5-6-2015

UL12 and ICP0 Regulate DNA Repair Pathway Choice During HSV-1 Infection

Samantha Smith
University of Connecticut - Storrs, smarques@uchc.edu

UL12 and ICP0 Regulate DNA Repair Pathway Choice During HSV-1 Infection

Samantha Smith, PhD

University of Connecticut, 2015

In order to promote lytic infection, HSV-1 manipulates components of the cellular DNA damage response (DDR). We hypothesized that correct pathway choice during HSV-1 infection is essential for productive infection. The central objective of this thesis was to determine whether UL12 acts a mediator of DDR pathway choice in order to produce DNA that is infectious and that can be packaged for productive infection. Previous studies have identified the classic non-homologous end joining (C-NHEJ) as antiviral, and we first sought to determine whether an incoming viral genome alone was sufficient to activate C-NHEJ. We transfected cells with purified virion DNA and monitored phosphorylation of RPA by DNA-PKcs. By adding 5' flaps to virion DNA, we were able to increase stimulation of DNA-PKcs activity, resulting in loss of infectivity. We showed that infectivity of the modified virion DNA could be restored by overexpression of ICP0 and in the cells deficient for DNA-PKcs. Thus, ICP0 may play an important role in promoting productive infection by inhibiting C-NHEJ. Since the UL12-null (AN-1) produces near wild type levels of DNA, but exhibits a severe growth defect, we next asked whether AN-1 DNA was infectious. By transfecting wild type and UL12-complementing Vero cells with purified AN-1 DNA, we determined that the DNA

produced in the absence of UL12 was aberrant and non-infectious. We hypothesized that in the absence of UL12, aberrant viral DNA is produced due to incorrect DDR pathway choice. To test this, we measured viral yields of UL12 mutant viruses on cells deficient for core C-NHEJ proteins and analyzed the DNA produced by pulsed field gel electrophoresis. We found that AN-1 grows better and produces less aberrant DNA on C-NHEJ-deficient cells. To determine whether UL12 and ICP0 are sufficient to effect pathway choice, we used a plasmid-based repair reporter that measures the ratio of C-NHEJ activity to MMEJ activity. We showed that both ICP0 and UL12 inhibit aspects of the C-NHEJ pathway in order to promote productive infection. This work demonstrates that C-NHEJ is antiviral, and that correct DDR pathway choice is essential for productive HSV-1 infection.

UL12 and ICP0 Regulate DNA Repair Pathway Choice During HSV-1 Infection

Samantha Smith

B.A., Western Connecticut State University, 2006

A Dissertation

Submitted in Partial Fulfillment of the

Requirements for the Degree of

Doctor of Philosophy

at the

University of Connecticut

2015

APPROVAL PAGE

Doctor of Philosophy Dissertation

UL12 and ICP0 Regulate DNA Repair Pathway Choice During HSV-1 Infection

Presented by

Samantha Smith, B.A.

Major Advisor_____

Sandra Weller

Associate Advisor_____

Chris Heinen

Associate Advisor_____

Bing Hao

Associate Advisor_____

Gordon Carmichael

University of Connecticut

2015

"Why are things as they are and not otherwise?"
- Johannes Kepler

"The capacity to blunder slightly is the real marvel of DNA. Without this special attribute, we would still be anaerobic bacteria and there would be no music."
- Lewis Thomas, Lives of the Cell

"Never ignore coincidence, unless of course, you're busy. In which case, always ignore coincidence."
-Doctor Who

ACKNOWLEDGEMENTS

"In everyone's life, at some time, our inner fire goes out. It is then burst into flame by an encounter with another human being. We should all be thankful for those people who rekindle the inner spirit."

-Albert Schweitzer

After the wild flurry of activity that completing and defending a dissertation entails, I relish this moment to stop and acknowledge those who have helped me reach this milestone. Without the help and support of my mentor, dissertation committee, colleagues, family and friends, I would not have achieved this goal.

First and foremost, I would like to thank my mentor, Sandy Weller. I am deeply grateful for her guidance and support throughout my graduate career. She has continually challenged me to become a more rigorous and thoughtful scientist. As a role model, her dedication to teaching, her candor, and her ability to provide both humor and humanity are all attributes that I will carry with me and strive for throughout my career. I would also like to thank my dissertation committee: Chris Heinen, Bing Hao, Shlomo Eisenberg, and Gordon Carmichael for their support and feedback.

To the members of the Weller lab, the ways that I am indebted to all of you are too numerous to list in this small section, but please know that I am deeply grateful for many things, including thoughtful feedback on data and practice talks, troubleshooting and assistance with experiments, friendship and laughs, and all the other ways that a lab family helps you get through each day. Thank you Renata Szczepaniak and Ping Bai for

training me and helping with experiments. My UL12 cohort: Lorry Grady, Nanda Balasubramanian, and April Schumacher, thank you for scholarly discussions. Anthar Darwish, for philosophical conversations, history lessons, and for coming to my rescue on numerous occasions. Brandon Albright, thank you for intellectual engagement, making me laugh until I cry, deftly composing song parodies, and washing our successes and failures down with many a pint. Kareem Mohni, my intellectual counterpoint, thank you for challenging me, for your generosity, for making me laugh, and above all for your friendship. Christine Livingston, my bosom friend, words cannot do justice- thank you for everything.

I give my deepest thanks to my family and friends. My parents, Chris and Ellen Smith, thank you for instilling me with a deep and unquenchable curiosity, and for supporting me throughout this long and arduous journey. I love you both so much. To my brother, Aaron, my sister-in-law Michele, my nephew Aiden, my cousin Steph, and my dear friends Mariah Perkins and John Redden, thank you for your love and support. Finally, thank you to my partner, Mark, for walking this path with me, sharing my triumphs and sorrows, and at times carrying me along. My life is infinitely better for having you in it, and I am profoundly thankful for all the ways you have helped me achieve my dreams.

TABLE OF CONTENTS

LIST OF FIGURES

CHAPTER 1.

CHAPTER 2.

CHAPTER 3.

CHAPTER 4.

CHAPTER 5.

LIST OF TABLES

CHAPTER 1.

CHAPTER 2.

CHAPTER 1

Introduction

Samantha Smith and Sandra K. Weller

Portions of the text and Figures 1.5, 1.6, and 1.8 from this chapter were submitted as a review manuscript for publication in Future Virology.

1.1. Herpes simplex virus I (HSV-1) Overview.

1.1.a. Characteristics of Herpesviridae family members.

Herpesvirales is a large and ancient order of viruses that is thought to have evolved approximately 500 million years ago. The *Herpesviridae* family is composed of more than 100 species, which infect a variety of reptilian, avian, and mammalian hosts. They are able to persist indefinitely within their hosts in a latent form, reactivating periodically to produce lytic infection. Members of *Herpesviridae,* commonly called herpesviruses, are grouped into three subfamilies (α, β, and γ herpesviruses) based on length of replicative cycle and the range of hosts they infect. Alphaherpesviruses have a short replication cycle and a broad host range; whereas, beta- and gammaherpesviruses have longer replication cycles and the range of host cells they infect are more restricted (Pellet and Roizman, 2007). Herpes simplex virus 1 & 2 (HSV-1, HSV-2) are alphaherpesviruses that cause lesions in the oral and genital mucosa, respectively. Varicella zoster virus (VZV or HHV-3), another alphaherpesvirus, causes chicken pox

(varicella) during primary infection, and shingles (zoster) during reactivation from latency. Epstein-Barr virus (EBV or HHV-4) is a gammaherpesvirus that causes mononucleosis and is associated with several types of cancer, including Burkitt's lymphoma. Human cytomegalovirus (HCMV or HHV-5), a betaherpesvirus, typically does not cause symptoms in healthy individuals, but can be deadly for immunocompromised individuals and newborn infants. HHV-6 and HHV-7 have not been as well researched as the other human herpesviruses. Both are betaherpesviruses and belong to the genus *roseolovirus* and are associated with febrile illness (Suga, Suzuki et al. 1998). HHV-6 causes sixth disease in young children, which can have serious complications. Kaposi's sarcoma-associated herpesvirus (KSHV or HHV-8) is a gammaherpesvirus, and is one of six known human oncoviruses[*] (Mesri, Feitelson et al. 2014).

Herpesviruses are extremely diverse with respect to tissue tropism and pathology; however, they all possess a similar virion structure (Figure 1.1). Herpesvirus virions contains a linear double strand DNA (dsDNA) genome that is relatively large (~124kb-241kb (Gray, Starnes et al. 2001, Davison, Dolan et al. 2003)) and contains terminal repeats and complementary single strand DNA (ssDNA) regions at each end (McGeoch, Rixon et al. 2006). The genome is housed within an icosahedral-shaped protein capsid, which is surrounded by a layer of viral proteins and mRNAs called the tegument. All of this is encased in a lipid bilayer envelope that is decorated with glycoproteins, which facilitate entry into the host cell. The herpesvirus lifecycle is biphasic, consisting of a primary lytic infection followed by latency (Figure 1.1).

[*] An **oncovirus** is a virus that can cause cancer.

1.1.b. Overview of the HSV-1 lifecycle.

Herpes simplex virus 1 (HSV-1) is a ubiquitous human pathogen responsible for significant disease during acute infection, HSV-1 lytic infection manifests in epithelial cells, most commonly of the oral and ocular mucosal, and results in cell death. Lytic infection is initiated when envelope glycoproteins on the virion bind to the attachment fact, heparin sulfate, and cell surface receptors, such as herpesvirus entry mediator (HVEM) and nectin-1 (Herold, WuDunn et al. 1991, Spear 2004). The envelope fuses with the cellular plasma membrane (Figure 1.2, top left). The capsid is then trafficked along microtubules by the dynein-dynactin motor complex, ultimately arriving at the nucleus (Sodeik, Ebersold et al. 1997, Dohner, Wolfstein et al. 2002, Mabit, Nakano et al. 2002). There it docks at the nuclear pore complex and releases its genome into the nucleoplasm (Batterson, Furlong et al. 1983, Lycke, Hamark et al. 1988). The incoming viral genome is a naked, linear dsDNA molecule that contains nicks and gaps (Kieff, Bachenheimer et al. 1971, Frenkel and Roizman 1972, Wilkie 1973, Biswal, Murray et al. 1974, Hirsch and Vonka 1974, Wadsworth, Hayward et al. 1976, Jacob and Roizman 1977, Roizman, Jacob et al. 1979). Within the nucleus, viral gene expression occurs in three kinetically distinct classes (described below). Viral gene expression, DNA replication, and packaging occur in large globular structures called replication compartments (RCs) (Quinlan, Chen et al. 1984, Lamberti and Weller 1996, Phelan, Dunlop et al. 1997). HSV-1 DNA replication produces highly branched, multimeric structures that must be resolved into linear, longer-than-unit length concatemers for packaging (Jacob and Roizman 1977, Jacob, Morse et al. 1979, Jongeneel and Bachenheimer 1981, Bataille and Epstein 1994, Severini, Morgan et al. 1994, Zhang,

Efstathiou et al. 1994, Severini, Scraba et al. 1996). DNA is packaged into preformed capsids. During egress from the nucleus, there is budding from the inner membrane, and fusion with the outer nuclear membrane, followed by a series of envelopment and de-envelopment steps (Enquist, Husak et al. 1998, Mettenleiter 2002). The tegument layer consists of 23 viral proteins and also viral (Loret, Guay et al. 2008). Although the nucleocapsid is thought to acquire components of the tegument layer in the cytoplasm, there is some evidence that some tegument proteins associate with nucleocapsids in the nucleus (Kelly, Fraefel et al. 2009). Finally, budding occurs at the cellular membrane, where the virion acquires its bi-lipid envelope and glycoproteins and is released into the extracellular space (Campadelli-Fiume, Amasio et al. 2007).

Following primary lytic infection, HSV-1 establishes a latent infection that can last for the life of the host with the potential for reactivation and recurrent disease. HSV-1 establishes latency in non-dividing sensory neurons within the trigeminal ganglion of its host. Sensory neurons can harbor anywhere between 10 to 100 copies of the HSV genome per cell (Sawtell, Poon et al. 1998, Wang, Lau et al. 2005). During latency, HSV-1 carries out minimal gene expression. The limited genes that are expressed during latency are called the latency associated transcripts, or LATs, which facilitate maintenance of the viral genome within the cell and allows for occasional reactivation from latency. It is thought that the ability to reactivate from latency and shed new virus is kept in check by cellular repressors and immune surveillance (Cantin, Hinton et al. 1995, Khanna, Bonneau et al. 2003).

1.1.c. The HSV-1 genome and gene expression.

The HSV-1 genome is approximately 152 kilobase pairs in length. It is composed of two unique regions (U_L and U_s), each of which is flanked by inverted repeat regions (Figure 1.3) (Hayward, Jacob et al. 1975, Sheldrick and Berthelot 1975, McGeoch, Dalrymple et al. 1988). Genomic inversions occur between the inverted repeats (Brown, Ritchie et al. 1973, Hayward 1974, Delius and Clements 1976, Zhang, Efstathiou et al. 1994). Thus, there are four possible isomers of the genome, which have been reported to be present in equimolar proportions during wild type infection (Bataille and Epstein 1997).

The genome encodes at least 74 proteins, which are temporally regulated and fall into three general kinetic classes: immediate early (IE, or α), early (E, or β), and late (L, or γ) (Honess and Roizman 1974). The five IE proteins (ICP0, ICP4, ICP22, ICP27, and ICP47) serve to promote a positive environment for productive viral replication and regulate viral gene expression. As the name implies, IE proteins are transcribed immediately and do not require protein synthesis for expression. IE transcription requires the viral tegument protein, VP16 (also called TIF, or α-trans-inducing factor) and the cellular transcription factors, Oct1 and HCF (Kristie and Roizman 1987, Kristie and Roizman 1988, Kristie and Sharp 1990). The E genes include DNA replication proteins and some envelope glycoproteins. Unlike IE genes, the E gene promoters do not require VP16, but they do contain elements that bind the cellular transcription factor, SP1 (Wagner, Guzowski et al. 1995, Kim and DeLuca 2002). In addition, E genes require IE gene expression. For example, ICP4 plays a very important role in stimulating E gene expression by binding directly to E promoters and helping to recruit TFIID and other

transcription factors (reviewed in DeLuca, 2011). L genes require DNA replication for their expression and they encode capsid proteins.

1.1.d. The earliest stages of HSV-1 infection.

HSV-1 DNA synthesis takes place in the infected cell nucleus in large globular domains called replication compartments. Replication compartments serve to concentrate and partition viral and cellular proteins that are required for productive infection. At the earliest stages of infection, cellular proteins are recruited to the vicinity of viral genomes in an attempt to thwart the infection. For instance, PML (promyelocytic leukemia protein) and other ND10 proteins form virus-induced PML-nuclear bodies (viPML-NB) that are associated with repression of vial gene expression (reviewed in (Everett 2001)). ViPML-NBs are subsequently disrupted by the E3 ubiquitin ligase activity of ICP0 (Everett, Meredith et al. 1999). As described below, other cellular proteins, many of which also exert antiviral effects, are also recruited to viral genomes including cellular histones as well as components of the DNA damage response pathways. HSV-1 has evolved to counteract antiviral mechanisms primarily through the action of ICP0. Some components of the DDR may also be beneficial to viral infection, and in this section we will discuss how HSV-1 navigates this complex cellular environment to create conditions that are conducive to productive viral infection.

1.1.e. HSV-1 DNA replication is closely associated with recombination.

The virus encodes seven essential replication proteins: the origin binding protein (UL9), the single strand DNA binding protein (SSB, ICP8), the heterotrimeric helicase/primase (UL5/8/52), the polymerase (UL30), and the polymerase processivity factor (UL42). Replication occurs in a biphasic manner, beginning with an UL9-dependent phase and later switching to a mechanism that does not require UL9 (Blümel and Matz 1995, Schildgen, Graper et al. 2005). The HSV genome contains three origins of replication: two copies of oriS and one oriL (Figure 1.3.A) (reviewed in (Weller and Coen 2012)). Current models suggest that together ICP8 and UL9 trigger the melting of one of these origins followed by recruitment of the helicase/primase complex and the HSV polymerase to carry out unwinding and elongation, respectively (Weller and Coen 2012).

HSV-1 DNA replication produces concatemers, which are required for the generation of progeny (Figure 1.3); however, the mechanism by which they are formed is unclear. It has long been recognized that HSV-1 genomes undergo a high degree of recombination (Wildy 1955, Brown, Ritchie et al. 1973, Hayward, Jacob et al. 1975, Sheldrick and Berthelot 1975, Delius and Clements 1976, Zhang, Efstathiou et al. 1994, Dutch, Bianchi et al. 1995, Fu, Wang et al. 2002). Although it has been proposed that the viral genome circularizes and rolling circle replication leads to the formation of concatemers (Poffenberger and Roizman 1985, Garber, Beverley et al. 1993, Deshmane, Raengsakulrach et al. 1995, Strang and Stow 2005), several lines of evidence suggest that HSV DNA replication is more complex. Controversy still remains over whether the incoming viral genome circularizes prior to replication, and recent evidence suggests that

circularization may actually be associated with latency (discussed in Chapter 2) (Jackson and DeLuca 2003, Strang and Stow 2005). HSV-1 replication proteins are able to catalyze rolling-circle replication *in vitro* (Skaliter and Lehman 1994, Skaliter, Makhov et al. 1996, Graves-Woodward, Gottlieb et al. 1997, Falkenberg, Lehman et al. 2000), but it has not been shown conclusively that rolling circle replication occurs during infection. Simple rolling circle replication does not explain the observation that genomic inversions occur as soon as viral DNA synthesis can be detected (Zhang, Efstathiou et al. 1994, Lamberti and Weller 1996, Severini, Scraba et al. 1996). In addition, replication of the HSV-1 genome produces X and Y branched structures that can be visualized by electron microscopy and 2D gel electrophoresis (Jacob and Roizman 1977, Severini, Scraba et al. 1996). These structures are reminiscent of recombination intermediates and suggest a more complex mode of replication. We have suggested that the HSV replication machinery promotes a unique form of DNA replication that utilizes a recombination-dependent mechanism to produce concatemers, which are required for packaging infectious virus (Wilkinson and Weller 2003, Weller and Sawitzke 2014).

The notion that HSV replication machinery promotes recombination-dependent replication is supported by experiments using HSV-1 as a helper virus to facilitate replication of other viruses and amplicons. For instance, replication of SV40 DNA by the six core HSV-encoded replication factors and SV40 large T-antigen produces concatemers composed of X-shaped DNA structures that may represent recombination intermediates (Blumel, Graper et al. 2000). Since SV40 replication normally produces two circular daughter molecules, it is noteworthy that the presence of HSV replication proteins can alter the mode of replication to generate complex concatemeric DNA (Matz

1987). In addition, adeno-associated virus (AAV) propagated using HSV as a helper virus produces high molecular weight forms of DNA that are not observed when adenovirus is used as a helper (Nicolas, Alazard-Dany et al. 2010). Thus, in the context of an HSV-1 infection, recombination may play a role in the generation of high molecular weight AAV concatemers that have a complex structure. Taken together, these data are consistent with the notion that the HSV replication machinery is inherently recombinogenic, giving rise to complex concatemeric DNA.

In addition to the core HSV replication machinery, we have identified a virus-encoded two-subunit recombinase that is reminiscent of the well-studied RedExo/β system of phage lambda (Stahl, Thomason et al. 1997, Reuven, Willcox et al. 2004). The lambda RedExo/β recombinase has been shown to perform strand annealing reactions *in vitro* (Stahl, Thomason et al. 1997, Reuven, Willcox et al. 2004). In addition, RedExo/β and related recombinases from other bacteriophages have been shown promote *in vivo* recombination-mediated genetic engineering using short homologies - "recombineering" in bacteria (reviewed in (Weller and Sawitzke 2014)). The HSV recombinase consists of UL12, a 5' to 3' exonuclease**,** and ICP8, which in addition to its role as a single strand DNA binding protein (SSB) can also function as a single strand DNA annealing protein (SSAP). UL12 and RedExo share conserved sequence elements, and both proteins interact with their partner SSAPs, ICP8 and Redβ, respectively (reviewed in (Weller and Sawitzke 2014)). The precise role of the UL12/ICP8 complex during infection remains unclear. We initially proposed that UL12 might be responsible for processing replication intermediates into a form suitable for encapsidation (Goldstein and Weller 1998); however, recent work has suggested that the viral recombinase may be involved at an

earlier step of infection during DNA synthesis to influence the mode of replication itself (Schumacher, Mohni et al. 2012). Thus, UL12 may stimulate a pathway of recombination-dependent replication required to produce concatemers that can be packaged into infectious virus.

A role for cellular DDR proteins in viral DNA replication has been suggested based on the observation that several cellular factors involved in HR including MRE11, RAD50, NBS1, and RAD51 are recruited to viral prereplicative sites and replication compartments (Wilkinson and Weller 2003, Taylor and Knipe 2004, Wilkinson and Weller 2004, Lilley, Carson et al. 2005, Shirata, Kudoh et al. 2005). In addition, both ICP8 and UL12 have been shown to interact with many DDR proteins (Taylor and Knipe 2004, Balasubramanian, Bai et al. 2010, Mohni, Mastrocola et al. 2011, Karttunen, Savas et al. 2014); however, attempts to identify the precise roles played by these proteins in HSV DNA replication have not been straightforward. For instance, although HSV may take advantage of cellular components to promote viral DNA replication, many DDR pathways promote antiviral mechanisms such as silencing and the induction of innate immune signaling. Because many components of cellular DDR pathways have complex and overlapping roles, it has been difficult to tease apart the precise functions of cellular DDR pathways during infection. Furthermore, DNA-PKcs, ATM, and the MRN complex also participate in other cellular processes and may play roles in HSV replication that are distinct from their roles in DDR pathways.

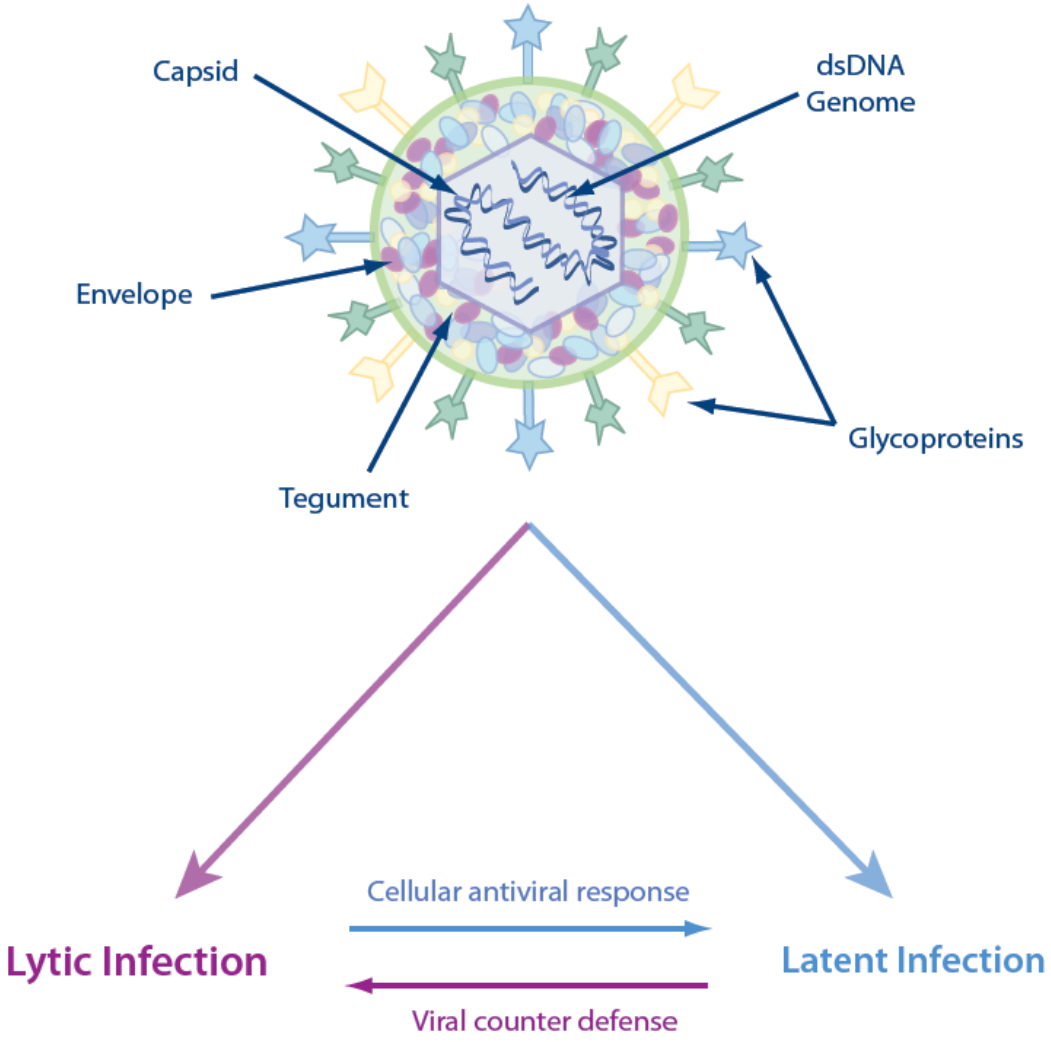

Figure 1.1. Herpesviruses share similar virion structures and have biphasic lifecycles. This figure illustrates the structural elements of the herpesvirus virion. The linear ds DNA genome is housed inside of a proteinaceous capsid. The capsid is surrounded by a layer tegument proteins and mRNAs. The tegument is enclosed within a lipid envelope layer that is decorated with glycoproteins. Viral and cellular factors influence whether viral infection manifests as lytic or latent.

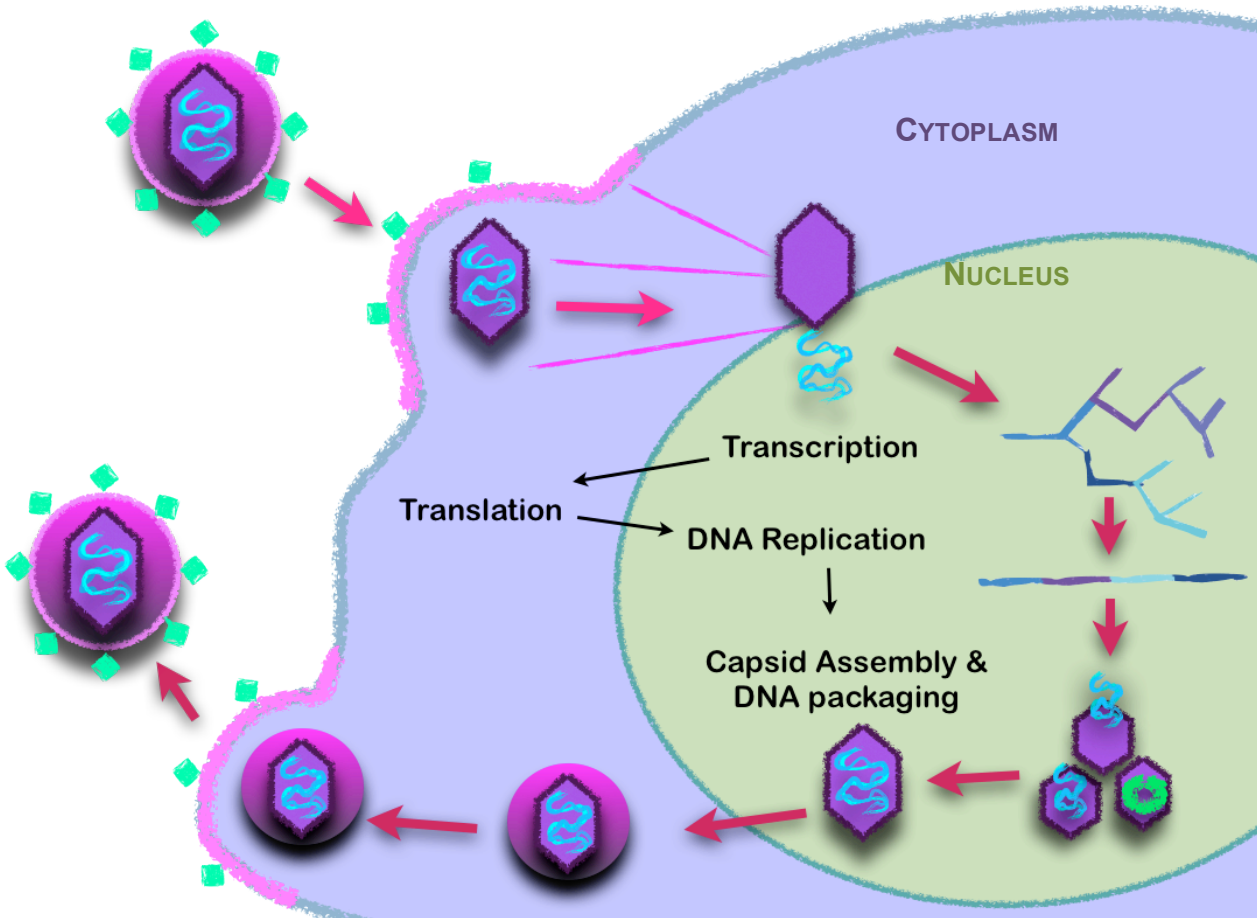

Figure 1.2. Diagram of the HSV-1 lytic life cycle. The HSV-1 virion binds to receptors on the surface of the host cell and fuses its envelope with the cellular plasma membrane (top left). The capsid is then transported on microtubules and docks at the nuclear pore complex where it injects its linear, dsDNA genome into the host cell nucleus. Within the nucleus, viral gene expression is initiated and occurs as three kinetically distinct classes. Viral genome replication results in complex, multimeric structures that must be resolved into linear, loner-than-unit length concatemers for packaging. The packaged capsid then undergoes a series of envelopment and de-envelopment steps during egress from the nucleus. In the cytoplasm, the tegument layer coats the capsid. Finally, budding occurs at the cellular membrane, where the virion acquires its bi-lipid envelope and glycoproteins.

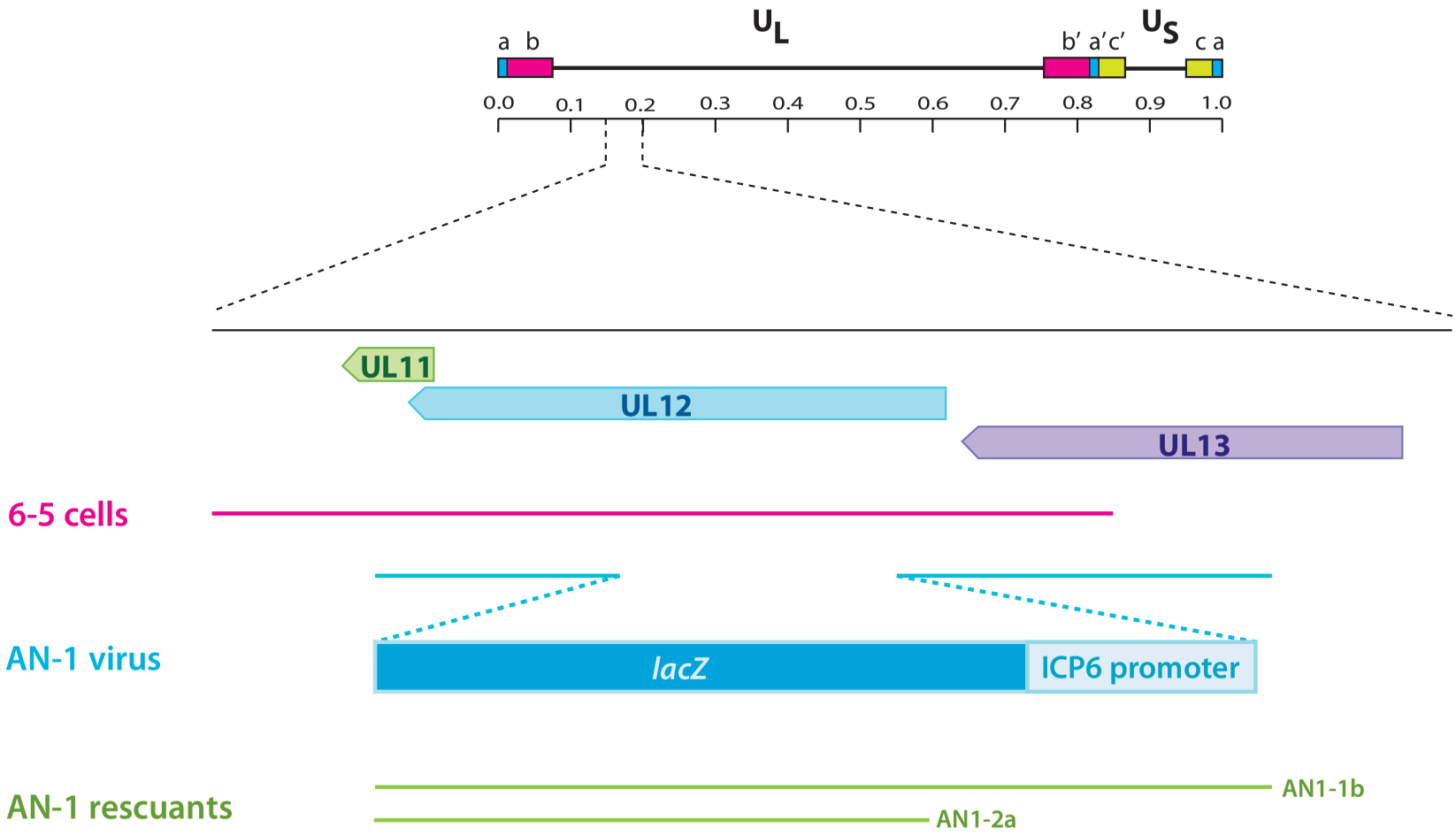
a b
UL
b′ a′c′
US
c a
0.0
0.1
0.2
0.3
0.4
0.5
0.6
0.7
0.8
0.9
1.0
UL11
UL12
UL13
6-5 cells
AN-1 virus
lacZ
ICP6 promoter
AN-1 rescuants
AN1-1b
AN1-2a

Figure 1.3. Diagram of the HSV-1 genome showing the region containing the *UL12* gene. The top of the diagram depicts the HSV-1 genome, below it are the physical map units. The region of the genome approximately spanning from map units 0.15 to 0.20 are enlarge to show the open reading frames encoding the *UL11, UL12,* and *UL13* genes. The pink bar indicates the portion of the genome that was used to create the UL12-complementing cell line, 6-5. The blue bar indicates the portion of *UL12* that was deleted and replaced with the *ICP6::lacZ* cassette to produce the UL12-null virus, AN-1. The green bars indicate portions of the genome that were used to produce rescuants of the AN-1 virus.

A.

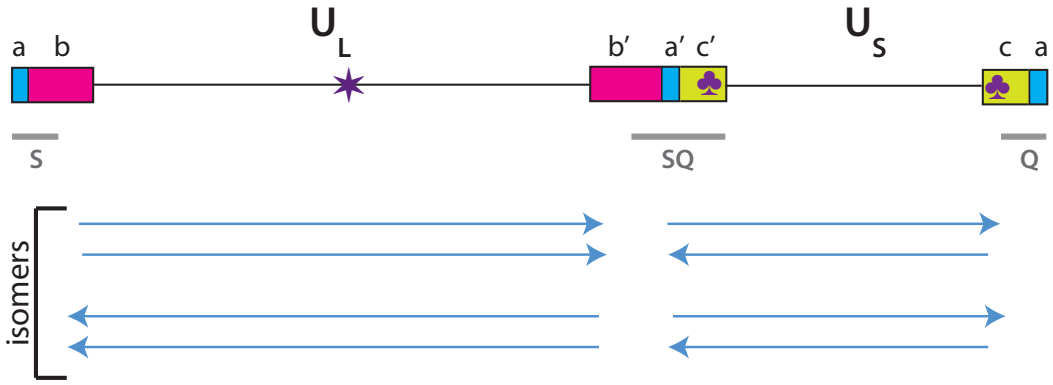
a b
U L
b′ a′ c′
U S
c a
S
SQ
Q
isomers

B.

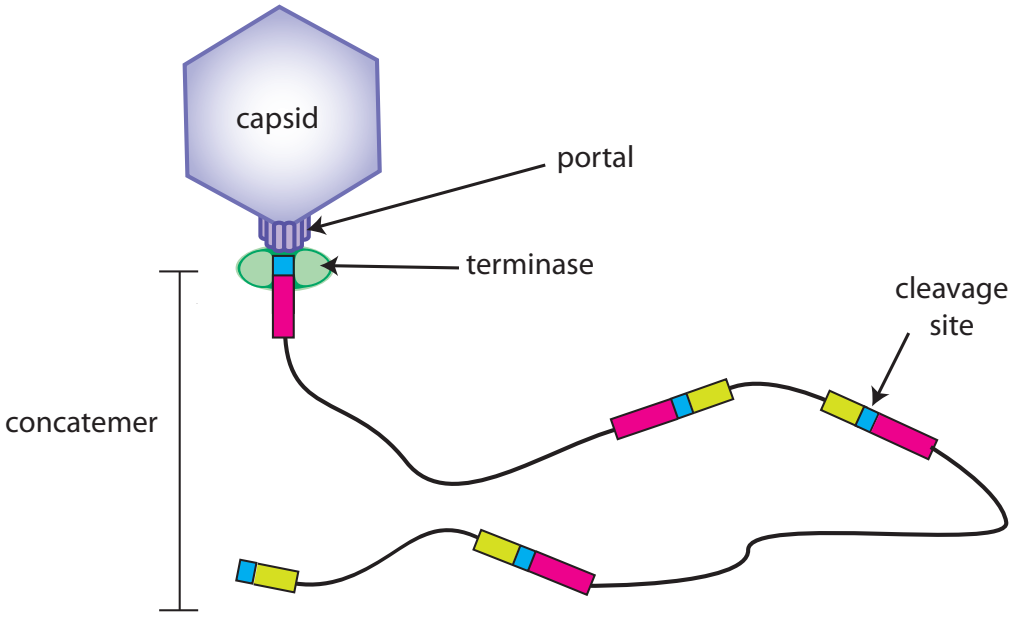
capsid
portal
terminase
cleavage site
concatemer

Figure 1.4. Diagram of the HSV-1 genome and concatemers. A. Schematic of the HSV-1 genome structure and key elements. U_L and U_S refer to the unique long and unique short regions, respectively. The inverted repeat sequences are labeled as a, b, and c. ✶ represents oriL, and ♣ represents oriS. The grey bars labeled S, SQ, and Q are restriction fragments produced by enzymatic digestion with *BamHI*. Below the genome, the four possible genome isomers are represented as blue arrows. *NB: Genomic elements are not proportionately to scale.* B. Diagram of the DNA packaging mechanism. A longer-than-unit length HSV-1 concatemer is required for packaging to occur. DNA molecules are expected to contain a higher proportion of junctions than terminal ends. On the other hand, genomes that have been cleaved for packaging are expected to contain equimolar ratios of junctions and termini.

Table 1.1. List of Abbreviations

Abbreviation	Name	Description
A-NHEJ	alternative nonhomologous end joining	DNA repair mechanism; also called MMEJ
AN-1	alkaline nuclease-1	Virus; mutant HSV-1 virus (KOS strain) that lacks the *UL12* gene
AT	Ataxia telaniectasia	Genetic disorder caused by mutations in the *ATM* gene
ATM	Ataxia telaniectasia mutated	Enzyme, kinase
BER	base excision repair	DNA repair mechanism
C-NHEJ	classic nonhomologous end joining	DNA repair mechanism
CMV	cytomegalovirus	Betaherpesvirus
DDR	DNA damage response	
DNA-PKcs	DNA-dependent protein kinase catalytic subunit	Enzyme, kinase; involved in the C-NHEJ repair pathway and the IRF-3 inducible innate immune response
DSBR	double strand break repair	DNA repair mechanism
dsDNA	double strand DNA	Molecule
EBV	Epstein-Barr virus	Gammaherpesvirus; infects humans
HCMV	human cytomegalovirus	Betaherpesvirus; infects humans
HR	homologous recombination	DNA repair mechanism
HSV	herpes simplex virus	Alphaherpesvirus
ICP0	infected cell protein 0	Viral (HSV-1) protein, E3 ubiquitin ligase

Abbreviation	Name	Description
IFI16	interferon inducible 16	Protein; DNA sensing protein; component of the IRF-3 inducible innate immune response
KSHV	Kaposi's sarcoma-associated herpesvirus	Gammaherpesvirus; infects humans
LIG I	DNA ligase I	Enzyme, ligase; associated with NER and MMEJ
LIG III	DNA ligase III	Enzyme, ligase; associated with BER and MMEJ
LIGIV	DNA ligase IV	Enzyme, ligase
MEF	mouse embryonic fibroblast	Cell line
MMEJ	microhomology mediated end joining	DNA repair mechanism; also called A-NHEJ
MMR	mismatch repair	DNA repair mechanism
MRE11	meiotic recombination 11 homolog A	
MRN	MRE11/RAD50/NBS1	Protein complex; involved in HR
NBS1	Nijmegen breakage syndrome 1	Protein; involved in HR; component of the MRN complex
NER	nucleotide excision repair	DNA repair mechanism
PAMP	pathogen-associated molecular pattern	Molecule; associated with groups of pathogens that are recognized by cells of the innate immune
PAR	poly (ADP-ribose)	Molecule, covalently attached to proteins and DNA as polymeric chains in response to DNA damage

Abbreviation	Name	Description
PARG	poly (ADP-ribose) glycosylase	Enzyme; involved in DNA repair; responsible for removal of PAR chains from proteins and DNA
PARP-1	poly (ADP-ribose) polymerase 1	Enzyme; involved in DNA repair and cellular stress response; catalyzes the covalent attachment of PAR chains to proteins and DNA
PFGE	pulsed-field gel electrophoresis	Assay for analyzing large DNA molecules
RAD50	radiation protein 50	Protein; involved in HR; component of the MRN complex
RNAP II	RNA polymerase II	Transcription protein
RPA	replication protein A	DNA binding protein involved in DNA repair and replication
SDSA	synthesis-dependent strand annealing	DNA repair mechanism; associated with repair of stalled replication forks
SSA	single strand annealing	DNA repair mechanism
ssDNA	single strand DNA	Molecule
U_L	unique long	Unique region of the HSV-1 genome that encodes *UL* genes
VZV	varicella zoster virus	Alphaherpesvirus
XLF	Cernunnos/XRCC4-like factor	Protein; involved in the C-NHEJ repair pathway
XRCC4	X-ray-cross-complementation gene 4	Protein; involved in the C-NHEJ repair pathway

Table 1.2. Properties of ICP0

***ICP0* gene**[7]	Also known as IE gene *1*
	Located in the R_L regions of the HSV-1 genome
	Immediate early (IE) expression kinetics
ICP0 protein	626 amino acids in length
	Approximately 110 kDa
	Also known as Vmw110
Enzymatic activity	RING finger E3 ubiquitin ligase
Other functions	Transactivator of viral gene expression
Some targets of ICP0 ubiquitin ligase activity[1,7]	PML, hDAXX, sp100, p53, NF-κB, CENP-A, CENP-B, CENP-C, DNA-PKcs[2,3], RNF8, RNF168, IFI16, PARG
Interacting partners	USP7, also called HAUSP; a ubiquitin-specific protease[4,5,6]
	Class II histone deacetylases[8]

[1]*Reviewed in* Lilley, Chaurushiya, et al. 2011; Lees-Miller, Long, et al. 1996; [3]Parkinson, Lees-Miller, et al. 1999; [4] Meredith, Orr, et al. 1994; [5]Meredith, Orr, et al. 1995; [6]Everett, Meredith, et al. 1997; [7]*Reviewed in* Smith, Boutell, et al. 2011; [8]Lomonte, Thomas, et al. 2004

Table 1.3. Properties of UL12

***UL12* gene**	Maps between approximately 0.168 and 0.175 map units on the HSV-1 genome, which is within the U_L region [1,2]
	Contained within a 2.3 kb mRNA that encodes a family of unspliced, 3' co-terminal mRNAs [2,3,4]
	Early (E) gene expression kinetics
UL12 protein	626 amino acids in length
	Approximately 85kDa
	Phosphoprotein
	Binds Mg^{2+}
Nuclease activity	Alkaline nuclease; *in vitro,* the nuclease activity is optimal in conditions between pH 8-9 [5]
	Possesses both exo- and endonuclease activity *in vitro* [6]
	5' to 3' exonuclease activity[7]
	Degrades ssDNA, dsDNA, and branched DNA structures[8]
Additional activities	Forms a putative two-subunit recombinase with ICP8[10] ↳ UL12/ICP8 catalyze strand exchange *in vitro*
	Stimulates SSA during HSV-1 infection[14]
Intracellular localization	Nuclear-diffuse[9]
	Detergent-resistant population in replication compartments, observable by immunofluorescence microcopy[9]
Interacting partners	ICP8, viral ssb
	MRN complex[9]
	MSH2/6 heterodimer[11]
	Ku70[12]
	FANCD2[13]

[1]Banks, Haliburton, et al. 1985; [2]Costa, Draper, et al. 1983; [3]Draper, Devi-Rao, et al. 1986; [4]McGeoch, Dolan et al. 1986; [5]Keir and Gold 1963; [6]Hoffman and Cheng 1978; [7]Knopf and Weisshart 1990; [8]Golstein and Weller 1998b; [9]Balasubramanian, Bai, et al. 2010; [10]Reuven, Staire, et al. 2003; [11]Mohni, Mastracola, et al., 2011; [12]Balasubramanian 2011; [13]Karttunen, Savas, et al. 2014; [14]Schumacher, Mohni, et al. 2012

1.2. HSV-1 and the cellular DNA damage response pathways.

1.2.a. Overview

In order to maintain its genetic integrity, the cell encodes a variety of mechanisms collectively termed the DNA damage response (DDR). The pathway by which cellular DNA is repaired depends on multiple factors, including cell type and cell cycle, as well as the nature and severity of the DNA lesion. Certain pathways are only activated during S phase at replication forks. Some types of repair require a template strand, while others do not, and some types of damage can be repaired by several mechanisms. The cell can utilize either direct chemical reversal of damage or excision repair to replace damaged or mismatched bases in DNA. Excision repair requires a template strand and the removal of stretches of nucleotides or bases. This mechanism encompasses base excision repair (BER), nucleotide excision repair (NER), and mismatch repair (MMR). For double strand breaks, the cell employs recombination-mediated repair. When DNA damage cannot be repaired by any of these strategies, the cell may utilize damage tolerance mechanisms, like translesion synthesis (TLS), post replication gap-filling, or replication fork regression. These mechanisms do not repair the damaged DNA, *per se*, but allow replication to proceed, often resulting in mutations. If damage is too great, the biological response tips from repair/tolerance toward cell cycle arrest and apoptosis.

1.2.b. Direct reversal and excision repair pathways.

Direct reversal of simple DNA adducts do not require a DNA template for repair. Instead, specific enzymes chemically reverse the lesion. For example, pyrimidine dimers

caused by exposure to UV can be repaired by photolyase[†], and O^6 methylguanine adducts are repaired by O^6 methylguanine methyltransferases (MGMT). Unlike the other types of repair, direct reversal does not require a template, neither does it involve breaking of the DNA backbone. Direct repair is, however, less versatile than other types of repair, due to the specificity required by each direct repair enzyme for a specific lesion.

Excision repair, which includes base excision repair (BER), nucleotide excision repair (NER), and mismatch repair (MMR), requires a template strand and involves the removal of stretches of nucleotides or bases. Pyrimidine dimers can be repaired via the nucleotide excision repair (NER) pathway, in addition to direct reversal. Of the three classes of excision repair, BER and NER are thought to occur throughout the cell cycle, whereas MMR is thought to occur primarily during replication (S-phase) (reviewed in (Branzei and Foiani 2008)).

Excision repair during HSV-1 infection. It is currently not known whether HSV-1 utilizes direct reversal or excision repair mechanisms to repair viral DNA. In a PCR-based assay, Millhouse, et al., demonstrated that repair of HSV-1 DNA damaged by UV irradiation can be repaired in Vero cells, but not in quiescently infected neuronal cells. Repair of viral DNA in Vero cells occurred in the absence of HSV pol, but appeared to be enhanced by HSV pol, even when viral replication was inhibited (Millhouse, Wang et al. 2012). In the absence of DNA replication, UV damage most commonly causes pyrimidine dimers. Thus, NER is likely responsible for the repair described in this paper, and it is possible that NER is active during HSV-1 infection.

[†] Although photolyase is expressed in a wide variety of organisms, humans lack this gene (Kato, Todo, et al. 1994).

1.2.c. Mismatch repair (MMR) proteins are required for efficient HSV-1 replication.

MMR overview. The MMR pathway is a highly conserved mechanism that is responsible for detecting and repairing mismatched bases, as well as insertion-deletions loops (IDLs) that arise during DNA replication. Single base mismatches and 1-2 base IDLs are recognized and bound by the MSH2/MSH6 heterodimer, while larger IDLs are bound by the MSH2/MSH3 heterodimer. The MLH1/PMS2 heterodimer is then recruited to help organize other MMR proteins, such as EXOI and replication protein A (RPA), onto mismatched DNA to facilitate resection and repair.

MMR and HSV. Both MSH2 and MLH1 are required for efficient replication of HSV-1 in normal human cells and are localized to viral replication compartments (Mohni, Mastrocola et al. 2011). In addition, interactions have been reported between ICP8 and UL12 and MMR proteins MSH2, MSH3, and MSH6 (Taylor and Knipe 2004, Mohni, Mastrocola et al. 2011). Interestingly, however, these proteins may have functions in HSV infection that are distinct from their canonical roles in recognizing mismatched DNA. MLH1 is recruited to viral genomes at the earliest stages of viral infection, and depletion of MLH1 in the context of viral infection inhibits immediate early gene expression (Mohni, Mastrocola et al. 2011). On the other hand, MSH2, which is generally thought to function before MLH1, is apparently recruited after MLH1 and may play a later role in HSV infection (Mohni, Mastrocola et al. 2011). These results suggest that although both MLH1 and MSH2 are required for efficient HSV infection, MLH1 may play a role in viral infection that is independent of MSH2 and may be distinct from the MMR pathway. MLH1 was also shown to be a component of PML-NBs, although unlike other components of these nuclear bodies, it is not degraded by ICP0 (Mohni, Mastrocola

et al. 2011). It will be of considerable interest to further explore the precise roles of both MLH1 and MSH2 during HSV infection.

1.2.d. HSV-1 influences pathway choice for double strand break repair (DSBR).

DBSR overview. Probably the most well studied type of DNA repair is double strand break repair (DSBR), which encompasses a variety of recombination-mediated pathways with distinct but overlapping functions. These mechanisms include: homologous recombination (HR), single strand annealing (SSA), classic nonhomologous end joining (C-NHEJ), and microhomology-mediated end joining (MMEJ) (Figure 1). The three pathways shown on the right side of Figure 1 (HR, SSA, and MMEJ) require some degree of homology; whereas, C-NHEJ does not. The homology driven pathways involve resection of DNA followed by annealing to a complementary strand. HR is generally more accurate than the other DSBR pathways, since HR employs strand invasion into a homologous chromosome or sister chromatid. SSA and MMEJ, on the other hand, are more error prone, often resulting in deletions or genomic translocations. Another type of homology driven repair, synthesis dependent strand annealing (SDSA) occurs during DNA replication in response to stalled replication forks. C-NHEJ does not require homology and can directly fuse unrelated DNA molecules (reviewed in (Dueva and Iliakis 2013)). Despite the potential for generating errors, C-NHEJ is the preferred mechanism of repair in higher eukaryotes and can occur during G1, S and G2 phases of the cell cycle.

DSBR and HSV. As shown in Figure 1.5, several cellular DDR mechanisms are available for recombination/repair during HSV-1 infection. In order to determine whether

HSV utilizes one or more of these pathways during infection, chromosomally integrated GFP correction assays were used to measure the frequency of DSBR by C-NHEJ, MMEJ, HR and SSA in infected cells (Schumacher, Mohni et al. 2012). Using these assays, we have shown that HSV infection stimulates SSA; however, HR, C-NHEJ and MMEJ were inhibited (Schumacher, Mohni et al. 2012). These results suggest that HSV has evolved to utilize SSA, and in the following sections we will explore possible reasons and mechanisms for the apparent inhibition of the other three pathways in infected cells.

1.2.e. HSV-1 inhibits classic non-homologous end joining (C-NHEJ).

C-NHEJ overview. As stated above, classic non-homologous end joining (C-NHEJ) involves the direct fusion of non-homologous dsDNA ends. This process involves at least three steps: recognition of DSB, end trimming/processing of non-ligatable termini, and ligation. C-NHEJ is promoted by the Ku70/86 heterodimer, which recognizes DSBs and binds to dsDNA ends. Ku70/86 recruits the DNA-dependent protein kinase catalytic subunit (DNA-PKcs), which aligns DNA ends. End processing occurs if the DNA ends are not easily ligatable, containing either non-homologous regions or unusual structures such as DNA hairpins. Cellular enzymes thought to play a role in the end-processing step include DNA-PKcs, Artemis, polynucleotide kinase phosphatase (PNKP), terminal deoxynucelotidyl transferase (Tdt), and polymerases (pols) λ and μ (reviewed in (Neal and Meek 2011)). The ligation step of C-NHEJ requires XRCC4, which interacts with both DNA Ligase IV (LIG IV) and DNA and is thought to be necessary for LIG IV recruitment to the DSB. XRCC4 also interacts with XLF; however, the precise role of XLF in NHEJ is not yet known.

C-NHEJ and HSV. The HSV genome contains nicks and gaps that are randomly located and present on both strands. Because the HSV-1 genome has dsDNA ends in addition to nicks and gaps, it is tempting to speculate that one or more of the DDR pathways might be activated by the genome as soon as it enters the nucleus. In fact, cells transfected with viral DNA exhibit RPA32 S4/S8 phosphorylation, a mark specific for DNA-PK activation (Smith, Reuven et al. 2014); however, DNA-PK is not activated in HSV-infected cells. It has been recognized since 1996 that DNA-PKcs activity is attenuated in HSV-infected cells in an ICP0-dependent manner (Figure 2) (Lees-Miller, Long et al. 1996, Parkinson, Lees-Miller et al. 1999, Smith, Reuven et al. 2014), leading to the suggestion that components of the C-NHEJ pathway are antiviral. In fact, HSV-1 replication is more efficient in cells lacking the catalytic subunit of DNA-dependent protein kinase (DNA-PKcs) (Parkinson, Lees-Miller et al. 1999), and in Ku-deficient murine embryonic fibroblasts, viral yields are increased by almost 50-fold (Taylor and Knipe 2004). In addition, we have recently demonstrated that ICP0 is required to relieve suppression of HSV-1 DNA infectivity caused by DNA-PKcs (Smith, Reuven et al. 2014). Possible reasons for the antiviral properties of C-NHEJ will be discussed below.

1.2.f. Homologous recombination (HR) components play positive and negative roles in HSV-1 infection.

HR overview. HR is mediated by the PI3 kinase-like kinase, ATM, which is activated when the MRN complex (MRE11, RAD50, and NBS1) senses a double strand break. ATM has numerous substrates, including the histone variant, H2AX, the phosphorylated form of which is called γH2AX (Rogakou, Pilch et al. 1998). The γH2AX

signal can spread as far as 1-2 megabases from the initial site of damage in an ATM and MDC1-dependent manner (Harper and Elledge 2007). This extensive phosphorylation is responsible for the appearance of damage foci observed by immunofluorescence microscopy (Fernandez-Capetillo, Celeste et al. 2003). Additional downstream effectors are then recruited to damage foci in a sequential fashion following ubiquitination of H2A-type histones by RNF8 and RNF168 (reviewed in (Jackson and Durocher 2013)). RNF8/RNF168-dependent ubiquitin conjugation is required to recruit and stabilize downstream repair proteins, such as BRCA1, 53BP1, and RAD51 ((Huen, Grant et al. 2007, Mailand, Bekker-Jensen et al. 2007, Stewart, Panier et al. 2009) and reviewed in (Jackson and Durocher 2013)). MRE11 and CtIP facilitate the initial end resection step, after which EXO1 and BLM carry out extensive resection (Williams, Williams et al. 2007, Bolderson, Tomimatsu et al. 2010). Following end resection, ssDNA is coated by RPA, which is important for activation of the ATR pathway (described below). RAD51 filaments assemble on RPA-coated DNA and facilitate strand invasion, resulting in a D-loop structure. During HR, this process results in Holliday junctions, which must be resolved to produce repaired, linear dsDNA. Strand invasion can also proceed via another mechanism, synthesis-dependent strand annealing (SDSA), which does not produce Holliday junctions (described below). Once the DSB has been repaired, DDR proteins dissociate from the DNA resulting in the resolution of damage foci.

Manipulation of the HR pathway during HSV-1 infection. Although chromosomal integration assays suggested that HR is suppressed during HSV-1 infection (Schumacher, Mohni et al. 2012), several components of the cellular HR machinery are required for efficient virus production. Virus production is deficient in cells lacking ATM,

MRN (MRE11, NBS1, RAD50), and WRN (Taylor and Knipe 2004, Lilley, Carson et al. 2005, Balasubramanian, Bai et al. 2010). In addition, we and others have demonstrated that HSV-1 induces ATM activation, as evidenced by the recruitment and phosphorylation of ATM, MDC1, NBS1, and CHK2 (Wilkinson and Weller 2004, Lilley, Carson et al. 2005, Shirata, Kudoh et al. 2005). Lilley et al., demonstrated that damage foci containing γH2AX and MDC1 are still able to form in IR-treated HSV-infected cells (Lilley, Carson et al. 2005); however, BRCA1 and 53BP1 are not recruited to damage foci because RNF8 and RNF168 are degraded by ICP0 (Figure 2) (Lilley, Chaurushiya et al. 2010). Thus, although ATM is activated in HSV infected cells, HR itself is inhibited, consistent with the observation that HR is inhibited in HSV-infected cells using the chromosomal reporter assay (Schumacher, Mohni et al. 2012). Interestingly, since HR proteins upstream of RNF8 and RNF168 are recruited to replication compartments and are required for efficient replication, it is possible that some of these components play positive roles during infection that are distinct from HR (Taylor and Knipe 2004, Lilley, Carson et al. 2005, Balasubramanian, Bai et al. 2010).

1.2.g. ATR-CHK1 signaling is disrupted in HSV-1 infected cells.

ATR-CHK1 pathway overview. In uninfected cells, the checkpoint kinase, ATR, is activated in response to stretches of ssDNA adjacent to dsDNA, like those found at stalled replication forks. ATR is also activated by substrates produced during ATM-mediated end-resection. Thus, ATM activation generally results in activation of the ATR pathway (Jazayeri, Falck et al. 2006, Sartori, Lukas et al. 2007). RPA is recruited to stretches of ssDNA and recruits ATR, and the ATR-interacting protein (ATRIP). ATR

signaling also requires the recruitment of the 9-1-1 (RAD9-RAD1-HUS1) checkpoint clamp, which in turn recruits the ATR-activator, TopBP1, which results in phosphorylation of CHK1 on S317 and S345 and RPA32 on S33.

ATR-CHK1 inhibition during HSV-1 infection. In uninfected cells, activation of ATM would be expected to result in the activation of ATR. Interestingly, ATR-CHK1 signaling is disrupted during HSV-1 infection even though HSV-1 DNA replication activates ATM signaling (Figure 2) (Wilkinson and Weller 2004, Lilley, Carson et al. 2005, Shirata, Kudoh et al. 2005, Mohni, Livingston et al. 2010). ATR is not activated in HSV-infected cells, even if these cells are treated with hydroxyurea (HU), which causes replication fork stalling (Gordin, Olshevsky et al. 1973, Mohni, Livingston et al. 2010). We have recently identified the mechanism by which HSV-1 inhibits ATR signaling: four replication proteins (ICP8 and the three components of the helicase/primase complex) can bind to substrates that contain ssDNA adjacent to dsDNA, which are similar to substrates recognized by RPA and ATR. Thus, these four viral proteins prevent the loading of the 9-1-1 complex and the subsequent recruitment of TopBP1, effectively disabling ATR signaling. It is still not clear why HSV has evolved to prevent ATR signaling. It is known that in uninfected cells ATR signaling can stabilize stalled forks and prevent fork collapse in order to prevent the formation of DSB (Peasland, Wang et al. 2011). Although DSB formation would be deleterious for cells, it may be beneficial during HSV replication, perhaps by stimulating recombination. This is supported by the observation that artificial activation of ATR results in reduced recombination between co-infecting viruses (Mohni, Dee et al. 2013). Although HR is inhibited in infected cells, other mechanisms of recombination such as SSA may be

stimulated under these conditions (discussed below). Despite the observation that ATR signaling is prevented in HSV-1 infected cells, ATR and several proteins in this pathway are recruited to viral replication compartments and are essential for efficient virus production (Mohni, Livingston et al. 2010, Mohni, Dee et al. 2013). These results suggest that ATR pathway proteins play positive roles in HSV-1 infection that are distinct from ATR signaling. Alternatively, it may be beneficial for HSV-1 to recruit these proteins to viral genomes as a way to inhibit cellular DNA replication.

1.2.h. The Fanconi anemia (FA) pathway plays a positive role in HSV-1 infection.

FA pathway overview. In uninfected cells, the Fanconi anemia (FA) pathway is activated by ATR during S-phase in response to replication stress caused by stalled forks and interstrand cross-links (ICLs) (Shigechi, Tomida et al. 2012, Tomida, Itaya et al. 2013). The FA pathway has been shown to promote replication restart by coordinating homology-mediated repair (HR and SSA) and translesion synthesis (TLS) (Nakanishi, Yang et al. 2005, Sale, Lehmann et al. 2012, Shigechi, Tomida et al. 2012), modulating MMR (Zhi, Wilson et al. 2009, Peng, Xie et al.) and suppressing C-NHEJ (Adamo, Collis et al. 2010). The FA pathway is composed of at least 15 proteins, which are divided into three functional groups: the core complex, the ID complex, and downstream effectors. Activation of the FA pathway requires monoubiquitination of the ID complex (FANCI and FANCD2) by the FA core complex (FANCA, B, C, E, F, G, L, and M), which together with FAAP24 and FAAP100 form a multi-subunit E3 ubiquitin ligase, and the E2-conjugating enzyme, UBE2T. FA activation is also dependent on phosphorylation of

FANCI and FANCD2 by ATR (Andreassen, D'Andrea et al. 2004, Ho, Margossian et al. 2006).

The FA pathway and HSV-1 infection. Recently, the Mohr lab demonstrated that FA proteins are necessary for efficient HSV-1 replication and transcription and suggested that these proteins act as regulators of DNA repair pathway choice during infection (Figure 1.8) (Karttunen, Savas et al. 2014). HSV-1 potently activates the FA pathway, by mono-ubiquitination of FANCI-D2, which seems to require HSV pol and DNA replication (Figure 2) (Karttunen, Savas et al. 2014). In addition, they demonstrated that FANCI interacts with ICP8, pol, UL42, UL12, and dUTPase and that FANCD2 interacts with the helicase subunit, UL5 (Karttunen, Savas et al. 2014). Furthermore, they showed that HSV-1 replication was restricted in FA-deficient cells, and that this restriction was partially eliminated by treatment with the DNA-PKcs inhibitor, NU7441(Karttunen, Savas et al. 2014). These results suggest that the FA pathway may play a role in restricting DNA-PKcs activity during HSV-1 infection. Previous reports demonstrate that FA pathway proteins stimulate SSA. This is consistent with the notion that these proteins direct repair toward the SSA pathway while inhibiting C-NHEJ in HSV-infected cells.

1.2.i. Single strand annealing (SSA) is stimulated in HSV-1 infected cells.

SSA overview. SSA is a form of homology-mediated repair, although it is more error-prone than HR, and can cause deletions and chromosomal translocations. SSA is initiated when a double strand break occurs between two repeated sequences oriented in the same direction. Homologous regions of single stranded DNA are exposed through extensive end resection by a 5’ to 3’ exonuclease. Annealing is facilitated by RAD52,

which is an SSAP (Singleton, Wentzell et al. 2002, Stark, Pierce et al. 2004). Following annealing, it is believed that non-homologous 3'overhangs are cleaved by ERCC1/XPF (reviewed in (Iyama and Wilson 2013)). GFP reporter assays have been used to identify the cellular components required for SSA, and interestingly, most appear to overlap with other DDR pathways (Singleton, Wentzell et al. 2002, Stark, Pierce et al. 2004, Bennardo, Cheng et al. 2008). For instance, the single strand annealing protein Rad52 is also involved in assembly of Rad51 filaments during HR, and ERCC1/XPF are also implicated in NER and MMEJ (reviewed in (Iyama and Wilson 2013).

HSV-1 stimulates SSA. GFP correction assays have demonstrated that HSV stimulates SSA, raising the question of whether SSA is carried out by viral or cellular proteins (or both). As mentioned above, HSV encodes a two-subunit recombinase (UL12 and ICP8). The alkaline nuclease (UL12) component of the HSV-1 recombinase is necessary and sufficient to stimulate SSA (Schumacher, Mohni et al. 2012). Stimulation of SSA was abrogated in the nuclease-dead mutant, UL12 D340E, suggesting that UL12 nuclease activity may be required for end-resection prior to SSA (Schumacher, Mohni et al. 2012). Direct involvement of ICP8 in this process has been difficult to demonstrate because ICP8 is also essential for DNA synthesis. Additional experimentation will be required to assess the possible involvement of cellular SSA proteins such as RAD52 and the ERCC1/XPF complex.

1.2.j. HSV-1 may also utilize MMEJ/SDSA to repair DSBs during replication.

MMEJ and SDSA overview. Perhaps the least understood DSBR mechanism is microhomology-mediated end joining (MMEJ). Like SSA, this process requires resection to expose regions of homology and annealing of homologous regions. Unlike SSA, however, MMEJ is thought to require a small amount of homology (5-25nt) for end joining to occur. Although MMEJ is not well defined, several proteins are thought to participate in this process, including: poly (ADP-ribose) polymerase 1 (PARP-1), XRCC1, ERCC1/XPF, LIG III, and possibly the MRN complex (Audebert, Salles et al. 2004, Wang, Wu et al. 2006, Rass, Grabarz et al. 2009, Xie, Kwok et al. 2009, Zhuang, Jiang et al. 2009, Cheng, Barboule et al. 2011). Interestingly, MMEJ has been shown to have an important role in the repair of DSBs at collapsed replication forks (Truong, Li et al. 2013) and may play a role in synthesis-dependent strand annealing (SDSA) [reviewed in (Ottaviani, LeCain et al. 2014)].

A model for A-NHEJ/SDSA during HSV-1 infection. As stated above, it is clear that recombination is tightly linked to DNA replication during HSV-1 infection. Thus, in addition to classic SSA, it is possible that the HSV-1 may use a synthesis dependent strand annealing (SDSA) mechanism (reviewed in (Weller and Sawitzke 2014)). SDSA utilizes strand exchange, in which the 5' end of dsDNA break is resected, and the 3' end is annealed to a homologous region at a single strand region of a growing replication fork (reviewed in (Ottaviani, LeCain et al. 2014)). Interestingly, the recombineering machinery employed by the lambda RedExo/β and other bacteriophage-encoded recombination systems such as RecE/T are also dependent on DNA synthesis (reviewed in (Weller and Sawitzke 2014)). Recombineering can be performed with either single or

double stranded oligonucleotides and is used to efficiently incorporate mutations into bacterial genomes. Single strand oligonucleotides are coated by an SSAP such as lambda Redß or RecT and inserted at the DNA replication fork. When double stranded oligonucleotides are used, the exonuclease degrades one entire strand. In the model shown in Figure 3A, the remaining strand is coated with the SSAP and incorporated on the lagging strand template (reviewed in (Weller and Sawitzke 2014)). A more elaborate situation has been proposed to occur during replication of viral genomes (Maresca, Erler et al.)(Figure 3B). According to this scenario, a DSB on one viral genome is concurrently resected and annealed at the lagging strand template. This model was originally proposed by A. Kuzminov [(Kuzminov 1999) and reviewed (Weller and Sawitzke 2014)]. Additional experiments will be required to determine whether HSV utilizes this type of synthesis dependent annealing reaction during replication; however, it is known that the HSV-1 recombinase, UL12/ICP8, is capable of performing strand exchange *in vitro* and that recombination is linked to DNA synthesis (Reuven, Willcox et al. 2004).

1.2.k. PARP/PARG may play positive and negative roles during HSV-1 infection.

PARP overview. PARP proteins utilize NAD+ to catalyze the covalent attachment of poly-ADP ribose (PAR) chains to proteins. Although there are 17 members of the PARP family, PARP-1 is responsible for nearly all PARylation that takes place in the cell, and only PARP-2 has been shown to complement a PARP-1 mutant (Huber, Bai et al. 2004). Interestingly, PARP-1 plays both pro- and anti-recombinogenic roles and regulates many DDR pathways. In addition to its role in MMEJ, PARP-1 also plays a crucial role in recovery from replication fork stalling through stimulation of HR. PARP-1 senses and

is recruited to nicks, ssDNA breaks, and dsDNA breaks and PARylates itself and other proteins. The PAR posttranslational modification is thought to control the activity and function of several DDR proteins such as MRE11, NBS1, and DNA-PKcs. Thus, PARP-1 plays an important role in chromatin remodeling and the recruitment and regulation of cellular DDR proteins. On the other hand, excess DNA damage can result in overactivation of PARP and lead to cell death. The enzyme, poly (ADPribose) glycohydrase (PARG), catalyzes the removal of PAR chains and is required to prevent cell death and promote replication restart via HR (Min, Cortes et al. 2010, Illuzzi, Fouquerel et al. 2014). In the absence of PARG, PAR chains are thought to accumulate on DNA, preventing RPA binding, and as a result, RPA32 phosphorylation by DNA-PKcs is inhibited (Illuzzi, Fouquerel et al. 2014). Thus, the PARP/PARG balance plays an important role in modulating the DNA damage response.

PARP/PARG and HSV-1. A study to examine metabolic changes in HSV-infected cells revealed that PARP is activated during infection. Vastag *et al.* reported that NAD^+ levels are decreased during HSV-1 infection (Vastag, Koyuncu et al. 2011), and PARylation carried out by activated PARP1/2 during HSV-1 infection was found to be responsible for the observed NAD^+ depletion (Grady, Hwang et al. 2012). Since PARP1/2 sense nicks and ssDNA breaks, it is possible that nicks and gaps in the viral genome are responsible for PARP activation. Whether nicks and gaps in viral genomes are repaired during the early stages of infection by DDR machinery is not known; however, PARP binding and the subsequent recruitment of repair proteins may represent an attempt to fill in gaps. Interestingly, PARG is degraded by ICP0 during HSV-1 infection (Grady, Hwang et al. 2012). Thus, it is possible that although PARP is activated

by infection, the downstream DNA repair processes facilitated by PARG are prevented by ICP0. This may be a mechanism by which HSV counteracts the antiviral activity of some DDR pathways such as C-NHEJ. Although ICP0 degrades DNA-PKcs in some cells, the activity DNA-PKcs is inhibited even in Vero cells in which DNA-PKcs is not degraded (Wilkinson and Weller 2004, Mohni, Smith et al. 2013, Smith, Reuven et al. 2014). As mentioned above, in the absence of PARG, DNA-PKcs activity is inhibited. The degradation of PARG by ICP0 may thus contribute to the inhibition of DNA-PKcs, implying that HSV has evolved more than one mechanism to inhibit DNA-PKcs and C-NHEJ. We are intrigued by the possibility that gap filling facilitated by PARP/PARG and circularization by C-NHEJ are antiviral and contribute to genome silencing. The ability of ICP0 to degrade both DNA-PKcs and PARG may be a means by which HSV prevents circularization, consistent with the demonstration by Jackson and Deluca that in the presence of ICP0, circularization of the viral genome is prevented (Jackson and DeLuca 2003). Further experimentation will be required to test this model and address the controversy over whether circularization occurs during lytic infection.

1.2.l. Some DDR proteins function as DNA sensors in intrinsic and innate immune responses.

DDR and Antiviral Defense. When HSV-1 infects a cell, the viral genome is released from the capsid into the host cell nucleus, which may be an intrinsically hostile environment for invading pathogens. Cellular defense strategies include three inter-related arms: intrinsic antiviral mechanisms, innate immune signaling and the adaptive immune responses. We are intrigued by the observation that DNA damage sensing

proteins are able to sense "foreign" DNA and trigger various types of antiviral responses. It is tempting to speculate that these responses are part of a larger network of antiviral defense mechanisms and that some DDR pathways may have evolved initially to counteract environmental pathogens such as viruses.

Intrinsic Antiviral Mechanisms. Intrinsic antiviral proteins are cellular factors that are constitutively expressed and poised to inhibit infection immediately following viral entry (Bieniasz 2004). The first recognized intrinsic factors target retroviruses, and the number of retroviral defense factors has now grown to include Fv-1, TRIM5α, APOBEC3G and SAMHD1. More recently, it has been recognized that nuclear factors such as PML (TRIM19) exert antiviral effects that target herpesviruses, especially HSV and HCMV (Tavalai, Papior et al. 2006, Boutell and Everett 2013). As described above, incoming viral genomes recruit PML into viPML-NBs that have been associated with repression of viral gene expression (Boutell and Everett 2013). Other proteins that are recruited to viral genomes at the earliest stages of infection may also be part of the intrinsic antiviral network. For example, DNA-PKcs may modulate transcription of viral genes through several mechanisms. It has been reported to modulate RNAP II activity and inhibit the ability of RNAP II to bypass DSBs (Maldonado, Shiekhattar et al. 1996, Pankotai, Bonhomme et al. 2012). Alternatively, if DNA-PKcs and Ku proteins are recruited to viral DNA ends, they might be expected to activate C-NHEJ resulting in the circularization of viral genomes and the subsequent promotion of chromatinization and epigenetic silencing (Lees-Miller, Long et al. 1996, Knipe and Cliffe 2008). Activation of RNF8 and RNF168 and the ubiquitination of H2A has also been suggested to cause genome silencing (Lilley, Chaurushiya et al. 2010). In addition, interferon-inducible

protein 16 (IFI16) is a DNA sensor involved in innate IRF-3-mediated signaling as well as intrinsic antiviral responses. IFI16 has also been shown to sense microbial DNA and promote epigenetic silencing of DNA lacking or loosely associated with chromatin, such as HSV-1 genomes (Orzalli, Conwell et al. 2013). Thus, the ability of various cellular components, including DDR proteins, to silence viral gene expression appears to be a common mechanism by which cells have evolved to counteract viral infections. The ability of ICP0 to degrade PML, DNA-PKcs, RNF8/168 and IFI16 demonstrates that HSV has evolved to evade intrinsically antiviral silencing mechanisms.

DDR proteins may act as DNA sensors that trigger innate immune responses. In addition to intrinsic defenses such as repression of viral gene expression, cells have elaborate signaling mechanisms to trigger innate and adaptive immune responses to viral infection. Viral nucleic acids are the predominant pathogen associated molecular patterns (PAMP) produced during viral infection and are recognized by pattern recognition receptors (PRRs). It has been suggested that the cell distinguishes between viral and endogenous nucleic acids based in part on their cellular compartmentalization and chemical differences in the DNA itself. For example, DNA that is present in a compartment other than the nucleus, such as in endosomes or in the cytoplasm, may be identified as foreign. Cytosolic sensors of viral/microbial DNA include: DNA-dependent activator of interferon (DAI), RNA polymerase III, PHYIN family proteins (such as: IFI16 and AIM2), DExD/H-box helicases (like RIG-I), DNA-PKcs, cGAS, and STING (reviewed in (Orzalli and Knipe 2014)). On the other hand, in the nucleus the cell relies on chemical differences in DNA to distinguish between foreign and endogenous DNA.

For example, unmethylated CpG DNA is chemically distinct from cellular DNA and will flag viral DNA as a PAMP (Unterholzner 2013).

In addition to the possible roles in intrinsic antiviral mechanisms described above, it appears that DNA-PKcs may also stimulate innate immune signaling. DNA-PKcs has been reported to sense and respond to DNA and to induce transcription of Cxcl10, IL-6, and IFN- β as part of the IRF-3 innate immune response (Ferguson, Mansur et al. 2012). In that report, Ferguson, et al. also demonstrated that HSV-1 infection stimulates IL-6 transcription in MEFs and that this stimulation is partially relieved in DNA-PKcs knockout cells (*Prkdc*$^{-/-}$ MEFs). It is thus possible that DNA-PK exerts its antiviral effects by several different mechanisms including initiating an innate signaling cascade. Recent studies have demonstrated that IFI16 also may play roles in both the intrinsic and innate antiviral responses (Unterholzner, Keating et al. 2010, Li, Yamauchi et al. 2012, Orzalli, DeLuca et al. 2012). HSV-1 triggers IRF-3 induction and activation of the inflammasome in human fibroblasts in an IFI16-dependent manner (Orzalli, DeLuca et al. 2012, Johnson, Chikoti et al. 2013). ICP0 degrades IFI16 as part of the immune-evasion strategy of HSV-1 (Orzalli, DeLuca et al. 2012).

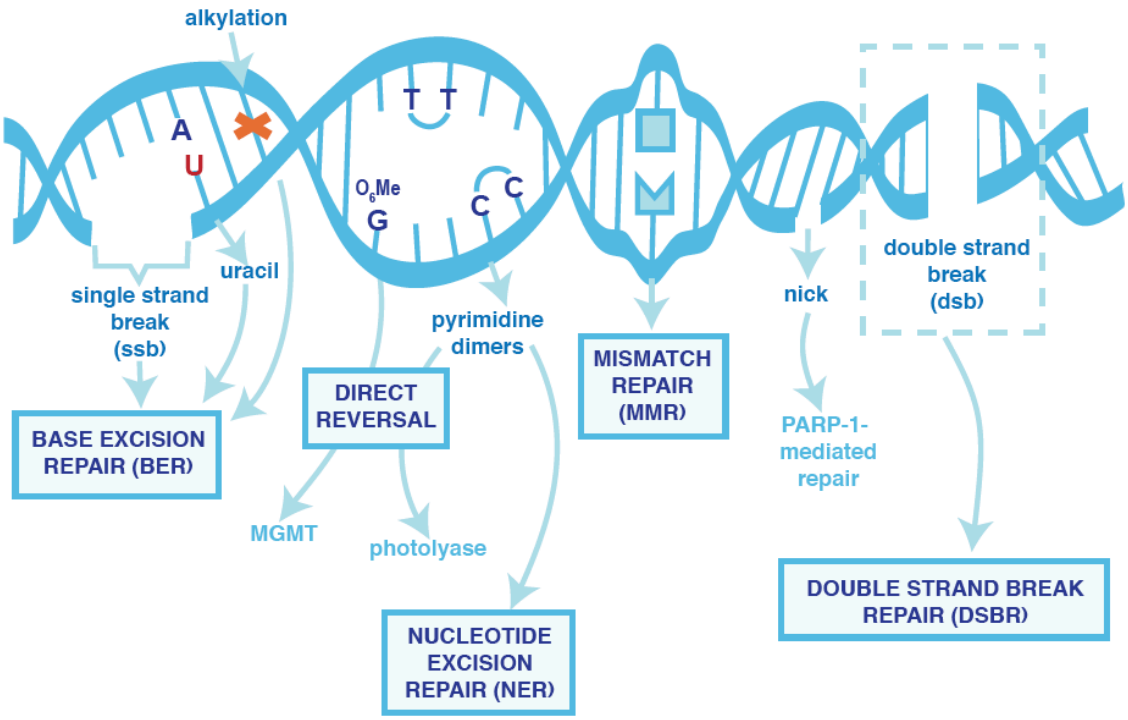

Figure 1.5. Diagram of the types of DNA damage and the cellular DNA repair strategies. Single strand breaks are produced by direct oxidative attack to the sugar phosphate backbone; alternatively, oxidative damage can indirectly cause ssDNA breaks by inducing base excision of damaged bases. In both instances, BER is required for repair (reviewed in (Ciccia and Elledge 2010)). Nicks can also arise from topoisomerase I activity. These nicks have intact 5'-P and 3'-OH ends, and are easily ligated back together. Some types of DNA damage, such as pyrimidine dimers and O_6 methylguanine can also be repaired by direct reversal; however, placental mammals do not express the photolyase enzyme (Kato, Todo, et al. 1994).

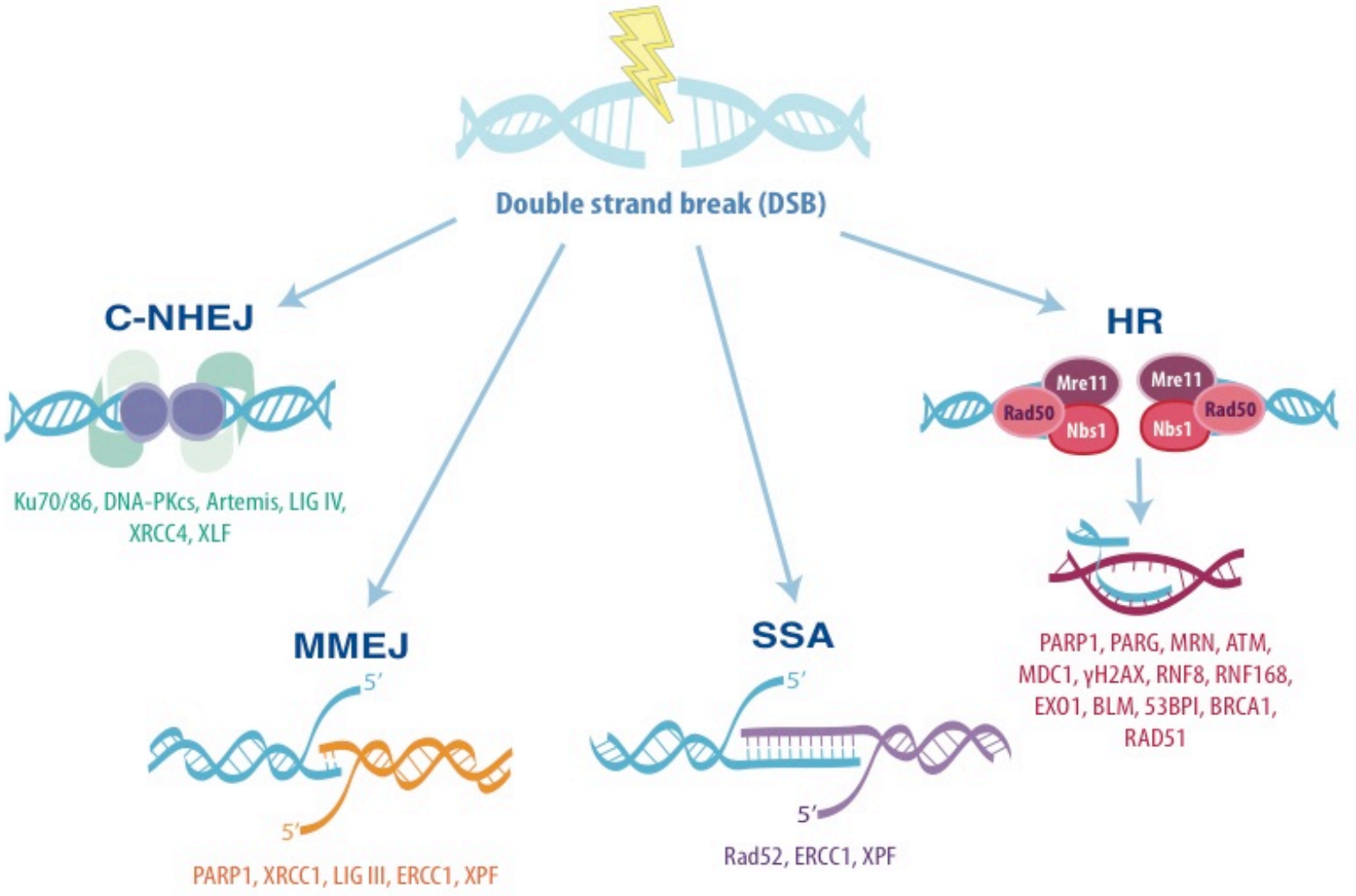
Double strand break (DSB)
C-NHEJ
Ku70/86, DNA-PKcs, Artemis, LIG IV, XRCC4, XLF
HR
Mre11
Rad50
Nbs1
Mre11
Rad50
Nbs1
PARP1, PARG, MRN, ATM, MDC1, γH2AX, RNF8, RNF168, EXO1, BLM, 53BPI, BRCA1, RAD51
MMEJ
5′
5′
PARP1, XRCC1, LIG III, ERCC1, XPF
SSA
5′
5′
Rad52, ERCC1, XPF

Figure 1.6. Diagram of the DNA double strand break repair (DSBR) pathways. In response to double strand breaks, DNA can be repaired by one of four major pathways: classic nonhomologous end joining (C-NHEJ), microhomology-mediated end joining (MMEJ), single strand annealing (SSA), and homologous recombination (HR). HR, SSA, and MMEJ are homology-directed forms of repair; whereas, C-NHEJ does not require homology. Double strand breaks arising at replication forks can also be repaired by synthesis-dependent strand annealing (SDSA) and break-induced repair (BIR) mechanisms via ATR-CHK1 signaling (not shown in figure).

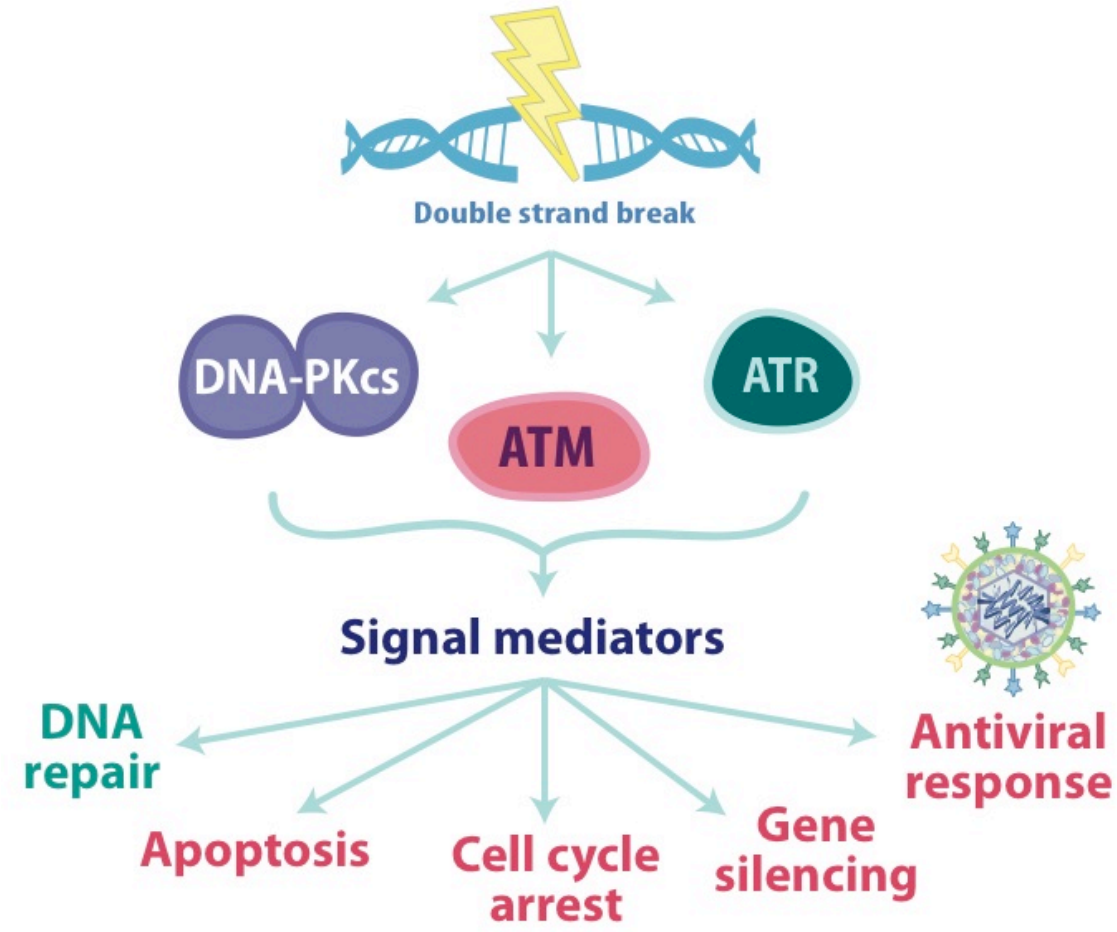

Figure 1.7. DNA damage is sensed by three PI3K-like kinases and has several possible consequences. DSBR is mediated by the PI3K-like kinases: DNA-PKcs, ATM, and ATR. These kinases activate signal mediators. Depending on the type and degree of damage, this signaling can result in DNA repair, apoptosis, cell cycle arrest, and/or gene silencing. When triggered by viral DNA, all of these consequences may contribute to an antiviral response.

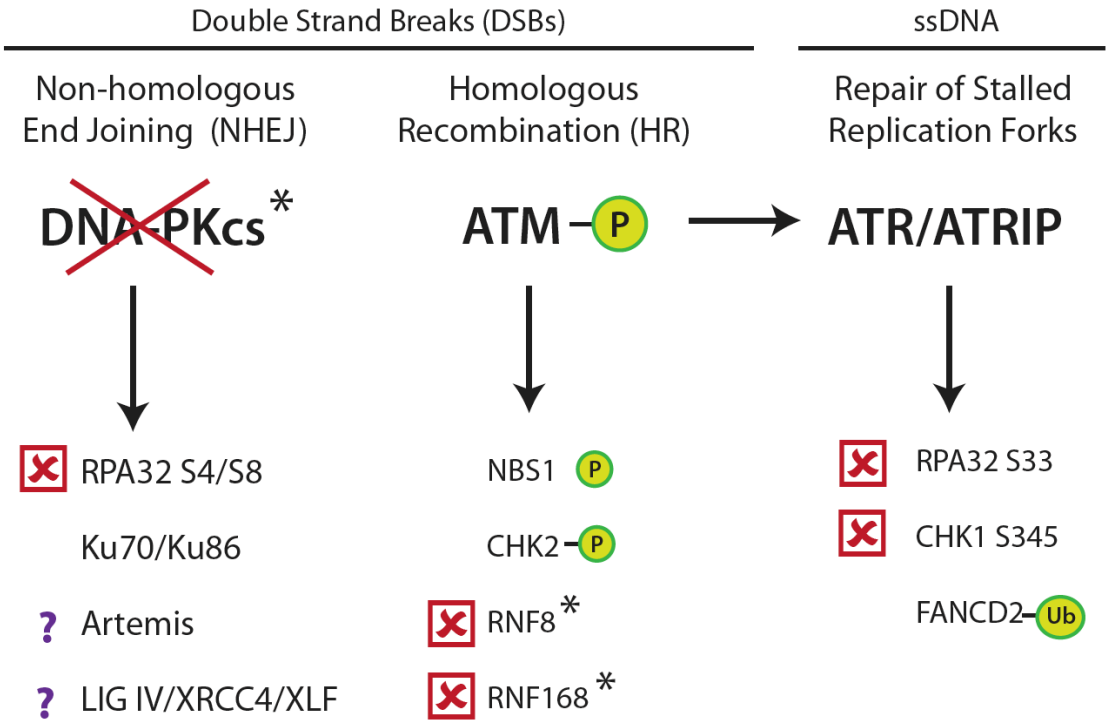

Figure 1.8. Schematic of how HSV-1 manipulates components of the cellular DNA damage response. During infection, HSV-1 inhibits phosphorylation of RPA32 S4/S8 by degrading or inhibiting DNA-PKcs in an ICP0-dependent fashion (Lees-Miller, Long et al. 1996, Wilkinson and Weller 2004, Smith, Reuven et al. 2014). Although ATM, NBS1, and CHK2 are phosphorylated during infection, the HR pathway is inhibited due to ICP0-dependent degradation of RNF8 and RNF168 (Wilkinson and Weller 2004, Lilley, Carson et al. 2005, Shirata, Kudoh et al. 2005, Lilley, Chaurushiya et al. 2010). ATR/ATRIP phosphorylation of CHK1 S345 and RPA32 S33 is inhibited; however, FANCD2 is activated by ubiquitination during HSV-1 infection (Mohni, Livingston et al. 2010, Mohni, Smith et al. 2013, Karttunen, Savas et al. 2014). Asterisk (*) indicates proteins that are degraded by ICP0.

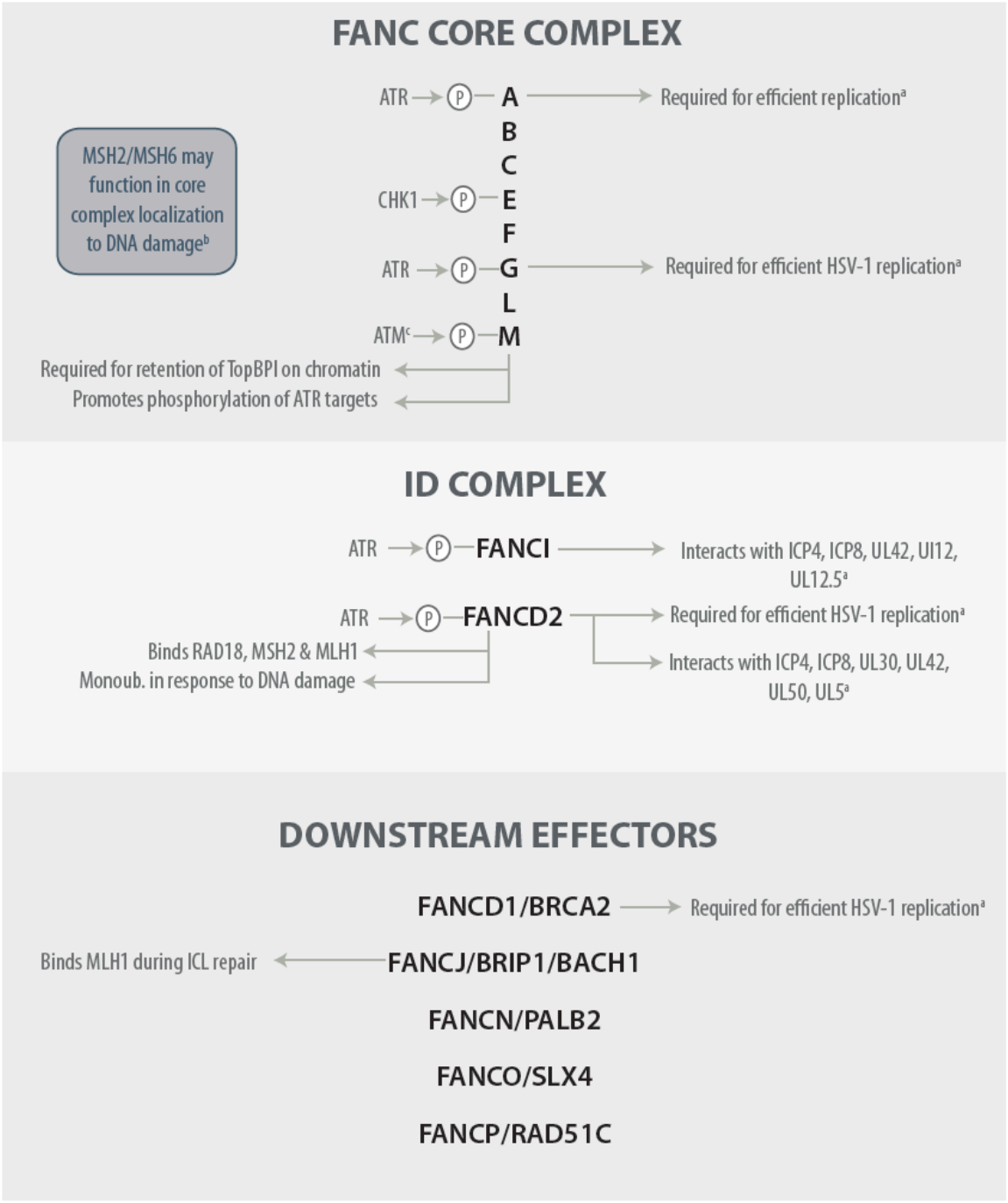

[a] Karttunen, et al., 2014;[b]Walden, 2014;[c]Sobeck, 2009
FA pathway in uninfected cells reviewed in Kupfer, 2013

Figure 1.9. Diagram of FA pathway protein functions in uninfected and HSV-1 infected cells.

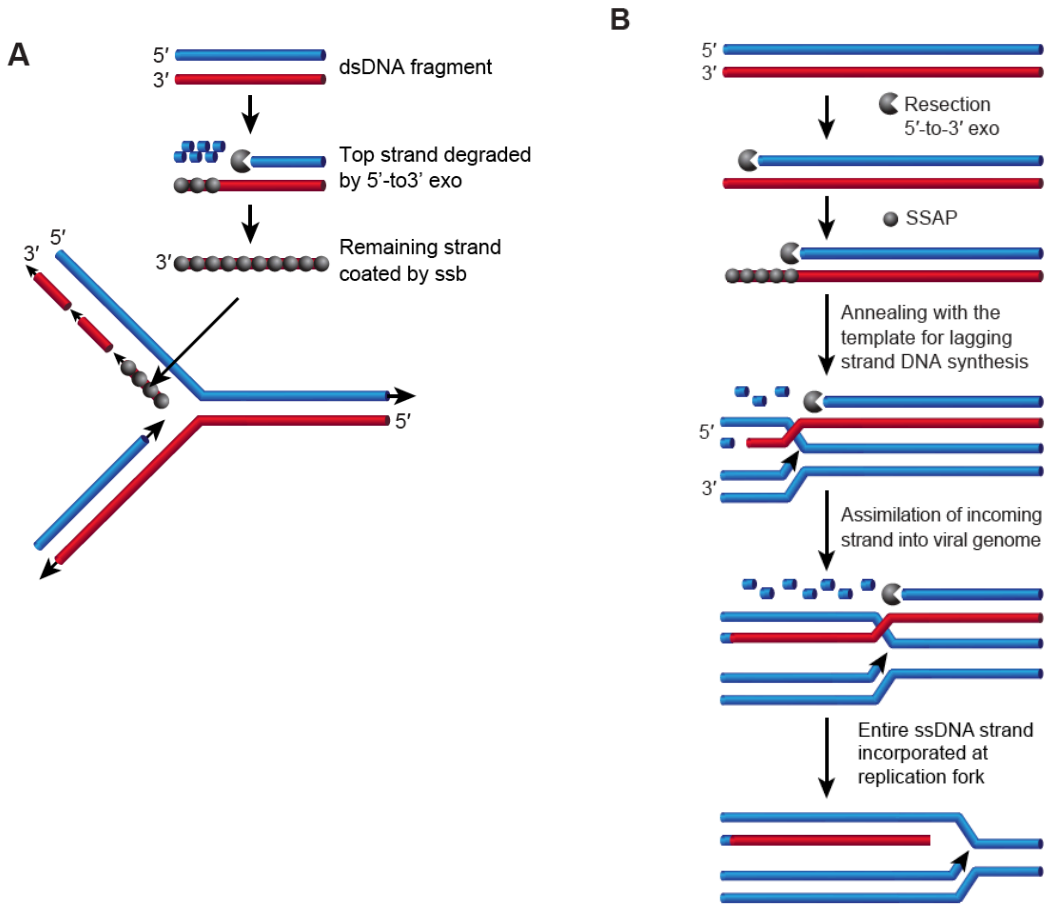

Figure 1.10. Possible SDSA strategies for recombination-dependent replication of HSV-1 DNA. A. Step-wise model for strand annealing. One entire strand of a dsDNA molecule is resected by exonuclease and the remaining strand is coated with SSAP prior to incorporation at the lagging strand of a replication fork. **B. Concerted model for strand annealing.** Resection of one strand of a long dsDNA molecule occurs concomitantly with strand annealing, resulting in incorporation of the entire strand into the lagging strand at a replication fork. This model was originally suggested by Kuzminov (1999), and adapted from Weller and Sawitzke (2014).

1.3. Thesis Objectives

The interaction between HSV-1 and the cell reflects an evolutionary tug of war in which cells have evolved antiviral mechanisms that are, in turn, counteracted by viral strategies that promote lytic infection. Because viruses rely on host cellular machinery during infection, they have evolved to usurp cellular processes. On the other hand, cells have intracellular antiviral defenses designed to fight viral infections. An important feature of the antiviral response is the cellular ability to sense viral DNA as "foreign", and components of the cellular DNA damage response (DDR) have been shown to function in this capacity. Thus, although HSV-1 may utilize some components of the DNA damage response machinery to replicate its genome, other components are antiviral, and HSV-1 has developed mechanisms to silence some DDR factors in order to avoid antiviral restriction.

In order to promote lytic infection, HSV-1 expresses IE proteins, which set the stage for viral replication by attenuating host antiviral factors and by facilitating gene expression. For example, the IE protein, ICP0, is an E3 ubiquitin ligase that promotes productive infection by targeting antiviral factors for proteasomal degradation. It is now becoming clear that, in addition to ICP0, there are other factors that influence the fate of the incoming genome by mediating DNA repair pathway choice. The viral alkaline nuclease, UL12, has been shown stimulate single strand annealing (SSA) (Schumacher, Mohni et al. 2012) and interact with cellular mediators of DDR pathway choice including the MRN complex and FANCD2 (Balasubramanian, Bai et al. 2010, Karttunen, Savas et al. 2014). The central hypothesis of this thesis is that **DDR pathway choice is essential for productive HSV-1 infection, and that UL12 acts a mediator of DDR pathway**

choice to produce DNA that is infectious and that can be packaged for productive infection.

SPECIFIC AIMS[‡]:

1) **<u>Hypothesis:</u> The molecular architecture of HSV-1 DNA affects its infectivity and its ability to induce a cellular DNA damage response.**
   a) Enzymatically manipulate HSV-1 DNA to determine structural requirements for infectivity.
   b) Determine whether 5' flapped DNA is not infectious because it triggers antiviral DNA damage response.
   c) Determine whether overexpression of ICP0 can rescue loss of infectivity of 5' flapped DNA.
   d) Determine whether infectivity of 5' flapped DNA is restored on C-NHEJ-deficient cells.

2) **<u>Hypothesis:</u> The growth defect observed in UL12-null (AN-1) infection is due to the production of aberrant DNA.**
   a) Determine whether AN-1 DNA is infectious by transfection of:
      i) Vero cells
      ii) UL12-complementing (6-5) cells.

[‡] In order to reflect the work that has been done, the aims presented here have been modified from those presented in the prospectus.

b) Determine whether AN-1 infection produces aberrant DNA on complementing cell lines.

   i) By pulsed field gel electrophoresis (PFGE)

   ii) By electron microscopy (EM)

c) Using sucrose gradient ultracentrifugation, determine whether AN-1 exhibits aberrant capsid packaging during infection of complementing cells.

3) <u>Hypothesis:</u> UL12 is required to inhibit DNA-PKcs-independent C-NHEJ.

a) Determine whether AN-1 virus yield is restored on cell lines deficient for C-NHEJ

b) Determine whether C-NHEJ is inhibited in AN-1 infected cells, compared to wild type infected cells.

CHAPTER 2

The structure of the HSV-1 genome: manipulation of nicks and gaps can abrogate infectivity and alter the cellular DNA damage response.

Samantha Smith, Nina Reuven, Kareem N. Mohni, April J. Schumacher, and Sandra K. Weller

This chapter was published in the Journal of Virology:

Smith, S., N. Reuven, K. N. Mohni, A. J. Schumacher, and S. K. Weller. 2014. Structure of the herpes simplex virus 1 genome: manipulation of nicks and gaps can abrogate infectivity and alter the cellular DNA damage response. Journal of virology 88:10146-10156.

Author contributions: N.R. performed the experiments and produced the figure for Figure 2.1. N.R. performed the experiments; S.S. performed the statistical analysis and produced the figure for Figure 2.2. N.R. performed the experiments and S.S. produced the figure for Figure 2.4. S.S. prepared the samples, A.J.S. performed the FACS analysis, and K.N.M. produced the figure Figure 2.5. S.S. prepared the samples, and K.N.M. performed the IF analysis and produced the figure Figure 2.7. All other experiments and figures were done by S.S.

2.1. ABSTRACT

The HSV-1 virion DNA contains nicks and gaps, and in this study a novel assay for estimating the size and number of gaps in virion DNA was developed. Consistent with previous reports, we estimate that there are approximately 15 gaps per genome, and we calculate the average gap length to be approximately 30 bases. Virion DNA was isolated and treated with DNA modifying enzymes in order to fill in the gaps and modify the ends. Interestingly, filling in gaps, blunting the ends, or the addition of random sequences to the 3' ends of DNA producing 3' flaps did not impair the infectivity of treated DNA following transfection of Vero cells. On the other hand, the formation of 5' flaps in the DNA following treatment resulted in a dramatic reduction (95-100%) in infectivity. Virion DNA stimulated DNA-PKcs activity in transfected cells, and DNA with 5' flaps stimulated a higher level of DNA-PKcs activity than that observed in cells transfected with untreated virion DNA. The infectivity of 5'-flapped DNA was restored in cells that do not express DNA-PKcs and in cells co-transfected with the immediate early protein, ICP0, which degrades DNA-PKcs. These results are consistent with previous reports that DNA-PK and the NHEJ repair pathway are intrinsically antiviral and that ICP0 can counteract this effect. We suggest that HSV-1 DNA with 5' flaps may induce an antiviral state due to the induction of a DNA damage response, primarily mediated by NHEJ, that renders the HSV-1 genome less efficient for lytic infection.

2.2. IMPORTANCE

For productive lytic infection to occur, HSV-1 must counteract a variety of cellular intrinsic antiviral mechanisms, including the DNA damage response (DDR).

DDR pathways have been associated with silencing of gene expression, cell cycle arrest and induction of apoptosis. In addition, the fate of viral genomes is likely to play a role in whether viral genomes adopt a configuration suitable for lytic DNA replication. This study demonstrates that virion DNA activates the cellular DDR kinase, DNA-PK, and that this response is inhibitory to viral infection. Furthermore, we show that HSV-1 ubiquitin ligase, ICP0, plays an important role in counteracting the negative effects of DNA-PK activation. These findings support the notion that DNA-PK is antiviral and suggest that the fate of incoming viral DNA has important consequences for the progression of lytic infection. This study underscores the complex evolutionary relationships between HSV and its host.

2.3. INTRODUCTION

Herpes Simplex Virus Type 1 has a double stranded linear DNA genome that is approximately 152 kbp in length. Both the replicating DNA and encapsidated viral genomes contain nicks and gaps (Kieff, Bachenheimer et al. 1971, Frenkel and Roizman 1972, Gordin, Olshevsky et al. 1973, Sheldrick, Laithier et al. 1973, Wilkie 1973, Biswal, Murray et al. 1974, Hirsch, Roubal et al. 1976, Jacob and Roizman 1977). In DNA isolated from virions, gaps have been reported to number 3-13 per genome (Ben-Porat and Rixon 1979, Sinden, Pettijohn et al. 1982). These gaps are randomly located, and are present on both strands (Kieff, Bachenheimer et al. 1971, Wilkie 1973, Hyman, Oakes et al. 1977). Little is known about how nicks and gaps arise, and it is anticipated that the study of nicks and gaps in the HSV genome may provide insight into host responses to incoming viral genomes and the mechanism of HSV-1 replication.

At the earliest stages of HSV infection, the viral genome is released from the capsid into the nucleus, where it becomes associated with a combination of viral and cellular proteins. Some of these proteins are factors utilized by the virus to initiate a robust program of viral gene expression and DNA synthesis, while others are now recognized for their ability to mount an intrinsic antiviral response. Several intrinsically antiviral pathways that act to silence viral gene expression have been identified, including: PML and other components of ND10 (Everett, Parada et al. 2008, Lukashchuk and Everett 2010), the interferon-inducible DNA sensor, IFI16 (Orzalli, DeLuca et al. 2012, Johnson, Chikoti et al. 2013, Pham, Kwon et al. 2013), and components of the DNA damage response (Lees-Miller, Long et al. 1996, Parkinson, Lees-Miller et al. 1999, Lilley, Chaurushiya et al. 2010, Lilley, Chaurushiya et al. 2011). HSV must counteract these intrinsically antiviral pathways to establish an environment conducive to lytic infection.

The cellular DNA damage response (DDR) is mediated by three phosphatidyl inositol 3-kinase-like serine/threonine protein kinases (PIKKs): DNA-PK (DNA-dependent protein kinase), ATM (Ataxia-telangiectasia mutated), and ATR (ATM and Rad3 related) (Abraham 2004, Cimprich and Cortez 2008, Ciccia and Elledge 2010). The DNA-PK complex, comprised of DNA-PKcs and the Ku70/Ku80 heterodimer, responds to double strand breaks and stimulates repair via non-homologous end joining (NHEJ) (Ciccia and Elledge 2010). ATM is activated by double strand breaks and stimulates repair via homologous recombination (HR) and single strand annealing (SSA). ATR is activated by stalled replication forks and stretches of ssDNA adjacent to dsDNA (Ciccia and Elledge 2010). DNA repair proteins play both positive and negative roles during

HSV infection, and HSV manipulates components of these pathways, activating some and disabling others (Lees-Miller, Long et al. 1996, Parkinson, Lees-Miller et al. 1999, Taylor and Knipe 2004, Wilkinson and Weller 2004, Lilley, Carson et al. 2005, Shirata, Kudoh et al. 2005, Muylaert and Elias 2007, Gregory and Bachenheimer 2008, Mohni, Livingston et al. 2010, Lilley, Chaurushiya et al. 2011, Mohni, Mastrocola et al. 2011, Mohni, Dee et al. 2013).

The incoming viral genome with double strand ends, nicks and gaps may be expected to be recognized by the cellular DDR and activate one or more of the DNA damage sensing kinases. Activation of a DNA damage response can initiate cell cycle arrest, gene silencing, and apoptosis, any of which could negatively impact the viral life cycle by suppressing viral gene expression and virus production. It is also possible that some DDR pathways may result in "repair" of DNA in a manner that is not consistent with lytic infection. In HSV-infected cells, several DNA damage-sensing elements are either degraded or their signaling is blocked. For instance, the immediate early protein ICP0 is a major player in counteracting cellular antiviral mechanisms by degrading antiviral proteins such as DNA-PKcs (Lees-Miller, Long et al. 1996, Parkinson, Lees-Miller et al. 1999). Interestingly, ICP0 is also a component of the viral tegument and is thus present at the earliest stages of viral infection even before immediate early protein synthesis (Yao and Courtney 1992, Loret, Guay et al. 2008, Delboy, Siekavizza-Robles et al. 2010). ATR-mediated phosphorylation of downstream targets, RPA and Chk1, is also inhibited by three hours post infection (Shirata, Kudoh et al. 2005, Wilkinson and Weller 2006, Mohni, Livingston et al.). Thus it appears that HSV has evolved to inactivate

several DDR elements that may recognize the unusual structure of the incoming viral genome.

In this paper we have explored the role of virion DNA in the activation of DDR kinases in the absence of the tegument using transfection-based assays. Virion DNA was treated with enzymes that would be expected to fill in gaps, extend 3' ends, ligate nicks, cleave regions of single stranded DNA or result in 5' flaps. These treatments were used to confirm the presence of approximately 15 gaps per viral genome. We were also able to estimate the average gap length to be approximately 30 bases. Virion DNA that had been enzymatically modified was tested for infectivity by transfection. Although many of the treatments did not affect infectivity, strand displacement synthesis resulting in 5' flaps and endonucleolytic digestion of ssDNA caused significant decreases in infectivity. Virion DNA containing 5' flaps activated robust DNA-PKcs activity that also correlated with the dramatic loss of infectivity. This suppression could be rescued by genetic deletion of DNA-PKcs or cotransfection with ICP0. These results are consistent with previous reports that DNA-PKcs represents a cellular antiviral response to infection.

2.4. MATERIALS AND METHODS

2.4.a. Cell lines.

Vero cells and HCT-116 cells were obtained from American Type Culture Collection (ATCC), and the derivative DNA-PK$^{-/-}$ cell line was generously provided by Eric A. Hendrickson (University of Minnesota Medical School, Minneapolis, MN), and has been previously described (Ruis, Fattah et al. 2008). Vero cells were grown in Dulbecco's modified minimal essential medium (DMEM) (Gibco) containing 5% fetal

bovine serum (FBS). HCT-116 cells and DNA-PK$^{-/-}$ cells were grown in McCoy's 5A medium (modified) (Gibco) containing 10% FBS.

2.4.b. Viruses and plasmids.

The KOS strain of HSV-1 was used as the wild-type virus. The recombinant virus, KOS-CMVGFP, contains the GFP gene under the control of the human cytomegalovirus (HCMV) promoter (2.0kbp insertion) in the intergenic region between UL26 and UL27 genes (Balliet, Kushnir et al. 2007). Wild type ICP0 (pCI-110) and ICP0 ΔRING-Finger (pCI-FXE) were generously provided by Roger Everett (MRC Virology Unit, Glasgow, Scotland).

2.4.c. Preparation of viral DNA.

Virion DNA was isolated as previously described (Goldstein and Weller 1988). Approximately 1 X 10^8 Vero cells were infected with KOS at a low m.o.i. (0.1-0.5). When maximum cytopathic effects were observed, infected cells were harvested by scraping and spun down at 1500rpm for 15 minutes at 4°C. Supernatant was removed and stored at 4°C for later use. The cell pellet was then resuspended in 3mL of cold 1X RSB, and incubated on ice for 10 minutes. Cells were then disrupted by dounce homogenization. Cell debris and nuclei were then removed by centrifugation, 1500 rpm for 10 minutes at 4°C. The supernatant was combined with the first supernatant and centrifuged, 9000 rpm for 60 minutes at 4°C. Virions were resuspended in 5 ml of TNE (10 mM Tris-Cl [pH 7.4], 10 mM NaCl, 30 mM $MgCl_2$,) and frozen at -80°C. Virions were thawed and SDS and Proteinase K were added to final concentrations of 1% and

100 μg/ml, respectively. The tube was gently inverted and then incubated for 5 hours at 37°C. Then DNA was either dialyzed overnight at 4°C against 1 L TE (10 mM Tris-Cl [pH 7.5], 1 mM EDTA, or DNA was gently extracted by phenol:chloroform:isoamyl alcohol (25:24:1), and precipitated by either adding 0.6 volumes of 20% polyethylene glycol 8000 (PEG 8000)- 2 M NaCl or by ethanol precipitation. DNA was incubated one hour on ice, and then centrifuged for 15 minutes at 20,000 x *g*. The pellet was washed with 70% ethanol, dried briefly, and resuspended in TE. The DNA was aliquoted and stored at -80°C.

2.4.d. Enzymes.

The Klenow Fragment of *E. coli* DNA polymerase I was from Boehringer Mannheim or New England Biolabs (NEB). T4 DNA polymerase, terminal transferase (TdT), calf intestine alkaline phosphatase (CIP), and mung bean nuclease were from NEB. T4 DNA ligase was from NEB or Invitrogen.

2.4.e. In vitro modification of virion DNA.

Virion DNA (200 ng, 2 fmol) was incubated with polymerases and other enzymes in a 25 μl reaction volume for 30 minutes, unless otherwise indicated. For reactions with Klenow polymerase and T4 DNA ligase, a buffer containing 10 mM Tris-Cl (pH 7.5), 5 mM $MgCl_2$, 7.5 mM dithiothreitol (DTT) was used. The manufacturer-supplied buffer (NEB) was used for reactions containing T4 polymerase, TdT, mung bean nuclease, and CIP. ATP was used at 1mM with T4 DNA ligase and CIP, unless otherwise noted, and

deoxynucleoside triphosphates (dNTPs) were used at 0.5mM where indicated. When different buffers were used, no-enzyme controls were run using the same buffer.

2.4.f. Measurement of nucleotide incorporation into DNA.

The incorporation of labeled nucleotides was performed using Klenow polymerase, T4 polymerase, and T4 DNA ligase (reactions described above) with [α^{32}P] dCTP included in the dNTP mixture. Reactions were incubated at 37°C for the times indicated in the figures, and stopped by adding 5 μl of 6X gel loading buffer (50% glycerol, 1 %SDS, 50 mM EDTA, 0.2% bromphenol blue). Half (15 μl) of each sample was loaded onto a 0.7% agarose TAE (0.04 M Tris-acetate, 0.001M EDTA) gel. The gel was dried onto DE81 paper (Whatman) and exposed to phosphorimager screens (National Diagnostics). Dilutions of the dNTP mix were spotted onto paper and exposed to the phosphorimager screen along with the gel in order to aid in the quantification of the amount of label incorporated. The ImageQuant version 5.0 software package was used for quantification of the results. Each time point was repeated independently at least three times. Adobe Photoshop (v.7.0) and Adobe Illustrator (v. 10) were used in preparation of the figures.

2.4.g. Calculation of gap number and length.

The incorporation of nucleotides by Klenow/ligase into 1 fmol of HSV genomes in a 40 minute incubation was compared to the incorporation into the same amount of DNA by Klenow fragment alone, 500 fmol and 3500 fmol, respectively. The number of gaps per genome was calculated by dividing the difference in incorporation between

Klenow alone and T4 pol, by the average length of Klenow strand-displacement (200 nucleotides [nt]):

$$\text{Gap number} = (\text{Incorporation}_{\text{Klenow}} - \text{Incorporation}_{\text{T4 pol}}) \div 200 \quad \textbf{(Equation 1)}$$

$$\text{Average gap length} = \text{Incorporation}_{\text{T4 pol}} \div \text{Gap number} \quad \textbf{(Equation 2)}$$

2.4.h. Infectivity assays.

Reactions were prepared and incubated as described above, without the labeled nucleotide. All cell types were transfected using Lipofectamine Plus reagent (Invitrogen) according to the manufacturer's suggested protocol. Vero cells at 50-70% confluence were transfected with incorporation products at a concentration of 200ng DNA/60mm dish. Samples were overlaid with DMEM containing 2% methylcellulose at 17-20 hours post-transfection. Plaques were fixed and stained with crystal violet four to five days later and plaques were counted. HCT-116 and DNA-PK$^{-/-}$ cells at 70% confluence were transfected with purified HSV DNA at a concentration of 0.5μg DNA/35mm dish. Samples were harvested at 48 hours following transfection and titrated on Vero cells. For co-transfection experiments, HCT-116 cells were plated on 35mm dishes at 70% confluence and transfected with 0.5μg of viral DNA and 1μg of plasmid DNA. Virus was collected at 48 hours following transfection and viral yield was determined by titration on Vero cells.

2.4.i. Pulsed-field gel electrophoresis.

Agarose gels were prepared using 1% pulsed-field gel-grade agarose (Bio-Rad) in 0.5X TBE buffer. Samples were diluted in 6X gel loading dye (NEB) and loaded directly into the wells. Electrophoresis was performed using a CHEF-DR III apparatus (Bio-Rad) with 0.5X TBE (45 mM Tris, 45 mM borate, 1 mM EDTA, pH 8.3) running buffer. Samples were separated using 6 V/cm (approximately 200V) for 24 h at 14 °C. Switch times ramped from 1 to 25 seconds. Lambda Ladder PFG Marker (NEB) and Vero cells infected with HSV-1 were used as size standards. Gels were stained with ethidium bromide, photographed, and were transferred by Southern blotting to GeneScreen Plus membranes (Dupont NEN) according to manufacturer's protocols. Membranes were probed with CDP-Star biotin detection reagent (NEB) and imaged using a ChemiDoc MP Imaging System (Bio-Rad).

2*.4.j. Western blot analysis.*

Vero cells were transfected with 2.5μg of untreated, Klenow-treated, or Klenow/ligase-treated infectious DNA (prepared as described above) per dish. Lipofectamine 2000 Reagent (Invitrogen) was used at a concentration of 10μL per transfection, as described by the manufacturer. Samples were harvested 24 hours following transfection and prepared for western blot analysis as previously described (Mohni, Dee et al. 2013). The primary antibodies used were mouse monoclonal anti-RPA32 (9H8) (1:1,000; GeneTex), polyclonal rabbit anti-phospho-RPA S33 (1:3,000; Bethyl), polyclonal rabbit anti-phospho-RPA S4/S8 (1:3,000; Bethyl), monoclonal mouse

anti-ICP0 5H7 (1:5,000; EastCoast Bio), monoclonal mouse anti-Ku70 Ab-4 (N3H10) (1:1,000; Neomarkers). Western blots were quantified using ImageJ software.

2.4.k. Gene expression assay.

Vero cells were transfected with modified KOS-GFP DNA. Samples were fixed with 4% paraformaldehyde at 24 hours post transfection and resuspended in PBS EDTA (5 mM). GFP-positive cells were measured using flow cytometry using a BD LSR II and analyzed using FlowJo software.

2.4.l. Immunofluorescence (IF).

IF analysis was performed as described previously (Livingston, DeLuca et al. 2008, Mohni, Mastrocola et al. 2011). Briefly, cells adhered to glass coverslips were washed with PBS, fixed with 4% paraformaldehyde, and permeabilized with 1% Triton X-100. Cells were blocked in 3% normal goat serum and reacted with antibodies as indicated below. Primary antibodies included monoclonal mouse anti-ICP0 5H7 (1:200; EastCoast Bio), and polyclonal rabbit anti-phospho-RPA32 S4/S8 (1:200; Bethyl Laboratories). Alexa Fluor secondary antibodies (1:200; Molecular Probes) were used with fluorophores excitable at a wavelength of 488, and 594 nm. Images were captured using a Zeiss LSM 510 confocal nonlinear optical (NLO) microscope equipped with argon and HeNe lasers and a Zeiss 63X objective lens (numerical aperture, 1.4). Images were processed and arranged using Adobe Photoshop CS3 and Illustrator CS3.

2.5. RESULTS

2.5.a. In vitro modification of HSV-1 DNA.

The HSV genome is packaged as a linear, double stranded DNA molecule that contains nicks and gaps. This unusual structure prompted us to ask how the presence of nicks and gaps might influence early steps in viral infection particularly with respect to host factors that respond to incoming DNA. HSV-1 DNA, purified from virions, is capable of initiating a productive infection in transfected cells. Transfection experiments thus permit us to explore the infectivity of virion DNA in the absence of tegument proteins that may act to promote or disable host factors responding to incoming viral genomes. To better understand how the structural attributes of virion DNA affect infectivity and host responses, DNA isolated from virions was enzymatically modified *in vitro* prior to transfection.

We first sought to confirm the presence of gaps in purified HSV DNA and to demonstrate that gaps could be repaired *in vitro* using a gap-filling polymerase. Purified DNA was treated with the Klenow fragment of *E. coli* DNA polymerase I, which was expected to recognize free 3' termini and incorporate nucleotides thereby filling in gaps. In a control reaction, virion DNA was denatured and primed with random hexamers. Figure 1A shows that labeled nucleotides incorporated into the boiled and random-primed DNA migrated as a smear (left side panels); whereas, nucleotides incorporated into virion DNA migrated primarily as a single species. The extent of incorporation was quantified and displayed in the graph shown in Figure 1B. Incorporation of label into non-denatured virion DNA reached a plateau after 5-10 minutes of incubation, indicating that the gaps in this DNA substrate had been filled. It is unlikely that the plateau is due to

inactivation of the enzyme or an exhaustion of the dNTPs, as the incorporation into the random-primed sample continues to be linear and does not reach a plateau in the same time frame.

2.5.b. Klenow polymerase strand-displacement activity can be used to measure gap number and length.

In order to measure the gap number and length of virion DNA, we compared nucleotide incorporation using DNA polymerases with different biochemical properties. The Klenow fragment of DNA polymerase I extends 3' termini at gaps, and is also capable of strand displacement synthesis. Because Klenow lacks 5'-3' exonuclease activity, nucleotides are displaced from the template ahead of the growing chain but are not cleaved, resulting in a 5' flap. T4 polymerase, on the other hand, does not possess strand displacement activity, and dissociates from the DNA template when it reaches the end of a gap (Panet, van de Sande et al. 1973). In addition, treatment with Klenow and T4 DNA ligase together prevents strand displacement synthesis because under these conditions, once Klenow has filled in the gap, the 3' terminus of the newly synthesized fragment is ligated to the 5' terminus of the adjacent strand.

Figure 2 shows the incorporation of labeled nucleotides into HSV DNA by Klenow polymerase alone, Klenow and ligase together, or the T4 DNA polymerase. While all three reactions reach a plateau, Klenow incorporates approximately 7-fold more label than the other two reactions. This is consistent with the known ability of Klenow to carry out strand displacement synthesis. On the other hand the inability of T4 DNA polymerase and Klenow/ligase to perform strand displacement synthesis is consistent

with the lower levels of incorporation observed for these conditions.

We took advantage of the known biochemical properties of T4 DNA ligase and Klenow polymerase to measure the number and length of gaps in HSV-1 DNA using Equation 1, as described in Materials and Methods. The difference in incorporation between Klenow treatment versus Klenow/ligase treatment (3000 fmol) represents the "extra" incorporation by Klenow resulting from strand displacement. Klenow polymerase is known to displace approximately 200 bases before it dissociates from a DNA template (Davey and Faust 1990, Kong, Kucera et al. 1993). To estimate the number of invasions, and consequently, the number of gaps, the value for "extra" incorporation was divided by 200. According to this calculation, the number of gaps in the HSV-1 genome is 15, which is comparable to previous determinations of 3-13 gaps per genome (Ben-Porat and Rixon 1979, Sinden, Pettijohn et al. 1982). Furthermore, using Equation 2, the average gap size is calculated to be 33 nucleotides.

The conditions under which the ligation was performed (low DNA concentration, high concentration of ligase at 37°C for 20 min) support complete sealing of the nicks, but are unlikely to result in any end-to-end ligation of molecules. In order to verify that the ends of the HSV-1 DNA were not ligated during the reaction, products were separated by pulsed-field gel electrophoresis. The untreated HSV-1 DNA migrates as a linear 152 kb monomer on this gel (Fig. 3, lane marked NT). After treatment with Klenow or Klenow/ligase together (Fig. 3, lanes marked K and KL, respectively) the DNA is still monomeric length, and no higher molecular weight species were observed, indicating that the ligase did not produce concatemers or circles. Species that are shorter than monomeric length were observed in all lanes, indicating that a portion of the DNA

was sheared. Since fragmentation is more noticeable in the untreated sample, it is likely that the nicked DNA was more vulnerable to breakage than DNA that had been repaired.

2.5.c. Filling in nicks and gaps does not affect infectivity.

The incorporation studies demonstrated that virion HSV-1 DNA contained gaps that were readily filled using purified DNA polymerases. We next asked whether the changes in DNA structure, made *in vitro,* affected the infectivity of the modified DNA, as measured by a plaque assay following transfection. Plaque numbers for the control DNA were in the range of 50-150 per 60 mm dish. Treatment of the DNA with T4 DNA ligase did not affect infectivity (Fig. 4). Likewise, DNA that was filled in and ligated by treatment with Klenow/ligase was fully infectious. This indicates that, at least in the context of transfection, gaps and nicks are not required for infectivity. Filling in nicks and gaps also did not potentiate the infection, as percent infectivity was similar to that of the untreated control.

2.5.d. Treatment with mung bean nuclease destroys infectivity, confirming the presence of gaps.

Infectivity was completely eliminated when HSV-1 DNA was incubated with mung bean nuclease, an endonuclease that degrades ssDNA (Fig. 4). This result confirms the presence of gaps in virion DNA, since digestion of the ssDNA at gaps would fragment the genome and abolish infectivity. On the other hand, virion DNA that had been treated with Klenow/ligase and then incubated with an excess of mung bean nuclease retained its infectivity. HSV has been reported to contain complementary single

3’ nucleotide overhangs at both ends (Mocarski and Roizman 1982, Davison and Rixon 1985). Treatment with mung bean nuclease following repair with Klenow/ligase would be expected to blunt the ends of the HSV genome by removing overhangs. These overhangs have been suggested to facilitate end ligation and contribute to circularization of the genome prior to replication (Strang and Stow 2005). The observation that HSV-1 DNA was still infectious after this treatment confirms that Klenow/ligase can fill in gaps and that 3’ overhangs are not required for infectivity.

2.5.e. Treatment with calf intestine alkaline phosphatase is tolerated.

End ligation and circularization of DNA would be expected to require the presence of a 5’ phosphate. In order to determine whether 5’ phosphates on viral DNA are required for infectivity, HSV-1 DNA was treated with calf intestine phosphatase. This treatment has no effect on infectivity, suggesting that incoming DNA does not need to be end-ligated (Fig. 4). We cannot, however, rule out the possibility that cellular kinases could re-phosphorylate viral DNA.

2.5.f. Virion DNA with 3’ flaps retains infectivity.

To further analyze the effects of *in vitro* modification on infectivity of virion DNA, we tested the effect of random 3’ tails added onto the DNA by terminal transferase (TdT). Treatment with TdT acts in a template-independent manner to catalyze the addition of deoxynucleotides to an available 3’ terminus. We used terminal transferase to add tails, which were approximately 100-300 nucleotides in length, onto the HSV-1 DNA (Roychoudhury, Jay et al. 1976, Tu and Cohen 1980, Chang and Bollum 1986, Boule,

Rougeon et al. 2001). Despite the fact that the 3' additions were random, and therefore non-homologous, these additions had no effect on the infectivity of the DNA (Fig. 4).

2.5.g. Treatment with Klenow polymerase abolishes infectivity.

Interestingly, DNA treated with Klenow alone produced only 0-10% of the number of plaques seen with untreated DNA (Fig.4). In the absence of nucleotides, Klenow treatment had no effect on infectivity demonstrating that incorporation of nucleotides into viral DNA was necessary for the loss of infectivity. In addition, if Klenow was prevented from generating 5' flaps by co-incubation with T4 DNA ligase, infectivity was not impaired. Thus the dramatic decrease in infectivity with Klenow-treated DNA was only seen when strand displacement synthesis was allowed. Since strand displacement synthesis is believed to result in the formation of 5' flaps, these results suggest that 5' flaps are responsible for the lack of infectivity of Klenow-treated DNA.

The drastic reduction in infectivity after Klenow treatment was not expected, and we were interested to determine its cause. To rule out the possibility that Klenow-treatment caused a reduction in transfection efficiency and thus reduced the number of genomes entering the nucleus, we measured gene expression from DNA that had been treated with either Klenow or Klenow/ligase. Virion DNA was prepared from cells that had been infected with a GFP-expressing virus and used to transfect Vero cells in the presence of PAA to prevent viral replication. Thus, gene expression is expected to originate only from input genomes, allowing for a direct comparison between treated and untreated virion DNA. GFP-positive cells were analyzed by fluorescence-activated cell

sorting (FACS). GFP expression was detected in cells transfected with untreated, Klenow-treated, or Klenow/ligase-treated KOS-GFP DNA. Figure 5 depicts histograms showing the distribution of GFP intensity plotted against the number of GFP-positive cells. These data indicate that transfection efficiencies are similar between treated and untreated samples, and that the loss of infectivity associated with Klenow treatment is not caused by differences in transfection efficiency.

2.5.h. Co-transfection of ICP0 with untreated and Klenow-treated HSV-1 DNA dramatically improves infectivity.

Co-transfection of ICP0 with infectious DNA has previously been shown to enhance plaque formation in Vero and U20S cells (Yao and Schaffer 1995). We were interested to see whether ICP0 could boost infectivity in cells transfected with Klenow-treated DNA. HCT-116 cells were co-transfected with wild-type or mutant ICP0, and purified HSV-1 DNA that was either untreated or treated with Klenow. The ICP0 mutant lacked the RING-finger domain (ICP0-FXE). Expression of wild-type ICP0 dramatically increased viral yield from Klenow-treated DNA by more than 3 orders of magnitude compared to co-transfection of an empty vector with Klenow-treated DNA (Table 1). Consistent with previous findings (Yao and Schaffer 1995), co-transfection with wild-type ICP0 also improved the infectivity of untreated virion DNA, although to a lesser extent. There was also a modest effect on the infectivity of both the untreated and Klenow-treated DNA when co-transfected with ICP0-FXE. This may be due to other functions of ICP0 that are unrelated to its ubiquitin-ligase activity. Similar results were also observed in Vero cells (data not shown). These results confirm that ICP0 expression

improves the infectivity of purified HSV-1 DNA. Interestingly, the presence of ICP0 is able to overcome the loss-of-infectivity exhibited by Klenow-treated virion DNA containing 5' flaps. Although it is unknown whether 5' flaps arise during HSV infection, it has been shown that replicating viral DNA adopts complex structures (Severini, Morgan et al. 1994, Severini, Scraba et al. 1996), and these structures may include 5' flaps.

2.5.i. HSV-1 DNA stimulates RPA32 phosphorylation in transfected cells, but not infected cells.

Since HSV virion DNA is linear, it has ends that may be recognized as double strand breaks by DNA-PK. Furthermore, it is possible that gaps in HSV DNA or other unusual structures could mimic the substrates that activate ATR (ssDNA adjacent to dsDNA). Therefore, the structure of the viral genome might be expected to result in activation of both ATR and DNA-PK. We have, however, previously reported that RPA, which is a target for phosphorylation by both kinases, is not phosphorylated during HSV infection (Wilkinson and Weller 2004, Mohni, Dee et al. 2013). HSV inactivates components of both NHEJ and HR pathways through the action of ICP0. As an immediate early protein, ICP0 is expressed very early in infection, but it is also present in the tegument of the incoming virion (Yao and Courtney 1992, Loret, Guay et al. 2008, Delboy, Siekavizza-Robles et al. 2010), potentially entering the nucleus at the time of DNA entry. These observations led us to examine whether virion DNA could induce DNA-PK and ATR kinase activity in transfected cells in which ICP0 and other viral proteins are not present. The cellular single-strand DNA-binding protein, replication protein A (RPA), is a well-known downstream target of both DNA-PKcs and ATR in

response to DNA damage (Anantha, Vassin et al. 2007). The S33 residue of the middle subunit, RPA32, is specifically phosphorylated by ATR (Vassin, Anantha et al. 2009), while the S4/S8 residues of RPA32 are phosphorylated by DNA-PK (Zernik-Kobak, Vasunia et al. 1997, Shao, Cao et al. 1999, Wang, Guan et al. 2001, Anantha, Vassin et al. 2007).

In uninfected Vero cells treated with UV, RPA32 is phosphorylated by DNA-PK and ATR, as detected using specific antibodies for phospho-RPA32 S4/S8 and phospho-RPA32 S33, respectively (Fig. 6). Consistent with our previous findings, no phosphorylated RPA was detected in HSV-infected cells (Fig. 6) (Wilkinson and Weller 2004, Wilkinson and Weller 2005, Mohni, Dee et al. 2013). On the other hand, phospho-RPA32 S4/S8 was detected in cells transfected with purified virion DNA demonstrating that DNA-PK is activated under these conditions (Fig. 6). Interestingly, phospho-RPA32 S33 was not detected, suggesting that incoming virion DNA is not a suitable substrate for ATR activation (Fig. 6).

The observation that DNA-PK is not activated in infected cells is consistent with the known ability of ICP0 to degrade DNA-PKcs at least in some cell types (Lees-Miller, Long et al. 1996, Parkinson, Lees-Miller et al. 1999, Davido, Von Zagorski et al. 2003, Lin, Noyce et al. 2004). Interestingly however, DNA-PKcs is not degraded in HSV-infected Vero cells (Wilkinson and Weller 2004), raising the possibility that DNA-PK might be inhibited by a mechanism other than degradation. Vero cells were transfected with ICP0 or an ICP0 RING-finger mutant (ICP0-FXE), which lacks ubiquitin ligase activity, UV-irradiated and analyzed by immunofluorescence with antibodies specific for ICP0 and pRPA-S4S8. Cells expressing ICP0 failed to induce RPA32 S4/S8

phosphorylation after UV damage, as there was no pRPA32 S4/S8 staining in cells that were positive for ICP0 expression (Fig. 7, top panel). Conversely, pRPA32 S4/S8 was observed in cells expressing ICP0-FXE, suggesting that the ubiquitin ligase activity of ICP0 is required for inhibition of RPA S4/S8 phosphorylation (Fig. 7, bottom panel). Thus, ICP0 is able to inhibit DNA-PK-dependent signaling, even in cell types in which DNA-PKcs is not degraded. These observations suggest that either ICP0 degrades another protein necessary for activation of DNA-PKcs, or that ubiquitination of DNA-PKcs is inhibitory even without degradation.

2.5.j. Addition of 5' flaps to virion DNA increases hyper-phosphorylation of RPA32.

We were intrigued by the dramatic loss of infectivity observed with the Klenow-treated DNA, and by the ability of ICP0 to rescue infectivity (Table 1, above). We hypothesized that DNA with 5' flaps may activate a more robust cellular DNA damage response than wild-type HSV-1 DNA. Given previous reports that DNA-PK is antiviral, we wanted to test the possibility that loss of infectivity may correlate with a robust DNA damage response. Therefore, we asked whether modifications to virion DNA could alter the DDR following transfection. Vero cells were transfected with virion DNA that was either untreated, Klenow-treated (containing 5' flaps), or treated with Klenow/ligase (filled-in and ligated). Untreated transfected DNA stimulated RPA32 S4/S8 phosphorylation, and Klenow/ligase-treated DNA exhibited a similar level of RPA32 S4/S8 phosphorylation as the untreated sample. Interestingly, Klenow-treated DNA elicited a greater pRPA S4/S8 signal than either the untreated and filled-in sample, perhaps due to the 5' flaps produced by Klenow treatment (Fig. 8).

2.5.k. Infectivity of Klenow-treated DNA is restored in the absence of DNA-PKcs.

As described above, virion DNA treated with Klenow polymerase exhibited a marked decrease in infectivity and increased levels of pRPA32 S4/S8 phosphorylation. Since pRPA32 S4/S8 is a substrate of DNA-PKcs, we wanted to determine if DNA-PKcs itself was responsible for the reduced virus yield seen with Klenow treated DNA. HCT-116 (wild-type) and DNA-PKcs$^{-/-}$ cells were transfected with untreated or Klenow-treated DNA, and infectivity was measured. Infectivity of Klenow-treated DNA in transfected HCT-116 cells was about 11% of untreated DNA in transfected HCT-116 (Fig. 9). This is a similar decrease to that observed when Klenow-treated DNA was compared to untreated DNA in transfected Vero cells (Fig. 4). In DNA-PKcs$^{-/-}$ cells transfected with Klenow-treated DNA, however, infectivity was 100% compared with untreated DNA in transfected DNA-PKcs$^{-/-}$ cells (Fig. 9). This suggests that DNA-PKcs plays a role in the loss of infectivity phenotype observed in wild-type cells.

2.6. DISCUSSION

2.6.a. Summary.

The results presented in this paper confirm that HSV-1 virion DNA has an unusual structure, containing multiple nicks and gaps. Virion DNA was treated with various combinations of enzymes that fill in gaps, ligate nicks, create 3' and 5' flaps, blunt the ends and fragment the genome at sites of ssDNA. Untreated virion DNA was as infectious as DNA whose nicks and gaps were filled in and ligated, suggesting that nicks and gaps are not required for virion DNA to be infectious. Other treatments including blunting of the termini, removal of 5' phosphates and production of 3' flaps are also tolerated. On the other hand, the formation of 5' flaps in the DNA following treatment with Klenow alone resulted in a dramatic reduction (95-100%) in infectivity. Untreated virion DNA was able to activate DNA-PK activity in transfected cells, a somewhat surprising result considering that DNA-PK is not activated in HSV-infected cells, even at early times post infection. Interestingly, virion DNA with 5' flaps stimulated an even more robust activation of DNA-PK, compared with untreated virion DNA. Infectivity of Klenow-treated DNA was restored in cells that do not express DNA-PK, and in cells co-transfected with the immediate early protein ICP0, which is known to degrade DNA-PKcs. Thus, we suggest that virion DNA with 5' flaps induces an antiviral state that is dependent on DNA-PK, and which can be suppressed by ICP0.

In this report we have used DNA with 5' flaps to explore how the cell responds to an unusual DNA structure. Although 5' flaps are unlikely to be present in virion DNA, the mechanisms of HSV DNA replication are poorly understood. Furthermore, it is clear that unusual and complex structures containing X and Y junctions arise in

infected cells, and it is thus possible that 5' flaps may arise during replication. We have been particularly interested in whether cells respond to unusual viral DNA conformations by signaling a damage response that could be antiviral. For instance the DDR response may silence or degrade viral DNA.

Using a novel assay based on the biochemical properties of the Klenow polymerase, we were also able to estimate that virion DNA contains on average 15 gaps per genome, consistent with published observations (Ben-Porat and Rixon 1979, Sinden, Pettijohn et al. 1982). The presence of gaps in virion DNA might have been expected to activate the ATR kinase; however, ATR signaling was not activated in cells transfected with virion DNA. It has been reported that ATR activation requires a stretch of ssDNA capable of binding at least two consecutive RPA complexes (approximately 65 nucleotides) (Blackwell and Borowiec 1994, Wold 1997). In this paper, we estimated that the average size of gaps in virion DNA was approximately 33 nucleotides, long enough bind a single RPA complex, but too short to activate ATR signaling. Thus, the incoming genome does not appear to be a suitable substrate for ATR activation.

The presence of nicks and gaps in HSV virion DNA has interesting implications for early stages of viral infection. Only a few other DNA viruses are known to package nicked and gapped genomes: Pseudorabies virus (PRV) and Marek's disease virus (MDV) have nicks and gaps that are randomly distributed (Reznikoff and Thomas 1969, Lee, Kieff et al. 1971, Ben-Porat, Stehn et al. 1976), while other DNA viruses contain nicks and gaps located at specific sites. For example, there are five major nicks in T5, which are thought to occur as a result of a virally encoded nicking enzyme, and may play a role in the two-step transfer mechanism for ejecting DNA into its host (Rogers

and Rhoades 1976, Scheible, Rhoades et al. 1977, Wang, Jiang et al. 2005). Like T5, T7 DNA also has single strand interruptions at specific sites, but these are thought to be the product of premature terminase activity during packaging (Khan, Hayes et al. 1995). Little is known, however, about whether the structure of viral genomes plays a role in infectivity or stimulation of host DDR.

2.6.b. Some cellular DNA damage response pathways are inhibited by HSV-1 infection.

Cells have several different DDR pathways that could be activated during infection, and it is possible that HSV has evolved to utilize those pathways that are conducive to productive infection while preventing pathways that inhibit lytic infection. Using GFP correction assays, we have recently reported that single-strand annealing (SSA) is increased in HSV-infected cells while NHEJ and HR are inhibited (Schumacher, Mohni et al. 2012). This "pathway choice" on the part of the virus may be facilitated by ICP0 consistent with its known ability to degrade components of the NHEJ and HR pathways. For instance, ICP0 is known to degrade DNA-PKcs, a component of the NHEJ pathway, as well as RNF8 and RNF168, which function in HR (Lees-Miller, Long et al. 1996, Lilley, Chaurushiya et al. 2010). DNA-PKcs and Ku, which are both essential components of the NHEJ pathway, are inhibitory to HSV infection: replication is more efficient in cells lacking DNA-PKcs (Parkinson, Lees-Miller et al. 1999), and viral yields are increased by almost 50-fold in Ku-deficient murine embryonic fibroblasts (Taylor and Knipe 2004). In this study, we show that ICP0 is able to inhibit DNA-PKcs-specific phosphorylation of RPA32 even in a cell type in which DNA-PKcs is not degraded (Table 1). The observation that HSV may utilize at least two different mechanisms to

inhibit the activity of DNA-PKcs underscores the apparent necessity for the virus to inactivate NHEJ.

Although the direct relationship between DNA-PK activation and loss-of-infectivity is not known, the observation that loss of infectivity of virion DNA with 5' flaps correlates with the robust activation of DNA-PK (Fig. 8) is consistent with the notion that DNA-PK is antiviral. Furthermore, infectivity of Klenow-treated DNA was restored in DNA-PK$^{-/-}$ cells (Fig. 9), suggesting that DNA-PKcs plays a role in the loss of infectivity phenotype observed in wild type cells. Taken together these results suggest that the activation of DNA-PK is associated with the drop in infectivity, and we are intrigued by the mechanism by which this occurs. It is possible that DNA with 5' flaps can recruit cellular proteins such as nucleases that are able to process the 5' flaps resulting in extreme fragmentation of the viral genome and loss of infectivity. This model, however, does not explain the observation that the absence of DNA-PK itself can rescue infectivity. Another model posits that 5' flaps either directly or indirectly activate DNA-PK, and this activation is antiviral. Support for this model comes from reports that DNA-PKcs kinase activity is potentiated by dsDNA with ssDNA ends compared to blunt ended dsDNA (DeFazio, Stansel et al. 2002, Martensson and Hammarsten 2002, Llorca and Pearl 2004, Rivera-Calzada, Maman et al. 2005). Additionally, DNA with a 5' overhang exhibits a greater increase in DNA-PK kinase activity than a 3' overhang (Pawelczak and Turchi 2008). The observation that in the absence of DNA-PK the 5' flap structure is tolerated supports the notion that the 5'-flapped genome represents a substrate for direct DNA-PK activation.

DNA-PK plays an important role in a variety of cellular processes, and the

specific mechanism by which DNA-PK inhibits lytic infection is not understood. It is possible that DNA-PK, acting as part of the NHEJ pathway, promotes circularization of the viral genome, which has been correlated with establishment of latent or quiescent infection (Rock and Fraser 1983, Efstathiou, Minson et al. 1986, Jackson and DeLuca 2003). The report by Jackson and Deluca that the presence of ICP0 can inhibit circularization (Jackson and DeLuca 2003) may be consistent with this suggestion; however, further experimentation will be required to elucidate the relationship between NHEJ and circularization of viral genomes. Regardless of whether circularization is the mechanism by which NHEJ exerts its antiviral effects, the fate of the viral genome and the choice of repair/recombination pathway activated during infection appear to have important consequences for the establishment of lytic infection.

Although the mechanism of recombination in HSV infection is not well understood, recent experiments from our laboratory suggest that HSV-1 activates the SSA pathway. During infection, SSA is stimulated in a manner that appears to be dependent on the viral 5' to 3' exonuclease, UL12 (Schumacher, Mohni et al. 2012). UL12 interacts with ICP8 to form a two-component recombinase capable of strand exchange (Reuven, Staire et al. 2003, Reuven, Willcox et al. 2004). We are intrigued by the possibility that UL12/ICP8 work together to promote recombination-dependent replication by SSA and that this pathway leads to the production of concatemeric DNA that can be packaged into infectious virus (Weller and Sawitke, manuscript in press). In addition, we are currently exploring the possible involvement of cellular proteins in the stimulation of SSA in HSV-infected cells.

Taken together these observations suggest that HSV has evolved mechanisms of

"pathway choice" that promote lytic replication by inhibiting NHEJ. Our findings suggest that the presence of nicks and gaps in incoming DNA may result in the recruitment of a combination of cellular and viral proteins that stimulates a repair pathway that is beneficial to lytic replication, such as SSA. This process underscores the complex evolutionary relationships between HSV and its host.

Acknowledgements: We wish to thank members of our laboratory for discussions and suggestions on the manuscript. This project was supported by National Institutes of Health grants awarded to SKW: AI069136 and AI021747.

TABLE 2.1. Viral yield from cells co-transfected with HSV-1 virion DNA and plasmid DNA

Viral DNA Treatment	Plasmid co-transfected	Viral titer (pfu/mL)	Std. Error	% Infectivity
Untreated (wild-type)	Empty vector	2.9×10^3	$\pm 1.7 \times 10^3$	100
	ICP0	4.1×10^5	$\pm 8.1 \times 10^4$	14,000
	ICP0 ΔFXE	1.2×10^4	$\pm 3.7 \times 10^3$	420
Klenow-treated	Empty vector	3.0×10^1	$\pm 1.1 \times 10^1$	1
	ICP0	1.3×10^5	$\pm 4.4 \times 10^4$	4,600
	ICP0 ΔFXE	1.0×10^3	$\pm 1.9 \times 10^2$	35

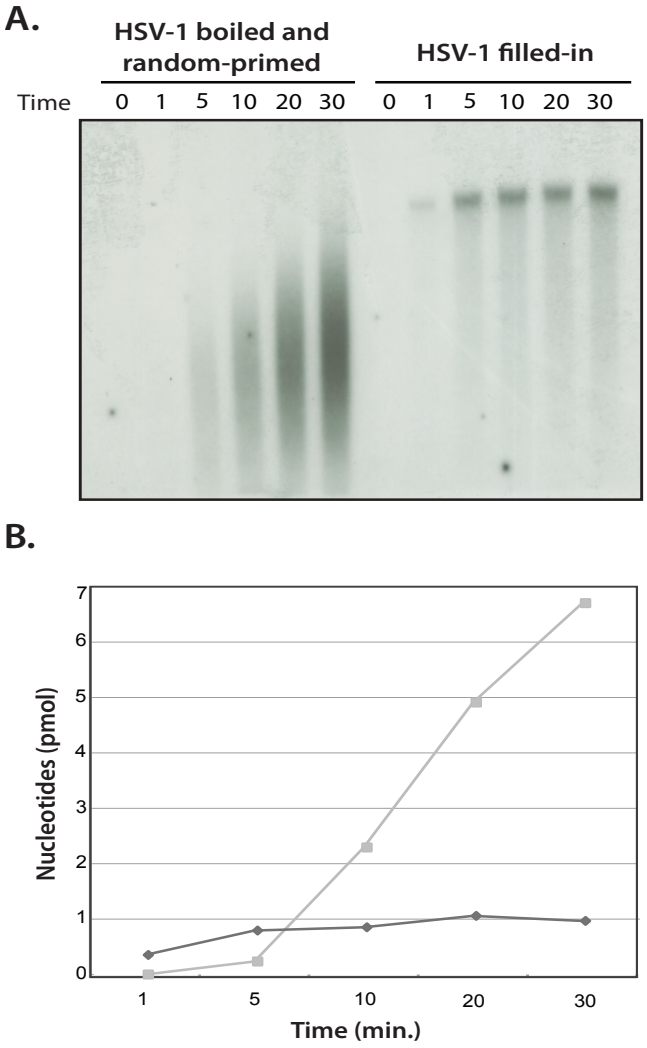

Figure 2.1. Purified HSV-1 DNA contains gaps than can be filled by DNA polymerase. (A) The incorporation of labeled nucleotides by the Klenow fragment of *E. coli* DNA polymerase I into 200ng HSV-1 DNA was performed as described in Methods. For lanes 1-6, prior to incubation in the reaction mix, the DNA was boiled 2 min and quick-cooled, and random primers were added. Samples were analyzed by agarose gel electrophoresis. (B) Quantification of labeled nucleotides incorporated into the HSV-1 DNA.

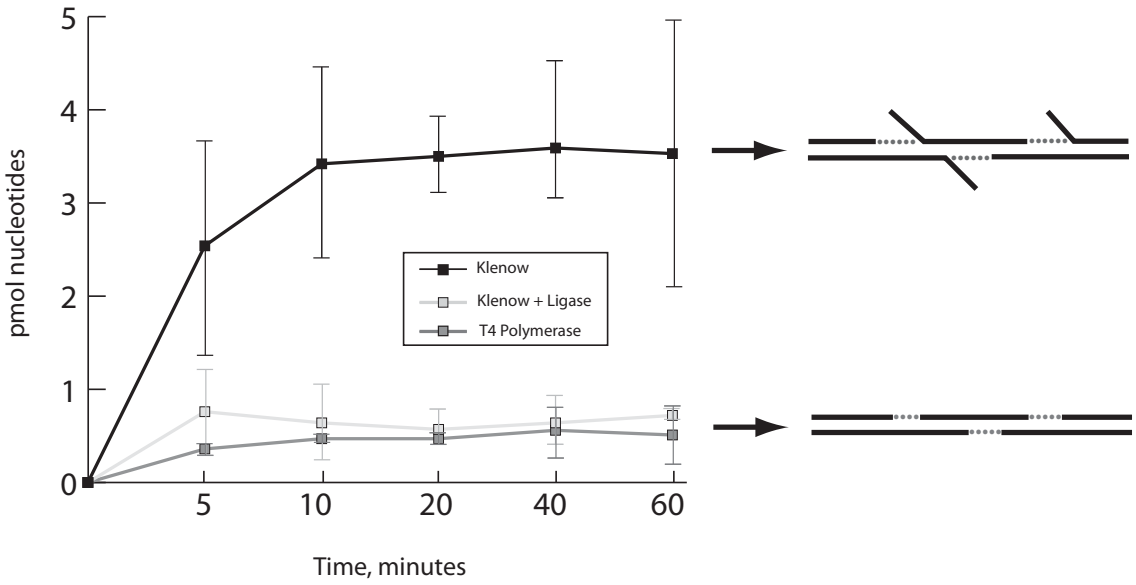

Figure 2.2. Incorporation of labeled nucleotides into HSV-DNA by Klenow fragment polymerase alone, Klenow and ligase together or T4 DNA polymerase. Purified HSV-1 DNA was incubated with labeled nucleotides and the following enzymes, as described in Methods: Klenow fragment, Klenow fragment together with T4 DNA ligase, T4 DNA polymerase.

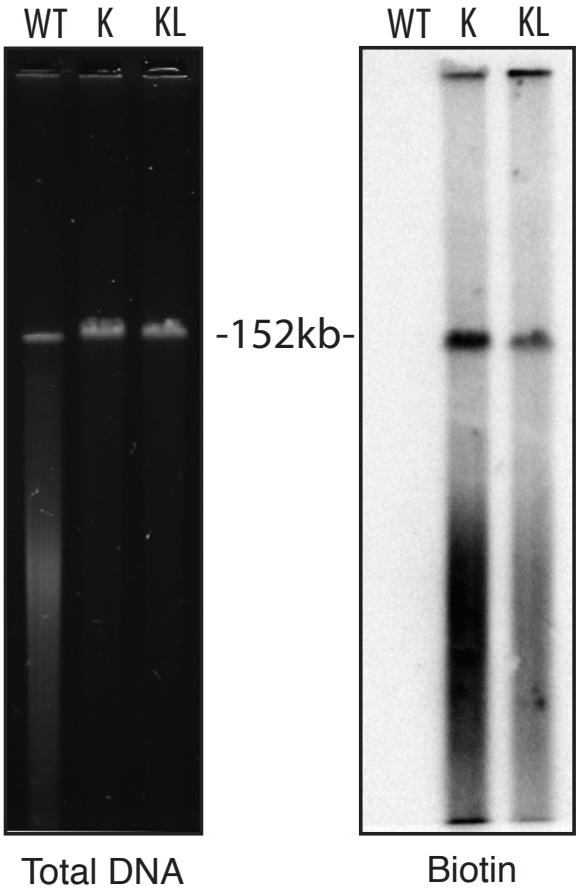

Figure 2.3. Virion DNA before and after treatment with Klenow or Klenow and ligase. Biotinylated nucleotides were incorporated into HSV DNA using Klenow alone, Klenow and ligase. Pulsed field gel electrophoresis was performed with untreated (C), Klenow-treated (K), and Klenow & ligase (KL) HSV virion DNA. The gel was probed with ethidium bromide (total DNA) and CDP-Star biotin detection reagent (incorporated nucleotides).

IN VITRO TREATMENT	DNA STRUCTURE	% INFECTIVITY
Wild-type		100
Ligase		116 ±9
Klenow	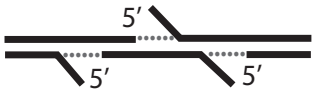	8 ±7
Klenow, no dNTPs		100 ±27
Klenow + ligase		109 ±14
Mung bean nuclease		0 ±5
Klenow + ligase, then mung bean nuclease		100 ±10
Terminal transferase	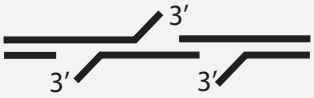	100 ±8
Alkaline phosphatase		100 ±10

Figure 2.4. Expected structure and measured infectivity of HSV virion DNA following various in vitro treatments. Virion DNA was treated with the indicated enzymes and tested for infectivity. The numbers of plaques have been normalized, with the plaque number obtained in control reactions set at 100%.

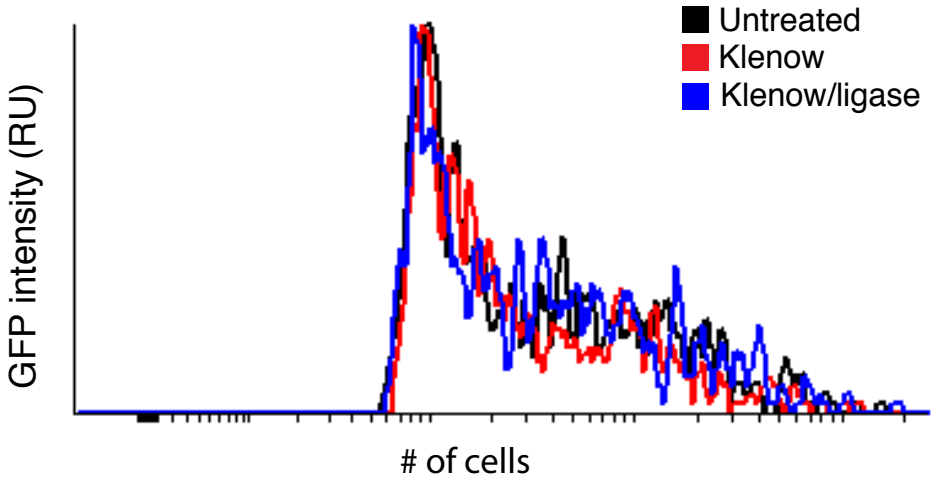

Figure 2.5. Transfection efficiency of treated and untreated KOS-GFP DNA. Vero cells were transfected with untreated (black), Klenow-treated (red), or Klenow/ligase-treated (blue) KOS-GFP DNA. The graph depicts overlayed histograms of cells sorted by FACS and gated for GFP-positive cells.

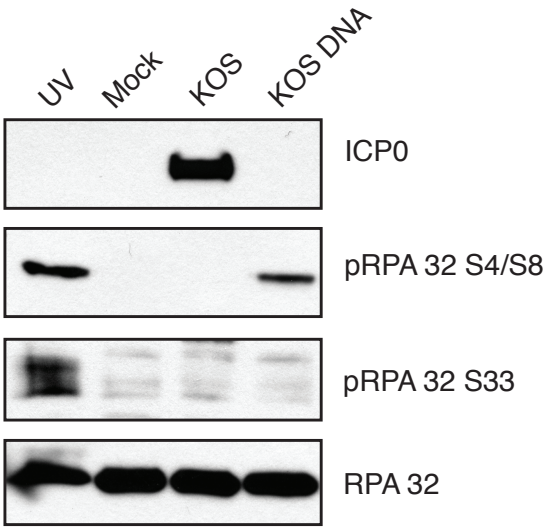

Figure 2.6. HSV-1 DNA stimulates RPA phosphorylation in transfected cells, but not infected cells. Vero cells were either infected with HSV-1 at MOI=10 and harvested at 3 h.p.i. (KOS), or transfected with 700ng of virion DNA and harvested 3h following serum addition (KOS DNA). As a positive control for pRPA S4/S8, Vero cells were treated with 50 J/m2 and allowed to recover for 1h at 37°C ("UV").

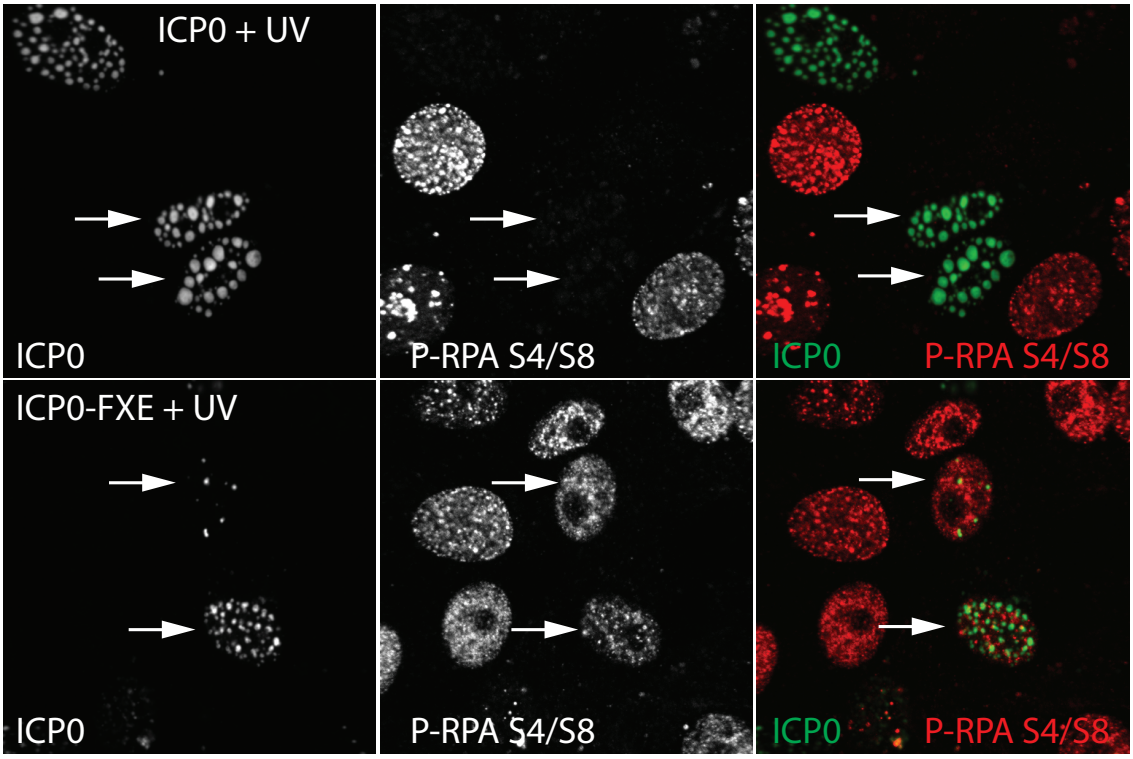

Figure 2.7. ICP0 prevents pRPA32 S4/S8 in Vero cells. Vero cells were transfected with wild-type ICP0 or the ICP0 ΔFXE mutant and then irradiated with 100 J/m2 UV. Cells were allowed to recover for 2 hours and then fixed and stained as indicated. Arrows highlight cells transfected with ICP0.

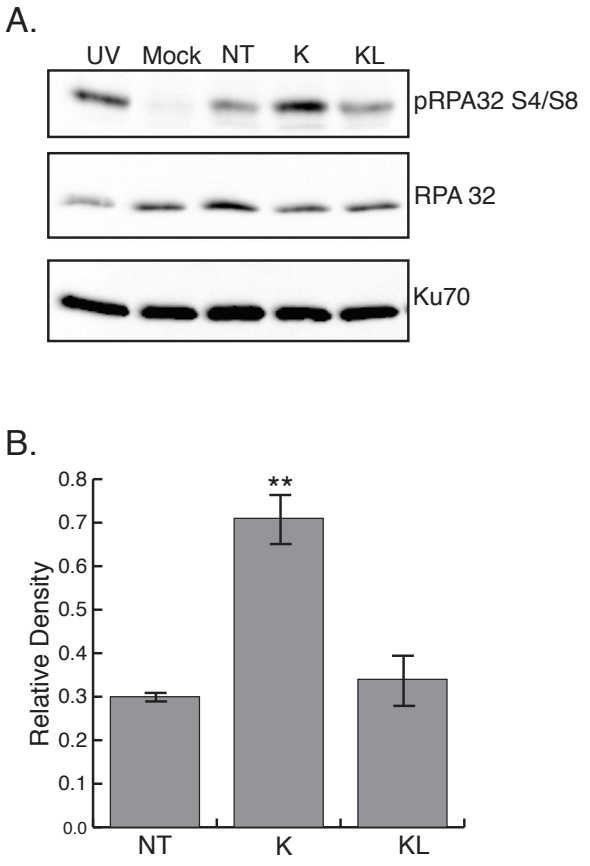

Figure 2.8. Addition of 5' flaps to virion DNA increases hyper-phosphorylation of RPA32. (A) Vero cells were transfected with purified KOS DNA that was either not treated (NT), Klenow-treated (K), or Klenow & ligase-treated (KL). Samples were harvested at 3h following serum addition. As a positive control for pRPA S4/S8, Vero cells were treated with 50 J/m2 and allowed to recover for 1h at 37°C ("UV"). (B) Densitometry analysis of western blot. Relative density was calculated by the ratio of the densities of pRPA S4/S8 and Ku70. **Indicates p=0.001.

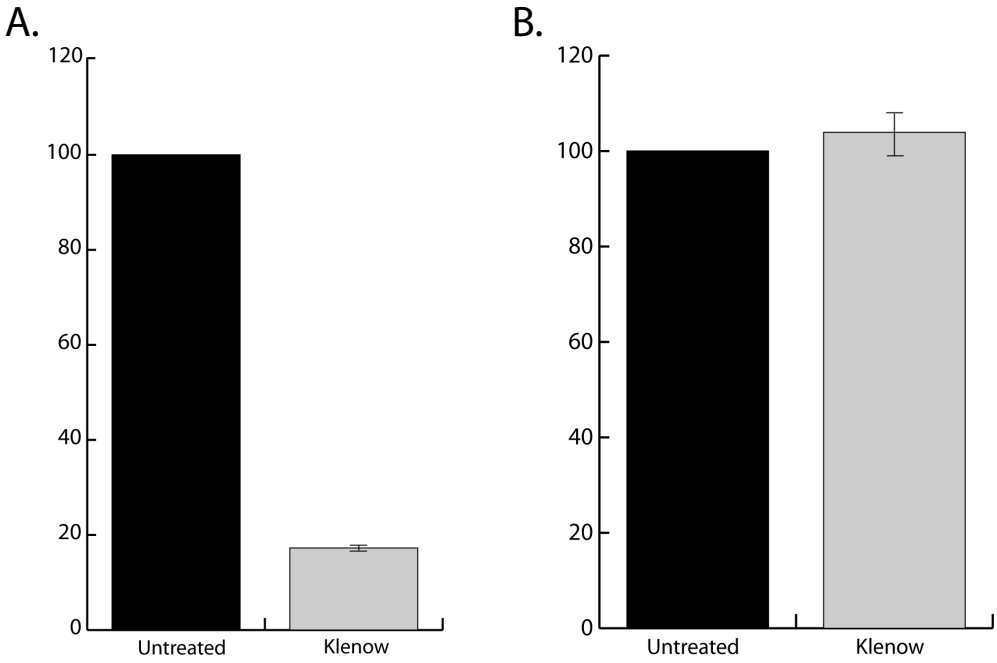

Figure 2.9. Infectivity of Klenow-treated DNA is rescued in the absence of DNA-PK. HCT-116 cells and DNA-PK$^{-/-}$ cells were transfected with 500ng of untreated or Klenow-treated virion DNA. Samples were harvested at 48h following serum addition, and titrated for virus yield on Vero cells. Infectivity is reported as percent of the untreated DNA control. Viral titers were normalized to untreated DNA control set at 100%.

CHAPTER 3.

Genomes produced by the HSV-1 alkaline nuclease-null virus, AN-1, are structurally aberrant and result in loss-of-infectivity.

Samantha Smith, Smaranda Wilcox, Renata Szczepaniak, Jack Griffith and Sandra K. Weller

Author contributions: S.W. performed the EM analysis and gp32 binding experiments shown in Figure 3.6 and Figure 3.7. R.S. performed the sucrose gradients for Figure 3.5. All other experiments and reagent preparations were done by S.S.

3.1. ABSTRACT

Herpes simplex virus type I (HSV-1) encodes an alkaline nuclease, UL12, which is required for efficient viral replication. UL12 has been shown to stimulate DNA repair by single strand annealing (SSA) in cells (Schumacher, Mohni et al. 2012), and participate in DNA strand exchange *in vitro* (Reuven, Willcox et al. 2004). The UL12-null virus, AN-1, produces aberrant DNA and exhibits defects in both virus yield and DNA packaging (Shao, Rapp et al. 1993, Martinez, Sarisky et al. 1996). Thus, it has been proposed that UL12 plays a role in facilitating the correct DNA repair pathway choice during infection in order to produce viral DNA that is infectious and suitable for packaging (Martinez, Sarisky et al. 1996, Goldstein and Weller 1998). This chapter

examines the phenotype of the AN-1 virus with respect to the infectivity and structure of DNA produced during infection. Purified AN-1 DNA was not infectious on Vero or complementing cells (6-5), and we determined that this is due to restriction of immediate early gene expression. Using pulsed field gel electrophoresis (PFGE), we found a species of aberrant viral DNA produced during AN-1 infection that was previously unreported. Interestingly, this species of DNA was not present during infection with the ANF-1 mutant virus, which does not express full-length UL12, but encodes the amino-terminally truncated UL12.5 protein that does not localize to the nucleus. It has previously been reported that AN-1 produces fewer C capsids and more A capsids than wild type virus (Shao, Rapp et al. 1993). We now show that this defect is partially relieved on complementing (6-5) cells. We tested the stability of purified C capsids and found that encapsidated AN-1 DNA appears to be as stable as encapsidated wild type DNA. EM analysis also suggested that AN-1 virion DNA may contain more ssDNA regions than wild type virion DNA. Taken together, these results suggest that UL12 is required to efficiently produce DNA that is infectious and suitable for packaging.

3.2. INTRODUCTION

Herpes simplex virus 1 (HSV-1) is a large double-stranded linear DNA virus that infects humans. The HSV-1 genome is approximately 152kb in length and is replicated in the nucleus of the host cell. The virus encodes seven essential replication proteins: the heterotrimeric helicase/primase (UL5/8/52), DNA polymerase (UL30), the polymerase processivity factor (UL42), the origin binding protein (UL9), and the single strand DNA binding protein (ICP8). These seven proteins together with an origin of replication (Ori)

sequence are considered to be the minimum requirements for viral DNA synthesis. Replication is thought to occur in a biphasic manner, beginning with origin-dependent, or theta, replication, and later switching to a mechanism capable of producing concatemeric DNA (Schildgen, Graper et al. 2005, Weller and Coen 2012)}. The production of concatemeric DNA is an essential step for the generation of progeny virus, as the packaging machinery must recognize longer-than-unit-length concatemers. The second phase of DNA replication, which is thought to be origin-independent, is poorly understood; however, several lines of evidence suggest that this phase may involve recombination-dependent DNA replication.

Despite the identification of cis- and trans-acting elements needed for HSV-1 DNA replication, the mechanism of replication is still poorly understood. It has been proposed that the viral genome circularizes and rolling circle replication leads to the formation of concatemers (Roizman, Jacob et al. 1979, Garber, Beverley et al. 1993); however, it is becoming increasingly apparent that the mechanism of HSV-1 utilizes a more complex and unusual mechanism for DNA replication. Simple rolling circle replication does not explain the observation that genomic inversions occur as soon as viral DNA synthesis can be detected (Zhang, Efstathiou et al. 1994, Lamberti and Weller 1996, Severini, Scraba et al. 1996). Furthermore, replicating HSV-1 DNA does not assume a linear concatemeric structure; instead, the products of HSV-1 DNA replication are large branched structures that contain X and Y shaped DNA elements that may represent recombination intermediates and replication forks, respectively (Jacob and Roizman 1977, Severini, Scraba et al. 1996, Bataille and Epstein 1997). The HSV-1 replication machinery can also produce complex structures when replicating SV40 DNA,

which when replicated using SV40 machinery produces concatenated DNA (Blumel, Graper et al. 2000). Generation of these complex structures by HSV-1 appears to be an inherent property of the replication machinery and does not require a specific sequence.

As alluded to earlier, we believe that HSV-1 utilizes a recombination-dependent mechanism to produce concatemeric DNA suitable for packaging. In support of this notion, the virus encodes a two-subunit recombinase, consisting of the alkaline nuclease, UL12, and ICP8. By analogy to the redα/β system of Lambda phage, UL12 is thought to resect 5' DNA ends to expose regions of homology, and ICP8 acts as a single strand annealing protein (SSAP) (Weller and Sawitzke 2014). We have previously shown that UL12 and ICP8 can catalyze a strand exchange reaction *in vitro* (Reuven, Willcox et al. 2004). More recently, we have utilized a cell-based GFP report assay to monitor DNA double strand break (DSB) repair during infection. Using this method, we have found that UL12 is sufficient to stimulate single strand annealing (SSA) (Schumacher, Mohni et al. 2012), and we believe that the viral recombinase may influence DNA repair pathway choice during infection in order to produce infectious viral DNA that is suitable for packaging.

The phenotype of the UL12-null virus (AN-1) is complex, affecting several stages of the virus life cycle. When AN-1 is propagated in Vero, HEK293, and BHK cells, viral yields are decreased by 2-3 logs, compared to growth on a complementing Vero cell line (6-5) (Weller, Seghatoleslami et al. 1990, Shao, Rapp et al. 1993, Balasubramanian, Bai et al. 2010). Viral DNA synthesis is not severely compromised in AN-1-infected Vero cells (50-90% of wild type levels) and terminal DNA ends can be detected by southern blot, suggesting that concatemers are cleaved; however, a more severe defect in

encapsidation and capsid egress was observed (Shao, Rapp et al. 1993). These results suggest that although DNA synthesis occurs and concatemers are cleaved for packaging, the DNA synthesized by AN-1 in Vero cells cannot be encapsidated efficiently into stable DNA-containing capsids that are competent for nuclear egress. We suggest that this could be the result of unresolved DNA recombination intermediates or other anomalies in DNA structure that diminish the efficiency of encapsidation. The observation that AN-1 DNA is more fragile and prone to fragmentation upon isolation than wild type DNA indicates that the structure of AN-1 DNA is abnormal compared to wild type (Goldstein and Weller 1998). The observation that the structure of AN-1 DNA is abnormal is consistent with the encapsidation defect. In this chapter we report that DNA isolated from virions that were produced in the absence of UL12 (AN-1 and ambUL12 infections) is not infectious on transfected Vero cells (Shao, Rapp et al. 1993, Porter and Stow 2004). Replicating DNA also appears to be aberrant in AN-1 infection: unlike wild-type replicating DNA, which can enter a pulsed-field gel after being digested by a restriction enzyme that cuts once per genome, similar treatment of replicating DNA from the AN-1 virus releases no discrete bands, which may suggest a more complex structure (Martinez, Sarisky et al. 1996).

Replicating DNA is complex, but packaged virion DNA is linear. Encapsidation requires that replicating DNA "mature" from a complex structure into an acceptable substrate for cleavage and packaging. The phenotype of the UL12-null virus (AN-1) supports the notion that UL12 is involved in some aspect of recombination-dependent replication- either through pathway choice, resolution of recombination intermediates or some combination of the two. This chapter examines the defects in viral infection with

the UL12-null virus, AN-1 in order to better understand the role of UL12 in these processes.

3.3. MATERIALS AND METHODS

3.3.a. Cell lines and viruses.

Vero, NHF, and HeLa cells were obtained from American Type Culture Collection (ATCC). Vero cells were grown in Dulbecco's modified minimal essential medium (DMEM) (Gibco) containing 5% fetal bovine serum (FBS). The UL12-expressing Vero cell line, 6-5, was previously described (Shao, Rapp et al. 1993). Vero and 6-5 cells were grown in Dulbecco's modified minimal essential medium (DMEM) (Gibco) containing 5% fetal bovine serum (FBS). 6-5 cells were supplemented with G418 to maintain selection for the UL12 cassette. HeLa cells were maintained in DMEM containing 10% FBS. The KOS strain of HSV-1 was used as the wild-type virus. The UL12-null virus, AN-1, was derived from KOS and lacks 917bp of the UL12 gene due to replacement with a LacZ insertion under the ICP6 promoter (Weller, Seghatoleslami et al. 1990).

3.3.b. Purification of viral DNA

Virion DNA was isolated as previously described (Goldstein and Weller 1988). Approximately 1 X 10^8 Vero cells were infected with KOS at a relatively low MOI (0.1 to 0.5 PFU/cell). When maximum cytopathic effects were observed, infected cells were harvested by centrifugation at 1500rpm for 15 minutes at 4°C. Supernatant was removed

and stored at 4°C for later use. The cell pellet was resuspended in 3mL of cold 1X RSB and incubated on ice for 10 minutes. Cells were disrupted by dounce homogenization and cell debris and nuclei were removed by centrifugation at 1500 rpm for 10 minutes at 4°C. The supernatant was combined with the first supernatant and centrifuged, 9000 rpm for 60 minutes at 4°C resulting in a suspension of intra and extracellular capsids, which were resuspended in 5 ml of TNE (10 mM Tris-Cl pH 7.4, 10 mM NaCl, 30 mM $MgCl_2$,) and frozen at -80°C. Virions were thawed, and SDS and Proteinase K were added to final concentrations of 1% and 100 μg/ml, respectively. The tube was gently inverted and incubated for 5 hours at 37°C to release virion DNA, which was gently extracted by phenol:chloroform:isoamyl alcohol (25:24:1) and precipitated with ice cold ethanol (100%). DNA was incubated one hour on ice, and then centrifuged for 15 minutes at 20,000 x *g*. The pellet was washed with 70% ethanol, dried briefly, and resuspended in TE buffer. Virion DNA was aliquoted and stored at -80°C for further use.

3.3c. Plaque assay.

Vero and 6-5 cells were seeded onto 60mm dishes at 50-70% confluence. Cells were transfected with either the specified virion DNA, or no DNA for the mock sample, at a concentration of 200ng DNA/dish using Lipofectamine Plus reagent (Invitrogen) according to the manufacturer's suggested protocol. Samples were overlaid with DMEM containing 2% methylcellulose at 17-20 hours post-transfection. When plaques were visible (approximately 4 to 5 days following transfection), samples were fixed with 8% formaldehyde in 1X PBS and stained with crystal violet and plaques were photographed and counted.

3.3.d. Pulsed-field gel electrophoresis (PFGE)

Infected cell plugs were prepared as follows: Cells were seeded in 60 mm dishes and infected at an MOI of 5 PFU/cell. At 20-24 h post infection, cells were harvested and centrifuged at 2,000 rpm for 5 min in a Beckman model TJ-6 tabletop centrifuge. The supernatant was then removed and cells were resuspended in approximately 600 µl of 55°C 1% low-melting-point agarose (BioRad LMP) in 0.5X TBE Buffer. Blocks were stored at 4°C in 50 mM EDTA (pH 8.0). Lysis of the cells in plugs was performed by incubation in 1% laurylsarcosine–0.4 M EDTA (pH 9.0) with proteinase K at 1 mg/ml for 24 h at 50°C. Blocks were then rinsed in 1X TE at 50°C, three times for 1 hour each, to remove the detergent and the proteinase K and stored at 4°C in TE. PFGE was performed as previously described (Smith, Reuven et al. 2014). Briefly, agarose gel was prepared using 1% Pulsed Field Gel-Grade agarose (Bio-Rad) gel in 0.5X TBE buffer. Samples were diluted in 6X Gel Loading Dye (NEB) and loaded directly into the wells. Electrophoresis was performed using a CHEF-DR III apparatus (Bio-Rad) with 0.5X TBE (45 mM Tris, 45 mM borate, 1 mM EDTA, pH 8.3) running buffer. Samples were separated using 6 V/cm (approximately 200V) for 24 h at 14 °C. Switch times ramped from 1-25 seconds. Lambda Ladder PFG Marker (NEB), MidRange II Marker (NEB), and Vero cells infected with HSV-1 were used as size standards. Gels were stained with ethidium bromide and imaged using a ChemiDoc MP imaging system (BioRad).

3.3.e. Southern blot analysis

Gels were transferred by vacuum blotting to GeneScreen Plus membranes (Dupont NEN) according to manufacturer's protocols. The *BamHI* K fragment probe was labeled by incorporation of dCTP [α-^{32}P] using the Random Primer DNA Labeling Kit (Life Technologies). The biotinylated *BamHI* S fragment probe was generated by PCR incorporation of Biotin-14-dATP (Forward primer, 5' CTCTCCGCATCACCACAGAA; Reverse primer, 5' AAAGGGGCCATGTGTAGGTG). Following PCR, probes were cleaned up using Qiaquick PCR Cleanup Kit (Qiagen). Membranes were, developed using the CDP-Star biotin detection reagent (NEB) and imaged using a ChemiDoc MP imaging system (Bio-Rad).

3.3.f. Western blot analysis

Samples were harvested 24 hours following transfection and prepared for western blot analysis as previously described (Mohni, Dee et al. 2013). The primary antibodies used were anti-UL12 antibody (BWpUL12), which detects UL12 was a gift from Joel Bronstein and Peter Weber (Parke-Davis Pharmaceutical Research), and monoclonal mouse anti-β-actin (1:15,000; Sigma). Western blots were imaged using a ChemiDoc MP imaging system (BioRad).

3.3.g. Preparation of capsids

To isolate capsids from infected cells, Vero cells were infected with either KOS or AN-1 virus, and 6-5 cells were infected with AN-1 virus at a multiplicity of infection of 3 pfu/cell. At 24 h post infection, samples were harvested and C capsids were

separated by analytical ultracentrifugation on a sucrose density gradient (50-20%). Purified C capsids were divided into 50μL aliquots and stored in a buffer containing 500mM MaCl and 35% sucrose at -20°C until further analysis.

3.3.h. Electron microscopy

To image virion DNA from purified C capsids, samples were stained using 1.7μL of cytochrome C in a total volume of 50μL, and allowed to develop for 90 seconds so that particles surface in a cytochrome film and picked up by the grid. For drop spreading, samples were diluted 1:10 in 10mM Tris and 250mM ammonium acetate and then immediately spread onto the grid by drop spreading. For the gp32 binding experiment, samples were digested in Proteinase K and then incubated with the T4 ssb, gp32 prior to analysis.

3.4. RESULTS

3.4.a. Purified AN-1 DNA is not infectious, even in cells expressing UL12.

Purified wild-type HSV-1 DNA is infectious when delivered by transfection into cells. On the other hand, it has previously been reported that virion DNA from the UL12-null virus, *amb*UL12, was not infectious (Porter and Stow 2004). In order to determine whether the AN-1 mutant virion DNA also exhibited a noninfectious phenotype, viral DNA was purified from AN-1-infected Vero cells and infectivity was measured. Transfection of Vero cells with 200μg of wild-type KOS DNA resulted in the formation of numerous plaques (Figure 3.1.A). In contrast, Figure 3.1.B. shows that no plaques

were observed in Vero cells transfected with 200μg of AN-1 DNA, and in a duplicate experiment, two plaques were observed. Similar results were observed in another experiment in which cells were transfected with 1-2 μg of AN-1 or KOS DNA (data not shown). The cell line, 6-5, expresses UL12 and has been shown to complement the growth of AN-1, albeit not quite to wild type levels. To determine whether infectivity could be restored by UL12 expression, 6-5 cells were transfected with AN-1 virion DNA. Again, the AN-1 DNA did not produce any plaques (Figure 3.1.B), suggesting that the loss of infectivity phenotype of purified AN-1 DNA cannot be rescued in the presence of UL12. We suggest that UL12 must be present at the time of DNA synthesis and that once aberrant DNA has been packaged it cannot be rescued by the presence of UL12 in transfected cells. As a control, transfection of 6-5 cells with KOS DNA resulted in numerous plaques (Figure 3.1.C), although there were fewer than seen on Vero cells. The KOS DNA produced numerous plaques on 6-5 cells; however, there appeared to be fewer plaques on 6-5 cells than on Vero cells (Figures 3.1C and 3.1.A, respectively). This is consistent with previous reports that KOS infection is not as efficient on 6-5 cells as on wild type Vero cells (Shao, Rapp et al. 1993).

3.4.b. Viral gene expression is not detectable in cells transfected with purified AN-1 DNA.

Next, we wanted to determine the stage of the HSV lifecycle at which the infectivity of AN-1 DNA was being restricted. We next examined whether viral gene expression could be detected in cells transfected with AN-1 DNA. To do this, Vero cells were transfected with 0.5μg of KOS or AN-1 virion DNA. Cell lysates were harvested at

24 h post transfection and analyzed by western blot for expression of the immediate-early protein, ICP4. Figure 3.2 shows that cells transfected with KOS virion DNA exhibit robust ICP4 expression at 24 h; whereas, no ICP4 expression is detected in the AN-1 sample. These results indicate that gene expression is markedly decreased in cells transfected with AN-1 DNA.

3.4.c. High molecular weight viral DNA is produced during AN-1 infection of non-complementing cell lines.

The lack of infectivity and viral gene expression of AN-1 DNA suggests that there may be an inherent flaw in the DNA itself. It has previously been reported that the DNA produced during AN-1 infection is extremely fragile, and replicating AN-1 DNA is aberrant and has a more complex structure than KOS DNA (Martinez, Sarisky et al. 1996, Goldstein and Weller 1998). With this in mind, we next wanted to compare AN-1 DNA produced in complementing and non-complementing cells. To do this, Vero, HeLa and 6-5 cells were infected with AN-1 or KOS. At 18 to 20 hours post infection, the samples were harvested, suspended in low melting point agarose, and subjected to pulsed field gel electrophoresis (PFGE) (Figure 3.3). At this time point, we expect to see replicating DNA, which remains in the well, and unit length (152kb) viral genomes, which have been cleaved and packaged (Figure 3.3.A). Figure 3.3.B shows a southern blot of the PFGE using a *BamHI* K fragment probe, which detects the junction region of the HSV-1 genome. The portion of the gel containing "well DNA" was removed from Figure 3.3.B to allow for longer exposure of DNA that has entered the gel. In lanes 1,2 and 3, samples from KOS- infected Vero, HeLa, and 6-5 cells are displayed.. All three of the KOS

samples exhibit sharp bands corresponding to unit-length packaged DNA (152kb). In contrast, all three of the AN-1 samples (Figure 3.3.B, lanes 4, 5, and 6) exhibit greatly diminished amounts of unit-length DNA, consistent with previous reports that AN-1 infection produces less DNase-protected (encapsidated) DNA (Shao, Rapp et al. 1993, Martinez, Sarisky et al. 1996). Furthermore, the 152kb bands seen in the AN-1 infected Vero and HeLa cell samples are more diffuse than the sharp bands of unit-length KOS DNA. The diffuse nature of this band may indicate heterogeneity in the size or structure of the packaged DNA. In contrast to the AN-1 DNA produced on Vero and HeLa cells, the 152kb DNA produced in AN-1 infected 6-5 cells appears to be more discrete, suggesting that the diffuse bands correlate with a non-productive infection.

Figure 3.3 also shows an additional slow-migrating species of viral DNA produced in AN-1 infected Vero and HeLa cells that is not present in wild-type samples or in AN-1 DNA from 6-5 cells. This species represents DNA that has migrated out of the well but is outside the linear range of separation by PFGE in what is termed the compression zone (CZ). The molecular weight of linear DNA migrating in the CZ ranges from > 300kbp to < 2Mbp; however, it is also possible that some branched molecules and very large, supercoiled circular DNA could also migrate at this position. If the CZ DNA has an unusual structure, its migration pattern would not be expected to reflect its molecular weight.

To determine whether viral CZ DNA was unique to the AN-1 virus PFGE was used to examine the DNA produced by another UL12 mutant virus, ANF-1. The ANF-1 virus is mutated in such a way that it does not express the full length UL12 gene, but still expresses an N-terminally truncated protein, UL12.5, expressed from a distinct mRNA

(Costa, Draper et al. 1983, Martinez, Shao et al. 1996 1983, Martinez, Goldstein et al. 2002, Corcoran, Saffran et al. 2009). CZ DNA was not observed in cells infected with ANF-1. (Figure 3.4.B). Thus, CZ DNA was only produced in non-permissive cells infected with a nuclease deficient virus.

3.4.d. Fewer C capsids are produced during AN-1 infection than during wild-type infection.

As mentioned in the introduction, we previously reported that cells in infected with AN-1, nearly wild type levels of viral DNA was produced and terminal fragments were detected, indicating cleavage of concatemeric products of viral DNA replication; however, a defect in stable encapsidation and egress from the nucleus was observed (Shao, Rapp et al. 1993). We therefore wanted to examine the capsids generated in AN-1 infection to determine whether a defect could be detected.

When infected cell lysates are subjected to centrifugation in a sucrose gradient, capsids band at three separate densities, labeled A, B, and C from least dense to greatest density, respectively (Figure 3.8, *far left*). Capsids assembled in HSV-1 infected cells (procapsids) are spherical and contain an internal scaffold that is cleaved prior to or concomitantly with DNA packaging. Scaffold containing procapsids are unstable angularize into scaffold containing capsids, which are designated as B-capsids following sucrose gradient sedimentation. Capsids that have successfully completed cleavage and packaging of virion DNA are C-capsids, which have replaced their scaffold with virion DNA. A-capsids are thought to represent capsids in which the packaging process has been initiated, and the scaffold has left the capsid; however, the DNA that enters the

capsid is not retained (Addison, Rixon et al. 1990). Thus, A capsids are devoid of scaffold and DNA and exhibit the least density of any capsid types.

We previously reported that, compared to wild type infection, a high proportion of A-capsids are produced in cells infected with AN-1, indicating that packaging may have been initiated but was subsequently aborted. Few, if any, DNA-containing C-capsids could be detected (Shao, Rapp et al. 1993). We have confirmed a defect in the production of stable C-capsids (Figure 3.5.A). Although C-capsids could be observed in cells infected with AN-1, they were much less numerous than those produced during KOS infection of Vero cells (Figure 3.5.A). We have also analyzed capsids from AN-1 infected NHFs and observe the same phenotype (Figure 3.5.B.). In addition, the C-capsids that are produced in AN-1 infected Vero and NHF cells appear to be more diffuse than those produced in KOS infection. We have also analyzed capsids produced in 6-5 cells infected with AN-1 infection and observed that fewer A-capsids and more C-capsids than in AN-1 infected Vero or NHF cells non-complementing cells infected. However, the phenotype does not appear to be completely rescued by the resident copy of UL12 in 6-5 cells, as capsids from AN-1 infected 6-5 cells contain more A-capsids and fewer C-capsids than the KOS sample (Figure 3.5). This result may be consistent with previous observations that the defects in AN-1 can only be partially complemented in 6-5 cells, since AN-1 yields are is improved on 6-5 cells compared to Vero and NHF but are still significantly less than the virus yield of KOS (Shao, Rapp et al. 1993).

3.4.e. Encapsidated AN-1 DNA appears to have more single strand regions, compared with that of wild type.

We hypothesized that encapsidated AN-1 DNA is less stable and thus more likely to be ejected from C-capsids, producing an abundance of A-capsids we observed by sucrose gradient sedimentation. To assess C-capsid stability, we treated C capsids isolated from KOS and AN-1 infections under various conditions to determine if the AN-1 capsids were more likely to disgorge or lose virion DNA than wild type C-capsids. Purified C-capsids were spread on EM grids and analyzed by rotary shadow EM. KOS and AN-1 C-capsids were first spread with cytochrome C in the high salt buffer in which they were stored (250mM NaCl). Neither the KOS nor the AN-1 capsids lost their DNA under these conditions (data not shown). We next diluted the salt to 125mM and again spread the capsids for EM analysis. Surprisingly, the KOS capsids ejected their DNA, but the AN-1 capsids appeared to maintain encapsidated DNA (data not shown). This indicates that wild type capsids may be more sensitive to changes in salt concentration, although we cannot rule out the possibility that some AN-1 capsids had already lost their DNA prior to the spreading and thus appeared to be undisrupted.

We also wanted to determine whether the encapsidated DNA from AN-1 C-capsids could be distinguished from those from KOS-infected cells. Capsids were diluted 1 to 10 in 10mM Tris buffer and drop spread for EM analysis. For both the KOS and AN-1 samples, the genomic DNA appeared as coils surrounding capsids. Because of the conformation of the genomic DNA, we were unable to determine the length or structure of the DNA with any accuracy. Thus, there were no observable differences between the DNA from AN-1 capsids and KOS capsids by this method (Figure 3.6).

One possible reason for the diffuse bands observed in unit-length AN-1 DNA by PFGE would be heterogeneity due to structural difference such as more single stranded DNA than in wild type genomes. This could also explain the diffuse nature of the C-capsids seen in AN-1-infected cells by sucrose gradient sedimentation. In Chapter 2, we demonstrated that, on average, wild type virion DNA contains approximately 15 gaps per genome, each with an average length of 33nt (Smith, Reuven et al. 2014). With this in mind, we wanted to compare the amount of ssDNA in AN-1 virion DNA to that of wild type. However, because purified AN-1 DNA is extremely fragile, we could not use the incorporation method for measurement of ssDNA, as we had done for wild type. Instead, we performed a binding experiment using an ssDNA binding protein (ssb) to qualitatively analyze ssDNA content by EM. To do this, we selected T4 phage gp32 protein as the ssb because it has a DNA footprint small enough to bind the gaps in the wild type genome. Figure 3.7 shows binding of the gp32 ssb protein to KOS (A) and AN-1 (B) from Vero cells and AN-1 from 6-5 cells (C). In each image, the arrows point to representative regions of viral DNA on which gp32 has bound. There appears to be more gp32 binding to the AN-1 DNA from infected Vero cells (Figure 3.7.B) than to KOS DNA from Vero cells. In addition, gp32-binding of AN-1 DNA from 6-5 cells appears to be similar in quantity to the KOS DNA. This result suggests that AN-1 grown on Vero cells has more ssDNA than KOS grown on Vero cells or AN-1 grown on 6-5 cells.

3.5. DISCUSSION

3.5.a. AN-1 DNA: quantity vs. quality.

The phenotype of the UL12-null virus is quite complex. Wild-type levels of DNA are observed in AN-1-infected cells; however, this DNA is not infectious. Furthermore, at least some AN-1 DNA is cleaved into approximately unit length molecules and terminal fragments are observed, indicating that encapsidation has been initiated; however, the production of stable C-capsids and the number of C capsids in the cytoplasm are greatly reduced compared to wild type infections. This complex phenotype may indicate that UL12 is needed for two distinct steps, DNA processing and production of stable capsids. However, the defects displayed by AN-1 may all be attributed to a single event, the production of aberrant DNA. Previously published findings are consistent with this notion. For example, although AN-1 synthesizes 60 to 90% of wild type DNA levels, viral yields of AN-1 are only 0.1 to 1% of wild type yields (Weller, Seghatoleslami et al. 1990, Shao, Rapp et al. 1993, Martinez, Shao et al. 1996). Furthermore, replicating DNA ("well DNA" in PFGE) has been shown to be more complex than in AN-1 infection than wild type infection, and virion DNA appears as a smear by PFGE (Martinez, Sarisky et al. 1996). Taken together, these results suggest that, although DNA is produced in AN-1 infection, it is unusual. We were intrigued by the possibility that the defect in AN-1 growth was due to the aberrant structure of DNA produced during AN-1 infection.

In this chapter, we demonstrated that purified viral DNA produced by the AN-1 mutant virus is not infectious because it cannot support immediate early gene expression in transfected cells. AN-1 DNA was also not infectious in cells that express the UL12

gene (6-5 cells). This may indicate that the loss of infectivity phenotype of purified AN-1 DNA cannot be rescued in the presence of UL12. It should be noted, however, that the UL12 gene in 6-5 cells is controlled by the ICP6 promoter (Shao, Rapp et al. 1993), and therefore requires immediate early gene expression to be activated. Since immediate early gene expression does not occur in cells transfected with AN-1 DNA, UL12 would not be present. Another consideration is that viral genes that are stably integrated into cellular genomes generally remain silent unless infected with virus, thus UL12 expression is not likely to occur in transfected cells. Wild type KOS DNA also appeared to produce fewer plaques on 6-5 cells than on Vero cells (Figure 3.1). There is currently no clear explanation for this observation; however, it may be due to variation in expression levels and kinetics between the UL12 gene in the viral genome versus the UL12 gene in 6-5 cells. UL12 is a potent exonuclease, and it is likely that its function must be regulated during infection, possibly by phosphorylation or other post-translational modifications. Further experiments will be required to confirm this hypothesis, but it is possible that overexpression of UL12 is not tolerated by wild type KOS because it cannot regulate excess amounts of UL12.

3.5.b. What is the nature of compression zone (CZ) DNA?

We are particularly intrigued by the notion that DNA produced in the absence of UL12 is aberrant, and we have begun characterization of the DNA produced in AN-1-infected cells. As shown in Figures 3.3 and 3.4, we identified a species of DNA that migrated in the "compression zone" (CZ DNA). CZ DNA was seen when AN-1 was grown in non-complementing cells but not detectable in partially permissive cells. By

definition, the CZ is beyond the linear range of separation in PFGE. Therefore, the species of AN-1 DNA migrating within the CZ could represent a large range of sizes and possibly structures. Further experiments will be required to better characterize this species of DNA. Better resolution of CZ DNA during PFGE may be achieved by altering the manner in which voltage is applied to the gel. The PFGE experiments presented in this chapter utilized a ramped switch time from 2 seconds to 70 seconds and a pulse angle 120°. Increasing the final switch time and decreasing the pulse angle from 120° to 94° may result in better resolution. It may be possible to determine whether CZ DNA contains unusual structures through treatment with structure specific endonucleases, such as T7 endonuclease I, which cleaves X and Y structures to produce linear DNA. Infected cell plugs could be treated with the enzyme and then PFGE could be employed to determine whether the treatment successfully resolved the CZ DNA. Although we would like to excise and purify CZ DNA from gels for EM analysis, this would likely be troublesome for two reasons. First, the CZ contains not only viral DNA but also cellular DNA, which would be present in all samples. Second, the amount of viral CZ DNA that can be separated in one PFGE well is very small. Because the CZ contains both cellular and viral DNA, the individual species within the CZ cannot be accurately quantified.

The observation that CZ DNA was not present in ANF-1 infected cells was surprising. ANF-1 only expresses the UL12.5 gene product, which cannot complement for UL12 for viral growth (Martinez, Goldstein et al. 2002). UL12.5 is lacks a nuclear localization signal (NLS), and is known to localize predominantly to the cytoplasm, specifically to the mitochondria (Corcoran, Saffran et al. 2009). Thus it has been assumed that it would not influence viral DNA replication, which takes place in the nucleus, There

are several interesting possibilities to explain why AN-F1 is defective for viral growth but does not produce the CZ DNA produce. First, although UL12.5 does not contain an NLS, it is possible that some UL12.5, which is active for nuclease, may still be getting to the nucleus and processing or eliminating CZ DNA; however, it is not a great enough quantity to affect viral titer. A more speculative possibility pertains to the fact that UL12.5 is required for the elimination of mitochondrial DNA that takes place during HSV-1 infection (Latchman 1988, Saffran, Pare et al. 2007). We know that HSV-1 infection results in an increased oxidation state (Palamara, Perno et al. 1995, Mathew, Bryant et al. 2010). What causes the increase in oxidation state is currently unknown; however, mitochondrial dysfunction is often associated with aberrant oxidation, and it is possible that elimination of mitochondrial DNA could contribute to the increased oxidation observed during HSV-1 infection. Oxidation and production of reactive oxygen species could result in extensive DNA damage, which in turn could stimulate DDR proteins that participate in recombination. Although UL12.5 is not required for efficient viral replication (Martinez, Goldstein et al. 2002), perhaps in the absence of full length UL12, UL12.5 provides an alternative mechanism to stimulate recombination dependent replication during HSV-1 infection. To further explore the contributions of UL12 and UL12.5 to the outcome of viral DNA replication, it would be valuable to examine the DNA produced during infection with the UL12 M127 mutant virus, which expresses UL12 but not UL12.5 (Martinez, Goldstein et al. 2002).

3.5.c. Does aberrant DNA account for the defects in C capsid formation during AN-1 infection?

AN-1 infection produces an abundance of A capsids, which are thought to be produced as a result of abortive packaging (Addison, Rixon et al. 1990, Shao, Rapp et al. 1993). This observation and the diffuse nature of AN-1 C capsids, led us to hypothesize that AN-1 C capsids were in some way more fragile than wild type C capsids. Thus, we were surprised to find that the C capsids produced during AN-1 infection were as stable as, if not more stable than, wild type C capsids. However, using an ssb-DNA binding experiment, we showed that encapsidated AN-1 DNA has more single strand regions than wild type DNA (Figure 3.7). It is unclear at this time whether the nature of the virion DNA contributes to the diffuse appearance of C capsids produced during AN-1 infection in non-complementing cells, which we observed by sucrose gradient sedimentation (Figure 3.5). In addition, it is tempting to speculate that these observations may correlate to the smeared appearance of unit-length AN-1 DNA by PFGE, because ssDNA may contribute to the fragility of DNA and result in breakage.

3.5.d. UL12, AN-1 DNA, and the cellular DNA damage response.

In this chapter, we have proposed that AN-1 DNA is not infectious because it contains structural abnormalities. We have previously shown (Chapter 2) that altering the structure of viral DNA can greatly affect DDR pathway choice and lead to loss of infectivity. In Chapter 2, we manipulated the structure of wild type DNA in order to determine the requirements for infectivity. We demonstrated that, although the virus tolerates some unusual DNA structures, introducing 5' flaps into virion DNA eliminates

the infectivity of KOS DNA (Smith, Reuven et al. 2014). In this situation, infectivity is lost because 5' flaps induce robust DNA-PKcs activity. DNA-PKcs has many antiviral properties, including its role as an activator of the classic non-homologous end joining (C-NHEJ) DNA repair pathway (Lees-Miller, Long et al. 1996, Taylor and Knipe 2004, Smith, Reuven et al. 2014). We have proposed that DNA-PKcs exerts its antiviral effects during HSV-1 infection by promoting incorrect pathway choice. One interesting explanation for the lack of infectivity of AN-1 DNA may be that this DNA is the result of incorrect pathway choice.

The production of aberrant DNA during AN-1 infection may illustrate the important role that UL12 plays in DNA repair pathway choice during HSV-1 infection. Because HSV-1 DNA replication remains poorly understood it is difficult to fully understand the function of UL12 in the HSV-1 virus life cycle. HSV-1 replication produces complex DNA structures, but the mechanism for this remains unknown. We have proposed that HSV-1 utilizes SSA to produce concatemers (Schumacher, Mohni et al. 2012), but how this is initiated and how the process plays out in the context of infection is also unclear. It is possible that UL12 is required to direct repair toward the correct pathway, either by resecting DNA at DSBs or recruiting DDR proteins. The role of UL12 in DNA repair pathway choice will be explored in more detail in Chapter 4.

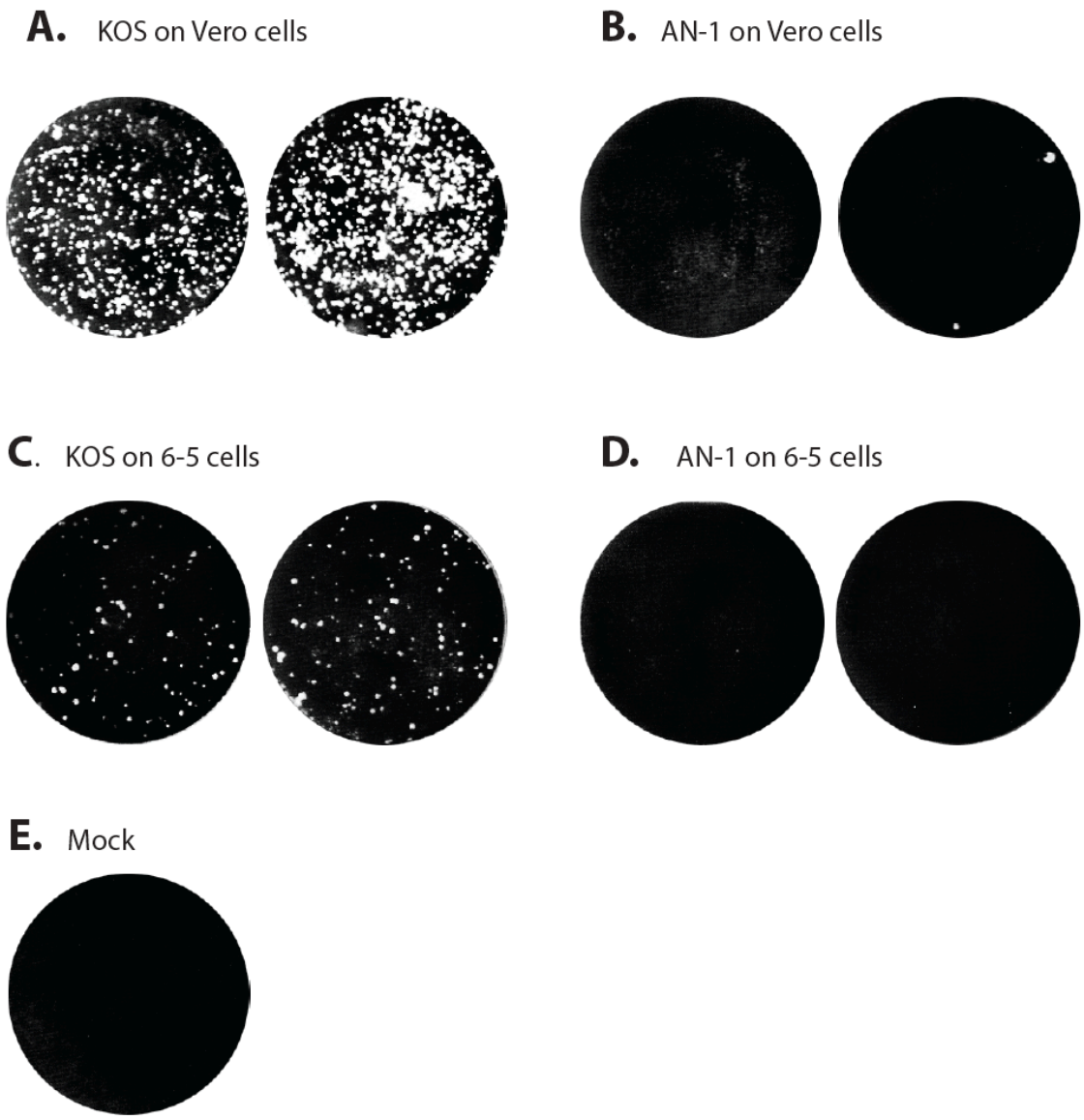

Figure 3.1. Plaque assay for cells transfected with purified virion DNA. A. Vero cells transfected with KOS DNA. B. Vero cells transfected with AN-1 DNA. C. 6-5 cells transfected with KOS DNA. D. 6-5 cells transfected with AN-1 DNA. E. Mock transfected Vero cells. Each sample has two replicates.

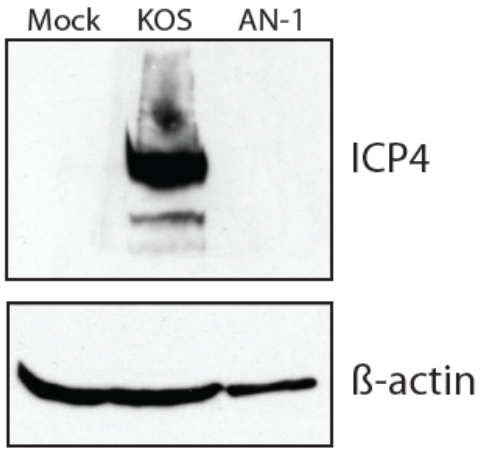

Figure 3.2. ICP4 is expressed in Vero cells transfected with purified KOS DNA, but not in Vero cells transfected with purified AN-1 DNA. Using Lipofectamine Plus Reagent (Invitrogen), Vero cells were transfected with 0.5μg of DNase resistant DNA was purifed from either KOS or AN-1 infection. Cells were harvested at ~24 hours following serum addition and analyzed by western blot with mAb α ICP4 (U.S. Biological) [1:1000], and mAb α ß-actin (Sigma) [1:5,000].

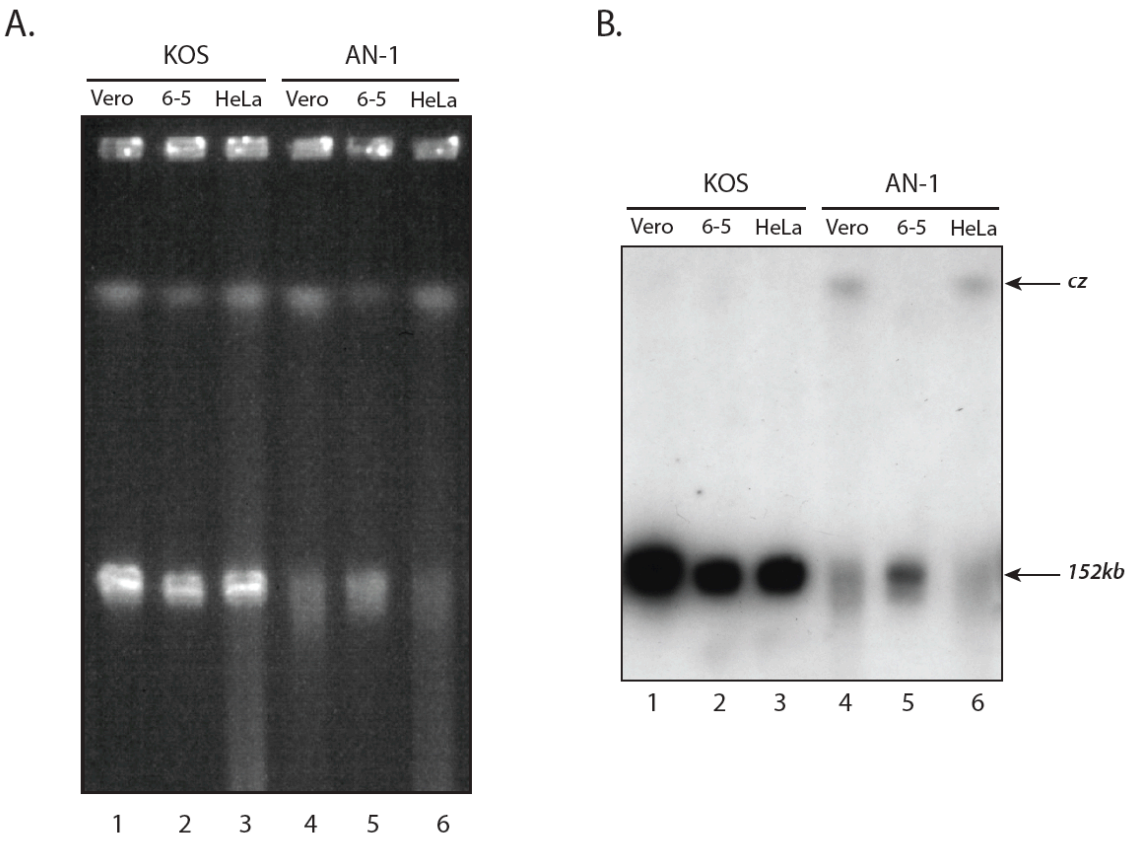

Figure 3.3. Pulsed field gel electrophoresis of KOS and AN-1 DNA. KOS and AN-1 -infected cells were embedded in agarose and treated with Proteinase K. Samples were then separated by PFGE. A. Ethidium bromide stain of total DNA B. Southern blot was performed with *BamHI* K probe (SQ fragment). Arrow for "cz" points to bands in compression zone (present in AN-1/Vero and AN-1/HeLa samples only). Numbers indicate lane numbers referred to in the text.

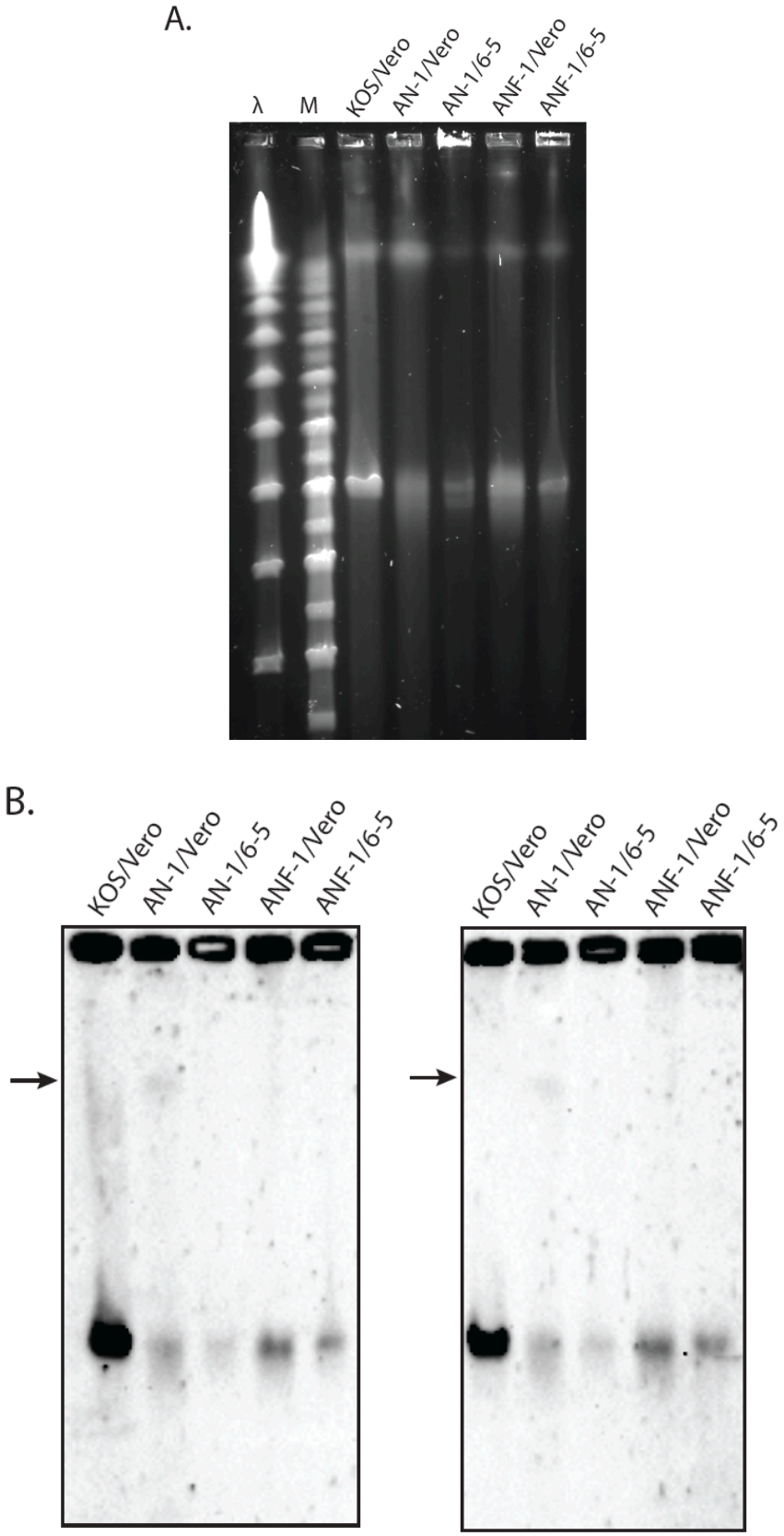
A.
λ
M
KOS/Vero
AN-1/Vero
AN-1/6-5
ANF-1/Vero
ANF-1/6-5
B.
KOS/Vero
AN-1/Vero
AN-1/6-5
ANF-1/Vero
ANF-1/6-5
KOS/Vero
AN-1/Vero
AN-1/6-5
ANF-1/Vero
ANF-1/6-5

Figure 3.4. Pulsed field gel electrophoresis of KOS, AN-1, and ANF-1 infected Vero and 6-5 cell plugs. A. SYBR Gold staining of total DNA. "λ" indicates lambda ladder (NEB) and "M" indicates Midrange II marker (NEB). This image correlates to the blot on the left side of panel B. B. Replicate southern blots with biotinylated *BamHI* S-fragment probe. Arrow points to bands in compression zone "cz" (present in AN-1/Vero samples only).

A.

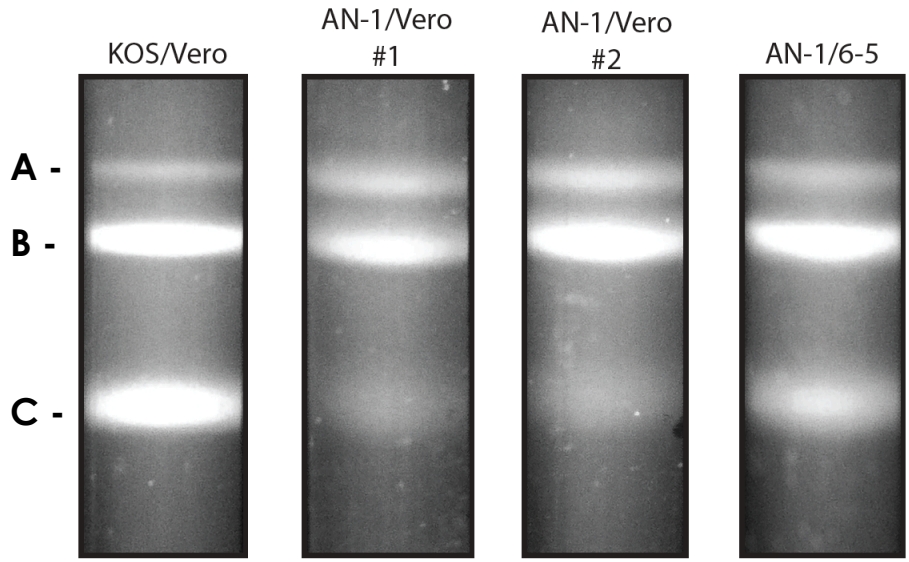
KOS/Vero
AN-1/Vero #1
AN-1/Vero #2
AN-1/6-5
A -
B -
C -

B.

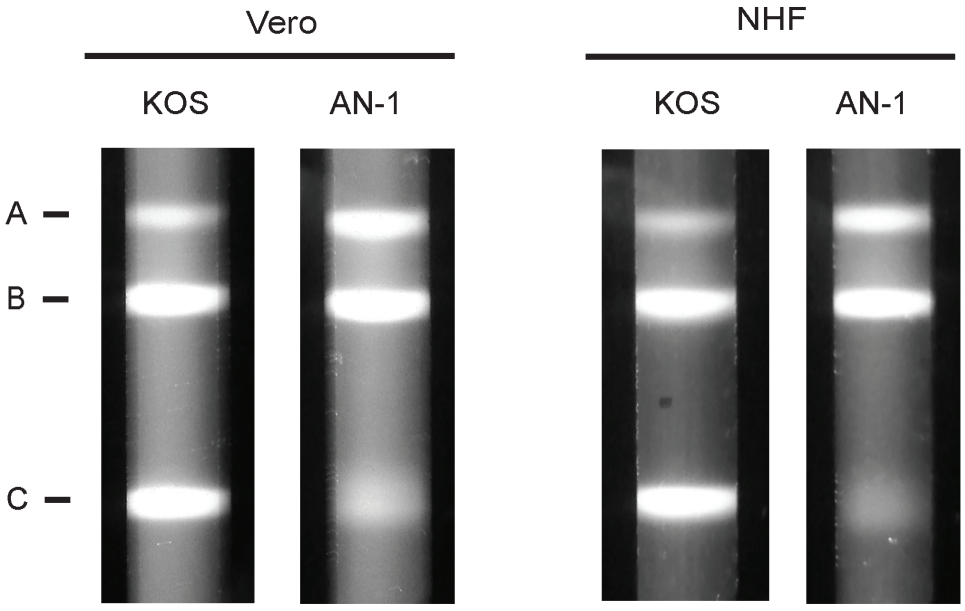
Vero
NHF
KOS
AN-1
KOS
AN-1
A
B
C

Figure 3.5. Sucrose gradient sedimentation of capsids isolated from KOS and AN-1 infected cells. Capsids were separated by analytical ultracentrifugation on a sucrose density gradient (50-20%). A. KOS and AN-1 infection on Vero cells and AN-1 infection on 6-5 cells. For AN-1/Vero samples, #1 and #2 represent replicate samples. B. KOS and AN-1 capsids from infected Vero and NHF cells.

A.

KOS from infected Vero cells

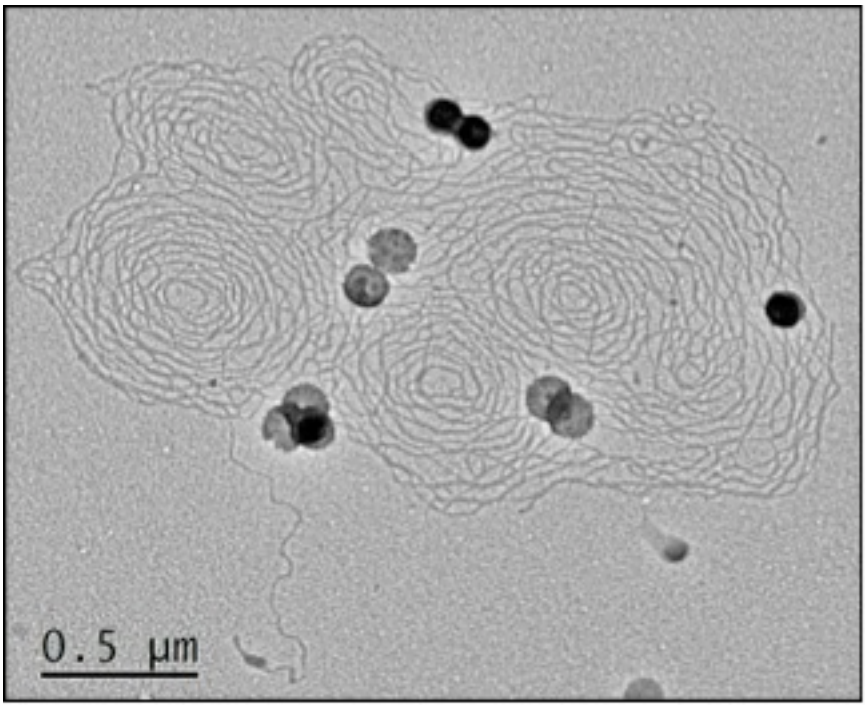

B.

AN-1 from infected Vero cells

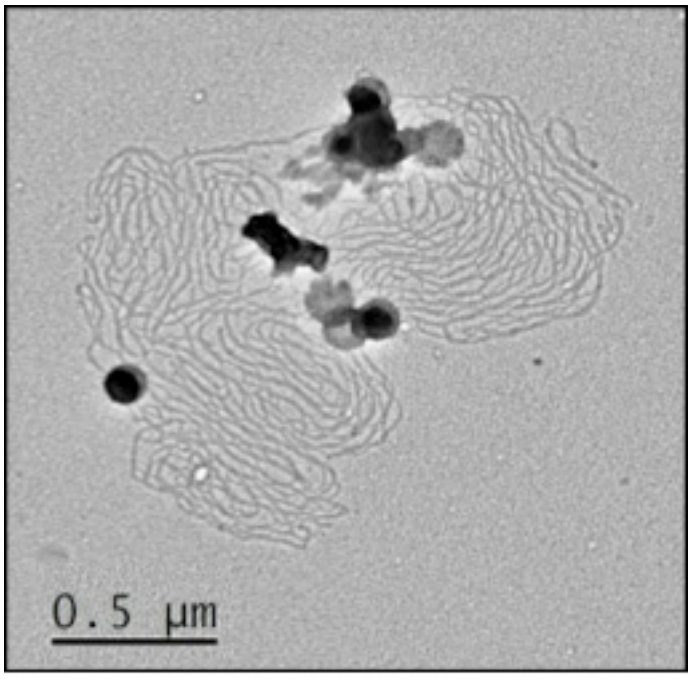

Figure 3.6. Genomes isolated from KOS and AN-1 C-capsids appear to be similar by electron microscopy (EM) analysis. C-capsids were isolated from KOS (A) and AN-1 (B) infected Vero cells using sucrose gradient ultracentifugation. Samples were diluted 1:10 in 10mM Tris & 250mM ammonium acetate. Samples were incubated in cytochrome C and then immediately spread onto an EM grid and imaged.

A.

KOS DNA from infected Vero cells

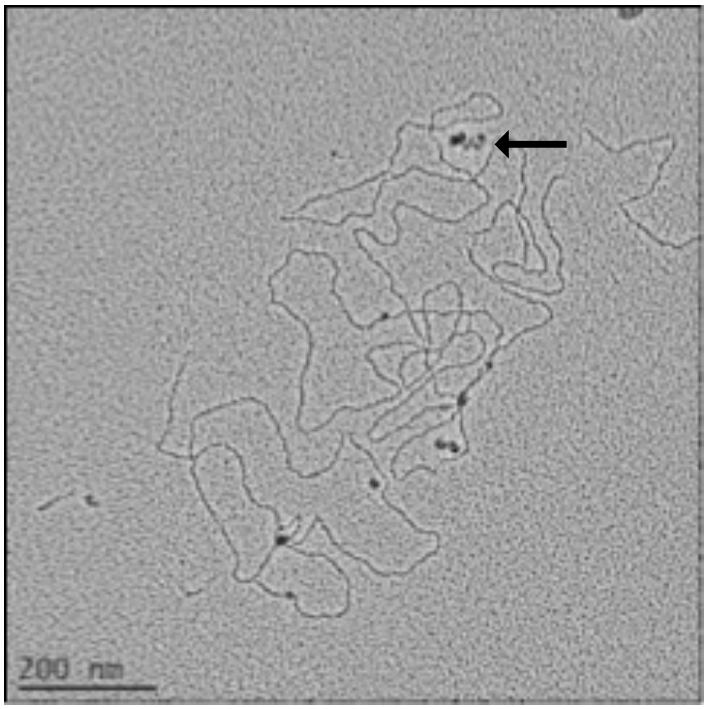

B.

AN-1 DNA from infected Vero cells

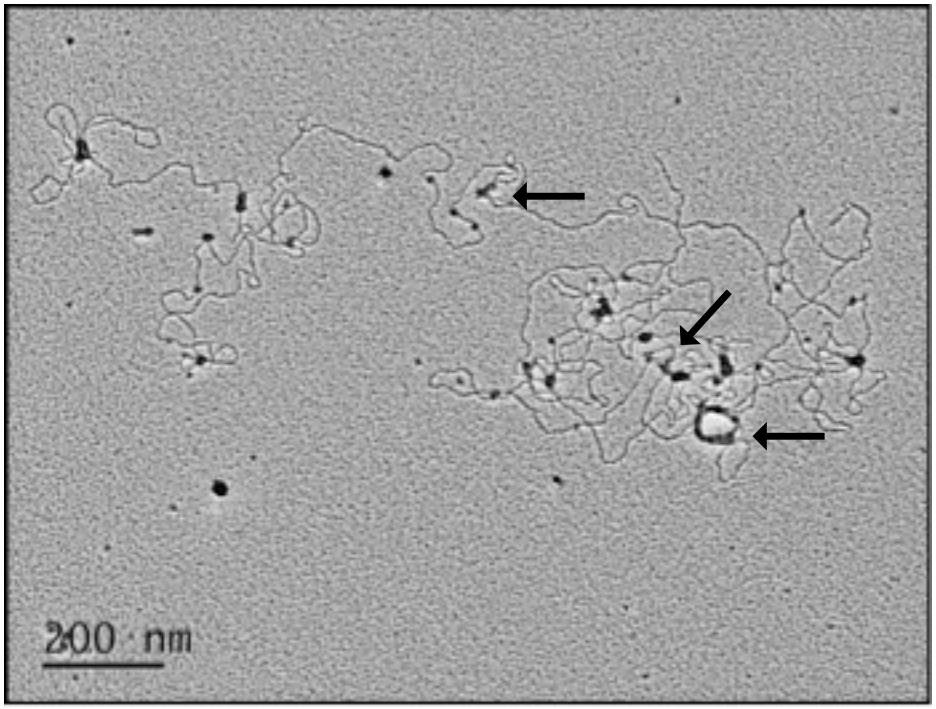

C.

AN-1 DNA from infected 6-5 cells

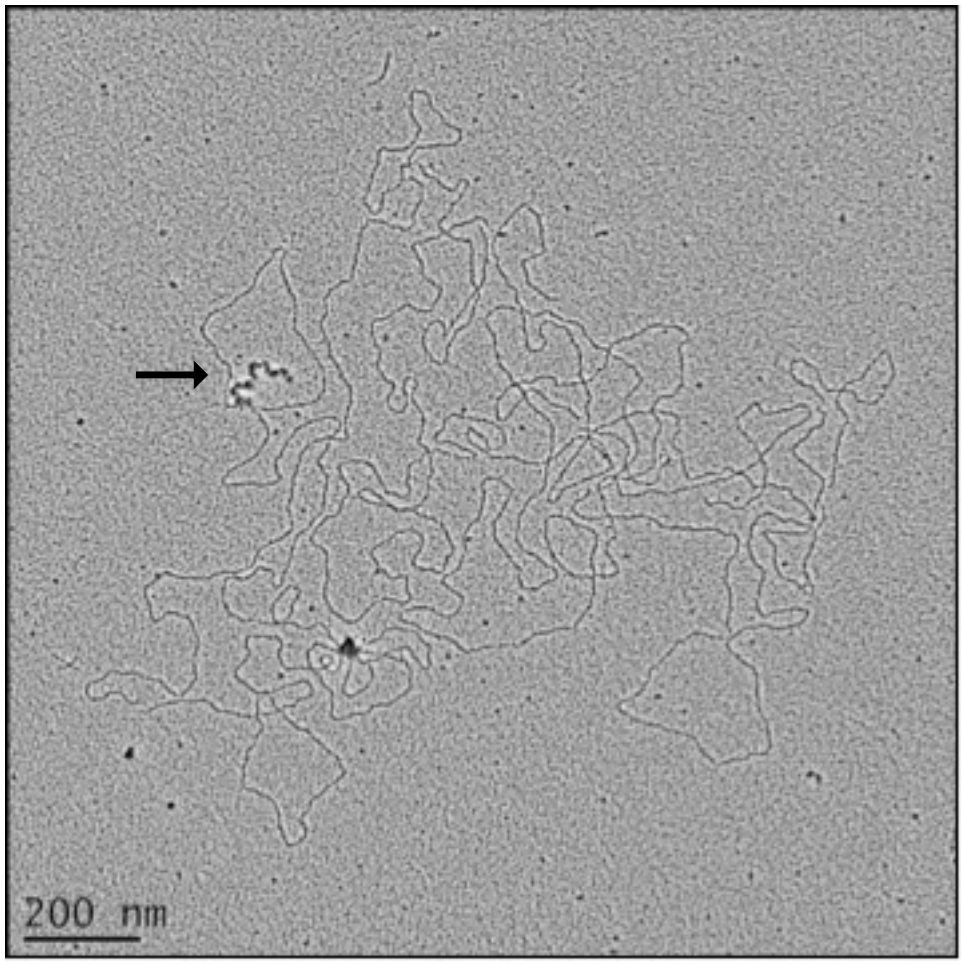

Figure 3.7. AN-1 DNA from C-capsids isolated from infection of non-complementing cells (Vero) contains more ssDNA than KOS. EM analysis of gp32-binding to KOS and AN-1 DNA from Proteinase K-treated C capsids. Arrows indicate examples of ssb bound to DNA.

CHAPTER 4.

The HSV-1 alkaline nuclease, UL12, inhibits Ligase IV-mediated NHEJ during infection.

Samantha Smith, Kareem N. Mohni, and Sandra K. Weller

Author contributions: KNM performed the experiments in Figure 4.4.B. All other experiments performed by S.S.

4.1. ABSTRACT

Replication of herpes simplex virus 1 (HSV-1) is associated with a high degree of recombination, and cellular DNA damage response (DDR) pathways have been shown to exert both positive and negative effects on this process. HSV-1 has evolved mechanisms to influence DDR pathway choice in order to establish productive infection. We have previously shown that HSV-1 stimulates the single strand annealing (SSA) pathway, while inhibiting homologous recombination (HR), classic non-homologous end joining (C-NHEJ), and microhomology-mediated end joining (MMEJ). We have now shown that knockout of the core C-NHEJ proteins, LIG IV and XRCC4, improves growth of wild type virus 2- to 3-fold, suggesting that these proteins are antiviral. The viral proteins, UL12 and ICP0, have both been implicated DDR pathway choice during infection. Therefore, in this chapter, we have set out to examine the roles of UL12 and ICP0 in the

suppression of C-NHEJ and MMEJ. Using knockout cell lines for core C-NHEJ proteins, we demonstrated that growth of the UL12-null virus (AN-1) was more robust on C-NHEJ deficient cells; whereas, ICP0-null (0β) growth was unchanged on these cells. In addition, using a reporter substrate that measures relative MMEJ and C-NHEJ activities, we found that C-NHEJ was more active in the absence of UL12, and MMEJ was more active in the absence of ICP0 compared to wild type. Taken together, these findings suggest that UL12 may play a role in suppressing C-NHEJ, and ICP0 may help to suppress the MMEJ pathway during infection.

4.2. INTRODUCTION

4.2.a. The cellular DNA damage response (DDR).

In order to maintain genetic integrity, cells encode a variety of mechanisms for the repair of DNA damage. The two main pathways for double strand break repair (DSBR) are homologous recombination (HR) and non-homologous end joining (NHEJ) (Figure 4.1). Although lower organisms rely on HR for most DSBR, vertebrates predominantly utilize NHEJ. HR requires extensive amounts of homology in order to facilitate repair; whereas, NHEJ requires little or no sequence homology at the dsDNA ends. HR encompasses at least two homology-dependent recombination mechanisms, including strand invasion (SI) and single strand annealing (SSA). NHEJ encompasses at least two discrete pathways that facilitate repair of DSBs through direct fusion of dsDNA ends, classic non-homologous end joining (C-NHEJ) and microhomology mediated end joining (MMEJ). These pathways differ in the proteins and mechanisms used to facilitate

end joining. The most well defined NHEJ pathway is classic (or canonical) non-homologous end joining (C-NHEJ).

C-NHEJ is initiated when the Ku70/86 heterodimer senses DSBs and binds dsDNA ends (Figure 4.2). This is a crucial step, as it not only promotes C-NHEJ, but also prevents end resection and thus inhibits other DNA repair pathways, such as HR, SSA, and some types of MMEJ. The DNA-dependent protein kinase catalytic subunit (DNA-PKcs) is recruited to dsDNA ends by Ku and phosphorylates other DNA-modifying enzymes. For example, DNA-PKcs binds and phosphorylates Artemis, the endonuclease activity of which is involved in end-trimming or other processing if the ends are not easily ligatable (Figure 4.2, right panel). The end ligation reaction is performed by DNA ligase IV (LIGIV), which forms a trimeric complex with its accessory factors, XRCC4 and XLF (Figure 4.2, left panel)(Lieber 2010).

The "core" components of the C-NHEJ pathway are thought to include the Ku70/86 heterodimer (hereafter Ku), DNA-dependent protein kinase catalytic subunit (DNA-PKcs), Artemis, DNA ligase IV (LIGIV), X-ray-cross- complementation gene 4 (XRCC4), and Cernunnos/XRCC4-like factor (XLF); however, some of these proteins may be dispensable for C-NHEJ (Figure 4.2). Genetic studies in conditional knockout cell lines using reporter plasmids biased for NHEJ have revealed that C-NHEJ can occur in the absence of Ku, ostensibly using only the LIGIV/XRCC4/XLF complex to facilitate repair (Oh, Harvey et al. 2014). Even though it is not absolutely required for C-NHEJ, Ku is an important factor in DSBR pathway choice, as its presence can inhibit other DDR pathways, such as LIGIII (DNA Ligase III)–mediated MMEJ (described below) (Oh, Harvey et al. 2014). XLF may also be dispensable, as it may functionally overlap DNA-

PKcs and ATM (Kumar, Alt et al. 2014). In addition, C-NHEJ that does not require end processing may proceed in the absence of DNA-PKcs and Artemis (Ma, Pannicke et al. 2002, Kumar, Alt et al. 2014). DNA-PKcs is an evolutionarily new protein, which does not exist in lower eukaryotes and prokaryotes. Because of this, C-NHEJ in higher organisms is sometimes referred to as D-NHEJ (DNA-PKcs-dependent C-NHEJ) (Dueva and Iliakis 2013). This is an important distinction, given that NHEJ is flexible with respect to the substrates it acts on and the components required.

Microhomology-mediated end joining (MMEJ) is another form of NHEJ present in higher organisms; however, it is only activated when C-NHEJ is inhibited. Thus, plasmid rejoining assays in cells that are genetically deficient for C-NHEJ have demonstrated that MMEJ can be "unleashed" and its activity stimulated (Fattah, Lee et al. 2010). Because of this, MMEJ is sometimes referred to as alternative-NHEJ (A-NHEJ) or backup-NHEJ (B-NHEJ), indicating that is activated only when C-NHEJ is prevented. Figure 4.1 shows a hierarchical schematic of how cells may rely on MMEJ for repair when other mechanisms fail. MMEJ is thought to be similar in mechanism to SSA, although MMEJ requires only 5 to 25 nt of homology; whereas, SSA requires >30 nt to occur. Both SSA and MMEJ result in deletions and can cause genomic translocations. The role of this pathway is still poorly understood, but there is evidence that MMEJ functions as more than just a backup mechanism for C-NHEJ in humans. MMEJ is believed to be an important mechanism for repair of collapsed replication forks, and microhomology has been detected at breakpoint junctions of chromosomal translocations in human cancer cells, implicating MMEJ in their repair (Bentley, Diggle et al. 2004, Mattarucchi, Guerini et al. 2008, Tsai, Lu et al. 2008, Truong, Li et al. 2013).

4.2.b. DDR during HSV-1 infection.

Herpes simplex virus 1 (HSV-1) is a dsDNA virus that replicates its linear 152kb genome in the nucleus of host cells. Replication of HSV-1 DNA is associated with a high degree of recombination, and cellular DNA damage response (DDR) pathways have been shown to exert both positive and negative effects on this process (Lilley, Chaurushiya et al. 2010, Lilley, Chaurushiya et al. 2011, Weitzman and Weller 2011, Smith and Weller 2015). HSV-1 has evolved mechanisms to influence DDR pathway choice in order to establish productive infection. Using cell-based GFP correction assays, Schumacher et al., demonstrated that HSV-1 infection potently stimulates SSA activity, and inhibits HR and NHEJ (Schumacher, Mohni et al. 2012). We believe that HSV-1 mediates DDR pathway choice by inactivating components of the C-NHEJ and HR pathways, which may be antiviral, while recruiting DDR elements that are favorable for productive infection.

In Chapter 2, we proposed that the viral ubiquitin ligase, ICP0, may be a key mediator of DDR pathway choice during infection. ICP0 degrades numerous proteins involved in the cellular antiviral and DNA damage responses, such as PML, IFI16, DNA-PKcs, RNF8, RNF168, and PARG (Lees-Miller, Long et al. 1996, Everett, Freemont et al. 1998, Lilley, Chaurushiya et al. 2010, Grady, Hwang et al. 2012, Johnson, Chikoti et al. 2013). In fact, several components of the C-NHEJ pathway have been shown to be antiviral. HSV-1 viral yields are 30 to 50-fold greater in Ku70-deficient MEFs, compared to growth on wild type MEFs (Taylor and Knipe 2004), and Parkinson, et al., have reported that HSV-1 virus yields were greater in human glioma cells that are deficient for DNA-PKcs (Parkinson, Lees-Miller et al. 1999). We and others have shown that DNA-

PKcs is degraded or inhibited in many cell types during infection (Lees-Miller, Long et al. 1996, Parkinson, Lees-Miller et al. 1999, Lin, Noyce et al. 2004, Taylor and Knipe 2004, Lilley, Carson et al. 2005, Smith, Reuven et al. 2014). Therefore, DNA-PKcs appears to be antiviral, and the ability of ICP0 to degrade DNA-PKcs provides one mechanism by which HSV-1 counteracts its activity. Furthermore, we have shown that even in cells in which DNA-PKcs is not degraded, ICP0 can directly inhibit its activity (Smith, Reuven et al. 2014).

It has been assumed that the inhibition of DNA-PKcs by ICP0 results in the inhibition of C-NHEJ; however, the recognition that DNA-PKcs-independent pathways of C-NHEJ exist in mammalian cells complicates this analysis (Figure 4.2). It is therefore important to look at how HSV-1 interacts with core components of the C-NHEJ pathway, such as LIGIV and XRCC4, in order to determine the mechanism by which C-NHEJ is inhibited during infection. It is clear that ICP0 plays a role in counteracting antiviral mechanisms, but there may be additional viral factors required to effect pro-viral pathway choice and inhibit C-NHEJ. In other words, other factors are likely to influence the fate of the viral genome and how it is replicated.

In this chapter, we will investigate whether the viral alkaline nuclease, UL12, also influences cellular DDR pathway choice during infection. Using GFP repair assays, we have shown that UL12 exonuclease activity potently stimulates SSA (Schumacher, Mohni et al. 2012). In addition, UL12 interacts with DDR proteins, such as Ku70 and the MRN (MRE11/RAD50/NBS1) complex (Balasubramanian, Bai et al. 2010, Balasubramanian 2011). Recently, UL12 was also shown to interact with FANCD2, which is a key mediator of DDR in uninfected cells and may contribute to inhibition of

C-NHEJ during infection (Karttunen, Savas et al. 2014). Although its precise function of UL12 in viral replication remains unclear, we have proposed that UL12 stimulates SSA in order to produce DNA concatemers that can be packaged into progeny virus. This notion is supported by the phenotype of two UL12-null viruses, AN-1 and *amb*UL12, which have been reported to produce structurally aberrant DNA that is inefficiently packaged into capsids (Shao, Rapp et al. 1993, Martinez, Sarisky et al. 1996, Porter and Stow 2004).

The picture that is emerging is that the DDR pathway chosen by HSV-1 during infection impacts the course of the infection in at least two ways. As mentioned above, some DDR pathways are antiviral and HSV has evolved mechanisms to counteract these. In addition it is important for HSV to generate concatemeric DNA suitable for encapsidation in order to produce infectious virus. HSV must walk a fine line, balancing these requirements. In this chapter, we will focus on the roles of UL12 and ICP0 in directing DNA repair pathway choice during infection. Because NHEJ has been shown to be antiviral, we will focus on the effects of both UL12 and ICP0 on the two types of NHEJ repair, classic non-homologous end joining (C-NHEJ) and microhomology-mediated end joining (MMEJ).

4.3. MATERIALS AND METHODS

4.3.a. Cell lines.

Vero, U2OS, and HCT-116 cells were obtained from American Type Culture Collection (ATCC), and the derivative cells lines: DNA-PK$^{-/-}$ (Ruis, Fattah et al. 2008), LIG IV$^{-/-}$ (Oh, Wang et al. 2013), XRCC4$^{-/-}$ (B. Ruis and E. A. Hendrickson, manuscript in preparation), and XLF$^{-/-}$ (Fattah, Kweon et al. 2014) were generously provided by Eric A. Hendrickson (University of Minnesota Medical School, Minneapolis, MN). The UL12-expressing Vero cell line, 6-5, was previously described (Shao, Rapp et al. 1993). Vero and 6-5 cells were grown in Dulbecco's modified minimal essential medium (DMEM) (Gibco) containing 5% fetal bovine serum (FBS). 6-5 cells were also supplemented with G418 to maintain selection for the UL12 cassette. HCT-116 and derivative cell lines were grown in McCoy's 5A medium (modified) (Gibco) containing 10% FBS. U2OS cells were grown in DMEM with 10% FBS.

4.3.b. Viruses.

The HSV-1 strain, KOS, was used as the wild-type virus in all experiments, unless otherwise noted. The UL12-null virus, AN-1, is derived from KOS and has been previously described (Weller, Seghatoleslami et al. 1990). The ICP0-null virus, 0β, was derived from KOS and contains *lacZ* insertions in both copies of the ICP0 gene. 0β was generously provided by Neal Deluca (University of Pittsburgh School of Medicine, Pittsburgh, PA). The HSV-1 strain 17+ viruses, *in1863* (wt) and *dl*1403/CMV*lacZ* (ΔICP0) were obtained from Chris Preston (MRC Virology Unit, Glasgow, Scotland). These viruses contain the *lacZ* gene under the control of the human cytomegalovirus

(HCMV) promoter/enhancer inserted into the *tk* gene (Strang and Stow 2007, Everett, Parada et al. 2008). KOS and *in1863* were grown and titrated on Vero cells. AN-1 was grown and titrated on 6-5 cells. 0β and *dl*1403/CMV*lacZ* were grown and titrated on U20S cells.

4.3.c. Western blot analysis.

Samples were harvested 24 hours following transfection and prepared for western blot analysis as previously described (Mohni, Dee et al. 2013). The primary antibodies used were polyclonal rabbit anti-Human DNA Ligase IV (1:1000; Abcam), monoclonal mouse anti-DNA-PKcs Ab-4 (Cocktail) (1:1,000; Neomarkers), and monoclonal mouse anti-b-actin (1:15,000; Sigma).

4.3.d. Pulsed-field gel electrophoresis (PFGE) and Southern blot analysis.

Cells were seeded in 60mm dishes and infected at an MOI of 5 for 24 h. Infected cells were then spun down and resuspended in 1200μL 1% low melting point agarose in 0.5X TBE buffer, except HCT-116* which was resuspened in 600 μL. Plugs were Proteinase K (Roche) digested overnight at 50ºC. Approximately 1/2 plug was loaded per well of 1% PFG grade agarose gel (BioRad) in 0.5X TBE buffer (45 mM Tris, 45 mM borate, 1 mM EDTA, pH 8.3). Electrophoresis was performed using a CHEF-DR III apparatus (Bio-Rad) with 0.5X TBE running buffer. Samples were separated at 6 V, switch times ramped from 2 to 70 s for 18 h at 14ºC. Following electrophoresis, gels were vacuum-transferred to GeneScreen Plus membranes (Dupont NEN), according to the manufacturer's protocols. Southern blot was performed using a biotinylated probe

specific for the *BamHI* S fragment of HSV-1. Detection was performed with CDP-Star reagent (NEB) on the BioRad Chemi-Doc MP imaging system.

4.3.e. Viral growth curves and yields.

Cells were seeded in 35mm dishes and infected at an MOI of 0.1 PFU/cell unless otherwise stated and harvested at the times described (0, 6, 12, 24, and 48 h post infection. KOS was titrated on Vero cells, AN-1 and D340E were titrated on 6-5 cells, and 0β was titrated on U2OS cells. When plaques were visible, the cells were fixed with 8% paraformaldehyde in 1X PBS (approximately 2 to 4 days post infection). Cells were stained using 0.1% crystal violet and plaques were counted.

4.3.f. Probability of plaque formation assay.

The probability of plaque formation assay was performed as previously described (Mohni, Livingston et al. 2010). Briefly, HCT-116, DNA-PK$^{-/-}$, and LIG IV$^{-/-}$ cells were infected with identical dilutions of in1863 and dl1403/CMVlacZ. Cells were fixed at 24 h postinfection with 2% paraformaldehyde for 1 h, and stained for β-galactosidase activity (5 mM potassium ferricyanide, 5 mM potassium ferricyanide, 2 mM MgCl2, and 1 mg/ml X-Gal [5-bromo-4-chloro-3- indolyl-β-D-galactopyranoside]). β-galactosidase-positive plaques were counted.

4.3.g. Microhomology assay.

The microhomology assay was performed as previously described (Verkaik, Esveldt-van Lange et al. 2002) with the following modifications. Briefly, cells were infected with wild type (KOS), UL12-null (AN-1), a recombinant virus expressing the nuclease-dead UL12 mutant (D340E), or ICP0-null (0β) virus at an MOI of 3. Cells were transfected with 1.5 μg of *EcoRV/AfeI*-linearized pDVG94 plasmid per well using Lipofectamine 2000 (Invitrogen) according to manufacturer's instructions. Cells were harvested at 48 h post transfection, and the repaired substrate was isolated using a modified Qiagen minipreparation protocol. Repaired products were PCR amplified using primer FM30 and DAR5 (Verkaik, Esveldt-van Lange et al. 2002). One half of the PCR product was digested with *BstXI* and one half was used as the undigested control. Samples were separated by polyacrylamide gel electrophoresis with using a 6% acrylamide gel and 1X TBE buffer. Gels were stained using SYBR Safe DNA stain (Invitrogen) and imaged using a ChemiDoc MP Imaging System (Bio-Rad). The 180bp and 120bp bands were quantified using ImageJ software.

4.4. RESULTS

4.4.a. DNA-PKcs inhibits probability of plaque formation, but not viral production in human epithelial cells.

As described in the introduction, various components of the C-NHEJ pathway have been shown to be antiviral. For instance, Parkinson et al., reported that virus production of wild type HSV-1 (syn17+ strain) DNA-PKcs deficient human glioma cells is 6 to 200-fold higher than on DNA-PKcs proficient cells (Parkinson, Lees-Miller et al. 1999). In order to further understand how and why C-NHEJ components are antiviral, we have explored the growth of wild type and mutant HSV-1 on cell lines deficient for DNA-PKcs and other components of the C-NHEJ pathway including LIGIV and XRCC4. If a cellular component such as DNA-PKcs is inhibitory to viral growth, viral replication is predicted to be more efficient on DNA-PKcs deficient cells. Furthermore, if the role of ICP0 is to inhibit an antiviral restriction factor, an ICP0 deficient mutant is predicted to grow better in cells deficient for that factor. We have used assays that either measure either virus production or the probability of plaque formation assay. The plaque formation assay reflects the probability that an incoming genome will commit the infected cell to lytic infection. This assay has proven a useful indication of whether a virus can overcome intrinsic antiviral mechanisms to establish a productive infection. The virus production assay measures total viral production and is not as sensitive for detecting early blocks to infection.

In order to confirm that DNA-PKcs is antiviral, we compared DNA-PKcs deficient and proficient versions of the human epithelial cell line (HCT-116) (Ruis, Fattah et al. 2008) in a plaque formation assay using *in*1863, a wild type 17syn+ strain

virus that contains a lac Z insertion. Figure 4.3.A shows that the *in*1863 exhibited no change in probability of plaque formation between wild type HCT-116 cells and DNA-PKcs$^{-/-}$ cells, a result that contrasts with that of Parkinson et al. (Parkinson, Lees-Miller et al. 1999). On the other hand, we were able to confirm the observation reported by Parkinson, et al. that virus production on DNA-PKcs$^{-/-}$ human glioma cells infected with an ICP0 deletion mutant (ΔICP0, *dl*1403) was up to 7-fold higher than on wild type cells (Parkinson, Lees-Miller et al. 1999). We were able to repeat this result using a probability of plaque formation assay. Figure 4.3.A shows that indeed, the probability of plaque formation by ΔICP0 is more than 5-fold greater on DNA-PKcs$^{-/-}$ cells than on wild type HCT-116 cells. Thus, in the absence of ICP0, DNA-PKcs inhibits viral growth confirming previous observations.

The observation that DNA-PKcs is antiviral may indicate that the C-NHEJ pathway itself is antiviral. However, in addition to its role in C-NHEJ, DNA-PKcs plays other roles in the cell including inhibition of transcription by RNAP II and DNA sensing as part of the IRF-3 immune response (Kuhn, Gottlieb et al. 1995, Ferguson, Mansur et al. 2012, Pankotai, Bonhomme et al. 2012). Thus, it is possible that DNA-PKcs is antiviral due to one of its additional functions apart from its role in C-NHEJ. If DNA-PKcs were antiviral due to its role in the C-NHEJ pathway, we would expect to see a greater probability of plaque formation on cells deficient for the essential C-NHEJ ligase, LIGIV, compared to wild type cells. Thus, to determine whether DNA-PKcs-independent C-NHEJ was antiviral, we measured the probability of plaque formation of wild type and ΔICP0 on an HCT-116 derivative cell line that was deficient for LIGIV (Oh, Wang et al. 2013). Again, we observed no change in probability of plaque formation on LIGIV$^{-/-}$ cells

infected with wild type virus (Figure 4.3.A). Interestingly, we also found that ΔICP0 did not exhibit increased probability of plaque formation in LIGIV$^{-/-}$ cells with ΔICP0-infected wild type cells. This suggests that the antiviral properties of DNA-PKcs may be related to a function other than C-NHEJ.

ICP0 is required to degrade or inhibit cellular factors that would otherwise restrict viral replication. The growth defects exhibited by ICP0-null viruses are much more pronounced at low multiplicities of infection presumably because the presence of restriction factors lowers the probability that the incoming viral genome will lead to lytic infection (Boutell and Everett 2013). Therefore, we wanted to determine whether virus production of the ICP0-null virus, 0β, would be inhibited by DNA-PKcs at very low multiplicities of infection (MOIs). We measured virus yields of 0β at very low MOIs on DNA-PKcs$^{-/-}$, and HCT-116 cells. We also tested virus yields for 0β on LIGIV$^{-/-}$ cells to determine whether a functional C-NHEJ mechanism would inhibit growth. Figure 4.4 shows that viral yields between the three cell types were not significantly different at any of the MOIs tested (MOI= 0.1, 0.05, 0.01, 0.005, and 0.001 PFU/cell). This was consistent with the findings in Parkinson et al. that ΔICP0 (*dl*14030 was not significantly inhibited by DNA-PKcs at very low MOIs (Parkinson, Lees-Miller et al. 1999).

Taken together, these results suggest that in the absence of DNA-PKcs plaque formation by an ICP0 mutant is enhanced, but virus production was not increased even at low multiplicities of infection. One explanation for this is that ICP0 degrades many proteins, some of which are antiviral, and depletion of DNA-PKcs alone may not be sufficient to overcome the defect caused by the absence of ICP0. Another interpretation is that that C-NHEJ is inhibited by a mechanism that does not involve ICP0 or

degradation/inhibition of DNA-PKcs. If C-NHEJ is inhibited even in the absence of ICP0, for example by another viral protein, then ΔICP0 viral yields would be unaffected by C-NHEJ deficiency. Since we know that C-NHEJ is inhibited during HSV-1 infection (Schumacher, Mohni et al. 2012), the results presented thus far suggest that an additional viral factor is required to inhibit C-NHEJ.

4.4.b. LIGIV and XRCC4 are antiviral.

HSV-1 may need to inhibit C-NHEJ in order to promote a DDR pathway that is beneficial for viral replication, and we were intrigued by the possibility that C-NHEJ may be inhibited by a mechanism other than degradation of DNA-PKcs. Therefore, we wanted to determine whether another viral factor was required to inhibit C-NHEJ during infection. We thought that UL12 may be implicated in DNA repair pathway choice and participate in inhibition of C-NHEJ, since UL12 has been shown to stimulate SSA repair (Schumacher, Mohni et al. 2012). In addition, UL12 has been shown to interact with cellular DDR proteins (Balasubramanian, Bai et al. 2010, Karttunen, Savas et al. 2014), although the biological significance of these interactions is not clear. Furthermore, we have shown that AN-1 (UL12-null) exhibits severe growth defects and produces aberrant DNA on non-complementing cells (Shao, Rapp et al. 1993, Martinez, Sarisky et al. 1996). We speculated that these defects were caused by the inability of AN-1 to induce a DDR pathway that would be conducive to productive infection. To assess whether UL12 plays a role in the manipulation of the cellular DDR, we asked whether AN-1 infection would be more efficient in cells defective for C-NHEJ. We also compared these results to KOS growth on the same cell lines. If our hypothesis is correct, we would expect that AN-1

yields would be greater on C-NHEJ deficient cells, and that the increase may be even more significant than the increase in KOS on LIG IV$^{-/-}$ and XRCC4$^{-/-}$.

In order to compare virus production from KOS and AN-1 infected C-NHEJ-deficient cells, we measured viral growth over time in wild type HCT-116 cells and the derivative cell lines DNA-PK$^{-/-}$, LIGIV$^{-/-}$, and XRCC4$^{-/-}$. Cells were infected at an MOI of 0.1 (PFU/mL). Samples were harvested at 0, 6, 12, 24, and 48 h post infection and titrated (as described in the Materials and Methods section). Figure 4.5.A shows the virus production over time in KOS-infected cells. Between 0 h and 24 h post infection, KOS viral yields were similar among the cell lines tested; however at 48 h post infection, growth yields of KOS on LIG IV$^{-/-}$ and XRCC4$^{-/-}$ cells were about 3 and 5 fold greater, respectively, than growth yields on either HCT-116 (wt) cells or DNA-PKcs$^{-/-}$ cells (Figures 4.5.A and 4.6). This result suggests that C-NHEJ is antiviral, since knocking out the core components of C-NHEJ, LIGIV and XRCC4, showed a small but reproducible improvement in viral growth. Furthermore, the observation that this effect was not seen on DNA-PKcs$^{-/-}$ cells supports the notion that the antiviral effect of C-NHEJ may be independent of DNA-PKcs.

We next wanted to determine whether C-NHEJ proteins inhibited AN-1 infection more efficiently than KOS infection. Figure 4.5.B shows viral growth curves for AN-1 on HCT-116, DNA-PKcs$^{-/-}$, LIGIV$^{-/-}$, and XRCC4$^{-/-}$ cells. As early as 12 h post infection, growth of AN-1 appears to be about 2-fold greater on all three knock out cell lines compared to growth HCT-116. By 48 h post infection, AN-1 growth is more than one log greater on XRCC4$^{-/-}$ cells than HCT-116 cells (Figures 4.5.B and 4.6.B). This increase is much more pronounced that than seen in KOS-infected LIGIV$^{-/-}$ and XRCC4$^{-/-}$ cells.

Thus, the core C-NHEJ proteins, LIGIV and XRCC4, are even more antiviral in the absence of UL12, suggesting that UL12 may play a role in inhibiting C-NHEJ during infection.

4.4.c. XLF may be dispensable for C-NHEJ.

We next asked whether XLF, another core C-NHEJ factor, was antiviral. During C-NHEJ, XLF interacts with DNA and forms filaments with XRCC4 and LIGIV to stabilize dsDNA ends and promote ligation (Gu, Lu et al. 2007, Ropars, Drevet et al. 2011, Mahaney, Hammel et al. 2013). We tested growth of KOS and AN-1 on HCT-116 and an $XLF^{-/-}$ derivative cell lines were infected at an MOI of 0.1, and viral yields were measured at 24 h and 48 h post infection. At these time points, KOS replication was approximately 2 to 3.5-fold less efficient on $XLF^{-/-}$ cells than on HCT-116 cells (Figure 4.6). The fact that virus production is decreased on XLF deficient cells suggests that XLF may have a beneficial role during KOS infection. In contrast, AN-1 grows approximately 2 to 3-fold more efficiently on $XLF^{-/-}$ cells than on HCT-116 cells. This result suggests that XLF may be antiviral but only in the absence of UL12. AN-1 growth on $XLF^{-/-}$ cells was considerably less efficient than on either $LIGIV^{-/-}$ or $XRCC4^{-/-}$ cells, suggesting that, like DNA-PKcs, XLF may be dispensable for C-NHEJ-mediated inhibition of HSV-1. In support of this notion, genetic studies have shown that XLF has overlapping roles with DNA-PKcs, 53BP1, and ATM, all of which have been implicated in DSBR pathway choice (Zha, Guo et al. 2011, Liu, Jiang et al. 2012, Oksenych, Kumar et al. 2013, Kumar, Alt et al. 2014). Furthermore, it has been suggested that these proteins may compensate for one and other in C-NHEJ. Thus, the fact that only a modest increase in virus

production was observed from AN-1 infection of XLF$^{-/-}$ cells may be due to compensatory roles of other proteins. Alternatively, given that XLF deficiency had opposite effects on wild type and AN-1 infections, it is possible that XLF exerts both positive and negative effects on infection. This may indicate that XLF plays more than one role during infection. Nevertheless, these results demonstrate that, in the absence of UL12, XLF is antiviral.

4.4.d. Aberrant DNA is produced in in cells that are non-permissive for AN-1 infection but not in semi-permissive DNA-PK$^{-/-}$ and LIG IV$^{-/-}$ cells.

We were intrigued by the possibility that UL12 is involved in pathway choice and contributes to the inhibition of C-NHEJ. Pulsed-field gel electrophoresis of viral DNA from AN-1-infected Vero or HeLa cells, which are non-permissive, revealed the presence of high molecular weight bands that do not resolve beyond the compression zone of the gel (CZ DNA) as well as a diffuse band of DNA at around 152 kb (*see* Chapter 3). On the other hand, KOS DNA and AN-1 DNA from complementing cells appears a discrete genome-length band at 152kb. We wanted to determine whether the unusual, aberrant structure of DNA produced when AN-1 is grown under non-permissive conditions was a result of an inappropriate DDR pathway choice. Because AN-1 replication was more efficient in cells deficient for C-NHEJ, we asked whether AN-1 DNA would appear less aberrant in cells deficient for C-NHEJ.

DNA from KOS and AN-1 infected cells was separated by PFGE and probed by southern blot for viral DNA (Figure 4.7). As shown on the left side of Figure 4.7, DNA from KOS-infected cells separated into two populations by PFGE. This is consistent with

previous reports that, when separated by PFGE, replicating HSV-1 DNA does not enter the gel and thus appears as "well" DNA, and genome-length HSV-1 DNA migrates at approximately 152kb (Martinez, Sarisky et al. 1996, Goldstein and Weller 1998). In addition, we observed that KOS infection produced significantly more genome-length DNA than AN-1 infection at the same MOI (consistent with the results presented in Chapter 3). AN-1 infection on HCT-116, HCT-116+3 (which express MLH1), and RAD52$^{-/-}$ all produce an aberrant, slow migrating band of viral DNA that appears in the compression zone (Figure 4.7, marked "*cz"*); however, AN-1 infected-DNA-PK$^{-/-}$ and LIG IV$^{-/-}$ cells do not. This result suggests that C-NHEJ may play a role in generating this aberrant phenotype.

Since the compression zone is beyond the limit of resolution in the PFGE, the exact size and structure of CZ DNA is not known. It is possible that the compression zone may contain genomes that are not linear; however, it seems likely that CZ DNA does not consist of simple circular genomes, since it does not migrate at the same position as the circular, bacmid-derived KOS genome (Figure 4.7, far right). Thus, CZ DNA is unlikely to be the result of simple end-to-end ligation of the genome, and may represent a more complex structure. Further experiments will be required to determine the precise structure(s) of DNA species within the CZ and the kinetics of CZ DNA formation during AN-1 infection.

4.4.e. UL12 may not require its nuclease activity to inhibit C-NHEJ.

Since UL12 is a potent exonuclease, and this activity is required for stimulation of SSA (Goldstein and Weller 1998, Schumacher, Mohni et al. 2012), we hypothesized that

UL12 nuclease activity might be needed to direct DDR pathway choice during infection. Specifically, we wanted to know whether UL12 nuclease activity was required to overcome viral inhibition by C-NHEJ. One possible mechanism by which UL12 could inhibit C-NHEJ could involve extensive resection of dsDNA ends. This resection could render dsDNA ends unsuitable for ligation by LIGIV. The D340E mutation in UL12 eliminates its exonuclease activity and is unable to stimulate SSA (Goldstein and Weller 1998, Schumacher, Mohni et al. 2012). If UL12 nuclease activity is required to inhibit C-NHEJ, then we would expect that growth of the UL12 D340E mutant would be greater on cells deficient for C-NHEJ proteins. Figure 4.8 shows virus yields for AN-1 and recombinant UL12 D340E virus at 24 and 48 h. Viral titers were measured following infection of HCT-116 cells and cells deficient for C-NHEJ proteins (DNA-PK$^{-/-}$, LIG IV$^{-/-}$, and XRCC4$^{-/-}$cell lines) at an MOI of 0.1. As shown in Figure 4.6, AN-1 grew better on cells that were deficient for core C-NHEJ proteins. In contrast, C-NHEJ proteins did not appear to be antiviral in the context of D340E infection, as viral growth was similar on all cell lines tested. In addition, D340E infection produced similar virus yields to AN-1 infection on LIG IV$^{-/-}$ and XRCC4$^{-/-}$ cells. This result suggests that UL12 does not require its nuclease activity in order to relieve the antiviral activity of C-NHEJ. Thus, UL12 may be inhibiting C-NHEJ by a mechanism that does not involve DNA end resection. Alternatively, UL12 may recruit another nuclease to perform end resection.

4.4.f. Measurement of MMEJ on C-NHEJ deficient HCT-116 cell lines.

Since UL12 appeared to inhibit the antiviral effects caused by C-NHEJ, we hypothesized that C-NHEJ may be more robust during AN-1 infection. To examine this

possibility, we measured the relative efficiency of MMEJ versus C-NHEJ during infection using the pDVG94 reporter substrate (Verkaik, Esveldt-van Lange et al. 2002, Lou, Chen et al. 2004). The pDVG94 plasmid is linearized by digestion with *AfeI* and *EcoRV* to produce a blunt-ended, dsDNA substrate that contains 6bp direct repeats at each end (Figure 4.9). End joining produces a circularized plasmid, which can then be recovered from transfected cells and PCR amplified. Repair of the substrate by MMEJ requires end resection, which removes one of the direct repeats, and thus creates a sequence that is sensitive to digestion by *BstXI* and appears as a 120bp band by polyacrylamide gel electrophoresis (PAGE). On the other hand, C-NHEJ generally preserves both direct repeats, and does not result in a *BstXI*-sensitive repair product, thus producing a 180bp uncut band by PAGE.

As mentioned earlier, C-NHEJ is the predominant mechanism of repair in vertebrates, and it has been proposed that MMEJ acts as a backup mechanism for repair if C-NHEJ fails (Dueva and Iliakis 2013, Oh, Harvey et al. 2014). This is supported by the observation that only about 1% of the total repaired pDVG94 plasmid recovered from wild type HCT-116 cells is *BstXI*-sensitive, which is to say that only about 1% of repair is facilitated by MMEJ ((Oh, Harvey et al. 2014) and Figure 4.10). On the other hand, almost all of the plasmid DNA recovered from C-NHEJ-deficient cells could be digested by *BstXI*, producing a 120 bp product ((Oh, Harvey et al. 2014) and Figure 4.10). Thus, MMEJ is the predominant form of repair in cells deficient for C-NHEJ proteins.

We used this assay to measure the relative frequency of repair by C-NHEJ versus MMEJ during wild type infection or infection with mutant viruses on the HCT-116 derivative cell lines. Cells were first infected with virus and transfected with the blunt-

ended linear pDVG94 substrate. At 48 h post infection, the repaired substrate was recovered, PCR amplified, subjected to *BstXI* digestion, and analyzed by PAGE. Figure 4.9 shows a representative experiment testing the effect of mock, KOS, AN-1, D340E, and 0β infections on MMEJ activity in the HCT-116 derivative cell lines. Table 4.2 shows the averages and statistics for replicate experiments and the average calculated relative frequency of MMEJ for each sample normalized to mock infection on HCT-116 cells.

In general, infection with the various viruses did not alter the predominant form of repair utilized in each of the cells lines. For example, C-NHEJ was the predominant repair mechanism in wild type HCT-116 cells (Figure 4.10, panel A), and the cell lines lacking components of the C-NEHJ predominantly utilized MMEJ for repair (Figure 4.10, panels B-E). We have previously shown that, using an HEK293 cell line with a chromosomally integrated reporter, MMEJ (A-NHEJ) is suppressed during infection (Schumacher, Mohni et al. 2012). This observation would seem to suggest that MMEJ is antiviral; however, the results shown in Figures 4.6 and 4.10 collectively suggest that KOS grows the same, if not a little better, on cells lines for which MMEJ is the predominant mechanism for end joining (i.e. DNA-PK$^{-/-}$, LIGIV$^{-/-}$, and XRCC4$^{-/-}$ cells). Thus, MMEJ activity may not be antiviral, even though it is suppressed in some cell types.

4.4.g. MMEJ is stimulated in 0β infected cells.

Because ICP0 degrades or inhibits DNA-PKcs in a variety of cell types (Lees-Miller, Long et al. 1996, Parkinson, Lees-Miller et al. 1999, Taylor and Knipe 2004, Smith, Reuven et al. 2014), we had initially thought that ICP0 was responsible for the inhibition of C-NHEJ during HSV-1 infection (Schumacher, Mohni et al. 2012). If this hypothesis were correct, we would have expected 0β to grow better on C-NHEJ deficient cells; however, this was not the case, since 0β did not grow better on LIGIV$^{-/-}$ cells (Figure 4.4). We therefore hypothesized that ICP0 may not be responsible for inhibition of C-NHEJ. To test this hypothesis, we used the pDVG94 reporter substrate, to measure repair by end joining during HSV-1 infection in the presence and absence of ICP0. If our hypothesis was correct, and ICP0 did not inhibit C-NHEJ, then we would expect the ratio of MMEJ to C-NHEJ to be similar in wild type and ICP0-null (0β) infected cells. For this assay we measured the proportion of end joining that was facilitated by microhomology (MMEJ) in HCT-116 and Vero cells during mock, KOS, AN-1 D340E, and 0β infections. The results were then normalized to the percent MMEJ for mock. Figure 4.11 represents the average of at least three individual experiments. We were surprised to find that in cells infected with 0β, the relative frequency of MMEJ was 2.5-fold (Vero) to 3-fold (HCT-116) greater than mock, meaning that C-NHEJ is more efficiently inhibited in the absence of ICP0. This suggests that rather than inhibiting C-NHEJ, ICP0 may play a role in inhibiting or at least regulating factors involved in MMEJ.

4.4.h. MMEJ is significantly reduced in AN-1 infected cells.

Figures 4.5 and 4.6 showed that AN-1 grew substantially better on LIGIV$^{-/-}$ and XRCC4$^{-/-}$ cells. Because of this, we thought that UL12 may play a role in inhibiting the C-NHEJ pathway during infection. Therefore, in the same assay described above, we also examined the effect of AN-1 infection on the relative frequency of MMEJ in HCT-116 and Vero cells. AN-1-infected HCT-116 cells exhibited 44% (about 2-fold) less MMEJ activity than mock-infected cells (Figure 4.11). MMEJ activity was further decreased in AN-1-infected Vero cells, about 33% (about 3-fold) less than mock-infected Vero cells. This suggests that MMEJ is significantly less active during AN-1 infection than it is in mock infection or in wild type KOS infection, and C-NHEJ is more robust in the absence of UL12 during infection. Thus, UL12 appears to play a role in the suppression of C-NHEJ during infection.

4.4.i. D340E infection stimulates MMEJ in HCT-116 cells, but inhibits MMEJ in Vero cells.

As mentioned earlier, C-NHEJ can occur in the absence of DNA-PKcs and Ku if the substrate being repaired has ends that are easily ligatable, and therefore do not require additional processing. Initially, we speculated that UL12 nuclease activity was required to resect DNA ends, rendering them unsuitable for ligation by LIGIV, and thereby inhibiting C-NHEJ. Thus, using the pDVG94 assay described above, we also tested whether the nuclease activity of UL12 was required to suppress C-NHEJ activity by measuring MMEJ activity during D340E infection of HCT-116 and Vero cells (Figure 4.11). An interesting discrepancy in the effect of D340E infection on MMEJ activity appeared between HCT-116 cells and Vero cells. MMEJ activity in HCT-116 cells

infected with D340E was significantly greater, about 4-fold, than in mock infected HCT-116 cells (Figure 4.11), suggesting that C-NHEJ is being inhibited. This finding is consistent with the observation that C-NHEJ does not appear to have an antiviral effect on D340E infection and supports our hypothesis that UL12 does not require nuclease activity to inhibit C-NHEJ during infection.

This observation, however, may be cell-type specific. In contrast to HCT-116 cells, Vero cells infected with the D340E exhibit significantly less MMEJ activity (nearly 2-fold less) compared to mock infected Vero cells (Figure 4.11, light green bars). This suggests that C-NHEJ may not be inhibited by D340E in this cell type. Thus, UL12 nuclease activity may affect MMEJ activity, perhaps by inhibiting C-NHEJ, in a cell-type specific manner. Another interesting explanation for this cell type dependence may be the presence of DNA-PKcs. We know that ICP0 degrades DNA-PKcs in HCT-116 cells, but not Vero cells [Mohni, unpublished data, (Wilkinson and Weller 2004)]. Furthermore, in Chapter 2, we demonstrated that DNA-PKcs signaling is inhibited in Vero cells, even though the protein is not degraded (Figure 2.7). Thus, in HSV-infected Vero cells, DNA-PKcs is present, but not catalytically active. Several studies have suggested that the presence of catalytically inactive DNA-PKcs is more deleterious to the cell than the absence of DNA-PKcs altogether because DNA-PKcs may still be able to inhibit other repair pathways, even in a catalytically inactive state (Calsou, Frit et al. 1999, Wang, Perrault et al. 2003, Perrault, Wang et al. 2004, Convery, Shin et al. 2005, Cui, Yu et al. 2005). It may be that, in cell types in which DNA-PKcs is not degraded, UL12 is required to overcome inhibition by DNA-PKcs and to stimulate more productive forms of repair.

Further experiments will be required to determine whether this is the case, and what affect inactive DNA-PKcs has on DDR pathway choice in the context of infection.

4.5. DISCUSSION

4.5.a. Summary

Cellular DNA damage response (DDR) pathways have been shown to exert both positive and negative effects on HSV-1 infection. Accordingly, HSV-1 has evolved mechanisms to influence DDR pathway choice in order to establish productive infection. Several lines of evidence suggest that C-NHEJ is antiviral, and that HSV-1 inhibits this pathway during infection. First, we have previously shown that NHEJ is inhibited during HSV-1 infection (Schumacher, Mohni et al. 2012). Furthermore, DNA-PKcs has been shown to moderately inhibit viral replication in infected human glioma cells (Parkinson, Lees-Miller et al. 1999). We have now shown that the knockout of the core C-NHEJ proteins, LIGIV and XRCC4, improves growth of wild type virus 2 to 3-fold, suggesting that these proteins are antiviral. The viral proteins, UL12 and ICP0, have both been shown to influence DDR pathway choice during infection, and we therefore sought to examine the roles of UL12 and ICP0 in the suppression of C-NHEJ and MMEJ activity.

Using knockout cell lines for core C-NHEJ proteins, we demonstrated that growth of the UL12-null virus (AN-1) was more robust on C-NHEJ deficient cells. Although growth of the ICP0-null virus (0β) was unchanged on C-NHEJ deficient cells, we found that viral gene expression was more robust on DNA-PKcs $^{-/-}$ cells (Figure 4.4). This result may suggest that DNA-PKcs has an auxiliary antiviral activity, which is separate from its role in C-NHEJ (discussed below). Finally, using a reporter substrate that measures

relative MMEJ and C-NHEJ activities, we found that C-NHEJ was more active in AN-1 infected cells, and MMEJ was more active in 0β infected cells, compared to mock infected cells (Figure 4.11). Taken together, these findings suggest that UL12 may play a role in suppressing C-NHEJ, and ICP0 may help to suppress the MMEJ pathway during infection; however, further studies will be required to determine the mechanisms underlying these observations.

The results described in this chapter demonstrate that both ICP0 and UL12 have essential and distinct roles in directing DDR pathway choice during HSV-1 infection. It has previously been shown that ICP0 acts as a "first line" of defense during HSV-1 infection by degrading or inhibiting components of ND10 and the DDR pathways in order to prevent silencing of the viral genome (Parkinson, Lees-Miller et al. 1999, Parkinson and Everett 2000, Lilley, Chaurushiya et al. 2011, Smith, Reuven et al. 2014). In addition, infection with an ICP0-null virus results in silencing of viral genomes in non-permissive cells (Jackson and DeLuca 2003). If ICP0 is unable to prevent genome silencing at early times, then the infection proceeds to latency. The phenotype of the UL12-null virus (AN-1), on the other hand, displays defects associated with later times during the HSV lifecycle, resulting in aberrant DNA structures and the accumulation of empty ("A") capsids (Shao, Rapp et al. 1993, Porter and Stow 2004). In this study we showed that C-NHEJ proteins, DNA-PKcs and LIGIV, may contribute to the production of aberrant, slow-migrating viral DNA during AN-1 infection, which has previously been observed in other non-complementing cell types (Figure 4.7 and Chapter 3). Thus, UL12 may influence viral replication at later times than ICP0 during infection.

4.5.b. UL12 may modulate cellular factors that influence DDR pathway choice, such as FANCD2, Ku70, and MRE11.

The mechanism by which a cell commits to a specific DNA repair pathway involves a variety of factors, including cell cycle, the nature of the damage, the structural complexity of DNA ends, and the repair proteins that initially respond to the DSB. Many of the details underpinning DDR pathway choice are still being disputed or remain unknown; however, it is clear that the inhibition or stimulation of DNA resection is a major determinant. HR, SSA, and MMEJ all require an initial end resection step; whereas, C-NHEJ does not (Lieber 2010, Truong, Li et al. 2013). In uninfected mammalian cells, the Ku70/86 heterodimer is thought to rapidly bind dsDNA ends in order to promote C-NHEJ (Fukushima, Takata et al. 2001, Zhang, Zhu et al. 2001, Beucher, Birraux et al. 2009, Shibata, Conrad et al. 2011) and inhibit HR, SSA, and MMEJ (Pierce, Hu et al. 2001, Stark, Pierce et al. 2004, Oh, Harvey et al. 2014). On the other hand, dsDNA end resection by MRE11 and CtIP is thought to disrupt Ku binding to DNA, and promote homology-mediated repair pathways (Shibata, Conrad et al. 2011, Truong, Li et al. 2013, Shibata, Moiani et al. 2014). In addition, the FA effector protein, FANCD2, has been shown to inhibit Ku70-binding to dsDNA ends by a similar mechanism, and thus inhibit C-NHEJ (Pace, Mosedale et al. 2010).

It is likely that end resection is also at the heart of DDR pathway choice during HSV-1 infection, and UL12 is strongly implicated in this process. We have previously shown that UL12 stimulates SSA in a nuclease-dependent fashion, perhaps by extensive resection at dsDNA ends (Schumacher, Mohni et al. 2012). We now also believe that UL12 plays a role in the inhibition of the C-NHEJ pathway during HSV-1 infection,

since the UL12-null virus (AN-1) grows significantly better on cells that are deficient for core C-NHEJ proteins. Interestingly, UL12 does not require its nuclease activity to inhibit C-NHEJ in HCT-116 cells (Figure 4.11). UL12 has been shown to interact with MRE11 (Balasubramanian, Bai et al. 2010) and FANCD2 (Karttunen, Savas et al. 2014), and perhaps recruits these factors in order to promote end resection and inhibit C-NHEJ. Ku70 has also been shown to interact with UL12 during HSV-1 infection (Balasubramanian, Bai et al. 2010); however, it is currently unclear whether UL12 exerts a positive or negative effect on Ku activity. In any case, UL12, by itself or with the help of interacting partners, may disrupt Ku binding at dsDNA ends (Figure 4.12). Future studies will be required to determine whether UL12 mediates DDR pathway choice, at least in part, through its interactions with cellular DDR factors, such as FANCD2, Ku70, and MRE11 (Balasubramanian, Bai et al. 2010, Balasubramanian 2011, Karttunen, Savas et al. 2014).

4.5.c. ICP0 and its complicated relationship with C-NHEJ

ICP0 acts as the special ops of HSV-1 infection; it eliminates cellular defenses that would otherwise silence the viral genome and inhibit infection. It is a fascinating protein because it inhibits and degrades numerous cellular factors during HSV-1 infection; however, the pleiotropic nature of ICP0 also makes it difficult to determine why it is beneficial for the virus to inhibit any individual target of ICP0. For instance, ICP0 degrades or inhibits DNA-PKcs signaling in numerous cell types, thus it is generally believed that ICP0 plays an important role in inhibiting C-NHEJ (Lees-Miller, Long et al. 1996, Parkinson and Everett , Smith, Reuven et al. 2014). Yet, DNA-PKcs is

not absolutely required for C-NHEJ, and the results presented in this paper suggest that ICP0 may inhibit DNA-PKcs in order to promote viral gene expression or evade other antiviral mechanisms.

ICP0 also degrades the cellular E3 ubiquitin ligase, RNF8 (Lilley, Chaurushiya et al. 2010). RNF8 is a DDR factor that is commonly associated with HR; however, it has also been shown to play an important role in facilitating resolution of C-NHEJ, by removing Ku86 from DSBs (Feng and Chen 2012). Thus, ICP0 may also help to inhibit C-NHEJ through degradation of RNF8. In order to determine whether this is the case, further experiments would be required to examine whether Ku86 is retained at DSBs in ICP0-null infected cells, and if so, what effect Ku86-retention may have on repair pathway choice during infection. In addition, it is possible that ICP0 affects DDR pathway choice through degradation of one of its other targets as well (discussed below).

4.5.d. ICP0-mediated degradation of PARG may inhibit MMEJ.

MMEJ remains poorly understood, in part because the factors required for this process are not completely defined. Nevertheless, several factors have been implicated in MMEJ. PARP-1 (poly (ADP-ribose) polymerase 1) is a molecular sensor of DNA breaks, and is thought to compete with Ku for binding of DNA ends (Wang, Wu et al. 2006). MRE11 has been shown to interact with PARP-1 and is recruited to DSBs to perform the initial end resection step required in order to expose regions of microhomology (Haince, McDonald et al. 2008, Bryant, Petermann et al. 2009, Pines, Mullenders et al. 2013). DNA ligase III (LIGIII) is thought to be the primary ligase involved in MMEJ, although DNA ligase I (LIGI) may compensate for LIGIII (Wang, Rosidi et al. 2005, Liang, Deng

et al. 2008). Other accessory factors implicated in MMEJ include XRCC1, CtIP, and DNA pol β (Ottaviani, LeCain et al. 2014), and additional proteins may yet be identified.

In this study, we have reported that MMEJ is stimulated in cells infected with the ICP0-null (0β) virus (Figure 4.11), suggesting that ICP0 may inhibit MMEJ during HSV-1 infection. Given that the components of MMEJ are not fully characterized, it is difficult to conjecture as to the mechanism by which ICP0 inhibits MMEJ; however, among the known degradation targets of ICP0, there may be at least one candidate. ICP0 has recently been shown to degrade the poly (ADP-ribose) (PAR) glycosylase (PARG) (Grady, Hwang et al. 2012). PARG plays an important role in the resolution of DNA damage foci by cleaving PAR polymers that are attached to DNA and proteins by PARP-1 in response to DNA damage. PARG promotes attachment of XRCC1 and LIG III at sites of DNA damage, which are factors associated with MMEJ. Thus, PARG may promote repair by MMEJ (Wei, Nakajima et al. 2013). With this in mind, it is tempting to speculate that ICP0 inhibits MMEJ during wild type (KOS) infection through degradation of PARG; however, additional experiments will be required to determine the exact mechanism by which ICP0 affects pathway choice.

4.5.e. The role of C-NHEJ proteins in HSV-1 infection.

Parkinson et al. reported that HSV-1 infection produced 6 to 200-fold more virus on DNA-PKcs deficient human glioma cells (M059J) compared with wild type cells (M059K)(Parkinson, Lees-Miller et al. 1999). On the other hand, we observed that DNA-PKcs deficiency did not have a significant effect on wild type HSV-1 growth in the HCT-116 cell line (Figure 4.6). We believe that the discrepancy between these findings may be

due to several differences between the M059J and HCT-116 DNA-PKcs$^{-/-}$ cell lines. First, the panel of HCT-116 cell lines used in our study are isogenic, meaning that they are genetically matched. Thus, the wild type HCT-116 cells and the DNA-PKcs$^{-/-}$ cells only differ in expression of DNA-PKcs (Ruis, Fattah et al. 2008). In contrast, the M059J cell line was isolated from a patient (Allalunis-Turner, Barron et al. 1993), and the DNA-PKcs deficiency was the result of a spontaneous mutation. Thus, M059J cells are not isogenically matched with the wild type (M059K) cell line. In fact, M059J cells are highly aneuploid (Anderson, Dunn et al. 2001) and contain mutations in numerous genes, including: ATM (Tsuchida, Yamada et al. 2002), p53 (Anderson and Allalunis-Turner 2000), FANCA (Halling-Brown, Bulusu et al. 2012). Therefore, although these cell lines have been extensively used to study DNA repair, it is unclear whether the observations reported by Parkinson et al., are directly due to DNA-PKcs deficiency (Parkinson, Lees-Miller et al. 1999). Although we do believe that DNA-PKcs is antiviral, it is possible that it is not as inhibitory to viral growth as previously reported and other components of the C-NHEJ pathway may restrict the virus more efficiently.

Although we have shown that NHEJ is inhibited during infection, there is conflicting evidence as to whether the core components of the C-NHEJ pathway, namely LIGIV and XRCC4, are antiviral. Muylaert et al., reported that RNAi knockdown of LIGIV and XRCC4 decreased viral yield at 20 h post infection by 8-fold and 19-fold, respectively, and (Muylaert and Elias 2007). This result is similar to our findings at earlier times post infection, where LIGIV$^{-/-}$ and XRCC4$^{-/-}$ cells appear to replicate HSV-1 less efficiently than wild type HCT-116 cells (Figure 4.5, Table 4.1). However, at 48 h post infection, we show that viral yields are about 3 fold greater on LIGIV$^{-/-}$ and XRCC4^{-}

$^{/-}$ cells compared to wild type HCT-116 cells (Figures 4.5 and 4.6, Table 4.1). Thus, although it was previously reported that LIGIV and XRCC4 are required for efficient viral replication, we now show that LIGIV and XRCC4 are antiviral.

Determining whether C-NHEJ plays a positive or negative role during HSV-1 infection is part of a bigger question regarding the mechanism of HSV-1 replication, which remains poorly understood. It has been proposed that the HSV-1 genome circularizes upon infection and undergoes rolling circle replication (Jacob, Morse et al. 1979, Mocarski and Roizman 1982, Poffenberger and Roizman 1985, Garber, Beverley et al. 1993). Muylaert and Elias reported that the LIGIV/XRCC4 complex was required for the formation of endless genomes (Muylaert and Elias 2007). From this observation, they proposed that the LIGIV/XRCC4 complex is required for circularization of the HSV-1 genome prior to rolling circle replication, suggesting that C-NHEJ plays a positive role during infection. The notion that HSV-1 undergoes rolling circle replication, however, has not been proven. In fact, there is evidence that circularization of the genome is associated with establishment of latent infection, rather than lytic infection (Rock and Fraser 1983, Efstathiou, Minson et al. 1986, Jackson and DeLuca 2003). Thus, the observation that LIGIV/XRCC4 are required for the formation of endless genomes may indicate that these proteins are antiviral and promote latent infection. Whether or not C-NHEJ activity causes circularization, the fate of the viral genome and the choice of repair/recombination pathway activated during infection appear to have important consequences for the establishment of lytic infection.

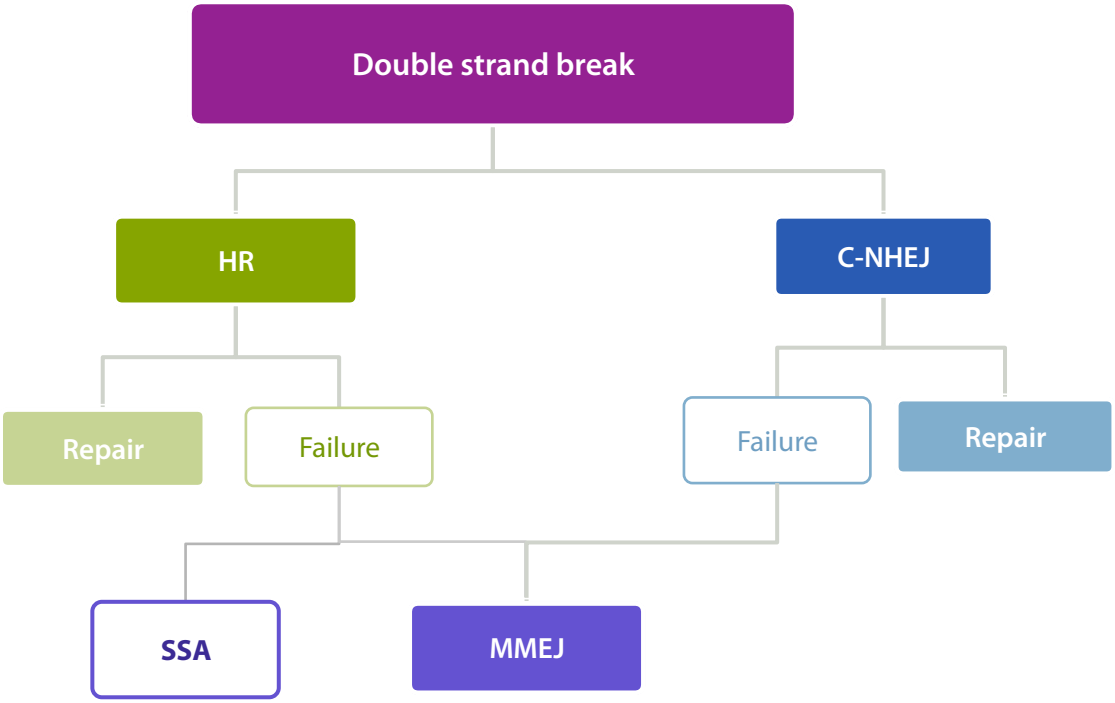

Figure 4.1. Schematic of the hierarchical model for DSBR pathway choice. In this model, homology directed repair (HR) and classic non-homologous end joining (C-NHEJ) are the predominant mechanisms for the repair of DNA double strand breaks (DSBs). In the event that repair by HR fails (left), the break can either be repaired by single strand annealing (SSA) or by microhomology mediated end joining (MMEJ). In the event that C-NHEJ fails, the break can be repaired by MMEJ (right).

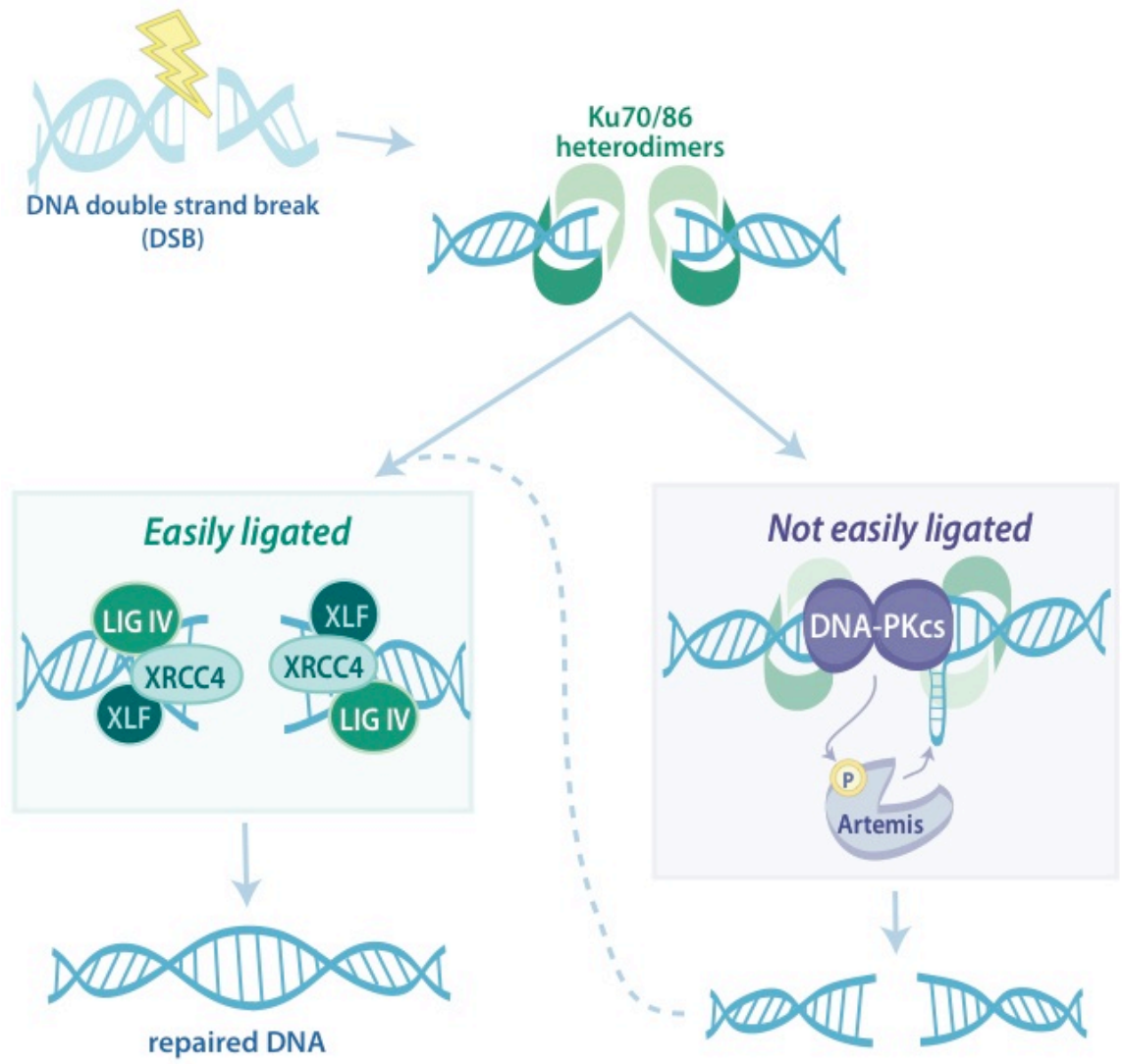

Figure 4.2. Diagram of the relationship between the classic non-homologous end joining (C-NHEJ) and DNA-PKcs-dependent (D-NHEJ) pathways. DNA double strand breaks (DSBs) are sensed and bound by the Ku70/86 heterodimer. C-NHEJ of DSBs that are easily ligatable (left panel) requires LIGIV/XRCC4/XLF. D-NHEJ occurs if DSB ends are not easily ligatable (right panel). For D-NHEJ, DNA-PKcs is required to activate end-processing enzymes, such as Artemis, to produce suitable DNA ends for C-NHEJ.

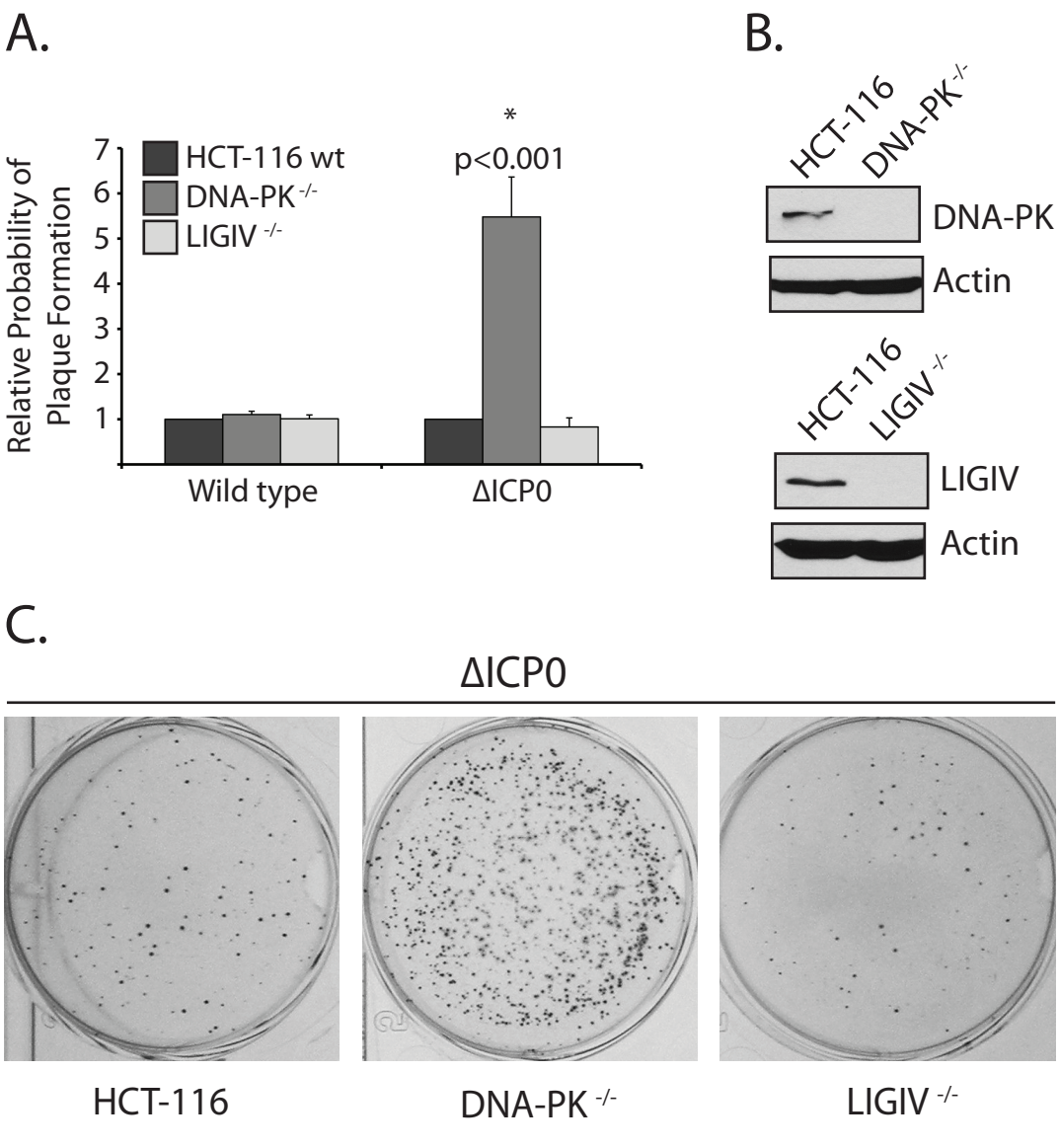
A.
B.
C.
Relative Probability of Plaque Formation
HCT-116 wt
DNA-PK -/-
LIGIV -/-
*
p<0.001
Wild type
ΔICP0
HCT-116
DNA-PK -/-
DNA-PK
Actin
HCT-116
LIGIV -/-
LIGIV
Actin
ΔICP0
HCT-116
DNA-PK -/-
LIGIV -/-

Figure 4.3. 0β has a greater probability of plaque formation on DNA-PK$^{-/-}$ cells.

(A) HCT-116 (wt), DNA-PK$^{-/-}$, and LIG IV $^{-/-}$ cells were plated and infected with identical dilutions of either wt (in1863) or ΔICP0 (dl1403/CMVlacZ). The relative probability of plaque formation was determined at each dilution. The values represent the averages of 5 independent experiments and the error represents the standard error. Representative plaque plates are shown for 1 dilution of ICP0 on each cell line. **(B)** Western blot for DNA-PKcs expression on wild type and DNA-PKcs$^{-/-}$ cell lines *(top panel)* and LIGIV expression on wild type and LIGIV$^{-/-}$ cell lines *(bottom panel)*. **(C)** Representative experiment showing LacZ staining of ΔICP0 (dl1403)-infected HCT-116, DNA-PKcs$^{-/-}$, and LIGIV$^{-/-}$ cells **Experimental data and figure produced by Kareem N. Mohni.

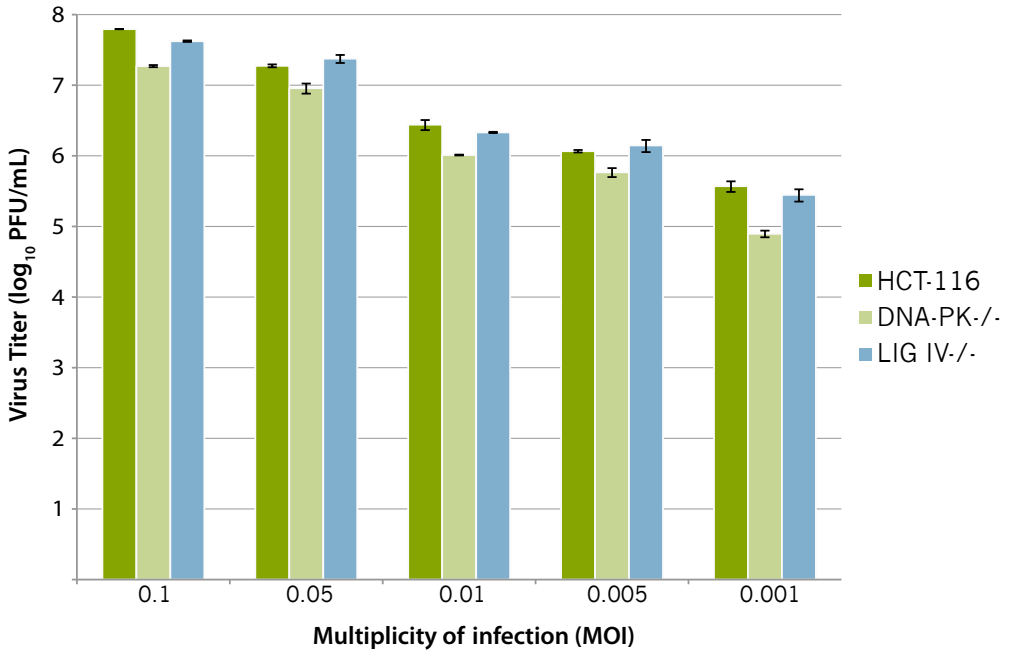

Figure 4.4. Neither DNA-PKcs nor LIGIV affect virus production from ΔICP0 infection at very low MOIs. HCT-116, DNA-PK$^{-/-}$, and LIG IV$^{-/-}$ cells were infected with the ICP0-null virus, 0β, at very low MOIs (0.1, 0.05, 0.01, 0.005, 0.001) for 48 hours. Infected cell lysates were harvested and viral yields were titrated on U2OS cells. Error bars represent standard error of the mean for three individual experiments.

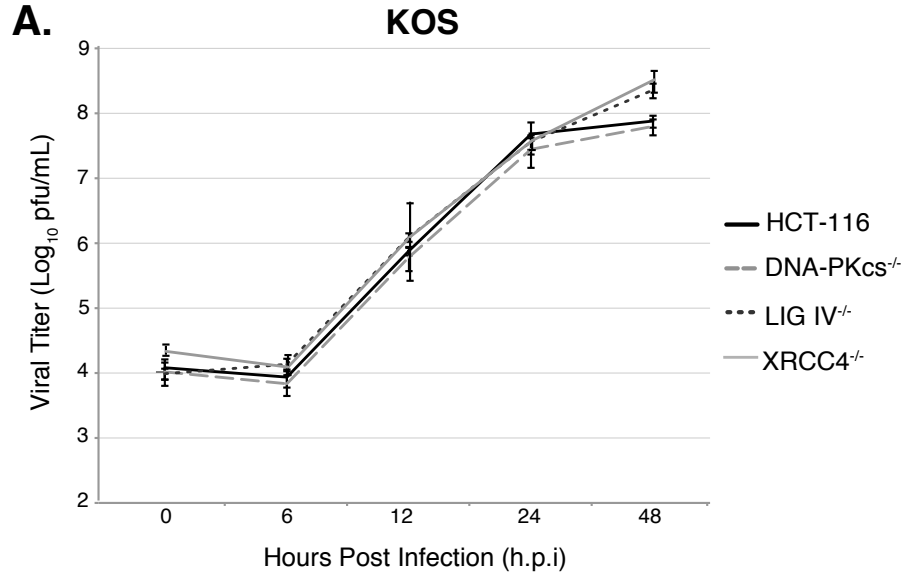
A.
KOS
Viral Titer (Log10 pfu/mL)
9
8
7
6
5
4
3
2
0
6
12
24
48
Hours Post Infection (h.p.i)
HCT-116
DNA-PKcs-/-
LIG IV-/-
XRCC4-/-

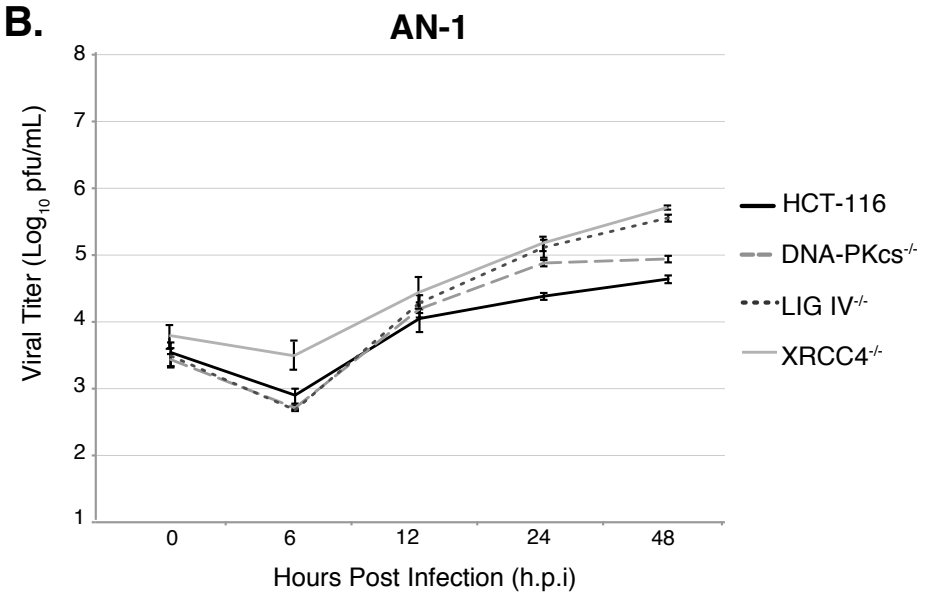
B.
AN-1
Viral Titer (Log10 pfu/mL)
8
7
6
5
4
3
2
1
0
6
12
24
48
Hours Post Infection (h.p.i)
HCT-116
DNA-PKcs-/-
LIG IV-/-
XRCC4-/-

Figure 4.5. Time course of KOS and AN-1 growth on C-NHEJ-deficient cell lines. HCT-116, DNA-PKcs$^{-/-}$, LIG IV$^{-/-}$, and XRCC4$^{-/-}$ cells were infected at an MOI of 0.1 pfu/cell. Samples were harvested at either 24 h post infection **(A)**, or 48 h post infection **(B)**, and titrated on their respective complementing cell lines *(see Materials and Methods section)*. Values represent the average of at least three independent experiments. Error bars represent standard error of the mean for each data point.

*p≤0.01; **p≤0.001; ***p≤0.0001

A.

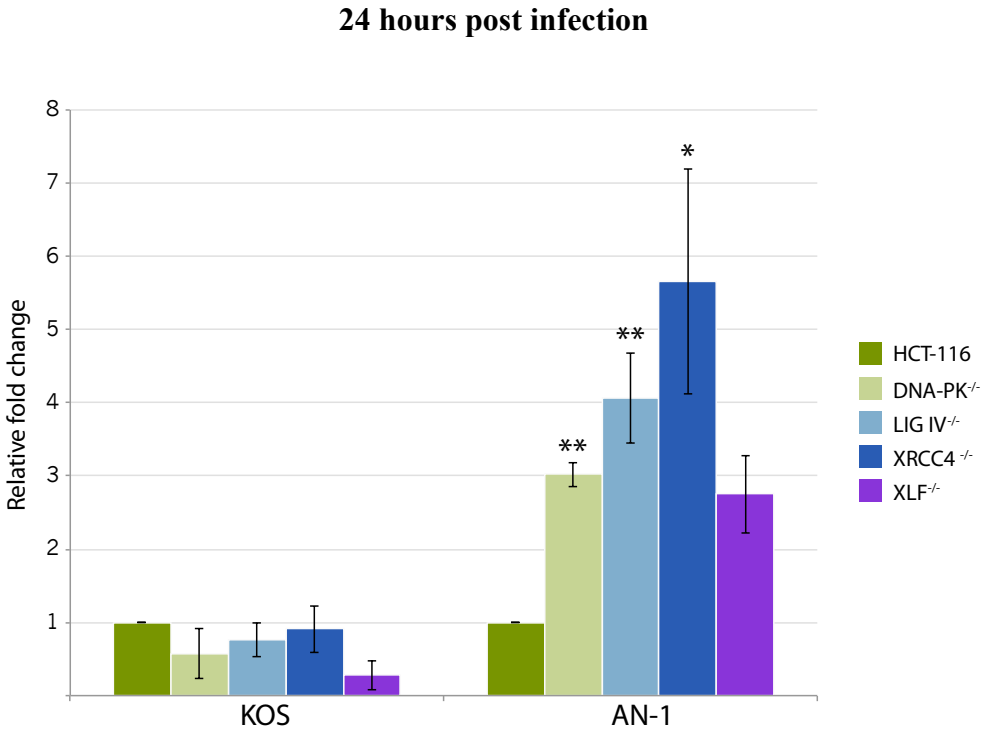
24 hours post infection
Relative fold change
8
7
6
5
4
3
2
1
**
**
*
KOS
AN-1
HCT-116
DNA-PK-/-
LIG IV-/-
XRCC4 -/-
XLF-/-

B.

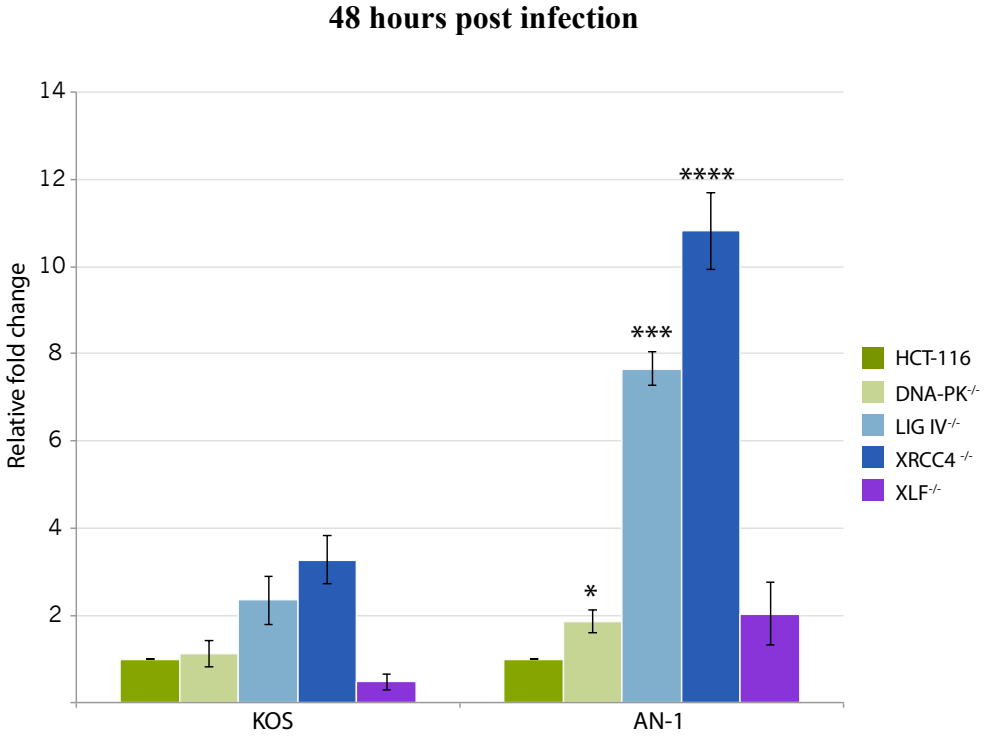
48 hours post infection
Relative fold change
14
12
10
8
6
4
2
*
***
****
KOS
AN-1
HCT-116
DNA-PK-/-
LIG IV-/-
XRCC4 -/-
XLF-/-

Figure 4.6. Fold change in KOS and AN-1 virus yield on DNA-PK$^{-/-}$, LIG IV$^{-/-}$, XRCC4$^{-/-}$, and XLF$^{-/-}$ cells relative to growth on HCT-116 cells. Fold change in virus yield was calculated relative to virus on HCT-116 for each virus. Values represent the average of at least three independent experiments. Error bars represent standard error of the mean for each data point. P values were calculated using the two-tailed student t-test with equal variance. *p≤0.01; **p≤0.001; ***p≤0.0001; ****p≤0.00001

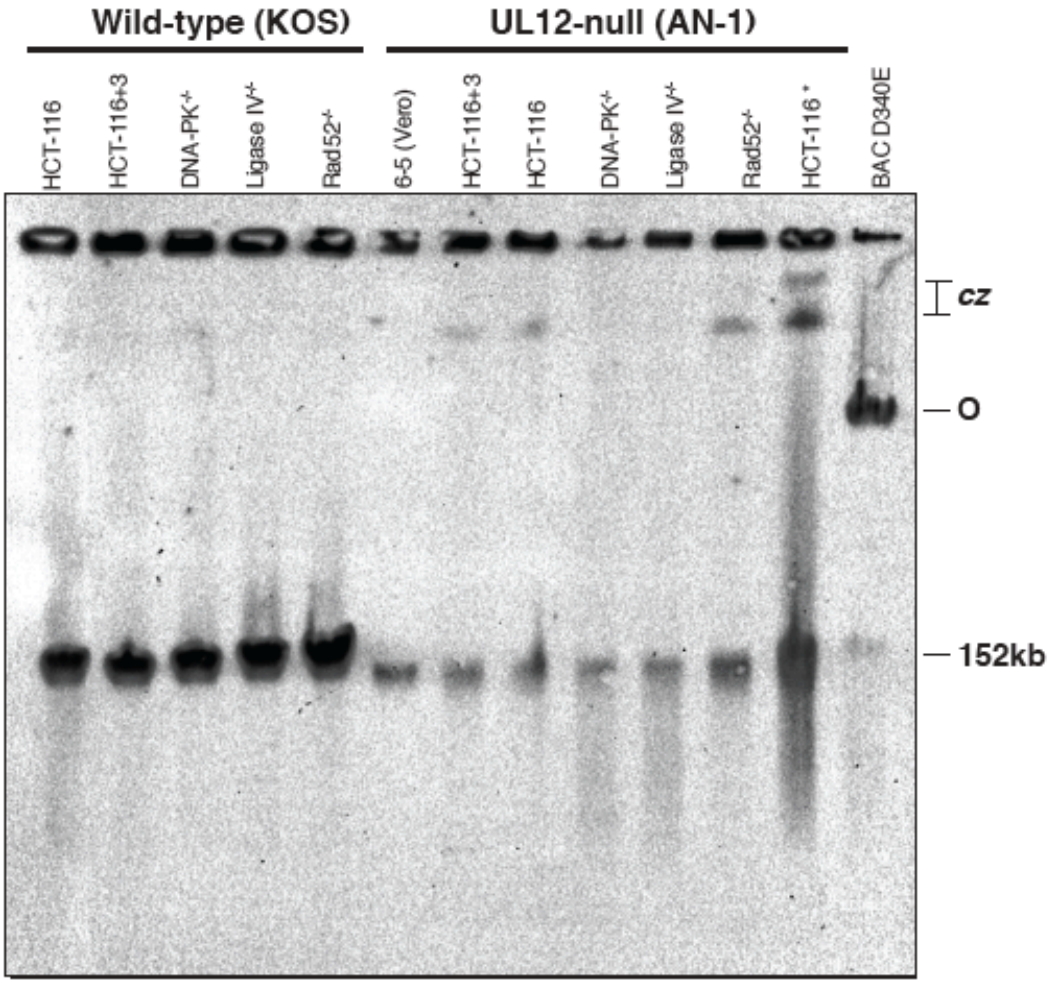

Figure 4.7. Southern blot of HSV-1 replicating and virion DNA separated by pulsed-field gel electrophoresis (PFGE). Pulsed field gel electrophoresis of KOS and AN-1 infected cells (cell lines indicated above). The label, "cz", indicates the compression zone of the gel. "O" indicates circular genome derived from HSV-1 BAC grown in *E. coli*. The 152kb mark indicates the size of HSV-1 monomeric genomes. Preparation of plugs is described in the Materials and Methods section. HCT-116* was prepared with 2X the amount of infected cells as the HCT-116 sample.

A.

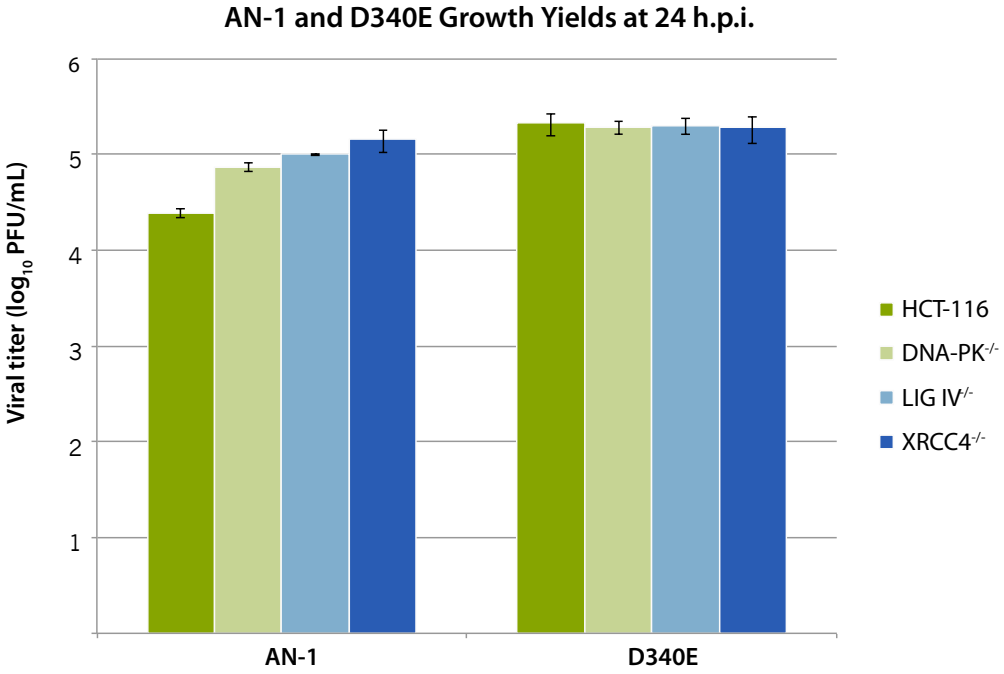
AN-1 and D340E Growth Yields at 24 h.p.i.
Viral titer (log10 PFU/mL)
6
5
4
3
2
1
AN-1
D340E
HCT-116
DNA-PK-/-
LIG IV-/-
XRCC4-/-

B.

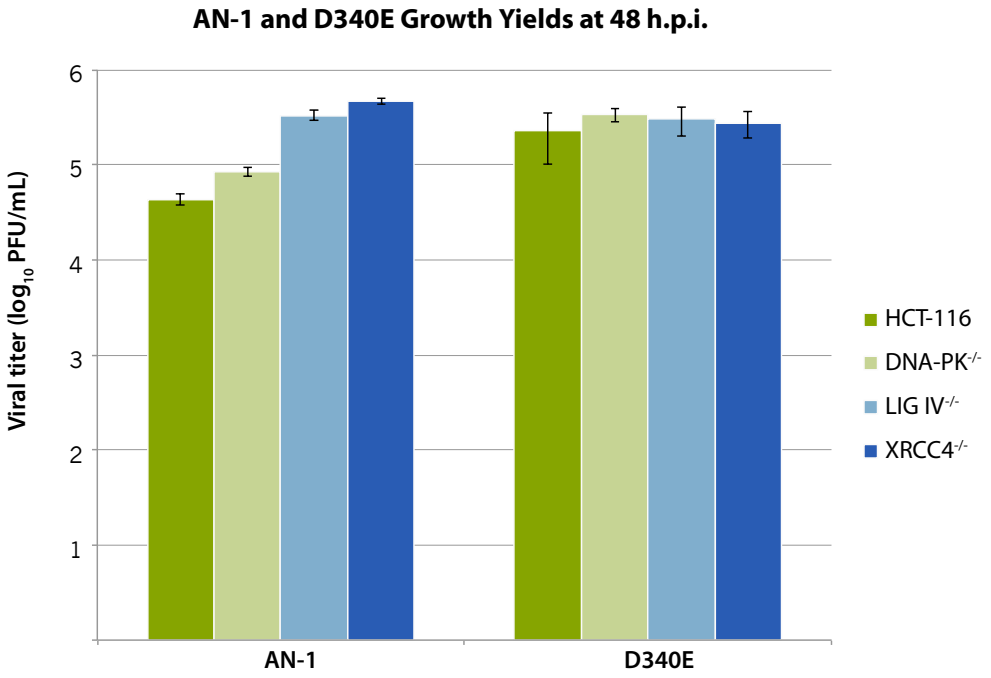
AN-1 and D340E Growth Yields at 48 h.p.i.
Viral titer (log10 PFU/mL)
6
5
4
3
2
1
AN-1
D340E
HCT-116
DNA-PK-/-
LIG IV-/-
XRCC4-/-

Figure 4.8. AN-1, and D340E virus growth yields on C-NHEJ-deficient cell lines. HCT-116 (wt) cells and cells deficient for components of the C-NHEJ pathway (DNA-PK$^{-/-}$, LIG IV$^{-/-}$, and XRCC4$^{-/-}$) were infected with AN-1 or D340E at an MOI of 0.1. Samples were harvested at either 24 h post infection **(A)**, or 48 h post infection **(B)**, and titrated on their respective complementing cell lines *(see Materials and Methods section)*.

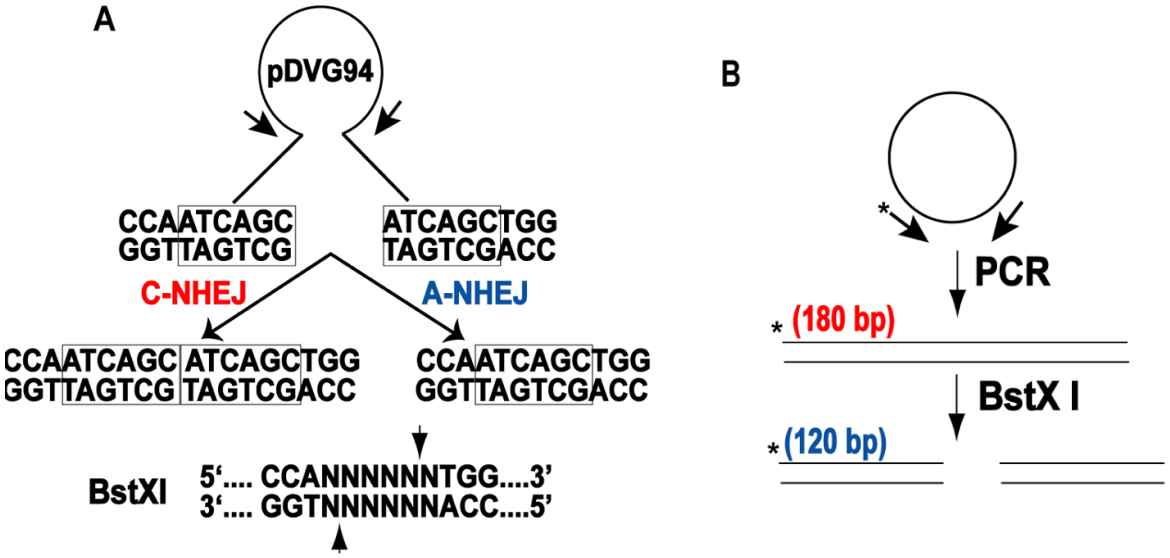
A
pDVG94
CCAATCAGC
GGTTAGTCG
ATCAGCTGG
TAGTCGACC
C-NHEJ
A-NHEJ
CCAATCAGC ATCAGCTGG
GGTTAGTCG TAGTCGACC
CCAATCAGCTGG
GGTTAGTCGACC
BstXI
5'.... CCANNNNNNTGG....3'
3'.... GGTNNNNNNACC....5'
B
PCR
(180 bp)
BstX I
(120 bp)

Figure 4.9. Schematic of the pDVG94 plasmid-based microhomology assay. (A) Diagram of the plasmid-based reporter substrate, pDVG94, which is biased for repair via microhomology-directed NHEJ (MMEJ). The plasmid is digested with *Afe I* and *EcoRV* to produce a blunt-ended linear substrate with 6-bp direct repeats regions (boxes) at both ends. DSB Repair by C-NHEJ will preserve a portion of both repeats. MMEJ results in the deletion of one repeat, leaving a single intact repeat, which is a substrate for *BstXI*. This panel is excerpted from Verkaik *et al*., 2002, Eur. J. Immunol., 32**:**701. **(B)** The experimental scheme for analysis of the plasmids recovered from transfected cells. Recovered plasmids were PCR amplified, products were digested *BstXI* restriction enzyme, and then analyzed via PAGE.

Panels A and B of this figure were taken from:

Fattah F, Lee EH, Weisensel N, Wang Y, et al. (2010) Ku Regulates the Non-Homologous End Joining Pathway Choice of DNA Double-Strand Break Repair in Human Somatic Cells. PLoS Genet 6(2): e1000855. doi:10.1371/journal.pgen.1000855

http://www.plosgenetics.org/article/info:doi/10.1371/journal.pgen.1000855

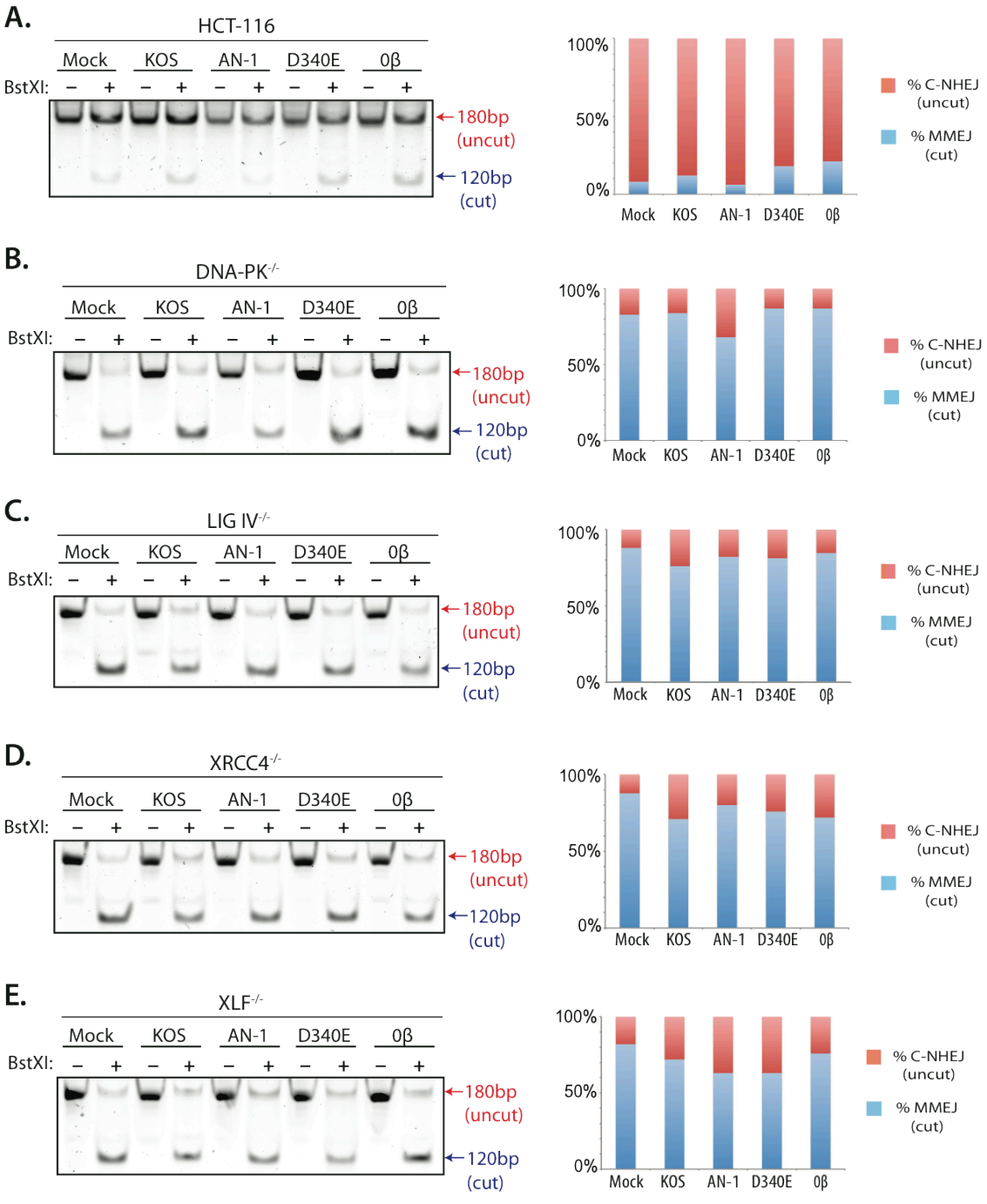
A.
HCT-116
Mock
KOS
AN-1
D340E
0β
BstXI:
180bp (uncut)
120bp (cut)
100%
50%
0%
% C-NHEJ (uncut)
% MMEJ (cut)
B.
DNA-PK-/-
C.
LIG IV-/-
D.
XRCC4-/-
E.
XLF-/-

Figure 4.10. Representative experiments measuring the effect of infection on MMEJ in wild type and C-NHEJ-deficient cell lines. Representative microhomology experiments were performed in HCT-116, DNA-PK$^{-/-}$, LIG IV$^{-/-}$, XRCC4$^{-/-}$, and XLF$^{-/-}$ cells infected with KOS, AN-1, D340E, and 0β**. Left Panels:** SYBR staining of undigested (control) and *BstXI*-digested PCR products separated by PAGE. The 180bp band (uncut) is substrate that had been repaired by C-NHEJ; whereas, the 120bp (cut) band is MMEJ-repaired substrate. **Right Panels:** The representative experiments shown on the left were quantitated using Image J software. Repair mediated by C-NHEJ or MMEJ are represented as percent of the total repaired substrate.

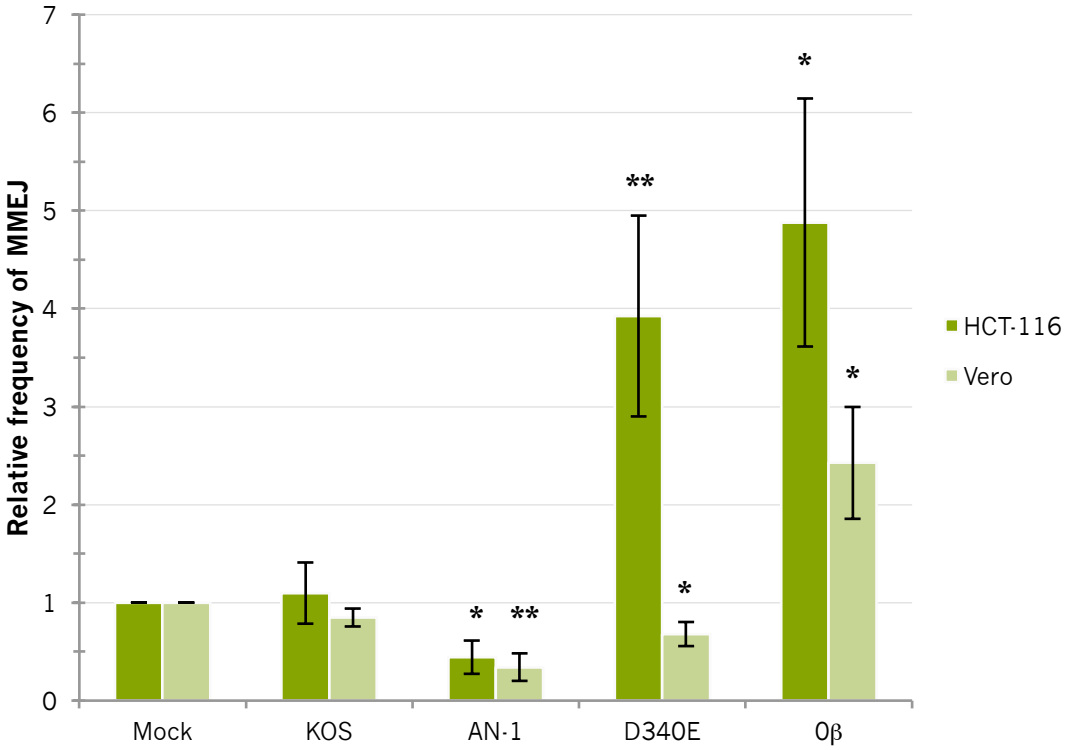

Figure 4.11. The effect of infection on the relative frequency of MMEJ in HCT-116 cells and Vero cells. HCT-116 cells and Vero cells were either mock infected, or infected with KOS, AN-1, D340E, or 0β at an MOI of 3. At 1 h post infection cells were transfected with the linearized pDVG94 reporter. The substrate was recovered at 48 h, PCR amplified, and digested with *BstXI*. Total repaired substrate was quantified using Image J software. Values are normalized to percent MMEJ in mock-infected cells. Values represent the average of three experiments. Error is calculated by standard error of the mean. P values were calculated using the two-tailed student t-test with equal variance.

* $p \leq 0.05$; ** $p \leq 0.01$

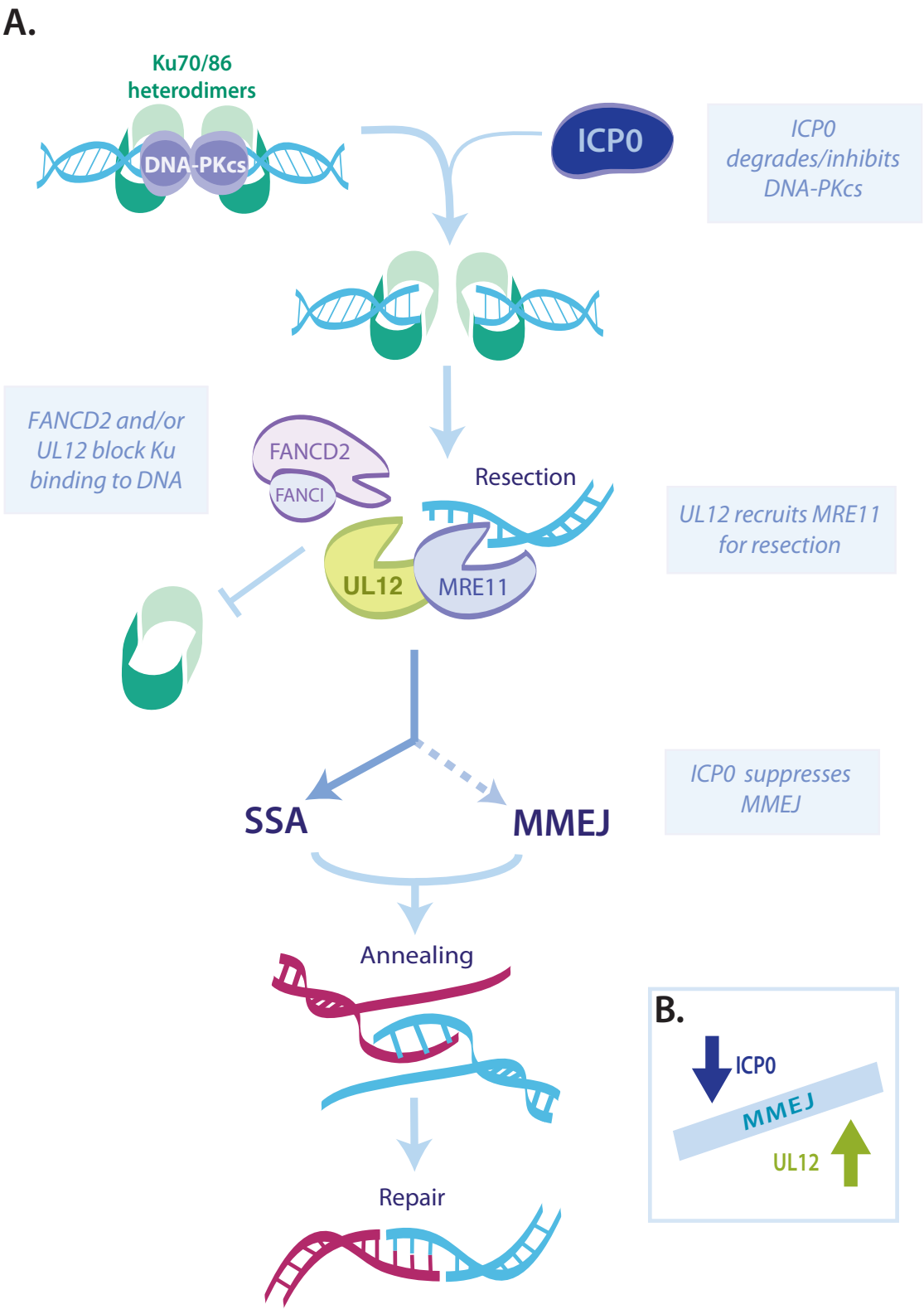
A.
Ku70/86
heterodimers
DNA-PKcs
ICP0
ICP0
degrades/inhibits
DNA-PKcs
FANCD2 and/or
UL12 block Ku
binding to DNA
FANCD2
FANCI
Resection
UL12
MRE11
UL12 recruits MRE11
for resection
SSA
MMEJ
ICP0 suppresses
MMEJ
Annealing
Repair
B.
ICP0
MMEJ
UL12

Figure 4.12. A model for the mechanisms by which ICP0 and UL12 may direct DNA repair pathway choice. (A) Diagram demonstrating how ICP0 and UL12 may work at different stages to inhibit C-NHEJ and promote SSA/MMEJ. At early stages, ICP0 degrades or inhibits DNA-PKcs (Lees-Miller, Long et al. 1996, Parkinson, Lees-Miller et al. 1999), perhaps to inhibit processing of DSBs for C-NHEJ. Inhibition of DNA-PKcs may also play a positive role in early viral gene expression. Once expressed (~2h post infection), UL12 interacts with Ku70, perhaps to prevent binding of Ku heterodimers to dsDNA ends (Balasubramanian 2011). The UL12-FANCD2 interaction may play a role in inhibiting Ku (Karttunen, Savas et al. 2014). UL12 has also been shown to interact with the MRN complex (Balasubramanian, Bai et al. 2010). This interaction may help recruit MRE11 to DSBs to perform limited end resection, either for MMEJ or as the first stage of resection for SSA. Finally, ICP0 may suppress MMEJ so that repair by SSA is favored. **(B)** ICP0 and UL12 may exert opposing forces on MMEJ.

CHAPTER 5.

Summary and Perspectives

Portions of the text from this chapter were submitted as a review manuscript by Samantha Smith and Sandra K. Weller, for publication in Future Virology.

5.1. SUMMARY

The overall goal of this thesis was to examine the factors that mediate DDR during HSV-1 infection, and the consequences of incorrect pathway choice. Specifically, we sought to determine whether UL12 acts as a mediator of DDR pathway choice in order to produce DNA that is infectious and that can be packaged for productive infection. The DNA produced in the absence of UL12 was found to be aberrant and non-infectious. We have provided evidence that the production of aberrant DNA may be the result of incorrect pathway choice. We showed that both ICP0 and UL12 inhibit aspects of the C-NHEJ pathway in order to promote productive infection. This work demonstrates that C-NHEJ is antiviral and that correct DDR pathway choice is essential for productive HSV-1 infection.

5.2. SPECIFIC AIMS*

Aim 1. Test the hypothesis that the molecular architecture of HSV-1 DNA affects its infectivity and the cellular DNA damage response.

This aim was addressed in Chapter 2, in which we enzymatically manipulated purified DNA to determine whether structural elements in viral DNA could alter infectivity. First, using a novel method, we calculated the number and length of gaps in the HSV-1 genome. This method measured incorporation of labeled nucleotides into the HSV-1 genome by Klenow polymerase. Confirming previous reports, we found HSV-1 genomes to contain about 15 gaps and that the gaps, on average, were about 33 nucleotides in length. We found that purified virion DNA activates DNA-PKcs in transfected cells. This was in contrast to infection, in which DNA-PKcs was not activated. DNA-PKcs is a component of the C-NHEJ pathway, which has been shown to be antiviral. ICP0 is known to degrade DNA-PKcs in some cell types (Lees-Miller, Long et al. 1996, Parkinson, Lees-Miller et al. 1999), and in Chapter 2 we showed that ICP0 is sufficient to inhibit DNA-PKcs activity even in cells in which DNA-PKcs is not degraded. In that study we also found that virion DNA with nicks and gaps was infectious but that some enzymatic treatments had a profound effect on infectivity. For instance, it is known that Klenow polymerase is capable of strand displacement synthesis, and when gaps were filled in with Klenow alone, the polymerase was able to displace the 5' ends of the next fragment, creating 5' flaps. Interestingly, Klenow-treated DNA lost infectivity. On the other hand, other alterations to the DNA structure, such as filling-in gaps with a polymerase that is not capable of strand displacement synthesis or addition of 3' flaps,

* In order to reflect the work that has been done, the aims presented here have been modified from those presented in the prospectus.

did not affect infectivity. The infectivity of virion DNA with 5' flaps could be restored by overexpression of ICP0 or by transfection of DNA-PKcs$^{-/-}$ cells. The observation that infectivity can be restored by ICP0 and in the absence of DNA-PKcs along suggests that ICP0 inhibits DNA-PKcs activation in order to promote productive infection.

Aim 2. Test the hypothesis that the growth defect observed in UL12-null (AN-1) infection is due to the production of aberrant DNA.

Experimental data supporting this hypothesis was presented in Chapter 3 and Chapter 4. First, we demonstrated that, although AN-1 growth is extremely defective in most cell types, the growth defects are much less pronounced in complementing cells and in DNA-PK $^{-/-}$ and LIG IV$^{-/-}$cells. In Chapter 3, we also showed that purified AN-1 DNA is not infectious when it is used to transfect Vero cells. Under these conditions, no viral gene expression could be observed. AN-1 DNA was also not infectious in UL12-expressing (6-5) cells. These observations are consistent with the hypothesis that the DNA produced during AN-1 infection is aberrant and contributes to the overall growth defect observed during AN-1 infection. Why AN-1 DNA does not support gene expression is not yet known; however, it is likely related to the fragile nature of purified AN-1 DNA and may be due to fragmentation. Further experiments will be required to determine whether the AN-1 genome is silenced because it elicits a robust DDR response than wild type DNA. For example, AN-1 DNA may induce a greater pRPA32 S4/S8 signal, as was observed with Klenow-treated DNA in Chapter 2 (Smith, Reuven et al. 2014). Another possibility is that, because AN-1 DNA is very fragile, pipetting the DNA for transfection may render the genome too fragmented to be infectious. In support of this

notion, in Chapter 2 we showed that fragmenting the wild type genome with mung bean nuclease rendered it noninfectious (Smith, Reuven et al. 2014). Finally, transfection efficiency should also be evaluated to rule out the possibility that uptake of AN-1 DNA is less efficient than uptake of wild type DNA.

We also analyzed AN-1 DNA by PFGE and showed that AN-1 DNA from non-complementing cells is different from AN-1 DNA from 6-5 cells in two important ways. First, the AN-1 DNA from non-complementing cells appears as a smear at the 152kb (genome length) mark. Second, there is an additional slower-migrating species present in the compression zone of the gel. In Chapter 3, we show that compression zone (CZ) DNA is present in AN-1-infected Vero and HeLa cells, neither of which complement UL12; however, the CZ DNA species is not present AN-1-infected 6-5 cells. In Chapter 4, we demonstrated that CZ DNA is also not present in AN-1-infected cells that are deficient for core C-NHEJ proteins (DNA-PK and LIG IV). This suggests that if C-NHEJ is active, the viral DNA that is produced is aberrant in some way. In Chapter 4 we demonstrated that AN-1 infection is more robust on C-NHEJ-deficient cell lines. Thus, the appearance of aberrant CZ DNA correlates with conditions in which AN-1 growth is most severely diminished. One explanation for these results is that C-NHEJ is antiviral, perhaps leading to a DDR pathway choice that is not conducive to productive infection, and the production of aberrant forms of viral DNA. It is possible that in cells infected with wild type virus, UL12 plays a role in inhibiting C-NHEJ and that in the absence of UL12, AN-1 is very sensitive to this pathway.

Aim 3. Test the hypothesis that UL12 plays a role in the inhibition of DNA-PKcs-independent C-NHEJ.

Previously, we showed that HSV-1 infection stimulates SSA while inhibiting HR and NHEJ (Schumacher, Mohni et al. 2012). It has previously been shown that HSV-1 viral growth is better on cells that do not express DNA-PKcs, a component of the C-NHEJ pathway (Parkinson, Lees-Miller et al. 1999). These results suggest that DNA-PKcs is antiviral and that ICP0 may play a role in counteracting antiviral effects. In fact, it was previously recognized that DNA-PKcs, is degraded by ICP0 in many cell types (Lees-Miller, Long et al. 1996, Parkinson, Lees-Miller et al. 1999, Davido, Von Zagorski et al. 2003, Lin, Noyce et al. 2004, Lilley, Carson et al. 2005, Gregory and Bachenheimer 2008); however, we and others have shown that DNA-PKcs is not degraded during infection in Vero cells. In Chapter 2, we demonstrated that ICP0 is sufficient to inhibit DNA-PKcs activity in Vero cells. Thus, ICP0 inhibits DNA-PKcs even in cells in which DNA-PKcs is not degraded. These results are consistent with the notion that DNA-PKcs is antiviral and that HSV has evolved at least two ICP0-dependent mechanisms to inhibit it. The observation that DNA-PKcs is not absolutely required for all C-NHEJ activity (Riballo, Kuhne et al. 2004, van Heemst, Brugmans et al. 2004, Mari, Florea et al. 2006) raised the question of whether other components of the C-NHEJ pathway are also antiviral. We asked whether two core components of this pathway, LIG IV and XRCC4, were also antiviral. In Chapter 4 we reported that the knockout of the core C-NHEJ proteins, LIG IV and XRCC4, improves growth of wild type virus 2- to 3-fold, suggesting that these proteins are antiviral. Interestingly, knockout of these proteins improves growth of the UL12-null 8-fold and 11-fold, respectively. These results suggest

that core C-NHEJ proteins are antiviral, and that in the presence of UL12, HSV-1 can overcome this antiviral mechanism; however, in the absence of UL12, infection is compromised. Unlike the null virus, the UL12 nuclease-dead mutant (D340E) grows equally well on wild type HCT-116 cells as it does on the C-NHEJ knockout cells lines, and D340E viral yields on these cell lines are equivalent to UL12-null on permissive cells (ie. XRCC4$^{-/-}$ and LIG IV$^{-/-}$). Thus the UL12-nuclease activity is not required for UL12-mediated suppression of C-NHEJ.

In addition, we performed experiments using a reporter substrate that measures relative MMEJ and C-NHEJ activities. It is now thought that MMEJ is "backup" pathway that is activated when C-NHEJ is inactive (Bennardo, Cheng et al. 2008, Fattah, Lee et al. 2010). We have used a transfection-based assay that can distinguish between MMEJ and C-NHEJ. In this assay if MMEJ activity is high, it indicates that C-NHEJ activity has been suppressed, and vice-versa. We have previously shown that HSV infection inhibits both pathways, and we now want to know which viral proteins are responsible. We have already shown that ICP0 is at least in part responsible for inhibition of DNA-PK (and presumably C-NHEJ), and we are now interested in how HSV inhibits MMEJ. In cells infected with AN-1, MMEJ is decreased by more than two fold. In this assay, low MMEJ indicates active C-NHEJ, suggesting that UL12 plays a role in suppression of C-NHEJ. The nuclease dead mutant (D340E) is still able to inhibit C-NHEJ, raising the interesting possibility that UL12 suppresses C-NHEJ through its interactions with DDR proteins such as FANCD2, MRE11, or Ku70 rather than through its own nuclease activity.

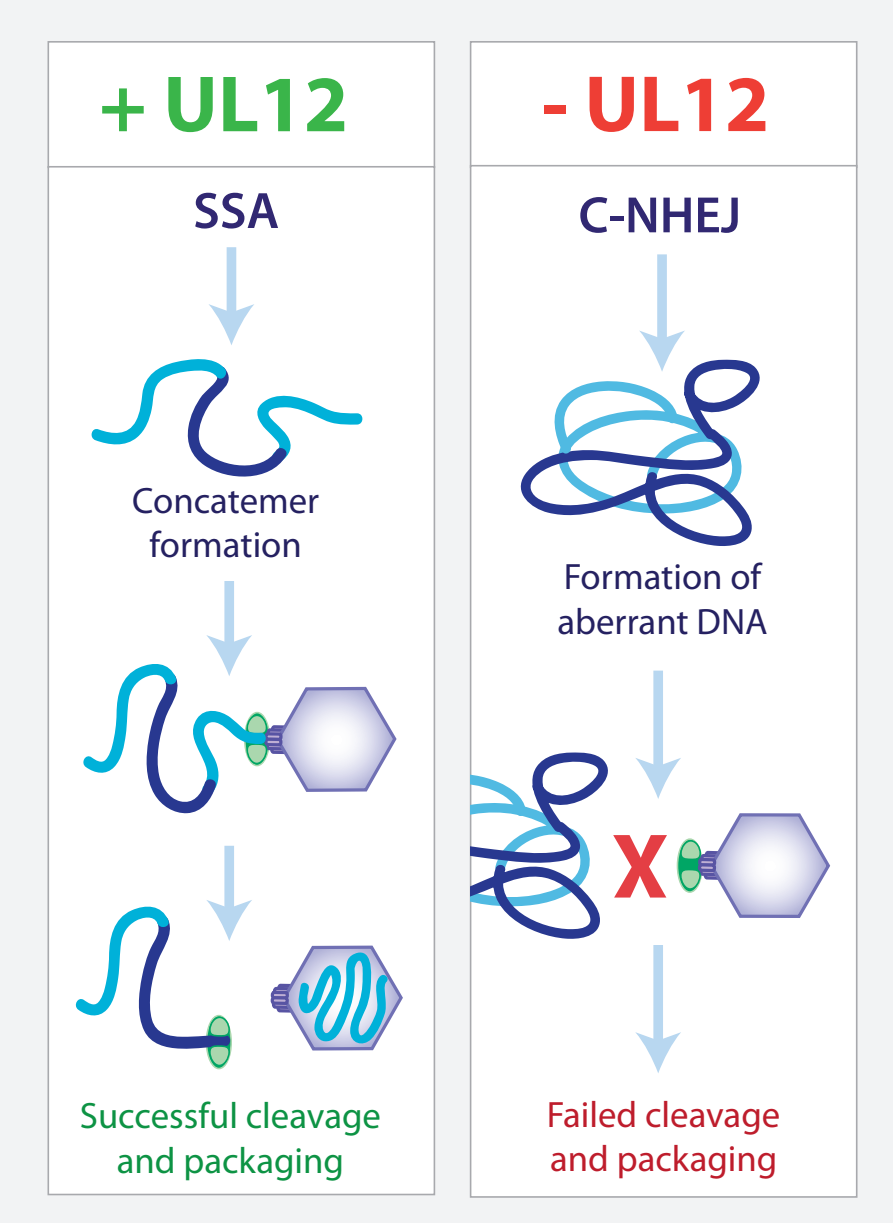

Figure 5.1. Diagram of the outcomes of DDR pathway choice, with and without UL12, during HSV-1 infection. *Left panel:* In the presence of UL12, SSA is stimulated and thus concatemer formation and successful cleavage and packaging of viral DNA is promoted. *Right panel:* In the absence of UL12, C-NHEJ is inefficiently inhibited and thus aberrant viral DNA is formed resulting in failed cleavage and packaging of viral DNA.

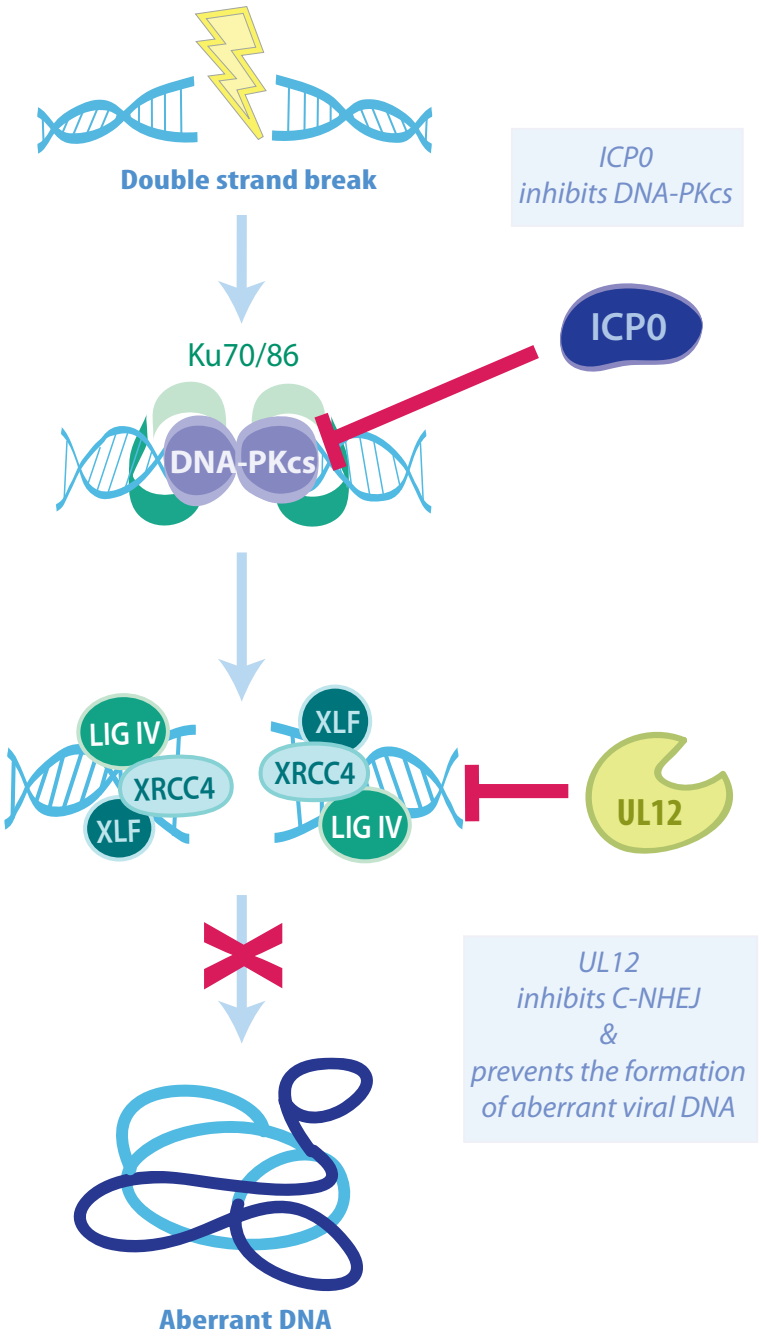

Figure 5.2. Model of the mechanism by which ICP0 and UL12 prevent the antiviral effects of C-NHEJ during HSV-1 infection. ICP0 degrades or inhibits DNA-PKcs activity. UL12 inhibits C-NHEJ activity and prevents the formation of aberrant DNA caused by incorrect DDR pathway choice.

5.3. Models and future directions.

As described above, we have now shown that both ICP0 and UL12 inhibit aspects of the C-NHEJ pathway in order to promote productive infection. In addition, we have demonstrated that the structure of the viral genome itself may also influence the outcome of DDR pathway choice at early stages during infection. Although the precise mechanisms by which UL12, ICP0, and the viral genome regulate repair pathway usage are not yet known, we have proposed several models:

5.3.a. UL12 may recruit cellular proteins to influence DDR pathway choice.

We have proposed that AN-1 DNA is not infectious because it contains structural abnormalities and that aberrant DNA is the result of incorrect pathway choice. The production of aberrant DNA during AN-1 infection may illustrate the important role that UL12 plays in DNA repair pathway choice during HSV-1 infection. Because HSV-1 DNA replication remains poorly understood it is difficult to fully understand the function of UL12 in the HSV-1 virus life cycle. HSV-1 replication produces complex DNA structures, but the mechanism for this remains unknown. We have proposed that HSV-1 utilizes SSA to produce concatemers (Schumacher, Mohni et al. 2012, Weller and Sawitzke 2014), but how this is initiated and how the process plays out in the context of infection is also unclear. It is possible that UL12 is required to direct repair toward the correct pathway, either by resecting DNA at DSBs or recruiting DDR proteins.

It is likely that end resection is also at the heart of DDR pathway choice during HSV-1 infection, and UL12 is strongly implicated in this process. We have previously shown that UL12 stimulates SSA in a nuclease-dependent fashion, perhaps by extensive resection at dsDNA ends (Schumacher, Mohni et al. 2012). We now also believe that UL12 plays a role in the inhibition of the C-NHEJ pathway during HSV-1 infection, since the UL12-null virus (AN-1) grows significantly better on cells that are deficient for core C-NHEJ proteins. In Chapter 4 we demonstrated that UL12 does not require its nuclease activity to inhibit C-NHEJ in HCT-116 cells (Figure 4.11). UL12 has been shown to interact with MRE11 (Balasubramanian, Bai et al. 2010) and FANCD2 (Karttunen, Savas et al. 2014), and perhaps recruits these factors in order to promote end resection and inhibit C-NHEJ. Ku70 has also been shown to interact with UL12 during HSV-1 infection (Balasubramanian, Bai et al. 2010); however, it is currently unclear whether UL12 exerts a positive or negative effect on Ku activity. In any case, UL12, by itself or with the help of interacting partners, may disrupt Ku binding at dsDNA ends (Figure 4.12). Future studies will be required to determine whether UL12 mediates DDR pathway choice, at least in part, through its interactions with cellular DDR factors, such as FANCD2, Ku70, and MRE11 (Balasubramanian, Bai et al. 2010, Balasubramanian 2011, Karttunen, Savas et al. 2014). In Chapter 4, we proposed that UL12 might recruit MRE11 to DSBs, and MRE11 may perform the initial end resection step required for either SSA or MMEJ (Figure 4.12). To test this, virus production, stimulation of SSA, and inhibition of NHEJ could be measured on the MRE11-H129N nuclease mutant cell line (Truong, Li et al. 2013), and compared to measurements of these properties on wild type cells.

5.3.b. ICP0 may inhibit C-NHEJ and MMEJ through degradation of antiviral factors.

The IE protein, ICP0, is an E3 ubiquitin ligase that promotes productive infection by targeting antiviral factors for proteasomal degradation. ICP0 degrades or inhibits DNA-PKcs signaling in numerous cell types, thus it is generally believed that ICP0 plays an important role in inhibiting C-NHEJ (Lees-Miller, Long et al. 1996, Parkinson and Everett , Smith, Reuven et al. 2014). The results presented in Chapter 4 suggest that ICP0 may also be required to inhibit MMEJ during infection. The mechanism by which ICP0 inhibits MMEJ is not yet known, but two previously characterized targets of ICP0 may be implicated in this process: RNF8 and PARG (Lilley, Chaurushiya et al. 2010, Grady, Hwang et al. 2012).

The E3 ubiquitin ligase, RNF8, functions in the cellular double strand break response (DSBR), is a target of ICP0, and is degraded during HSV-1 infection (Lilley, Chaurushiya et al. 2010). RNF8 recruits HR and C-NHEJ proteins to sites of damage, and aiding in the resolution of DNA damage foci (Huen, Grant et al. 2007, Kolas, Chapman et al. 2007, Mailand, Bekker-Jensen et al. 2007). More recently, Ku86 has been identified as a target of RNF8 for ubiquitin ligase-mediated degradation (Feng and Chen 2012). RNF8 degrades Ku86 after the Ku70/86 heterodimer binds dsDNA ends. This is an essential step in the resolution of C-NHEJ. In the absence of RNF8, Ku would be expected to remain bound at dsDNA ends. Thus, completion of C-NHEJ would be inhibited. Additionally, DNA bound by Ku would be protected from end resection, and therefore other homology-mediated repair mechanisms may also be inhibited. Thus, ICP0 may also help to inhibit C-NHEJ and MMEJ through degradation of RNF8. If this were the case, we would expect to see Ku retained at DSBs during HSV-1 infection. In support

of this notion, it has been previously reported that Ku86 is present in replication compartments (Taylor and Knipe 2004). Further experiments would be required to examine whether Ku86 is retained at DSBs in replication compartments, and if so, what effect Ku86-retention may have on repair pathway choice during infection. It was also be important to determine whether ICP0 is sufficient to induce retention of Ku at sites of DNA damage. To do this, the persistence of Ku at sites of DNA damage could be monitored using immunofluorescence microscopy of cells transfected with ICP0. The same type of experiment could also be done with infected cells by comparing persistence of Ku in wild type-infected cells versus ICP0-null infected cells.

It is also possible that ICP0 affects DDR pathway choice through degradation of one of its other targets as well. The DDR protein, PARG [†], is also a target of ICP0-mediated degradation during HSV-1 infection (Grady, Hwang et al. 2012). PARG plays an important role in the resolution of DNA damage foci by cleaving PAR polymers that are attached to DNA and DDR proteins in response to DNA damage. In addition, PARG promotes attachment of XRCC1 and LIG III at sites of DNA damage, which are factors associated with MMEJ (Wei, Nakajima et al. 2013). Thus, PARG may promote repair by MMEJ. In Chapter 4, we demonstrated that ICP0 plays a role in the inhibition of MMEJ during HSV-1 infection. One possible model for the inhibition of MMEJ by ICP0 during wild type (KOS) infection is through the degradation of PARG. Additional experiments will be required to determine whether ICP0-mediated degradation of PARG contributes to inhibition of MMEJ during infection; however, this may be difficult, since ICP0 targets so many cellular proteins.

[†] Poly (ADP-ribose) (PAR) glycosylase

Determining whether C-NHEJ plays a positive or negative role during HSV-1 infection is part of a bigger question regarding the mechanism of HSV-1 replication, which remains poorly understood. It has been proposed that the HSV-1 genome circularizes upon infection and undergoes rolling circle replication (Jacob, Morse et al. 1979, Mocarski and Roizman 1982, Poffenberger and Roizman 1985, Garber, Beverley et al. 1993). On the other hand, it is possible that DNA-PKcs and the C-NHEJ pathway promote circularization of the viral genome, as an antiviral mechanism to establish latent or quiescent infection (Rock and Fraser 1983, Efstathiou, Minson et al. 1986, Jackson and DeLuca 2003). This notion is supported by that observation made by Jackson and Deluca, that ICP0 can inhibit circularization, and that circular viral genomes are more prevalent during infection in the absence of ICP0 (Jackson and DeLuca 2003). In any case, further experimentation will be required to fully understand how C-NHEJ and circularization of viral genomes are antiviral. Regardless of whether circularization is the mechanism by which C-NHEJ exerts its antiviral effects, the fate of the viral genome and the choice of repair/recombination pathway activated during infection appear to have important consequences for the establishment of lytic infection.

5.4.Perspectives: Virus-host interactions and the evolutionary arms race.

Peter Wildy first observed genetic recombination between strains of HSV in 1955 (Wildy 1955). At the time, knowledge of DNA repair mechanisms was limited, and it has only been in the last decade that particular DNA damage response (DDR) pathways have been examined in the context of viral infections. One of the first reports addressing the interaction between a cellular DDR protein and HSV-1 was that DNA-PKcs levels were depleted in an ICP0-dependent manner during HSV-1 infection (Lees-Miller, Long et al. 1996). Since then, there have been numerous reports describing the interactions between HSV infection and cellular DDR pathways (Wilkinson and Weller 2003, Everett 2006, Lilley, Schwartz et al. 2007, Weitzman, Lilley et al. 2010, Weller 2010). The interaction between HSV-1 and the cell reflects an evolutionary tug of war in which cells have evolved antiviral mechanisms that are, in turn, counteracted by viral strategies that promote lytic infection. Because viruses rely on host cellular machinery during infection, they have evolved to usurp cellular processes. On the other hand, cells have intracellular antiviral defenses designed to fight viral infections. An important feature of the antiviral response is the cellular ability to sense viral DNA as "foreign", and components of the cellular DNA damage response (DDR) have been shown to function in this capacity. Thus, although HSV-1 may utilize some components of the DNA damage response machinery to replicate its genome, other components are antiviral, and HSV-1 has developed mechanisms to silence some DDR factors in order to avoid antiviral restriction.

The work presented in this thesis examines how the cellular NHEJ pathways are manipulated by HSV-1 infection. It is likely that researchers have only scratched the surface regarding the identification of cellular proteins that can trigger antiviral responses. We predict that additional cellular factors that exert antiviral effects by sensing foreign DNA will be identified. Cellular DDR pathways have no doubt influenced how HSV-1 has evolved an unusual mechanism by which to replicate its genome. If filling in nicks and gaps and circularization are antiviral as we have suggested, it is possible that recombination-dependent replication pathways using SSA and SDSA provide a mechanism that evades these antiviral mechanisms and produces DNA concatemers that can be packaged into infectious virus. We are struck by the fact that linear DNA viruses from bacteria, protozoa, yeast, mammals and insects that replicate through concatemeric DNA all encode two subunit recombinases similar to UL12 and ICP8. The evolutionary conservation between the recombinases from these different DNA viruses suggests that they have evolved replication strategies that are distinct from cellular replication mechanisms and utilize an unusual form of recombination-dependent DNA replication. In the case of HSV-1, which has co-evolved with its mammalian host, there has also been evolutionary pressure to evade intrinsic and innate antiviral mechanisms.

A relevant example of a protein that may have evolved to avert viral infection is the DNA sensing kinase, DNA-PKcs. This protein is absent in prokaryotes and lower eukaryotes, and thus, is evolutionarily speaking, a relatively new protein. It has been speculated that the emergence of DNA-PKcs as a component of the C-NHEJ may be part of the reason that this pathway is the predominant mechanism for repair in vertebrates and other higher eukaryotes (Mladenov and Iliakis 2011). In addition to its role in C-

NHEJ, DNA-PKcs functions as part of the host innate response to foreign DNA. In this role, DNA-PKcs acts as a DNA sensor, along with IFI16, to induce the IRF-3 dependent innate response (Ferguson, Mansur et al. 2012). It would be interesting to examine how viral proteins that interact with the C-NHEJ pathway have evolved to accommodate and counteract the advent of DNA-PKcs, and whether DNA-PKcs arose from a need to combat viral pathogens, such as HSV-1.

It is often discussed that viruses and their hosts are involved in an evolutionary arms race, and indeed, herpesviruses are a prehistoric family that has existed before the first mammal. The subfamily of Alphaherpesviruses is estimated to have arisen 400 million years ago, and coevolved with our first synapsid relatives (Grose 2012). As we gain a better understanding of virus-host interactions, we also gain insight into the evolutionary genealogy of the individual organisms. When a virus infects a new species of host, it is often extremely virulent, and it is believed that virulence is attenuated as the virus coevolves with its new host species. Since herpes is an ancient virus, it is tempting to speculate that our very existence- the fact that we have brains and spines and fingers to type on all sorts of technology- the fact that we are *humans,* we may at least, in part, have herpes to thank. Maybe we evolved to avoid infection, and became more complex in order to outwit the virus. At the very beginning of our evolution, the results could have been dramatic.

CHAPTER 6.

References

Abraham, R. T. 2004. PI 3-kinase related kinases: 'big' players in stress-induced signaling pathways. DNA Repair (Amst) 3:883-887.

Adamo, A., S. J. Collis, C. A. Adelman, N. Silva, Z. Horejsi, J. D. Ward, E. Martinez-Perez, S. J. Boulton, and A. La Volpe. 2010. Preventing nonhomologous end joining suppresses DNA repair defects of Fanconi anemia. Mol Cell 39:25-35.

Addison, C., F. J. Rixon, and V. G. Preston. 1990. Herpes simplex virus type 1 UL28 gene product is important for the formation of mature capsids. J Gen Virol 71 (Pt 10):2377-2384.

Alekseev, O., K. Donovan, and J. Azizkhan-Clifford. 2014. Inhibition of ataxia telangiectasia mutated (ATM) kinase suppresses herpes simplex virus type 1 (HSV-1) keratitis. Invest Ophthalmol Vis Sci 55:706-715.

Allalunis-Turner, M. J., G. M. Barron, R. S. Day, 3rd, K. D. Dobler, and R. Mirzayans. 1993. Isolation of two cell lines from a human malignant glioma specimen differing in sensitivity to radiation and chemotherapeutic drugs. Radiat Res 134:349-354.

Anantha, R. W., V. M. Vassin, and J. A. Borowiec. 2007. Sequential and Synergistic Modification of Human RPA Stimulates Chromosomal DNA Repair. Journal of Biological Chemistry 282:35910-35923.

Anderson, C. W., and M. J. Allalunis-Turner. 2000. Human TP53 from the malignant glioma-derived cell lines M059J and M059K has a cancer-associated mutation in exon 8. Radiat Res 154:473-476.

Anderson, C. W., J. J. Dunn, P. I. Freimuth, A. M. Galloway, and M. J. Allalunis-Turner. 2001. Frameshift mutation in PRKDC, the gene for DNA-PKcs, in the DNA repair-defective, human, glioma-derived cell line M059J. Radiat Res 156:2-9.

Andreassen, P. R., A. D. D'Andrea, and T. Taniguchi. 2004. ATR couples FANCD2 monoubiquitination to the DNA-damage response. Genes Dev 18:1958-1963.

Audebert, M., B. Salles, and P. Calsou. 2004. Involvement of poly(ADP-ribose) polymerase-1 and XRCC1/DNA ligase III in an alternative route for DNA double-strand breaks rejoining. J Biol Chem 279:55117-55126.

Bacon, T. H., M. J. Levin, J. J. Leary, R. T. Sarisky, and D. Sutton. 2003. Herpes simplex virus resistance to acyclovir and penciclovir after two decades of antiviral therapy. Clin Microbiol Rev 16:114-128.

Balasubramanian, N. 2011. HSV-1 exonuclease UL12 interacts with host recombination factors and is essential for viral growth. University of Connecticut.

Balasubramanian, N., P. Bai, G. Buchek, G. Korza, and S. K. Weller. 2010. Physical interaction between the herpes simplex virus type 1 exonuclease, UL12, and the DNA double-strand break-sensing MRN complex. J Virol 84:12504-12514.

Balliet, J. W., A. S. Kushnir, and P. A. Schaffer. 2007. Construction and characterization of a herpes simplex virus type I recombinant expressing green fluorescent protein: acute phase replication and reactivation in mice. Virology 361:372-383.

Banks, L., D. J. Purifoy, P. F. Hurst, R. A. Killington, and K. L. Powell. 1983. Herpes simplex virus non-structural proteins. IV. Purification of the virus-induced deoxyribonuclease and characterization of the enzyme using monoclonal antibodies. J Gen Virol 64 (Pt 10):2249-2260.

Banks, L. M., I. W. Halliburton, D. J. Purifoy, R. A. Killington, and K. L. Powell. 1985. Studies on the herpes simplex virus alkaline nuclease: detection of type-common and type-specific epitopes on the enzyme. J Gen Virol 66 (Pt 1):1-14.

Bataille, D., and A. Epstein. 1994. Herpes simplex virus replicative concatemers contain L components in inverted orientation. Virology 203:384-388.

Bataille, D., and A. L. Epstein. 1997. Equimolar generation of the four possible arrangements of adjacent L components in herpes simplex virus type 1 replicative intermediates. Journal of virology 71:7736-7743.

Batterson, W., D. Furlong, and B. Roizman. 1983. Molecular genetics of herpes simplex virus. VIII. further characterization of a temperature-sensitive mutant defective in release of viral DNA and in other stages of the viral reproductive cycle. J Virol 45:397-407.

Baumruker, T., R. Sturm, and W. Herr. 1988. OBP100 binds remarkably degenerate octamer motifs through specific interactions with flanking sequences. Genes Dev 2:1400-1413.

Ben-Porat, T., and F. J. Rixon. 1979. Replication of herpesvirus DNA. IV: analysis of concatemers. Virology 94:61-70.

Ben-Porat, T., B. Stehn, and A. S. Kaplan. 1976. Fate of parental herpesvirus DNA. Virology 71:412-422.

Bennardo, N., A. Cheng, N. Huang, and J. M. Stark. 2008. Alternative-NHEJ is a mechanistically distinct pathway of mammalian chromosome break repair. PLoS Genet 4:e1000110.

Bentley, J., C. P. Diggle, P. Harnden, M. A. Knowles, and A. E. Kiltie. 2004. DNA double strand break repair in human bladder cancer is error prone and involves microhomology-associated end-joining. Nucleic Acids Res 32:5249-5259.

Beucher, A., J. Birraux, L. Tchouandong, O. Barton, A. Shibata, S. Conrad, A. A. Goodarzi, A. Krempler, P. A. Jeggo, and M. Lobrich. 2009. ATM and Artemis promote homologous recombination of radiation-induced DNA double-strand breaks in G2. EMBO J 28:3413-3427.

Bieniasz, P. D. 2004. Intrinsic immunity: a front-line defense against viral attack. Nat Immunol 5:1109-1115.

Biswal, N., B. K. Murray, and M. Benyesh-Melnick. 1974. Ribonucleotides in newly synthesized DNA of herpes simplex virus. Virology 61:87-99.

Blackwell, L. J., and J. A. Borowiec. 1994. Human replication protein A binds single-stranded DNA in two distinct complexes. Mol Cell Biol 14:3993-4001.

Blümel, J., S. Graper, and B. Matz. 2000. Structure of simian virus 40 DNA replicated by herpes simplex virus type 1. Virology 276:445-454.

Blümel, J., and B. Matz. 1995. Thermosensitive UL9 gene function is required for early stages of herpes simplex virus type 1 DNA synthesis. The Journal of general virology 76 (Pt 12):3119-3124.

Bolderson, E., N. Tomimatsu, D. J. Richard, D. Boucher, R. Kumar, T. K. Pandita, S. Burma, and K. K. Khanna. 2010. Phosphorylation of Exo1 modulates homologous recombination repair of DNA double-strand breaks. Nucleic Acids Res 38:1821-1831.

Boule, J. B., F. Rougeon, and C. Papanicolaou. 2001. Terminal deoxynucleotidyl transferase indiscriminately incorporates ribonucleotides and deoxyribonucleotides. J Biol Chem 276:31388-31393.

Boutell, C., and R. D. Everett. 2013. Regulation of alphaherpesvirus infections by the ICP0 family of proteins. J Gen Virol 94:465-481.

Branzei, D., and M. Foiani. 2008. Regulation of DNA repair throughout the cell cycle. Nature reviews. Molecular cell biology 9:297-308.

Brown, S. M., D. A. Ritchie, and J. H. Subak-Sharpe. 1973. Genetic studies with herpes simplex virus type 1. The isolation of temperature-sensitive mutants, their arrangement into complementation groups and recombination analysis leading to a linkage map. J Gen Virol 18:329-346.

Bryant, H. E., E. Petermann, N. Schultz, A. S. Jemth, O. Loseva, N. Issaeva, F. Johansson, S. Fernandez, P. McGlynn, and T. Helleday. 2009. PARP is activated at stalled forks to mediate Mre11-dependent replication restart and recombination. EMBO J 28:2601-2615.

Calsou, P., P. Frit, O. Humbert, C. Muller, D. J. Chen, and B. Salles. 1999. The DNA-dependent protein kinase catalytic activity regulates DNA end processing by means of Ku entry into DNA. J Biol Chem 274:7848-7856.

Campadelli-Fiume, G., M. Amasio, E. Avitabile, A. Cerretani, C. Forghieri, T. Gianni, and L. Menotti. 2007. The multipartite system that mediates entry of herpes simplex virus into the cell. Rev Med Virol 17:313-326.

Cantin, E. M., D. R. Hinton, J. Chen, and H. Openshaw. 1995. Gamma interferon expression during acute and latent nervous system infection by herpes simplex virus type 1. J Virol 69:4898-4905.

Chang, L., and F. J. Bollum. 1986. Molecular Biology of Terminal Transferas. CRC Critical Reviews in Biochemistry 21:27-52.

Chen, B. P. C., M. Li, and A. Asaithamby. 2012. New insights into the roles of ATM and DNA-PKcs in the cellular response to oxidative stress. Cancer letters 327:103-110.

Cheng, Q., N. Barboule, P. Frit, D. Gomez, O. Bombarde, B. Couderc, G. S. Ren, B. Salles, and P. Calsou. 2011. Ku counteracts mobilization of PARP1 and MRN in chromatin damaged with DNA double-strand breaks. Nucleic Acids Res 39:9605-9619.

Ciccia, A., and S. J. Elledge. 2010. The DNA damage response: making it safe to play with knives. Mol Cell 40:179-204.

Cimprich, K. A., and D. Cortez. 2008. ATR: an essential regulator of genome integrity. Nat Rev Mol Cell Biol 9:616-627.

Convery, E., E. K. Shin, Q. Ding, W. Wang, P. Douglas, L. S. Davis, J. A. Nickoloff, S. P. Lees-Miller, and K. Meek. 2005. Inhibition of homologous recombination by variants of the catalytic subunit of the DNA-dependent protein kinase (DNA-PKcs). Proc Natl Acad Sci U S A 102:1345-1350.

Corcoran, J. A., H. A. Saffran, B. A. Duguay, and J. R. Smiley. 2009. Herpes simplex virus UL12.5 targets mitochondria through a mitochondrial localization sequence proximal to the N terminus. J Virol 83:2601-2610.

Costa, R. H., K. G. Draper, L. Banks, K. L. Powell, G. Cohen, R. Eisenberg, and E. K. Wagner. 1983. High-resolution characterization of herpes simplex virus type 1 transcripts encoding alkaline exonuclease and a 50,000-dalton protein tentatively identified as a capsid protein. J Virol 48:591-603.

Cui, X., Y. Yu, S. Gupta, Y. M. Cho, S. P. Lees-Miller, and K. Meek. 2005. Autophosphorylation of DNA-dependent protein kinase regulates DNA end processing and may also alter double-strand break repair pathway choice. Mol Cell Biol 25:10842-10852.

Davey, S. K., and E. A. Faust. 1990. Murine DNA polymerase alpha fills gaps to completion in a direct assay. Altered kinetics of de novo DNA synthesis at single nucleotide gaps. J Biol Chem 265:4098-4104.

Davido, D. J., W. F. Von Zagorski, G. G. Maul, and P. A. Schaffer. 2003. The differential requirement for cyclin-dependent kinase activities distinguishes two functions of herpes simplex virus type 1 ICP0. J Virol 77:12603-12616.

Davison, A., and F. Rixon. 1985. Cloning of the DNA of Alphaherpesvirinae, p. 103-124. In J. H. Yechiel Becker (ed.), Recombinant DNA Research and Viruses, vol. 5. Springer US, Boston, MA.

Davison, A. J., A. Dolan, P. Akter, C. Addison, D. J. Dargan, D. J. Alcendor, D. J. McGeoch, and G. S. Hayward. 2003. The human cytomegalovirus genome revisited: comparison with the chimpanzee cytomegalovirus genome. J Gen Virol 84:17-28.

DeFazio, L. G., R. M. Stansel, J. D. Griffith, and G. Chu. 2002. Synapsis of DNA ends by DNA-dependent protein kinase. EMBO J 21:3192-3200.

Delboy, M. G., C. R. Siekavizza-Robles, and A. V. Nicola. 2010. Herpes simplex virus tegument ICP0 is capsid associated, and its E3 ubiquitin ligase domain is important for incorporation into virions. J Virol 84:1637-1640.

Delius, H., and J. B. Clements. 1976. A partial denaturation map of herpes simplex virus type 1 DNA: evidence for inversions of the unique DNA regions. J Gen Virol 33:125-133.

Deluca, N. 2011. Functions and Mechanism of Action of the Herpes Simplex Virus Regulatory Protein ICP4, p. 17-38. *In* S. K. Weller (ed.), Alphaherpesviruses. Caister Academic Press, Norfolk, UK.

Deshmane, S. L., B. Raengsakulrach, J. F. Berson, and N. W. Fraser. 1995. The replicating intermediates of herpes simplex virus type 1 DNA are relatively short. J Neurovirol 1:165-176.

Ditch, S., and T. T. Paull. 2012. The ATM protein kinase and cellular redox signaling: beyond the DNA damage response. Trends in biochemical sciences 37:15-22.

Dodding, M. P., and M. Way. 2011. Coupling viruses to dynein and kinesin-1. EMBO J 30:3527-3539.

Dohner, K., A. Wolfstein, U. Prank, C. Echeverri, D. Dujardin, R. Vallee, and B. Sodeik. 2002. Function of dynein and dynactin in herpes simplex virus capsid transport. Mol Biol Cell 13:2795-2809.

Draper, K. G., G. Devi-Rao, R. H. Costa, E. D. Blair, R. L. Thompson, and E. K. Wagner. 1986. Characterization of the genes encoding herpes simplex virus type 1 and type 2 alkaline exonucleases and overlapping proteins. J Virol 57:1023-1036.

Dueva, R., and G. Iliakis. 2013. Alternative pathways of non-homologous end joining (NHEJ) in genomic instability and cancer. Transl. Cancer Res. 2:163-177.

Dutch, R. E., V. Bianchi, and I. R. Lehman. 1995. Herpes simplex virus type 1 DNA replication is specifically required for high-frequency homologous recombination between repeated sequences. J Virol 69:3084-3089.

Efstathiou, S., A. C. Minson, H. J. Field, J. R. Anderson, and P. Wildy. 1986. Detection of herpes simplex virus-specific DNA sequences in latently infected mice and in humans. J Virol 57:446-455.

Enquist, L. W., P. J. Husak, B. W. Banfield, and G. A. Smith. 1998. Infection and spread of alphaherpesviruses in the nervous system. Adv Virus Res 51:237-347.

Everett, R. D. 2001. DNA viruses and viral proteins that interact with PML nuclear bodies. Oncogene 20:7266-7273.

Everett, R. D. 2006. Interactions between DNA viruses, ND10 and the DNA damage response. Cell Microbiol 8:365-374.

Everett, R. D., P. Freemont, H. Saitoh, M. Dasso, A. Orr, M. Kathoria, and J. Parkinson. 1998. The Disruption of ND10 during Herpes Simplex Virus Infection Correlates with the Vmw110- and Proteasome-Dependent Loss of Several PML Isoforms. Journal of Virology 72:6581-6591.

Everett, R. D., M. Meredith, and A. Orr. 1999. The ability of herpes simplex virus type 1 immediate-early protein Vmw110 to bind to a ubiquitin-specific protease contributes to its roles in the activation of gene expression and stimulation of virus replication. J Virol 73:417-426.

Everett, R. D., C. Parada, P. Gripon, H. Sirma, and A. Orr. 2008. Replication of ICP0-null mutant herpes simplex virus type 1 is restricted by both PML and Sp100. Journal of virology 82:2661-2672.

Falkenberg, M., I. R. Lehman, and P. Elias. 2000. Leading and lagging strand DNA synthesis in vitro by a reconstituted herpes simplex virus type 1 replisome. Proc Natl Acad Sci U S A 97:3896-3900.

Fattah, F., E. H. Lee, N. Weisensel, Y. Wang, N. Lichter, and E. A. Hendrickson. 2010. Ku regulates the non-homologous end joining pathway choice of DNA double-strand break repair in human somatic cells. PLoS genetics 6:e1000855.

Ferguson, B. J., D. S. Mansur, N. E. Peters, H. Ren, and G. L. Smith. 2012. DNA-PK is a DNA sensor for IRF-3-dependent innate immunity. Elife 1:e00047.

Fernandez-Capetillo, O., A. Celeste, and A. Nussenzweig. 2003. Focusing on foci: H2AX and the recruitment of DNA-damage response factors. Cell Cycle 2:426-427.

Frenkel, N., and B. Roizman. 1972. Separation of the Herpesvirus Deoxyribonucleic Acid Duplex into Unique Fragments and Intact Strand on Sedimentation in Alkaline Gradients. Journal of Virology 10:565-572.

Fu, X., H. Wang, and X. Zhang. 2002. High-frequency intermolecular homologous recombination during herpes simplex virus-mediated plasmid DNA replication. J Virol 76:5866-5874.

Fukushima, T., M. Takata, C. Morrison, R. Araki, A. Fujimori, M. Abe, K. Tatsumi, M. Jasin, P. K. Dhar, E. Sonoda, T. Chiba, and S. Takeda. 2001. Genetic analysis of the DNA-dependent protein kinase reveals an inhibitory role of Ku in late S-G2 phase DNA double-strand break repair. J Biol Chem 276:44413-44418.

Garber, D. A., S. M. Beverley, and D. M. Coen. 1993. Demonstration of circularization of herpes simplex virus DNA following infection using pulsed field gel electrophoresis. Virology 197:459-462.

Gibson, W., and B. Roizman. 1972. Proteins specified by herpes simplex virus. 8. Characterization and composition of multiple capsid forms of subtypes 1 and 2. J Virol 10:1044-1052.

Goldstein, D. J., and S. K. Weller. 1988. Factor(s) present in herpes simplex virus type 1-infected cells can compensate for the loss of the large subunit of the viral ribonucleotide reductase: characterization of an ICP6 deletion mutant. Virology 166:41-51.

Goldstein, J. N., and S. K. Weller. 1998a. The exonuclease activity of HSV-1 UL12 is required for in vivo function. Virology 244:442-457.

Goldstein, J. N., and S. K. Weller. 1998b. In vitro processing of herpes simplex virus type 1 DNA replication intermediates by the viral alkaline nuclease, UL12. Journal of virology 72:8772-8781.

Gordin, M., U. Olshevsky, H. S. Rosenkranz, and Y. Becker. 1973. Studies on herpes simplex virus DNA: denaturation properties. Virology 55:280-284.

Grady, S. L., J. Hwang, L. Vastag, J. D. Rabinowitz, and T. Shenk. 2012. Herpes simplex virus 1 infection activates poly(ADP-ribose) polymerase and triggers the degradation of poly(ADP-ribose) glycohydrolase. J Virol 86:8259-8268.

Graves-Woodward, K. L., J. Gottlieb, M. D. Challberg, and S. K. Weller. 1997. Biochemical analyses of mutations in the HSV-1 helicase-primase that alter ATP hydrolysis, DNA unwinding, and coupling between hydrolysis and unwinding. J Biol Chem 272:4623-4630.

Gray, W. L., B. Starnes, M. W. White, and R. Mahalingam. 2001. The DNA sequence of the simian varicella virus genome. Virology 284:123-130.

Gregory, D. A., and S. L. Bachenheimer. 2008. Characterization of mre11 loss following HSV-1 infection. Virology 373:124-136.

Grose, C. 2012. Pangaea and the Out-of-Africa Model of Varicella-Zoster Virus Evolution and Phylogeography. J Virol 86:9558-9565.

Gu, J., H. Lu, A. G. Tsai, K. Schwarz, and M. R. Lieber. 2007. Single-stranded DNA ligation and XLF-stimulated incompatible DNA end ligation by the XRCC4-DNA ligase IV complex: influence of terminal DNA sequence. Nucleic Acids Res 35:5755-5762.

Haince, J. F., D. McDonald, A. Rodrigue, U. Dery, J. Y. Masson, M. J. Hendzel, and G. G. Poirier. 2008. PARP1-dependent kinetics of recruitment of MRE11 and NBS1 proteins to multiple DNA damage sites. J Biol Chem 283:1197-1208.

Halling-Brown, M. D., K. C. Bulusu, M. Patel, J. E. Tym, and B. Al-Lazikani. 2012. canSAR: an integrated cancer public translational research and drug discovery resource. Nucleic Acids Res 40:D947-956.

Harper, J. W., and S. J. Elledge. 2007. The DNA damage response: ten years after. Mol Cell 28:739-745.

Hayward, G. S. 1974. Unique double-stranded fragments of bacteriophage T5 DNA resulting from preferential shear-induced breakage at nicks. Proceedings of the National Academy of Sciences of the United States of America 71:2108-2112.

Hayward, G. S., R. J. Jacob, S. C. Wadsworth, and B. Roizman. 1975. Anatomy of herpes simplex virus DNA: evidence for four populations of molecules that differ in the relative orientations of their long and short components. Proceedings of the National Academy of Sciences of the United States of America 72:4243-4247.

Herold, B. C., D. WuDunn, N. Soltys, and P. G. Spear. 1991. Glycoprotein C of herpes simplex virus type 1 plays a principal role in the adsorption of virus to cells and in infectivity. J Virol 65:1090-1098.

Hirsch, I., J. Roubal, and V. Vonka. 1976. Replicating DNA of herpes simplex virus type 1. Intervirology 7:155-175.

Hirsch, I., and V. Vonka. 1974. Ribonucleotides linked to DNA of herpes simplex virus type 1. Journal of virology 13:1162-1168.

Ho, G. P., S. Margossian, T. Taniguchi, and A. D. D'Andrea. 2006. Phosphorylation of FANCD2 on two novel sites is required for mitomycin C resistance. Mol Cell Biol 26:7005-7015.

Hoffmann, P. J., and Y. C. Cheng. 1978. The deoxyribonuclease induced after infection of KB cells by herpes simplex virus type 1 or type 2. I. Purification and characterization of the enzyme. The Journal of biological chemistry 253:3557-3562.

Honess, R. W., and B. Roizman. 1974. Regulation of herpesvirus macromolecular synthesis. I. Cascade regulation of the synthesis of three groups of viral proteins. J Virol 14:8-19.

Huber, A., P. Bai, J. M. de Murcia, and G. de Murcia. 2004. PARP-1, PARP-2 and ATM in the DNA damage response: functional synergy in mouse development. DNA Repair (Amst) 3:1103-1108.

Huen, M. S., R. Grant, I. Manke, K. Minn, X. Yu, M. B. Yaffe, and J. Chen. 2007. RNF8 transduces the DNA-damage signal via histone ubiquitylation and checkpoint protein assembly. Cell 131:901-914.

Hyman, R. W., J. E. Oakes, and L. Kudler. 1977. In vitro repair of the preexisting nicks and gaps in herpes simplex virus DNA. Virology 76:286-294.

Illuzzi, G., E. Fouquerel, J. C. Ame, A. Noll, K. Rehmet, H. P. Nasheuer, F. Dantzer, and V. Schreiber. 2014. PARG is dispensable for recovery from transient replicative stress but required to prevent detrimental accumulation of poly(ADP-ribose) upon prolonged replicative stress. Nucleic Acids Res 42:7776-7792.

Ivanchenko, M., J. Zlatanova, and K. van Holde. 1997. Histone H1 preferentially binds to superhelical DNA molecules of higher compaction. Biophysical Journal 72:1388-1395.

Iyama, T., and D. M. Wilson, 3rd. 2013. DNA repair mechanisms in dividing and non-dividing cells. DNA Repair (Amst) 12:620-636.

Jackson, S. A., and N. A. DeLuca. 2003. Relationship of herpes simplex virus genome configuration to productive and persistent infections. Proc Natl Acad Sci U S A 100:7871-7876.

Jackson, S. P., and D. Durocher. 2013. Regulation of DNA damage responses by ubiquitin and SUMO. Mol Cell 49:795-807.

Jacob, R. J., L. S. Morse, and B. Roizman. 1979. Anatomy of herpes simplex virus DNA. XII. Accumulation of head-to-tail concatemers in nuclei of infected cells and their role in the generation of the four isomeric arrangements of viral DNA. Journal of virology 29:448-457.

Jacob, R. J., and B. Roizman. 1977. Anatomy of herpes simplex virus DNA VIII. Properties of the replicating DNA. J Virol 23:394-411.

Jazayeri, A., J. Falck, C. Lukas, J. Bartek, G. C. Smith, J. Lukas, and S. P. Jackson. 2006. ATM- and cell cycle-dependent regulation of ATR in response to DNA double-strand breaks. Nat Cell Biol 8:37-45.

Johnson, K. E., L. Chikoti, and B. Chandran. 2013. Herpes simplex virus 1 infection induces activation and subsequent inhibition of the IFI16 and NLRP3 inflammasomes. J Virol 87:5005-5018.

Jongeneel, C. V., and S. L. Bachenheimer. 1981. Structure of replicating herpes simplex virus DNA. Journal of virology 39:656-660.

Karttunen, H., J. N. Savas, C. McKinney, Y. H. Chen, J. R. Yates, 3rd, V. Hukkanen, T. T. Huang, and I. Mohr. 2014. Co-opting the Fanconi anemia genomic stability pathway enables herpesvirus DNA synthesis and productive growth. Mol Cell 55:111-122.

Kato, T. Jr., T. Todo, H. Ayaki, T. Morita, S. Mitra, and M. Ikenaga. 1994. Cloning of the marsupial DNA photolyase gene and the lack of related nucleotide sequences in placental mammals. Nuc Acid Res 22(20):4119-4124.

Keir, H.M. and E. Gold. 1963. Deoxyribonucleic acid nucleotidyltransferase and deoxyribonuclease from cultured cells infected with herpes simplex virus. Biochimica et biophysica acta 72: 263-276.

Kelly, B. J., C. Fraefel, A. L. Cunningham, and R. J. Diefenbach. 2009. Functional roles of the tegument proteins of herpes simplex virus type 1. Virus Res 145:173-186.

Khan, S. A., S. J. Hayes, E. T. Wright, R. H. Watson, and P. Serwer. 1995. Specific single-stranded breaks in mature bacteriophage T7 DNA. Virology 211:329-331.

Khanna, K. M., R. H. Bonneau, P. R. Kinchington, and R. L. Hendricks. 2003. Herpes simplex virus-specific memory CD8+ T cells are selectively activated and retained in latently infected sensory ganglia. Immunity 18:593-603.

Kieff, E. D., S. L. Bachenheimer, and B. Roizman. 1971. Size, composition, and structure of the deoxyribonucleic acid of herpes simplex virus subtypes 1 and 2. Journal of virology 8:125-132.

Kim, D. B., and N. A. DeLuca. 2002. Phosphorylation of transcription factor Sp1 during herpes simplex virus type 1 infection. J Virol 76:6473-6479.

Knipe, D. M., and A. Cliffe. 2008. Chromatin control of herpes simplex virus lytic and latent infection. Nat Rev Microbiol 6:211-221.

Kong, H., R. B. Kucera, and W. E. Jack. 1993. Characterization of a DNA polymerase from the hyperthermophile archaea Thermococcus litoralis. Vent DNA polymerase, steady state kinetics, thermal stability, processivity, strand displacement, and exonuclease activities. Journal of Biological Chemistry 268:1965-1975.

Krishnakumar, R., M. J. Gamble, K. M. Frizzell, J. G. Berrocal, M. Kininis, and W. L. Kraus. 2008. Reciprocal binding of PARP-1 and histone H1 at promoters specifies transcriptional outcomes. Science (New York, NY) 319:819-821.

Kristie, T. M., and B. Roizman. 1987. Host cell proteins bind to the cis-acting site required for virion-mediated induction of herpes simplex virus 1 alpha genes. Proc Natl Acad Sci U S A 84:71-75.

Kristie, T. M., and B. Roizman. 1988. Differentiation and DNA contact points of host proteins binding at the cis site for virion-mediated induction of alpha genes of herpes simplex virus 1. J Virol 62:1145-1157.

Kristie, T. M., and P. A. Sharp. 1990. Interactions of the Oct-1 POU subdomains with specific DNA sequences and with the HSV alpha-trans-activator protein. Genes Dev 4:2383-2396.

Kuhn, A., T. M. Gottlieb, S. P. Jackson, and I. Grummt. 1995. DNA-dependent protein kinase: a potent inhibitor of transcription by RNA polymerase I. Genes Dev 9:193-203.

Kumar, V., F. W. Alt, and V. Oksenych. 2014. Functional overlaps between XLF and the ATM-dependent DNA double strand break response. DNA repair 16:11-22.

Kuzminov, A. 1999. Recombinational repair of DNA damage in Escherichia coli and bacteriophage lambda. Microbiol Mol Biol Rev 63:751-813, table of contents.

Lamberti, C., and S. K. Weller. 1996. The herpes simplex virus type 1 UL6 protein is essential for cleavage and packaging but not for genomic inversion. Virology 226:403-407.

Latchman, D. S. 1988. Effect of herpes simplex virus type 2 infection on mitochondrial gene expression. J Gen Virol 69 (Pt 6):1405-1410.

Lee, L. F., E. D. Kieff, S. L. Bachenheimer, B. Roizman, P. G. Spear, B. R. Burmester, and K. Nazerian. 1971. Size and composition of Marek's disease virus deoxyribonucleic acid. Journal of virology 7:289-294.

Lees-Miller, S. P., M. C. Long, M. A. Kilvert, V. Lam, S. A. Rice, and C. A. Spencer. 1996. Attenuation of DNA-dependent protein kinase activity and its catalytic subunit by the herpes simplex virus type 1 transactivator ICP0. J Virol 70:7471-7477.

Li, Z., Y. Yamauchi, M. Kamakura, T. Murayama, F. Goshima, H. Kimura, and Y. Nishiyama. 2012. Herpes simplex virus requires poly(ADP-ribose) polymerase activity for efficient replication and induces extracellular signal-related kinase-dependent phosphorylation and ICP0-dependent nuclear localization of tankyrase 1. J Virol 86:492-503.

Liang, L., L. Deng, S. C. Nguyen, X. Zhao, C. D. Maulion, C. Shao, and J. A. Tischfield. 2008. Human DNA ligases I and III, but not ligase IV, are required for microhomology-mediated end joining of DNA double-strand breaks. Nucleic Acids Res 36:3297-3310.

Lieber, M. R. 2010. The mechanism of double-strand DNA break repair by the nonhomologous DNA end-joining pathway. Annual review of biochemistry 79:181-211.

Lilley, C. E., C. T. Carson, A. R. Muotri, F. H. Gage, and M. D. Weitzman. 2005. DNA repair proteins affect the lifecycle of herpes simplex virus 1. Proc Natl Acad Sci U S A 102:5844-5849.

Lilley, C. E., M. S. Chaurushiya, C. Boutell, R. D. Everett, and M. D. Weitzman. 2011. The intrinsic antiviral defense to incoming HSV-1 genomes includes specific DNA repair proteins and is counteracted by the viral protein ICP0. PLoS pathogens 7:e1002084.

Lilley, C. E., M. S. Chaurushiya, C. Boutell, S. Landry, J. Suh, S. Panier, R. D. Everett, G. S. Stewart, D. Durocher, and M. D. Weitzman. 2010. A viral E3 ligase targets RNF8 and RNF168 to control histone ubiquitination and DNA damage responses. EMBO J 29:943-955.

Lilley, C. E., M. S. Chaurushiya, and M. D. Weitzman. 2009. Chromatin at the intersection of viral infection and DNA damage. Biochimica et biophysica acta.

Lilley, C. E., R. A. Schwartz, and M. D. Weitzman. 2007. Using or abusing: viruses and the cellular DNA damage response. Trends Microbiol 15:119-126.

Lin, R., R. S. Noyce, S. E. Collins, R. D. Everett, and K. L. Mossman. 2004. The herpes simplex virus ICP0 RING finger domain inhibits IRF3- and IRF7-mediated activation of interferon-stimulated genes. J Virol 78:1675-1684.

Liu, X., W. Jiang, R. L. Dubois, K. Yamamoto, Z. Wolner, and S. Zha. 2012. Overlapping functions between XLF repair protein and 53BP1 DNA damage response factor in end joining and lymphocyte development. Proc Natl Acad Sci U S A 109:3903-3908.

Livingston, C. M., N. A. DeLuca, D. E. Wilkinson, and S. K. Weller. 2008. Oligomerization of ICP4 and rearrangement of heat shock proteins may be important for herpes simplex virus type 1 prereplicative site formation. Journal of virology 82:6324-6336.

Llorca, O., and L. H. Pearl. 2004. Electron microscopy studies on DNA recognition by DNA-PK. Micron 35:625-633.

Loret, S., G. Guay, and R. Lippe. 2008. Comprehensive characterization of extracellular herpes simplex virus type 1 virions. J Virol 82:8605-8618.

Lou, Z., B. P. Chen, A. Asaithamby, K. Minter-Dykhouse, D. J. Chen, and J. Chen. 2004. MDC1 regulates DNA-PK autophosphorylation in response to DNA damage. J Biol Chem 279:46359-46362.

Lukashchuk, V., and R. D. Everett. 2010. Regulation of ICP0-null mutant herpes simplex virus type 1 infection by ND10 components ATRX and hDaxx. Journal of virology 84:4026-4040.

Lycke, E., B. Hamark, M. Johansson, A. Krotochwil, J. Lycke, and B. Svennerholm. 1988. Herpes simplex virus infection of the human sensory neuron. An electron microscopy study. Arch Virol 101:87-104.

Ma, Y., U. Pannicke, K. Schwarz, and M. R. Lieber. 2002. Hairpin opening and overhang processing by an Artemis/DNA-dependent protein kinase complex in nonhomologous end joining and V(D)J recombination. Cell 108:781-794.

Mabit, H., M. Y. Nakano, U. Prank, B. Saam, K. Dohner, B. Sodeik, and U. F. Greber. 2002. Intact microtubules support adenovirus and herpes simplex virus infections. J Virol 76:9962-9971.

Mailand, N., S. Bekker-Jensen, H. Faustrup, F. Melander, J. Bartek, C. Lukas, and J. Lukas. 2007. RNF8 ubiquitylates histones at DNA double-strand breaks and promotes assembly of repair proteins. Cell 131:887-900.

Maldonado, E., R. Shiekhattar, M. Sheldon, H. Cho, R. Drapkin, P. Rickert, E. Lees, C. W. Anderson, S. Linn, and D. Reinberg. 1996. A human RNA polymerase II complex associated with SRB and DNA-repair proteins. Nature 381:86-89.

Maresca, M., A. Erler, J. Fu, A. Friedrich, Y. Zhang, and A. F. Stewart. 2010. Single-stranded heteroduplex intermediates in lambda Red homologous recombination. BMC Mol Biol 11:54.

Mari, P. O., B. I. Florea, S. P. Persengiev, N. S. Verkaik, H. T. Bruggenwirth, M. Modesti, G. Giglia-Mari, K. Bezstarosti, J. A. Demmers, T. M. Luider, A. B. Houtsmuller, and D. C. van Gent. 2006. Dynamic assembly of end-joining complexes requires interaction between Ku70/80 and XRCC4. Proc Natl Acad Sci U S A 103:18597-18602.

Martensson, S., and O. Hammarsten. 2002. DNA-dependent protein kinase catalytic subunit. Structural requirements for kinase activation by DNA ends. J Biol Chem 277:3020-3029.

Martinez, R., J. N. Goldstein, and S. K. Weller. 2002. The product of the UL12.5 gene of herpes simplex virus type 1 is not essential for lytic viral growth and is not specifically associated with capsids. Virology 298:248-257.

Martinez, R., R. T. Sarisky, P. C. Weber, and S. K. Weller. 1996. Herpes simplex virus type 1 alkaline nuclease is required for efficient processing of viral DNA replication intermediates. Journal of virology 70:2075-2085.

Martinez, R., L. Shao, J. C. Bronstein, P. C. Weber, and S. K. Weller. 1996. The product of a 1.9-kb mRNA which overlaps the HSV-1 alkaline nuclease gene (UL12) cannot relieve the growth defects of a null mutant. Virology 215:152-164.

Mathew, S. S., P. W. Bryant, and A. D. Burch. 2010. Accumulation of oxidized proteins in Herpesvirus infected cells. Free Radic Biol Med 49:383-391.

Mattarucchi, E., V. Guerini, A. Rambaldi, L. Campiotti, A. Venco, F. Pasquali, F. Lo Curto, and G. Porta. 2008. Microhomologies and interspersed repeat elements at genomic breakpoints in chronic myeloid leukemia. Genes Chromosomes Cancer 47:625-632.

Matz, B. 1987. Herpes simplex virus infection generates large tandemly reiterated simian virus 40 DNA molecules in a transformed hamster cell line. J Virol 61:1427-1434.

McGeoch, D. J., M. A. Dalrymple, A. J. Davison, A. Dolan, M. C. Frame, D. McNab, L. J. Perry, J. E. Scott, and P. Taylor. 1988. The complete DNA sequence of the long unique region in the genome of herpes simplex virus type 1. The Journal of general virology 69 (Pt 7):1531-1574.

McGeoch, D. J., A. Dolan, and M. C. Frame. 1986. DNA sequence of the region in the genome of herpes simplex virus type 1 containing the exonuclease gene and neighbouring genes. Nucleic acids research 14:3435-3448.

McGeoch, D. J., F. J. Rixon, and A. J. Davison. 2006. Topics in herpesvirus genomics and evolution. Virus Res 117:90-104.

Mesri, E. A., M. A. Feitelson, and K. Munger. 2014. Human viral oncogenesis: a cancer hallmarks analysis. Cell Host Microbe 15:266-282.

Mettenleiter, T. C. 2002. Herpesvirus assembly and egress. J Virol 76:1537-1547.

Millhouse, S., X. Wang, N. W. Fraser, L. Faber, and T. M. Block. 2012. Direct evidence that HSV DNA damaged by ultraviolet (UV) irradiation can be repaired in a cell type-dependent manner. Journal of neurovirology 18:231-243.

Min, W., U. Cortes, Z. Herceg, W. M. Tong, and Z. Q. Wang. 2010. Deletion of the nuclear isoform of poly(ADP-ribose) glycohydrolase (PARG) reveals its function in DNA repair, genomic stability and tumorigenesis. Carcinogenesis 31:2058-2065.

Mladenov, E., and G. Iliakis. 2011. Induction and repair of DNA double strand breaks: the increasing spectrum of non-homologous end joining pathways. Mutation research 711:61-72.

Mocarski, E. S., and B. Roizman. 1982. Structure and role of the herpes simplex virus DNA termini in inversion, circularization and generation of virion DNA. Cell 31:89-97.

Mohni, K. N., A. R. Dee, S. Smith, A. J. Schumacher, and S. K. Weller. 2013. Efficient herpes simplex virus 1 replication requires cellular ATR pathway proteins. J Virol 87:531-542.

Mohni, K. N., C. M. Livingston, D. Cortez, and S. K. Weller. 2010. ATR and ATRIP are recruited to herpes simplex virus type 1 replication compartments even though ATR signaling is disabled. J Virol 84:12152-12164.

Mohni, K. N., A. S. Mastrocola, P. Bai, S. K. Weller, and C. D. Heinen. 2011. DNA mismatch repair proteins are required for efficient herpes simplex virus 1 replication. J Virol 85:12241-12253.

Mohni, K. N., S. Smith, A. R. Dee, A. J. Schumacher, and S. K. Weller. 2013. Herpes simplex virus type 1 single strand DNA binding protein and helicase/primase complex disable cellular ATR signaling. PLoS Pathog 9:e1003652.

Morrison, J. M., and H. M. Keir. 1968. A new DNA-exonuclease in cells infected with herpes virus: partial purification and properties of the enzyme. J Gen Virol 3:337-347.

Muylaert, I., and P. Elias. 2007. Knockdown of DNA ligase IV/XRCC4 by RNA interference inhibits herpes simplex virus type I DNA replication. Journal of Biological Chemistry 282:10865-10872.

Nakanishi, K., Y. G. Yang, A. J. Pierce, T. Taniguchi, M. Digweed, A. D. D'Andrea, Z. Q. Wang, and M. Jasin. 2005. Human Fanconi anemia monoubiquitination pathway promotes homologous DNA repair. Proc Natl Acad Sci U S A 102:1110-1115.

Neal, J. A., and K. Meek. 2011. Choosing the right path: does DNA-PK help make the decision? Mutat Res 711:73-86.

Nicolas, A., N. Alazard-Dany, C. Biollay, L. Arata, N. Jolinon, L. Kuhn, M. Ferro, S. K. Weller, A. L. Epstein, A. Salvetti, and A. Greco. 2010. Identification of rep-associated factors in herpes simplex virus type 1-induced adeno-associated virus type 2 replication compartments. J Virol 84:8871-8887.

O'Hare, P., and C. R. Goding. 1988. Herpes simplex virus regulatory elements and the immunoglobulin octamer domain bind a common factor and are both targets for virion transactivation. Cell 52:435-445.

O'Neill, E. A., and T. J. Kelly. 1988. Purification and characterization of nuclear factor III (origin recognition protein C), a sequence-specific DNA binding protein required for efficient initiation of adenovirus DNA replication. J Biol Chem 263:931-937.

Oh, S., A. Harvey, J. Zimbric, Y. Wang, T. Nguyen, P. J. Jackson, and E. A. Hendrickson. 2014. DNA ligase III and DNA ligase IV carry out genetically distinct forms of end joining in human somatic cells. DNA repair:1-14.

Oh, S., Y. Wang, J. Zimbric, and E. A. Hendrickson. 2013. Human LIGIV is synthetically lethal with the loss of Rad54B-dependent recombination and is required for certain chromosome fusion events induced by telomere dysfunction. Nucleic acids research 41:1734-1749.

Oksenych, V., V. Kumar, X. Liu, C. Guo, B. Schwer, S. Zha, and F. W. Alt. 2013. Functional redundancy between the XLF and DNA-PKcs DNA repair factors in V(D)J recombination and nonhomologous DNA end joining. Proceedings of the National Academy of Sciences 110:2234-2239.

Orzalli, M. H., S. E. Conwell, C. Berrios, J. A. DeCaprio, and D. M. Knipe. 2013. Nuclear interferon-inducible protein 16 promotes silencing of herpesviral and transfected DNA. Proc Natl Acad Sci U S A 110:E4492-4501.

Orzalli, M. H., N. A. DeLuca, and D. M. Knipe. 2012. Nuclear IFI16 induction of IRF-3 signaling during herpesviral infection and degradation of IFI16 by the viral ICP0 protein. Proc Natl Acad Sci U S A 109:E3008-3017.

Orzalli, M. H., and D. M. Knipe. 2014. Cellular sensing of viral DNA and viral evasion mechanisms. Annu Rev Microbiol 68:477-492.

Ottaviani, D., M. LeCain, and D. Sheer. 2014. The role of microhomology in genomic structural variation. Trends Genet 30:85-94.

Palamara, A. T., C. F. Perno, M. R. Ciriolo, L. Dini, E. Balestra, C. D'Agostini, P. Di Francesco, C. Favalli, G. Rotilio, and E. Garaci. 1995. Evidence for antiviral activity of glutathione: in vitro inhibition of herpes simplex virus type 1 replication. Antiviral Res 27:237-253.

Panet, A., J. H. van de Sande, P. C. Loewen, H. G. Khorana, A. J. Raae, J. R. Lillehaug, and K. Kleppe. 1973. Physical characterization and simultaneous purification of bacteriophage T4 induced polynucleotide kinase, polynucleotide ligase, and deoxyribonucleic acid polymerase. Biochemistry 12:5045-5050.

Pankotai, T., C. Bonhomme, D. Chen, and E. Soutoglou. 2012. DNAPKcs-dependent arrest of RNA polymerase II transcription in the presence of DNA breaks. Nat Struct Mol Biol 19:276-282.

Parkinson, J., and R. D. Everett. 2000. Alphaherpesvirus Proteins Related to Herpes Simplex Virus Type 1 ICP0 Affect Cellular Structures and Proteins. Journal of virology.

Parkinson, J., S. P. Lees-Miller, and R. D. Everett. 1999. Herpes simplex virus type 1 immediate-early protein vmw110 induces the proteasome-dependent degradation of the catalytic subunit of DNA-dependent protein kinase. J Virol 73:650-657.

Pawelczak, K. S., and J. J. Turchi. 2008. A mechanism for DNA-PK activation requiring unique contributions from each strand of a DNA terminus and implications for microhomology-mediated nonhomologous DNA end joining. Nucleic Acids Res 36:4022-4031.

Peasland, A., L. Z. Wang, E. Rowling, S. Kyle, T. Chen, A. Hopkins, W. A. Cliby, J. Sarkaria, G. Beale, R. J. Edmondson, and N. J. Curtin. 2011. Identification and evaluation of a potent novel ATR inhibitor, NU6027, in breast and ovarian cancer cell lines. Br J Cancer 105:372-381.

Peng, M., J. Xie, A. Ucher, J. Stavnezer, and S. B. Cantor. 2014. Crosstalk between BRCA-Fanconi anemia and mismatch repair pathways prevents MSH2-dependent aberrant DNA damage responses. EMBO J 33:1698-1712.

Perrault, R., H. Wang, M. Wang, B. Rosidi, and G. Iliakis. 2004. Backup pathways of NHEJ are suppressed by DNA-PK. Journal of cellular biochemistry 92:781-794.

Perry, L. J., and D. J. McGeoch. 1988. The DNA sequences of the long repeat region and adjoining parts of the long unique region in the genome of herpes simplex virus type 1. J Gen Virol 69 (Pt 11):2831-2846.

Pham, T. H., K. M. Kwon, Y.-E. Kim, K. K. Kim, and J.-H. Ahn. 2013. DNA sensing-independent inhibition of herpes simplex virus 1 replication by DAI/ZBP1. Journal of virology 87:3076-3086.

Phelan, A., J. Dunlop, A. H. Patel, N. D. Stow, and J. B. Clements. 1997. Nuclear sites of herpes simplex virus type 1 DNA replication and transcription colocalize at early times postinfection and are largely distinct from RNA processing factors. J Virol 71:1124-1132.

Pierce, A. J., P. Hu, M. Han, N. Ellis, and M. Jasin. 2001. Ku DNA end-binding protein modulates homologous repair of double-strand breaks in mammalian cells. Genes Dev 15:3237-3242.

Pines, A., L. H. Mullenders, H. van Attikum, and M. S. Luijsterburg. 2013. Touching base with PARPs: moonlighting in the repair of UV lesions and double-strand breaks. Trends Biochem Sci 38:321-330.

Poffenberger, K. L., and B. Roizman. 1985. A noninverting genome of a viable herpes simplex virus 1: presence of head-to-tail linkages in packaged genomes and requirements for circularization after infection. Journal of virology 53:587-595.

Porter, I. M., and N. D. Stow. 2004. Virus particles produced by the herpes simplex virus type 1 alkaline nuclease null mutant ambUL12 contain abnormal genomes. The Journal of general virology 85:583-591.

Quinlan, M. P., L. B. Chen, and D. M. Knipe. 1984. The intranuclear location of a herpes simplex virus DNA-binding protein is determined by the status of viral DNA replication. Cell 36:857-868.

Rass, E., A. Grabarz, I. Plo, J. Gautier, P. Bertrand, and B. S. Lopez. 2009. Role of Mre11 in chromosomal nonhomologous end joining in mammalian cells. Nat Struct Mol Biol 16:819-824.

Reuven, N. B., A. E. Staire, R. S. Myers, and S. K. Weller. 2003. The herpes simplex virus type 1 alkaline nuclease and single-stranded DNA binding protein mediate strand exchange in vitro. Journal of virology 77:7425-7433.

Reuven, N. B., S. Willcox, J. D. Griffith, and S. K. Weller. 2004. Catalysis of strand exchange by the HSV-1 UL12 and ICP8 proteins: potent ICP8 recombinase activity is revealed upon resection of dsDNA substrate by nuclease. J Mol Biol 342:57-71.

Reznikoff, W. S., and J. Thomas, C A. 1969. The anatomy of the SP50 bacteriophage DNA molecule. Virology 37:309-317.

Riballo, E., M. Kuhne, N. Rief, A. Doherty, G. C. Smith, M. J. Recio, C. Reis, K. Dahm, A. Fricke, A. Krempler, A. R. Parker, S. P. Jackson, A. Gennery, P. A. Jeggo, and M. Lobrich. 2004. A pathway of double-strand break rejoining dependent upon ATM, Artemis, and proteins locating to gamma-H2AX foci. Mol Cell 16:715-724.

Rice, S. A., M. C. Long, V. Lam, P. A. Schaffer, and C. A. Spencer. 1995. Herpes simplex virus immediate-early protein ICP22 is required for viral modification of host RNA polymerase II and establishment of the normal viral transcription program. J Virol 69:5550-5559.

Rivera-Calzada, A., J. D. Maman, L. Spagnolo, L. H. Pearl, and O. Llorca. 2005. Three-dimensional structure and regulation of the DNA-dependent protein kinase catalytic subunit (DNA-PKcs). Structure 13:243-255.

Rock, D. L., and N. W. Fraser. 1983. Detection of HSV-1 genome in central nervous system of latently infected mice. Nature 302:523-525.

Rogakou, E. P., D. R. Pilch, A. H. Orr, V. S. Ivanova, and W. M. Bonner. 1998. DNA double-stranded breaks induce histone H2AX phosphorylation on serine 139. J Biol Chem 273:5858-5868.

Rogers, S. G., and M. Rhoades. 1976. Bacteriophage T5-induced endonucleases that introduce site-specific single-chain interruptions in duplex DNA. Proceedings of the National Academy of Sciences of the United States of America 73:1576-1580.

Roizman, B., R. J. Jacob, D. M. Knipe, L. S. Morse, and W. T. Ruyechan. 1979. On the structure, functional equivalence, and replication of the four arrangements of herpes simplex virus DNA. Cold Spring Harbor symposia on quantitative biology 43 Pt 2:809-826.

Rolton, H. A., and H. M. Keir. 1974. Deoxycytidylate deaminase evidence for a new enzyme in cells infected by the virus of herpes simplex. Biochem J 143:403-409.

Ropars, V., P. Drevet, P. Legrand, S. Baconnais, J. Amram, G. Faure, J. A. Marquez, O. Pietrement, R. Guerois, I. Callebaut, E. Le Cam, P. Revy, J. P. de Villartay, and J. B. Charbonnier. 2011. Structural characterization of filaments formed by human Xrcc4-Cernunnos/XLF complex involved in nonhomologous DNA end-joining. Proc Natl Acad Sci U S A 108:12663-12668.

Roychoudhury, R., E. Jay, and R. Wu. 1976. Terminal labeling and addition of homopolymer tracts to duplex DNA fragments by terminal deoxynudeotidyl transferase. Nucleic acids research.

Ruis, B. L., K. R. Fattah, and E. A. Hendrickson. 2008. The catalytic subunit of DNA-dependent protein kinase regulates proliferation, telomere length, and genomic stability in human somatic cells. Molecular and cellular biology 28:6182-6195.

Saffran, H. A., J. M. Pare, J. A. Corcoran, S. K. Weller, and J. R. Smiley. 2007. Herpes simplex virus eliminates host mitochondrial DNA. EMBO reports 8:188-193.

Sale, J. E., A. R. Lehmann, and R. Woodgate. 2012. Y-family DNA polymerases and their role in tolerance of cellular DNA damage. Nat Rev Mol Cell Biol 13:141-152.

Sartori, A. A., C. Lukas, J. Coates, M. Mistrik, S. Fu, J. Bartek, R. Baer, J. Lukas, and S. P. Jackson. 2007. Human CtIP promotes DNA end resection. Nature 450:509-514.

Sawtell, N. M., D. K. Poon, C. S. Tansky, and R. L. Thompson. 1998. The latent herpes simplex virus type 1 genome copy number in individual neurons is virus strain specific and correlates with reactivation. J Virol 72:5343-5350.

Scheible, P. P., E. A. Rhoades, and M. Rhoades. 1977. Localization of single-chain interruptions in bacteriophage T5 DNA I. Electron microscopic studies. Journal of virology 23:725-736.

Schildgen, O., S. Graper, J. Blumel, and B. Matz. 2005. Genome replication and progeny virion production of herpes simplex virus type 1 mutants with temperature-sensitive lesions in the origin-binding protein. J Virol 79:7273-7278.

Schreiber, V., F. Dantzer, J.-C. Ame, and G. De Murcia. 2006. Poly (ADP-ribose): novel functions for an old molecule. Nature reviews. Molecular cell biology 7:517-528.

Schumacher, A. J., K. N. Mohni, Y. Kan, E. A. Hendrickson, J. M. Stark, and S. K. Weller. 2012. The HSV-1 exonuclease, UL12, stimulates recombination by a single strand annealing mechanism. PLoS Pathog 8:e1002862.

Sciortino, M. T., M. Suzuki, B. Taddeo, and B. Roizman. 2001. RNAs extracted from herpes simplex virus 1 virions: apparent selectivity of viral but not cellular RNAs packaged in virions. J Virol 75:8105-8116.

Severini, A., A. R. Morgan, D. R. Tovell, and D. L. Tyrrell. 1994. Study of the structure of replicative intermediates of HSV-1 DNA by pulsed-field gel electrophoresis. Virology 200:428-435.

Severini, A., D. G. Scraba, and D. L. Tyrrell. 1996. Branched structures in the intracellular DNA of herpes simplex virus type 1. J Virol 70:3169-3175.

Shao, L., L. M. Rapp, and S. K. Weller. 1993. Herpes simplex virus 1 alkaline nuclease is required for efficient egress of capsids from the nucleus. Virology 196:146-162.

Shao, R. G., C. X. Cao, H. Zhang, K. W. Kohn, M. S. Wold, and Y. Pommier. 1999. Replication-mediated DNA damage by camptothecin induces phosphorylation of RPA by DNA-dependent protein kinase and dissociates RPA:DNA-PK complexes. The EMBO journal 18:1397-1406.

Sheldrick, P., and N. Berthelot. 1975. Inverted repetitions in the chromosome of herpes simplex virus. Cold Spring Harb Symp Quant Biol 39 Pt 2:667-678.

Sheldrick, P., M. Laithier, D. Lando, and M. L. Ryhiner. 1973. Infectious DNA from herpes simplex virus: infectivity of double-stranded and single-stranded molecules. Proceedings of the National Academy of Sciences of the United States of America 70:3621-3625.

Shibata, A., S. Conrad, J. Birraux, V. Geuting, O. Barton, A. Ismail, A. Kakarougkas, K. Meek, G. Taucher-Scholz, M. Lobrich, and P. A. Jeggo. 2011. Factors determining DNA double-strand break repair pathway choice in G2 phase. EMBO J 30:1079-1092.

Shibata, A., D. Moiani, A. S. Arvai, J. Perry, S. M. Harding, M.-M. Genois, R. Maity, S. van Rossum-Fikkert, A. Kertokalio, F. Romoli, A. Ismail, E. Ismalaj, E. Petricci, M. J. Neale, R. G. Bristow, J.-Y. Masson, C. Wyman, P. A. Jeggo, and J. A. Tainer. 2014. DNA Double-Strand Break Repair Pathway Choice Is Directed by Distinct MRE11 Nuclease Activities. Molecular cell 53:7-18.

Shigechi, T., J. Tomida, K. Sato, M. Kobayashi, J. K. Eykelenboom, F. Pessina, Y. Zhang, E. Uchida, M. Ishiai, N. F. Lowndes, K. Yamamoto, H. Kurumizaka, Y. Maehara, and M. Takata. 2012. ATR-ATRIP kinase complex triggers activation of the Fanconi anemia DNA repair pathway. Cancer Res 72:1149-1156.

Shirata, N., A. Kudoh, T. Daikoku, Y. Tatsumi, M. Fujita, T. Kiyono, Y. Sugaya, H. Isomura, K. Ishizaki, and T. Tsurumi. 2005. Activation of ataxia telangiectasia-mutated DNA damage checkpoint signal transduction elicited by herpes simplex virus infection. J Biol Chem 280:30336-30341.

Simpson-Holley, M., R. C. Colgrove, G. Nalepa, J. W. Harper, and D. M. Knipe. 2005. Identification and functional evaluation of cellular and viral factors involved in the alteration of nuclear architecture during herpes simplex virus 1 infection. J Virol 79:12840-12851.

Sinden, R. R., D. E. Pettijohn, and B. Francke. 1982. Organization of herpes simplex virus type 1 deoxyribonucleic acid during replication probed in living cells with 4,5',8-trimethylpsoralen. Biochemistry 21:4484-4490.

Singleton, M. R., L. M. Wentzell, Y. Liu, S. C. West, and D. B. Wigley. 2002. Structure of the single-strand annealing domain of human RAD52 protein. Proc Natl Acad Sci U S A 99:13492-13497.

Skaliter, R., and I. R. Lehman. 1994. Rolling circle DNA replication in vitro by a complex of herpes simplex virus type 1-encoded enzymes. Proc Natl Acad Sci U S A 91:10665-10669.

Skaliter, R., A. M. Makhov, J. D. Griffith, and I. R. Lehman. 1996. Rolling circle DNA replication by extracts of herpes simplex virus type 1-infected human cells. J Virol 70:1132-1136.

Smith, S., N. Reuven, K. N. Mohni, A. J. Schumacher, and S. K. Weller. 2014. Structure of the herpes simplex virus 1 genome: manipulation of nicks and gaps can abrogate infectivity and alter the cellular DNA damage response. J Virol 88:10146-10156.

Sodeik, B., M. W. Ebersold, and A. Helenius. 1997. Microtubule-mediated transport of incoming herpes simplex virus 1 capsids to the nucleus. J Cell Biol 136:1007-1021.

Spear, P. G. 2004. Herpes simplex virus: receptors and ligands for cell entry. Cell Microbiol 6:401-410.

Stahl, M. M., L. Thomason, A. R. Poteete, T. Tarkowski, A. Kuzminov, and F. W. Stahl. 1997. Annealing vs. invasion in phage lambda recombination. Genetics 147:961-977.

Stark, J. M., A. J. Pierce, J. Oh, A. Pastink, and M. Jasin. 2004. Genetic steps of mammalian homologous repair with distinct mutagenic consequences. Mol Cell Biol 24:9305-9316.

Stewart, G. S., S. Panier, K. Townsend, A. K. Al-Hakim, N. K. Kolas, E. S. Miller, S. Nakada, J. Ylanko, S. Olivarius, M. Mendez, C. Oldreive, J. Wildenhain, A. Tagliaferro, L. Pelletier, N. Taubenheim, A. Durandy, P. J. Byrd, T. Stankovic, A. M. R. Taylor, and D. Durocher. 2009. The RIDDLE Syndrome Protein Mediates a Ubiquitin-Dependent Signaling Cascade at Sites of DNA Damage. 136:420-434.

Strang, B. L., and N. D. Stow. 2005. Circularization of the herpes simplex virus type 1 genome upon lytic infection. J Virol 79:12487-12494.

Strang, B. L., and N. D. Stow. 2007. Blocks to herpes simplex virus type 1 replication in a cell line, tsBN2, encoding a temperature-sensitive RCC1 protein. J Gen Virol 88:376-383.

Suga, S., K. Suzuki, M. Ihira, H. Furukawa, T. Yoshikawa, and Y. Asano. 1998. Clinical features of primary HHV-6 and HHV-7 infections. Nihon Rinsho 56:203-207.

Sze, P., and R. C. Herman. 1992. The herpes simplex virus type 1 ICP6 gene is regulated by a 'leaky' early promoter. Virus Res 26:141-152.

Tavalai, N., P. Papior, S. Rechter, M. Leis, and T. Stamminger. 2006. Evidence for a role of the cellular ND10 protein PML in mediating intrinsic immunity against human cytomegalovirus infections. J Virol 80:8006-8018.

Taylor, T. J., and D. M. Knipe. 2004. Proteomics of herpes simplex virus replication compartments: association of cellular DNA replication, repair, recombination, and chromatin remodeling proteins with ICP8. J Virol 78:5856-5866.

Tomida, J., A. Itaya, T. Shigechi, J. Unno, E. Uchida, M. Ikura, Y. Masuda, S. Matsuda, J. Adachi, M. Kobayashi, A. R. Meetei, Y. Maehara, K. Yamamoto, K. Kamiya, A. Matsuura, T. Matsuda, T. Ikura, M. Ishiai, and M. Takata. 2013. A novel interplay between the Fanconi anemia core complex and ATR-ATRIP kinase during DNA cross-link repair. Nucleic Acids Res 41:6930-6941.

Truong, L. N., Y. Li, L. Z. Shi, P. Y. Hwang, J. He, H. Wang, N. Razavian, M. W. Berns, and X. Wu. 2013. Microhomology-mediated End Joining and Homologous Recombination share the initial end resection step to repair DNA double-strand breaks in mammalian cells. Proc Natl Acad Sci U S A 110:7720-7725.

Tsai, A. G., H. Lu, S. C. Raghavan, M. Muschen, C. L. Hsieh, and M. R. Lieber. 2008. Human chromosomal translocations at CpG sites and a theoretical basis for their lineage and stage specificity. Cell 135:1130-1142.

Tsuchida, R., T. Yamada, M. Takagi, A. Shimada, C. Ishioka, Y. Katsuki, T. Igarashi, L. Chessa, D. Delia, H. Teraoka, and S. Mizutani. 2002. Detection of ATM gene mutation in human glioma cell line M059J by a rapid frameshift/stop codon assay in yeast. Radiat Res 158:195-201

Tu, C. P., and S. N. Cohen. 1980. 3'-end labeling of DNA with [alpha-32P]cordycepin-5'-triphosphate. Gene 10:177-183.

Unterholzner, L. 2013. The interferon response to intracellular DNA: why so many receptors? Immunobiology 218:1312-1321.

Unterholzner, L., S. E. Keating, M. Baran, K. A. Horan, S. B. Jensen, S. Sharma, C. M. Sirois, T. Jin, E. Latz, T. S. Xiao, K. A. Fitzgerald, S. R. Paludan, and A. G. Bowie. 2010. IFI16 is an innate immune sensor for intracellular DNA. Nat Immunol 11:997-1004.

van Heemst, D., L. Brugmans, N. S. Verkaik, and D. C. van Gent. 2004. End-joining of blunt DNA double-strand breaks in mammalian fibroblasts is precise and requires DNA-PK and XRCC4. DNA Repair (Amst) 3:43-50.

van Velzen, M., T. Missotten, F. B. van Loenen, R. J. Meesters, T. M. Luider, G. S. Baarsma, A. D. Osterhaus, and G. M. Verjans. 2013. Acyclovir-resistant herpes simplex virus type 1 in intra-ocular fluid samples of herpetic uveitis patients. J Clin Virol 57:215-221.

Vassin, V. M., R. W. Anantha, E. Sokolova, S. Kanner, and J. A. Borowiec. 2009. Human RPA phosphorylation by ATR stimulates DNA synthesis and prevents ssDNA accumulation during DNA-replication stress. J Cell Sci 122:4070-4080.

Vastag, L., E. Koyuncu, S. L. Grady, T. E. Shenk, and J. D. Rabinowitz. 2011. Divergent effects of human cytomegalovirus and herpes simplex virus-1 on cellular metabolism. PLoS Pathog 7:e1002124.

Verkaik, N. S., R. E. E. Esveldt-van Lange, D. v. Heemst, H. T. Brüggenwirth, J. H. J. Hoeijmakers, M. Z. Zdzienicka, and D. C. v. Gent. 2002. Different types of V(D)J recombination and end-joining defects in DNA double-strand break repair mutant mammalian cells. European journal of immunology 32:701.

Wadsworth, S., G. S. Hayward, and B. Roizman. 1976. Anatomy of herpes simplex virus DNA. V. Terminally repetitive sequences. 17:503-512.

Wagner, E. K., J. F. Guzowski, and J. Singh. 1995. Transcription of the herpes simplex virus genome during productive and latent infection. Prog Nucleic Acid Res Mol Biol 51:123-165.

Wang, H., J. Guan, H. Wang, A. R. Perrault, Y. Wang, and G. Iliakis. 2001. Replication protein A2 phosphorylation after DNA damage by the coordinated action of ataxia telangiectasia-mutated and DNA-dependent protein kinase. Cancer research 61:8554-8563.

Wang, H., A. R. Perrault, Y. Takeda, W. Qin, H. Wang, and G. Iliakis. 2003. Biochemical evidence for Ku-independent backup pathways of NHEJ. Nucleic Acids Res 31:5377-5388.

Wang, H., B. Rosidi, R. Perrault, M. Wang, L. Zhang, F. Windhofer, and G. Iliakis. 2005. DNA ligase III as a candidate component of backup pathways of nonhomologous end joining. Cancer Res 65:4020-4030.

Wang, J., Y. Jiang, M. Vincent, Y. Sun, H. Yu, J. Wang, Q. Bao, H. Kong, and S. Hu. 2005. Complete genome sequence of bacteriophage T5. Virology 332:45-65.

Wang, K., T. Y. Lau, M. Morales, E. K. Mont, and S. E. Straus. 2005. Laser-capture microdissection: refining estimates of the quantity and distribution of latent herpes simplex virus 1 and varicella-zoster virus DNA in human trigeminal Ganglia at the single-cell level. J Virol 79:14079-14087.

Wang, M., W. Wu, W. Wu, B. Rosidi, L. Zhang, H. Wang, and G. Iliakis. 2006. PARP-1 and Ku compete for repair of DNA double strand breaks by distinct NHEJ pathways. Nucleic Acids Res 34:6170-6182.

Wei, L., S. Nakajima, C. L. Hsieh, S. Kanno, M. Masutani, A. S. Levine, A. Yasui, and L. Lan. 2013. Damage response of XRCC1 at sites of DNA single strand breaks is regulated by phosphorylation and ubiquitylation after degradation of poly(ADP-ribose). J Cell Sci 126:4414-4423.

Weitzman, M. D., C. E. Lilley, and M. S. Chaurushiya. 2010. Genomes in conflict: maintaining genome integrity during virus infection. Annu Rev Microbiol 64:61-81.

Weitzman, M. D., and S. K. Weller. 2011. Interactions between HSV-1 and the DNA damage response, p. 257-268. *In* S. K. Weller (ed.), Alphaherpesviruses: Molecular Virology. Caister Academic Press, Norfolk, UK.

Weller, S. K. 2010. Herpes simplex virus reorganizes the cellular DNA repair and protein quality control machinery. PLoS Pathog 6:e1001105.

Weller, S. K., and D. M. Coen. 2012. Herpes simplex viruses: mechanisms of DNA replication. Cold Spring Harb Perspect Biol 4:a013011.

Weller, S. K., and J. A. Sawitzke. 2014. Recombination promoted by DNA viruses: phage lambda to herpes simplex virus. Annu Rev Microbiol 68:237-258.

Weller, S. K., M. R. Seghatoleslami, L. Shao, D. Rowse, and E. P. Carmichael. 1990. The herpes simplex virus type 1 alkaline nuclease is not essential for viral DNA synthesis: isolation and characterization of a lacZ insertion mutant. The Journal of general virology 71 (Pt 12):2941-2952.

Whitley RJ. Herpesviruses. In: Baron S, editor. Medical Microbiology. 4th edition. Galveston (TX): University of Texas Medical Branch at Galveston; 1996. Chapter 68. Available from: http://www.ncbi.nlm.nih.gov/books/NBK8157/

Wildy, P. 1955. Recombination with herpes simplex virus. J Gen Microbiol 13:346-360.

Wilkie, N. M. 1973. The synthesis and substructure of herpesvirus DNA: the distribution of alkali-labile single strand interruptions in HSV-1 DNA. The Journal of general virology 21:453-467.

Wilkinson, D. E., and S. K. Weller. 2003. The role of DNA recombination in herpes simplex virus DNA replication. IUBMB Life 55:451-458.

Wilkinson, D. E., and S. K. Weller. 2004. Recruitment of cellular recombination and repair proteins to sites of herpes simplex virus type 1 DNA replication is dependent on the composition of viral proteins within prereplicative sites and correlates with the induction of the DNA damage response. Journal of virology 78:4783-4796.

Wilkinson, D. E., and S. K. Weller. 2005. Inhibition of the herpes simplex virus type 1 DNA polymerase induces hyperphosphorylation of replication protein A and its accumulation at S-phase-specific sites of DNA damage during infection. Journal of virology 79:7162-7171.

Wilkinson, D. E., and S. K. Weller. 2006. Herpes simplex virus type I disrupts the ATR-dependent DNA-damage response during lytic infection. Journal of cell science 119:2695-2703.

Williams, R. S., J. S. Williams, and J. A. Tainer. 2007. Mre11-Rad50-Nbs1 is a keystone complex connecting DNA repair machinery, double-strand break signaling, and the chromatin template. Biochem Cell Biol 85:509-520.

Wold, M. S. 1997. Replication protein A: a heterotrimeric, single-stranded DNA-binding protein required for eukaryotic DNA metabolism. Annual review of biochemistry 66:61-92.

Wysocka, J., and W. Herr. 2003. The herpes simplex virus VP16-induced complex: the makings of a regulatory switch. Trends Biochem Sci 28:294-304.

Xie, A., A. Kwok, and R. Scully. 2009. Role of mammalian Mre11 in classical and alternative nonhomologous end joining. Nat Struct Mol Biol 16:814-818.

Yan, Z., K. F. Bryant, S. M. Gregory, M. Angelova, D. H. Dreyfus, X. Z. Zhao, D. M. Coen, T. R. Burke, Jr., and D. M. Knipe. 2014. HIV integrase inhibitors block replication of alpha-, beta-, and gammaherpesviruses. MBio 5:e01318-01314.

Yao, F., and R. J. Courtney. 1992. Association of ICP0 but not ICP27 with purified virions of herpes simplex virus type 1. Journal of virology 66:2709-2716.

Yao, F., and P. A. Schaffer. 1995. An activity specified by the osteosarcoma line U2OS can substitute functionally for ICP0, a major regulatory protein of herpes simplex virus type 1. Journal of virology 69:6249-6258.

Zernik-Kobak, M., K. Vasunia, M. Connelly, C. W. Anderson, and K. Dixon. 1997. Sites of UV-induced phosphorylation of the p34 subunit of replication protein A from HeLa cells. Journal of Biological Chemistry 272:23896-23904.

Zha, S., C. Guo, C. Boboila, V. Oksenych, H. L. Cheng, Y. Zhang, D. R. Wesemann, G. Yuen, H. Patel, P. H. Goff, R. L. Dubois, and F. W. Alt. 2011. ATM damage response and XLF repair factor are functionally redundant in joining DNA breaks. Nature 469:250-254.

Zhang, X., S. Efstathiou, and A. Simmons. 1994. Identification of novel herpes simplex virus replicative intermediates by field inversion gel electrophoresis: implications for viral DNA amplification strategies. Virology 202:530-539.

Zhang, Z., L. Zhu, D. Lin, F. Chen, D. J. Chen, and Y. Chen. 2001. The three-dimensional structure of the C-terminal DNA-binding domain of human Ku70. J Biol Chem 276:38231-38236.

Zhi, G., J. B. Wilson, X. Chen, D. S. Krause, Y. Xiao, N. J. Jones, and G. M. Kupfer. 2009. Fanconi anemia complementation group FANCD2 protein serine 331 phosphorylation is important for fanconi anemia pathway function and BRCA2 interaction. Cancer Res 69:8775-8783.

Zhuang, J., G. Jiang, H. Willers, and F. Xia. 2009. Exonuclease function of human Mre11 promotes deletional nonhomologous end joining. J Biol Chem 284:30565-30573.